2007

Novel Sulfated 4-Hydroxycinnamic Acid Oligomers as Potent Anticoagulants

Brian Lawrence Henry
Virginia Commonwealth University

NOVEL SULFATED 4-HYDROXYCINNAMIC ACID OLIGOMERS AS POTENT ANTICOAGULANTS

A Dissertation submitted in partial fulfillment of the requirements for the degree of Doctor of Philosophy at Virginia Commonwealth University.

by

BRIAN LAWRENCE HENRY
B.S. in Biology, James Madison University, 2001

Director: UMESH R. DESAI
PROFESSOR, DEPARTMENT OF MEDICINAL CHEMISTRY

Virginia Commonwealth University
Richmond, Virginia
July 2007

Acknowledgement

I would like to thank Dr. Desai for his support as my advisor over the last two-and-half years. He took me in after I was orphaned by my previous advisor and gave me a fantastic project to work on. Our DHP work was exactly the type of project I had hoped to do because of its translational and practical nature. He was always available to answer questions and provide direction but he also trusted my scientific judgment and afforded me great latitude in my work.

I would also like to thank our MD/PhD program director Dr. Gordon Archer for his amazing work to improve our program. Over the past 5 years, our program has improved tremendously, and he is largely responsible for that. He also interviewed me for the PhD portion of the MD/PhD program and was the only interviewer that thought I was capable of becoming a physician scientist. I greatly appreciate VCU extending me an MD/PhD position and taking a chance on a student that no other programs were interested in. I would also like to thank the Dean of the School of Medicine, Dr. Jerry Strauss for his strong commitment to the MD/PhD program. Dr. Archer and Dr. Strauss have worked hard to restore full tuition and stipend scholarships to those of us in the MD/PhD program that were not receiving them and that gesture is greatly appreciated.

I would like to thank my committee members for reading my dissertation and my grant for my oral examination. I would also like to thank them for attending my oral examination and my dissertation defense. I would specifically like to thank my

committee member, Dr. Ross Mikkelsen, because he interviewed me for medical school and apparently thought it was a good idea for me to be accepted at VCU. Since most people did not think it was a good idea for me to attend their medical school, I appreciate him seeing something in me that other did not and recommending that I be given a shot.

I would like to thank all the people I have worked with in labs here at VCU and JMU (the Desai lab, the Brophy lab, the Reynolds lab, the Archer lab, the Schwartz lab, the Kendler lab, the Abraham lab and the Wiggins lab at JMU). I learned something at every stop and I appreciate their efforts to teach me something new.

I would be remiss if I did not thank my first two mentors at the National Cancer Institute (NIH) in Frederick, MD, Dr. Clay Stephens and Dr. Cherie Winkler. Clay gave me my first job in science at age 17 working in bioinformatics. After he left the NIH, Cherie took me into her lab because she saw my potential as a scientist and was the single most important influence in my decision to become a physician scientist. Her willingness to mentor me and employ me in her lab every summer is the reason that I am where I am today. I also developed tremendous professional and personal relationships with my co-workers in Cherie's lab as well as the other labs in our hallway at NCI. Specifically, I have to thank my co-workers Beth Binns, Mark Konsovich, Leo Kenefic and Dr. An-Ping for their daily mentoring of my intellectual curiosities. They taught me literally thousands of little things about science and lab work that are not in books and I have benefited tremendously from their mentorship.

I would like to thank my fellow colleagues in the Desai lab for many great times, whether it was doing lab work, having a conversation to kill time or traveling to Georgia for an ACS conference. I **MUST** thank Research Assistant Professor Dr. Muhammad Riaz for teaching us about humanism, being political, the effects of Mountain Dew, the German people and about things that are "bunie." I have to thank Dr. Bernhard Monien for synthesizing the DHPs used in my experiments. I want to also thank Arjun "the golden boy" Raghuraman, Jay Thakker, Dr. Ayie Liang, Chandravel Krishnasamy and Tim King.

I would like to thank the following collaborators: Mike Hindel for his help with mass spect. in chapter 3, Erika Martin and Don Brophy for their help with the experiments in Chapter 4 and Paul Bock for providing the exosite I ligand used in the Chapter 5 experiments.

Finally, I want to thank my family and friends for their support over these last years. Without their support, I would not have been able to achieve the things I have. Although, come to think of it, I they had not made me go drinking with them so often, I may have achieved so much more.

Table of Contents

Page

List of Tables

Page

List of Figures

Page

Abstract

NOVEL SULFATED 4-HYDROXYCINNAMIC ACID OLIGOMERS AS POTENT ANTICOAGULANTS

By Brian Lawrence Henry, Ph.D.

A Dissertation submitted in partial fulfillment of the requirements for the degree of Doctor of Philosophy at Virginia Commonwealth University.

Virginia Commonwealth University, 2007

Major Director: Umesh R. Desai
Professor, Department of Medicinal Chemistry

The occurrence of thrombosis in several pathophysiological conditions creates a huge need for anticoagulation therapy. Thrombin and factor Xa have been prime targets for regulation of clotting through the direct and indirect mechanism of inhibition.

This work investigates chemo-enzymatically prepared oligomers of 4-hydroxycinnamic acids (DHPs) as potential anticoagulants. Oligomers were prepared through peroxidase-catalyzed oxidative coupling of 4-hydroxycinnamic acids. The products resulting from this reaction are called CDs, FDs and SDs. Structurally, these

sulfated DHPs are unique and do not resemble any of the anticoagulants known in the literature.

DHP oligomers were found to increase clotting times at concentrations comparable to heparin. Studies in blood and plasma show that DHPs possess an anticoagulation profile similar to enoxaparin. To understand the mechanism of action of DHPs, we studied the inhibition of thrombin, FXa, FIXa, and FVIIa in the presence and absence of antithrombin. CDs and FDs display a preference for direct inhibition of thrombin and FXa, and exhibit a high level of specificity over FIXa and FVIIa. In the presence of AT, CDs and FDs displayed weaker inhibition of FXa and thrombin suggesting that binding to AT is a competitive side reaction. SDs exhibited potent inhibition of FXa and thrombin in the absence of antithrombin, but was inactive against FIXa and FVIIa representing the best selectivity among the DHPs. For SDs, inhibition of all the pro-coagulant enzymes favored the antithrombin dependent pathway.

Binding studies were performed to determine how CDs directly inhibits thrombin. Competitive binding studies suggest that CDs interacts with exosite II and disrupts the catalytic triad of thrombin. These results indicate that the preferred mechanism of CDs action is exosite II mediated allosteric disruption of thrombin. CDs appears to be the first exosite II mediated DTI and this represents a novel mechanism of inhibitor function.

The inhibition characteristics of DHPs are unique and radically different in structure from all the current clinically used anticoagulants. To the best of our knowledge this dual mechanism of anticoagulation and unique binding mode has not been described as yet in literature and represents a novel strategy that our laboratory has discovered.

Chapter 1: Introduction

1.1 Coagulation Cascade

The human body is designed to maintain an intricate network of vasculature that is capable of continuously circulating blood for decades. It is also responsible for its own repair when internal or external forces disrupt the integrity of this system. The major physiologic pathway that is responsible for this endogenous repair is the coagulation cascade (Figure 1). It is composed of two separate, but likeminded, pathways known as the extrinsic (or tissue factor) pathway and the intrinsic (or contact factor) pathway. The extrinsic pathway has the greatest effect on normal and pathologic hemostasis [1]. The extrinsic pathway begins when factor VIIa (FVIIa) and tissue factor (TF) coalesce. TF is the most important initiator of coagulation [2]. TF is a transmembrane glycoprotein that is expressed in regions of the body where, if disrupted, coagulation would be necessary. In normal vessels, TF is found in the adventia smooth muscle cells of the vessel media [3]. TF is expressed on subendothelial cells and is generally barricaded from the blood by the endothelial barrier of the vasculature. The initiation of the extrinsic pathway is triggered by the exposure of TF to the blood, indicating a hemorrhagic event has occurred [4]. TF exposure can also occur when endotoxins and cytokines stimulate cells to increase TF expression, which is common during an inflammatory response or sepsis [5].

Although segregated from TF, FVIIa is always circulating in the blood at low basal levels. When TF is exposed to the blood, it forms a complex with circulating free FVIIa to form a TF/FVIIa complex, which can be considered the initiation of thrombin generation [6]. During the initiation phase, the TF/FVIIa complex activates factor X to factor Xa (FXa). Also, the TF/FVIIa complex activates more FVII. Complexation with TF greatly enhances the activity of FVIIa [7]. The earliest FXa formed is free FXa, which activates a small amount of prothrombin to thrombin, which in turn activates a small number of platelets. FXa first cleaves the peptide bond immediately following Arg320 in prothrombin generating meizothrombin. Next, the peptide bond immediately following Arg271 is cleaved by FXa to generate thrombin and prothrombin fragment 1.2 [8]. The activity of the TF/FVIIa complex is also referred to as the extrinsic pathway.

After clotting has been initiated by the exposure of TF, large amounts of fibrin and activated platelets are needed to stop the hemorrhage. In a very short time, high concentrations of thrombin are necessary for the production of fibrin and activated platelets. The series of biochemical events that ultimately lead to the mass production of thrombin is known as the amplification phase. During the amplification phase, thrombin continues to activate platelets [9] as well as FVIII [10], FV [11] and FXI [12]. FIX is activated by FXIa which allows for the formation of the intrinsic tenase complex which is composed of FIXa, FVIIIa, anionic phospholipids and Ca^{+2}. The intrinsic tenase complex activates FX which can now form its own complex, know as the prothrombinase complex. This prothrombinase complex is composed of FXa, FVa, phospholipids and Ca^{+2}. The prothrombinase complex generates thrombin over 100,000 times faster than free FXa, so it

is this complex formation that results in an explosion of thrombin [13]. At the beginning of the intrinsic pathway, factor XIIa can activate FXI to FXIa. FXIa in turn activates FIX, which binds with the catalytically inactive FVIIIa. FIXa and FVIIIa cooperate to activate FX to FXa. Factor Xa represents the confluence of the two kindred pathways (extrinsic and intrinsic) and forms the beginning of the common pathway in the coagulation cascade. FXa activates prothrombin to thrombin. Small amounts of thrombin feeds back to activate FVII to FVIIa. FVIIa activates FX to FXa. FXa activates more prothrombin to thrombin. This is a positive feedback system whereby thrombin is capable of amplifying its own creation, ultimately leading to an explosion in thrombin levels and subsequently, the rapid development of a clot. To create a clot, thrombin converts fibrinogen to fibrin and FXIII to FXIIIa. The proteolytic production of fibrin from fibrinogen allows for the non-covalent self-association of the fibrin monomers [14]. FXIIIa is a transglutaminase that covalently links the Gln and Lys residues of the growing non-covalent fibrin polymer [15]. This creates a strong fibrin polymer that affords structural integrity to the clot.

During thrombogenesis, clotting factors become ensnared in the growing fibrin meshwork and become bound to fibrin. These clot-bound procoagulant proteases include thrombin, FXa, prothrombinase complex and likely other procoagulant elements. The clot bound factors continue to remain active, making them important for thrombogenicity and the evolution of clot maturation [16, 17]. These clot bound factors can not be accessed by AT and are therefore resistant to AT-dependent drugs [18, 19].

Another example of this positive feed back system occurs when thrombin activates FXI [12]. FXIa activates FIX and FIXa complexes with FVIIIa to activate FX which

ultimately results in a further increase in thrombin concentration. In this light, it is also possible to think of the intrinsic pathway, not as a separate pathway, but as another avenue to amplify the extrinsic pathway.

Figure 1. The coagulation cascade. Green arrows and blue arrows, indicate the processes of the intrinsic and extrinsic pathways, respectively. The dotted red lines are reactions catalyzed by thrombin. Factors inhibited by antithrombin are shown by the black arrows.

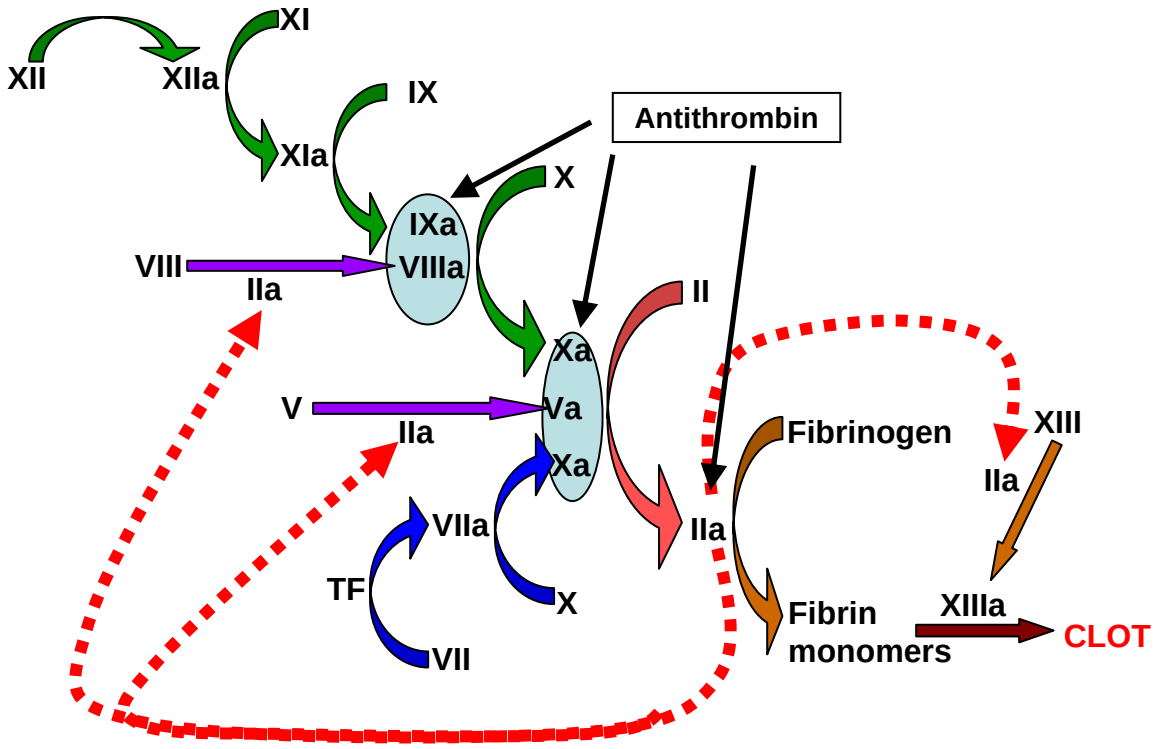

Although the goal of the coagulation cascade is to form a stable clot and seal off the area of hemorrhage, there needs to exist an internal adversary which is capable of regulating the clotting process. Within our bodies, there are several naturally occurring

anticoagulants that serve to regulate the procoagulant enzymes of the blood. The three major endogenous anticoagulants are antithrombin III (AT), activated protein C (APC) and tissue factor pathway inhibitor (TFPI) [20]. These endogenous inhibitors have several different mechanisms to restrain hypercoagulation or regulate accelerated clot formation. Tissue factor pathway inhibitor (TFPI) inhibits the TF/FVIIa/FXa complex [21]. Antithrombin is a suicide inhibitor that regulates thrombin, FXa, FIXa and to lesser degree FVIIa and FXIa [21]. AT inhibition of these factors is greatly accelerated by the presence of heparin. Paradoxically, thrombin, the most important procoagulant enzyme also behaves as an anticoagulant by interacting with thrombomodulin to activate protein C, which in turn inhibits FVa and FVIIIa. While, AT and APC begin to inhibit their targets while the coagulation response is in the process of amplifying, TFPI inhibits the coagulation response during the earliest steps of coagulation [22].

Although the two systems are antagonistic, coagulation and fibrinolysis both share a common associate. Thrombin is able to activate thrombin-activated fibrinolysis inhibitor (TAFI) [23]. TAFIa removes the C-terminal K and R residues from partially degraded fibrin [24]. Fibrin containing these residues is a necessary cofactor for plasminogen activation and plasmin is a key enzyme is clot catabolism. This allows TAFIa to inhibit fibrinolysis and further extend the influence of thrombin as a procoagulant enzyme. Inhibition of thrombin generation can reduce TAFI activation and reduce resistance to fibrinolysis.

1.2 Current Anticoagulants

For decades, drug design of anticoagulants has focused on the two most prominent serine proteases of the coagulation cascade, thrombin and FXa [25]. The mechanism of action for these anticoagulants has relied on both direct inhibition of the enzymes as well as indirect inhibition utilizing the endogenous anticoagulant systems or disrupting metabolic pathways. Direct inhibitors bind to the enzyme and disrupt its catalytic ability by occluding the active site or through allosteric modulation. Indirect inhibitors do not bind to procoagulant enzymes but their interaction with other proteins ultimately yields an anticoagulant effect. Common anticoagulants, like warfarin or heparin and its derivatives are indirect inhibitors which work through a conduit, such as vitamin K or antithrombin, respectively. These inhibitors are mentioned briefly below, while direct inhibitors are discussed more thoroughly.

1.2.1 ***Warfarin*** is a vitamin K antagonist (figure 2). Warfarin is capable of inhibiting the enzyme vitamin K epoxide reductase, which prevents the production of reduced vitamin K, a necessary cofactor for the action of γ-carboxylase. The function of γ-carboxylase is to add carboxyl groups to glutamic acid residues in thrombin, FXa, FIXa and FVIIa. Without proper γ-carboxylation, calcium can not bind to the serine proteases, thereby disrupting the pro-coagulant reactions. γ-carboxylase utilizes vitamin K as a reducing cofactor, which in turn is oxidized to vitamin K epoxide. Vitamin K epoxide reductase converts the oxidized vitamin K back to its useful, reduced state. Therefore, warfarin is indirectly able to act as

an anticoagulant by depleting vitamin K, resulting in decreased γ-carboxylase activity, which in turn produces catalytically inactive pro-coagulant serine proteases [26].

Figure 2. The structure of Warfarin.

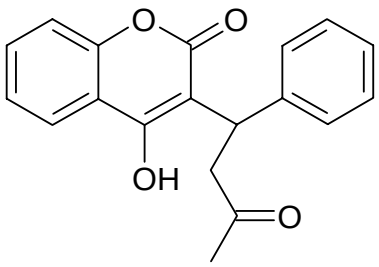

WARFARIN

1.2.3 Heparin** and **low molecular weight derivatives are popular anticoagulants because they are effective and easily accessible (figure 3). Heparin is isolated from mammalian sources, most commonly from porcine intestine. Structurally, heparin is composed of glucosamine and iduronic acid residues that are connected in a 1- 4 linkage, which creates a linear polymer [27]. Despite the simplistic primary structure of heparin, it is a highly sulfated complex, heterogeneous, polydisperse molecule. Thus, a heparin preparation has numerous fragments with different structures that range in size from 3-50 kDa. Within these sequences is a specific sequence motif referred to as the antithrombin pentasaccharide sequence. It is this sequence that gives heparin its anticoagulant activity [28].

Figure 3. The general structure of heparin.

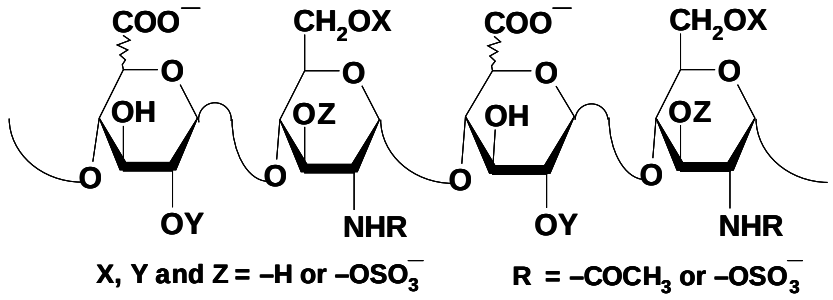

The large sulfated polymers create a high negative charge density along the heparin molecule. In addition to binding antithrombin, this polyanionic polymer is capable of nonspecifically binding to a large number of plasma proteins, which is a putative cause for many of heparin's undesirable side effects as well as its most common mechanism of action [29].

The raw preparations taken directly from porcine sources are considered to be unfractionated heparin (UFH). UFH has variable pharmacokinetics and numerous undesirable side effects. To combat these problems, low molecular weight heparins (LMWHs) were produced by filtering out some of the higher molecular weight species in an attempt to better concentrate the active pentasaccharide sequence. This results in a drug that has less side effects and more predictable pharmacokinetics. UFH and LMWHs bind to antithrombin via their specific pentasaccharide sequence and accelerates antithrombin's inhibition of thrombin and FXa. The mechanism of inhibition is slightly different for each serine protease. UFH/LMWH binds to antithrombin and changes its conformation, which accelerates its rate of FXa inhibition (figure 4). To inhibit thrombin, an additional step is

required. Following change in antithrombin conformation, heparin utilizes its long, polyanionic chain to bind thrombin and bring it into close association with antithrombin. This is referred to as the bridging mechanism of heparin. If the heparin fragment is too short, then the bridging mechanism will not proceed [30]. Factor IXa is inhibited by heparin utilizing both the bridging mechanism and the conformational change mechanism.

Figure 4. The mechanism of inhibition of procoagulant serine proteases by heparin.

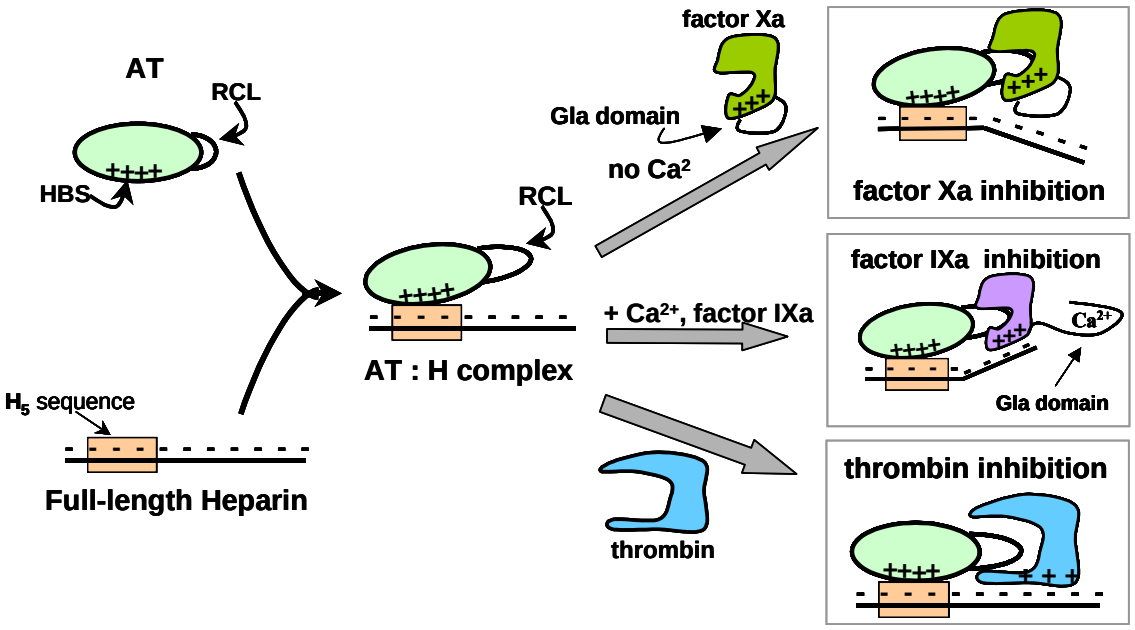

1.2.4 Fondaparinux is a synthetically prepared analogue of the highly specific pentasaccharide found in heparin (figure 5). Fondaparinux binds to antithrombin, an endogenous regulator of procoagulant serine proteases, and accelerates its inhibition of FXa [31]. Since fondaparinux is short compared to unfractionated and low molecular weight heparin and can not bridge thrombin and antithrombin, it is unable to inhibit

thrombin effectively. Just like its predecessors, fondaparinux is parenterally administered and can not inhibit clot bound or platelet bound FXa. However, it also does not bind platelet factor 4 (PF4). This is significant because the heparin:PF4 complex is potentially antigenic and is the epitope for the production of auto-antibodies which cause heparin-induced thrombocytopenia. Unfortunately, fondaparinux is not susceptible to the protamine sulfate antidote like larger heparins [21].

Figure 5. The structure of the pentasaccharide binding sequence.

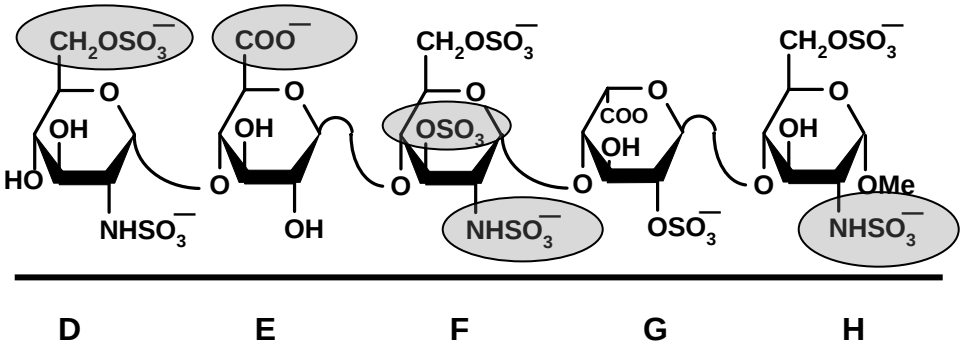

1.2.5 ***Hirudin*** is an example of a direct inhibitor which directly inhibits thrombin. It is a 65-amino acid protein that is produced in the salivary glands of *Hirudo medicinalis*, a common medical leech [32] (figure 6). Recombinant hirudin is commercially available as **lepirudin** and **desirudin**, which are approved for several indications. These recombinant hirudins lack a sulfate group on the phenol of Tyr 63, which is present in natural hirudin. This loss of anionic character results in a decrease in the thrombin binding potency [33]. Once in the blood stream, hirudin's anionic carboxy-terminal region binds to the

fibrinogen binding domain (exosite I), while its bulky, amino-terminal region binds in the active site of thrombin [34] (figures 7, 8 and 9). This type of binding is known as bivalent direct inhibition. Although the binding is strictly noncovalent, the complex is so tight (Ki= 20 fM) that it is practically irreversible. The thrombin Ki values for lepirudin and desirudin are 60 fM and 200 fM, respectively [35, 36]. This ultra tight binding is unfortunate because no antidote can be given to reverse thrombin inhibition. Hirudin is highly selective for thrombin over other serine proteases (10^9-fold more selective) [33, 35]. Several derivatives of this peptide have been produced and are now obtainable for clinical applications [37]. Since hirudin is a large polypeptide, and therefore not orally available, a great deal of energy is being put forth to develop an orally bioavailable direct thrombin inhibitor. These small molecules are being synthesized as prodrugs that target the thrombin active site. Furthermore, hirudin has been shown to be as or more effective than heparin in various indications, especially the treatment of deep vein thrombosis (DVT). However, it has a narrow therapeutic window, carries a significant bleeding risk and can cause anaphylaxis [21, 38]. Major bleeding has been observed in 18-20% of patients receiving lepirudin, with a 2.5% risk of hemorrhagic death [38]. Since the hirudins are foreign peptides, they are highly immunogenic, resulting in potentially life threatening anaphylaxis [38].

Figure 6. The primary sequence of a naturally occurring hirudin. Recombinant hirudins do not contain a sulfate at Tyr63. Residues in red (E49-Q65) consist of the C-terminal exosite I recognition sequence, while the first three residues in blue bind in the thrombin

active site. The black lines connecting Cys residues denote disulfide bonds. This figure is adapted from [39].

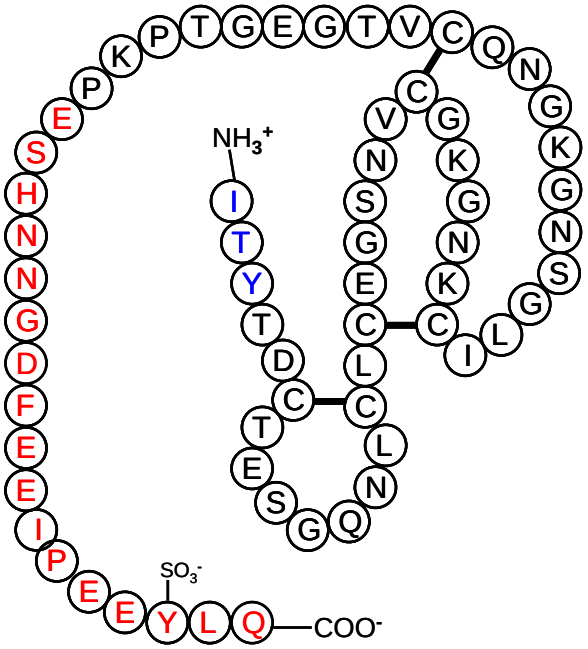

Figure 7. An illustration of thrombin (*left*), which includes are the active site as well as the substrate recognition sites (exosites) and Na^+ binding site. The second illustration (*right*) shows hirudin interacting with exosite I and the active site of thrombin.

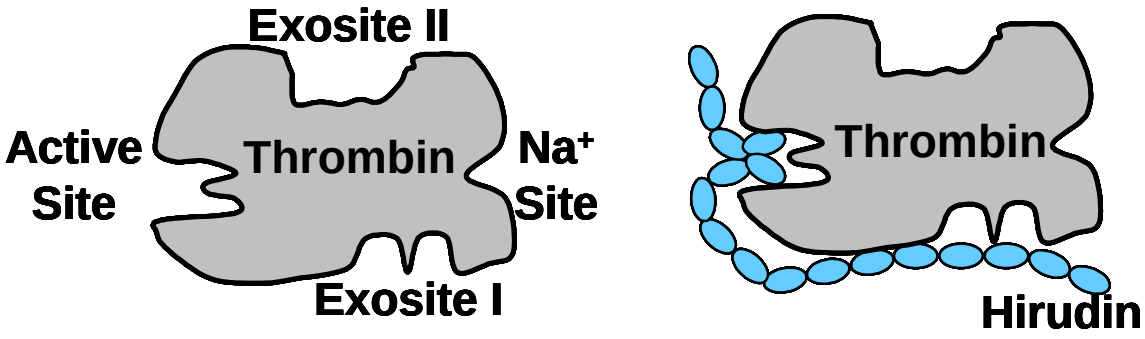

Figure 8. This is a ribbon structure of the thrombin (light blue), hirudin (red) complex. The N-terminus of hirudin occludes the active site and the C-terminus stretches along exosite I of thrombin. This image was created from the PDB file 4HTC using sybyl 7.2.

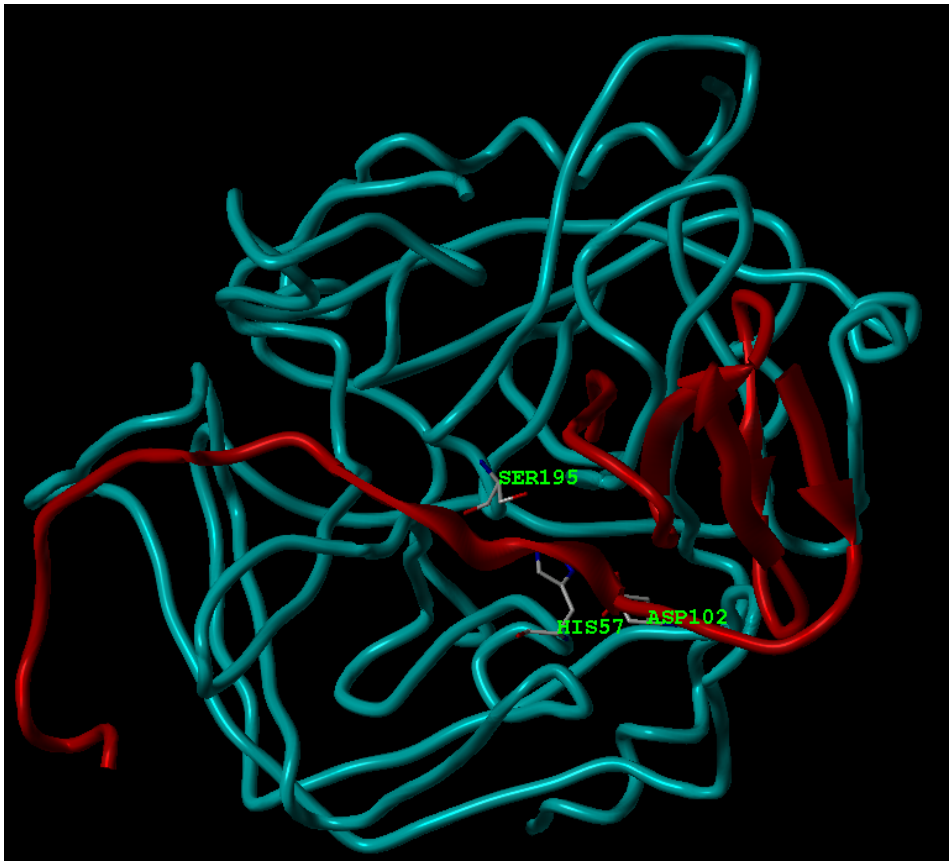

Figure 9. This is a mixed rendering of the thrombin (space filled model), hirudin (green) complex. The N-terminus of hirudin occludes the active site and the C-terminus stretches along exosite I of thrombin. This image was created from the PDB file 4HTC using sybyl 7.2.

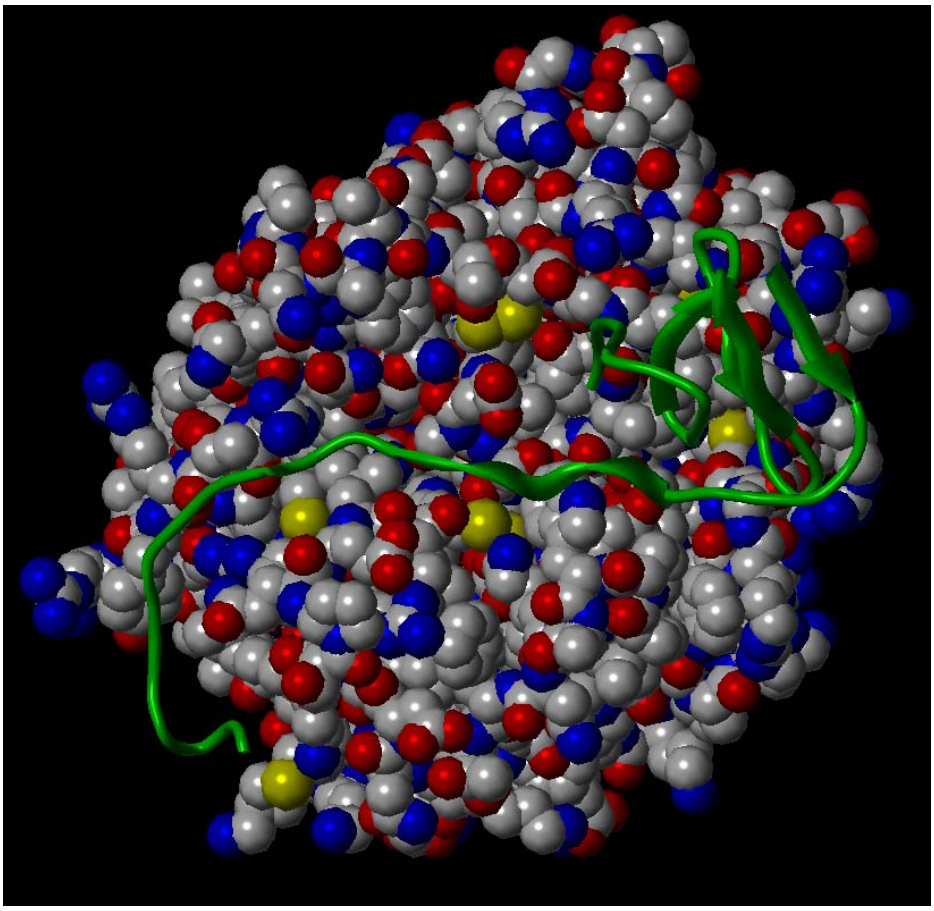

1.2.6 Bivalirudin is a synthetic, 20-amino acid (2180 Da) analog of hirudin (generically referred to as a hirulog), which is a potent reversible inhibitor of thrombin [40]. Structurally, bivalirudin (and hirulogs) can be considered a "bare bones" version of hirudin with only most important residues retained for activity (figure 10). The N-terminus contains the sequence, D-Phe-Pro-Arg-Pro, which binds in the active site of thrombin. The C-terminus is a dodecapeptide that binds thrombin exosite I. These two sequences are connected by a four glycine linker to one another (figure 11) [41]. It forms a 1:1 complex with thrombin but the Pro-Arg bond that binds the active site is cleaved allowing thrombin to regenerate its activity [42]. Initially, bivalirudin exhibits irreversible thrombin binding, but eventually bivalirudin begins to exhibit reversible thrombin binding kinetics (kcat= 0.01/sec) [43]. Bivalirudin (or hirulog-1) inhibits small chromogenic peptide hydrolysis by thrombin with a Ki= 1.9-2.3 nM [40, 43]. The C-terminal portion of bivalirudin alone inhibits the fibrinogen clotting activity of thrombin with a Ki= 144 nM but it can not inhibit thrombin hydrolysis of small peptides. Bivalirudin, like hirudin, is specific for thrombin over other serine proteases including FXa, plasmin and trypsin. Bivalirudin is twice as potent as hirudin in increasing APTT in human plasma [40]. Since bivalirudin has a 25 minute half-life [44] and a predictable anticoagulant response, it is considered to be as good or superior to heparin in certain surgical procedures while carrying a decreased bleeding risk [21]. Unlike hirudin, bivalirudin is not considered immunogenic [38].

Figure 10. The primary sequence of bivalirudin. The exosite I recognition sequence is shown in red, which is connected to the active site recognition sequence in blue by a four Gly linker.

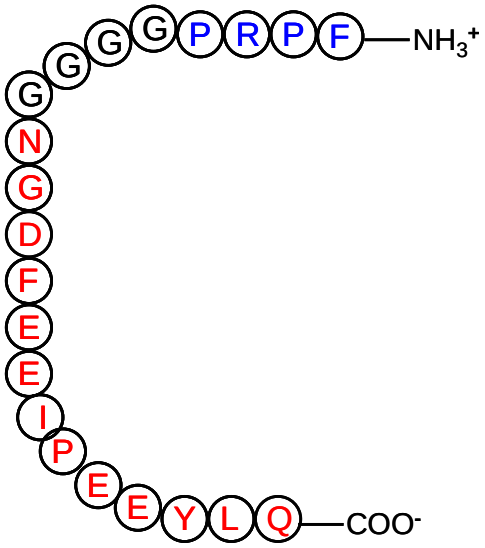

Figure 11. An illustration of thrombin bound to bivalirudin. The exosite I recognition sequence is connected to the active site recognition sequence by a four Gly linker.

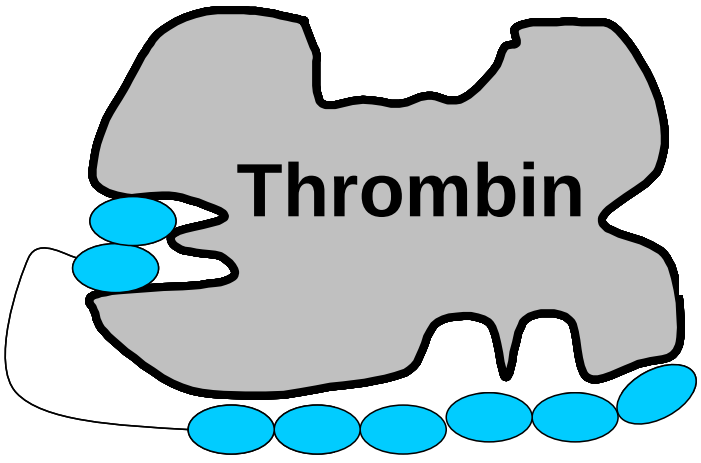

1.2.7 Argatroban (**1**) is a reversible, competitive active site directed thrombin inhibitor (figure 12) [45]. It has a molecular mass of 527 Da and displays good selectivity and potency for thrombin (Ki= 38 nM) [37]. Although argatroban is approved for use in patients with heparin-induced thrombocytopenia (HIT), or patients believed to be at high risk for developing HIT, its usefulness is limited by a short plasma half-life and its parenteral route of administration. Argatroban lacks oral bioavailability due to its guanidine moiety which is positively charged under physiological conditions. Additionally, argatroban is not antigenic [46] and it is able to inhibit clot bound thrombin [47].

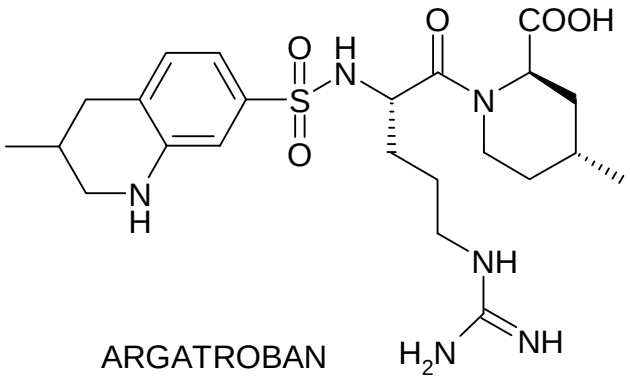

1

Ximelagatran (**2**) represents the first orally active direct thrombin inhibitor which was approved for the treatment of venous thromboembolic diseases. Ximelagatran is a prodrug of the active compound melagtran. The prodrug is created by the amidoxime group and an ester [48]. Ximelagatran transforms to melagatran via two intermediate metabolites which involves ester hydrolysis and reduction of the hydroxyl group [49]. The conversion can occur in two ways. There can either be a reduction of hydroxyamidine to ethylmelagatran

followed by hydrolysis or hydrolysis to hydroxymelagatran and then reduction to melagatran [50]. Ximelagatran has greatly increased lipophilic character over melagatran and it remains uncharged in the gastrointestinal tract [48]. Both these factors contribute to ximelagatran's superior permeability (80-fold) and oral absorption [51]. Melagatran is a peptide mimic of part of fibrinopeptide, specifically; it mimics the D-Phe-Pro-Arg sequence [52]. It has a benzamidine in place of Arg, Pro is mimicked by azetidine 2-carboxylic acid and the Phe is replaced by cyclohexylglycine. Based on this design, melagatran is an active site inhibitor of thrombin (figure 12) and it is capable of inhibiting both free thrombin and fibrin bound thrombin [53]. Melagatran has a molecular weight of 429 Da [37]. While ximelagatran and hydroxyamidine melagatran are devoid of anticoagulant activity, ethyl melagatran is considered to possess similar anticoagulant activity to melagatran [51]. It can not be considered selective because its Ki against thrombin is 3 nM, while its Ki is 4 nM against trypsin. However, selectivity is achieved over the other serine proteases [49]. In Europe, ximelagatran (Exanta®) was approved for preventing thrombosis in orthopedic surgical patients. Although ximelagatran does not have any known drug-drug or drug-food interactions like warfarin, liver toxicity is a major safety issue [54] and unfortunately, this has prevented its wide spread use. The FDA rejected Exanta® in 2004 citing concerns over hepatotoxicity in some patients [37] and this concern ultimately killed its future as a drug. Using ximelagatran as a lead, **AZD0837** (**3**) was created as an orally bioavailable, active site mediated, thrombin inhibitor [55].

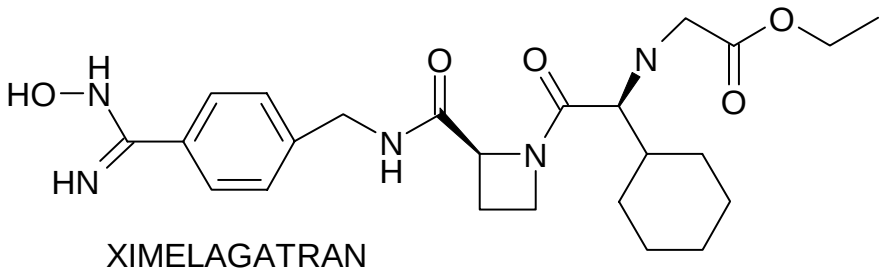

XIMELAGATRAN

2

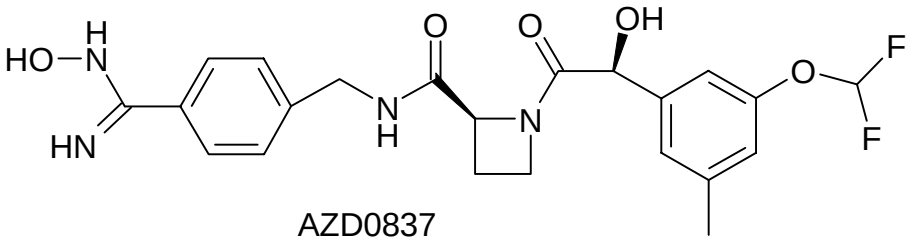

AZD0837

3

Figure 12. An illustration of synthetic small molecules interacting with the thrombin active site. Note that peripheral exosites are not involved in mediating enzyme-inhibitor interactions.

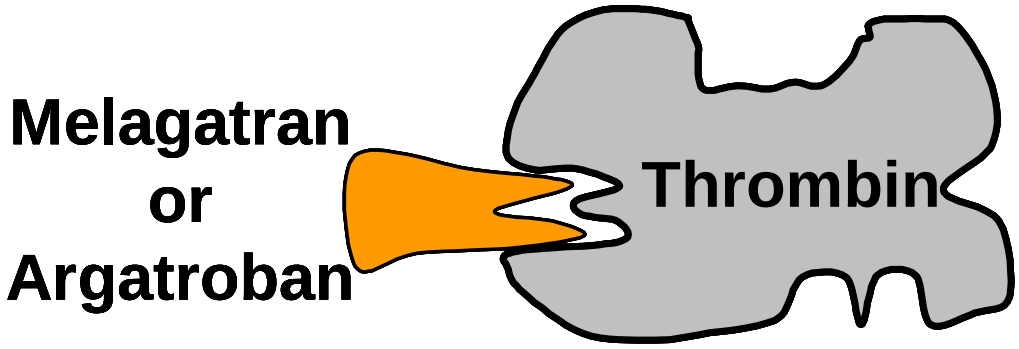

1.3 Major limitations of current anticoagulants

Although indirect inhibitors are commonly used in anticoagulant therapy, they suffer from several limitations including enhanced chance of bleeding, variable patient responses, heparin-induced thrombocytopenia (HIT) and the inability to inhibit clot bound thrombin [18, 19, 56]. Because of these limitations, newer direct inhibitors of thrombin and factor Xa are considered to be a superior alternative to indirect inhibitors. An important advantage of direct inhibition is that both circulating and clot-bound thrombin can be inhibited [47]. During thrombogenesis, clotting factors become ensnared in the growing fibrin meshwork and become bound to fibrin. These clot-bound procoagulant proteases include thrombin, FXa, prothrombinase complex and likely other procoagulant elements. Clot bound factors are important for thrombogenicity and the evolution of clot maturation [16, 17]. These clot bound factors can not be accessed by AT and therefore are resistant to AT-dependent drugs [18, 19]. Some currently approved therapies, like hirudin, its derivatives and argatroban are not orally bioavailable and have short durations of action. The first orally active anticoagulant since warfarin, ximelagatran, was never approved and ultimately discontinued because of liver toxicity.

1.4 Challenges in designing inhibitors of coagulation

Development of these molecules has been challenging including difficulties establishing enzyme binding affinity that is not associated with excessive bleeding, achieving inhibition of both free and clot-bound thrombin and avoiding liver toxicity [37]. Furthermore, the development of selective compounds, especially compounds that do not also inhibit

trypsin, is difficult. It is also unknown what inhibitor strategy will yield the best anticoagulant effects and be hampered the least by side effects. It may also be the case that dual inhibition of the coagulation cascade or poly-pharmacy will end up being the most efficacious. Regardless, these numerous unanswered questions make the field anticoagulation drug design extremely exciting, compelling and challenging.

1.5 The trypsin family of serine proteases

In general, the active sites of this family are composed of a specificity pocket (S1), a proximal hydrophobic pocket (S2) and a distal hydrophobic pocket (S3) [57]. Although the active sites are similar, there are differences between them that allow for the development of specific, potent inhibitors. All serine protease have the same catalytic triad in the S1 pocket, Ser-His-Asp [58]. The active site of trypsin is considered to be more open and less sterically restricted then the other proteases [59]. By skillfully designing and probing the active sites, one can eventually develop specific, potent inhibitors.

1.6 Inhibitors of initiation of coagulation

1.6.1 General Mechanism of Action and Rationale for Designing Inhibitors

These molecules target and inhibit the formation and amplification of the FVIIa/TF complex, by inhibiting factor VIIa, TF or the FVIIa/TF complex. It is believed that inhibition of TF/FVIIa complex, instead of thrombin or FXa, will allow for a better separation of the desirable antithrombotic effects from the deleterious hemorrhagic side effects common to thrombin and FXa inhibition [60]. Since the TF/FVIIa complex is only

formed at sites of TF exposure, an inhibitor will only work locally without the global complications caused by inhibiting other coagulation enzymes.

1.6.2 FVIIa active site

The active site of FVIIa is similar to that of other serine proteases but specific differences do exist (figures 13 and 14). The binding of tissue factor radically alters the active site geometry into a conformation with superior catalytic potential. The three pockets of the active site are the specificity pocket (S1), the proximal hydrophobic pocket (S2) and the distal hydrophobic pocket (S3). In the S1 pocket, FVIIa differs at 2 positions from the other serine proteases. Residue 190 is a serine in FVIIa while it is an alanine in thrombin and FXa [61]. Residue 192 is a Lys while other serine proteases have a Gln and thrombin has a unique Glu [59]. In the S2 pocket, FVIIa is the only serine protease with an anionic group at residue 60 (Asp) and the pocket is comparatively large and open [59]. The S3 pocket is considered to be open and hydrophobic.

Figure 13. The structure of FVIIa. The active site residues are displayed for reference. This image was created from the PDB file 1CVW using sybyl 7.2.

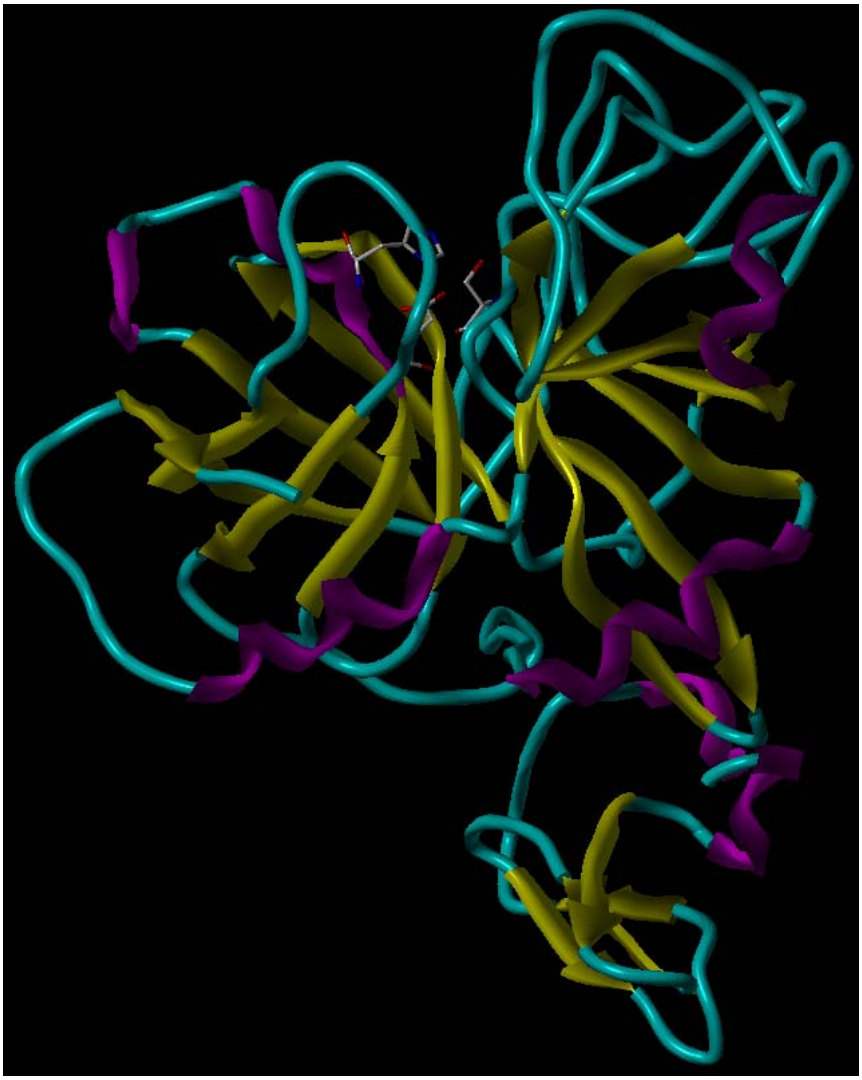

Figure 14. The structure of FVIIa active site. The active site residues and other key residues are displayed for reference. This image was created from the PDB file 1CVW using sybyl 7.2.

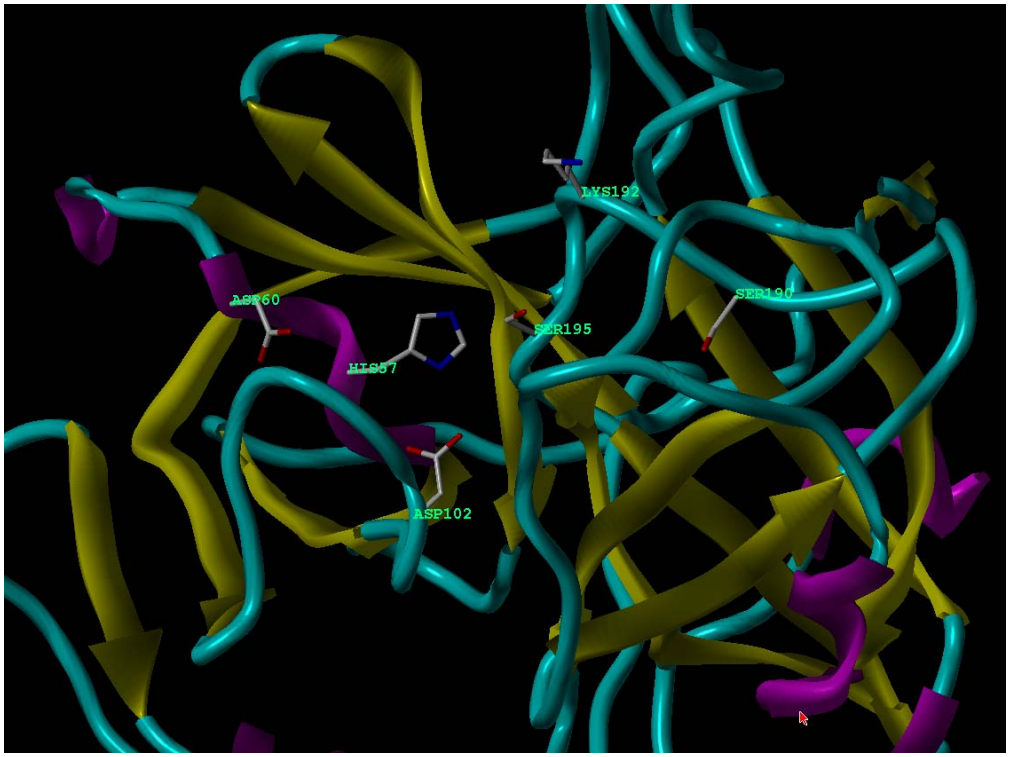

***1.6.3 2-Aryl substituted 4H-3, 1-Benzoxazin-4ones*:** Their mechanism of action is the selective acylation of the FVIIa Ser 195 by the benzoxazinone lactone [62]. The two factors that affect this mechanism are the electronegative groups present on the 2-aryl ring and on the benzoxazinone ring at positions 5, 6, 7 and 8. Substitutions at these positions alter the reactivity of the lactone by changing its polarity. The best substitution pattern is 2,6-difluoro on the 2-aryl ring and an electronegative group at positions 5, 6, 7 or 8 of the benzoxazinone ring, exemplified by the inhibitor **4**. The IC_{50} for FX activation by the

TF/FVIIa complex is 0.82 μM, while the IC_{50} towards FXa and thrombin is 112 μM and >200 μM, respectively.

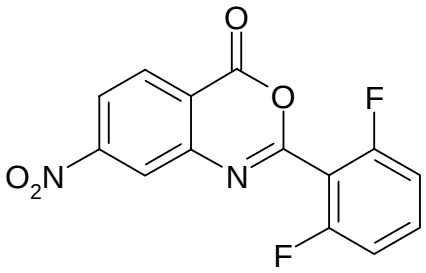

4

***1.6.4 Biarylamide inhibitors*:** both inhibitors of this group (**5, 6**) have a TF/FVIIa IC_{50}= 12-13 nM and **5** has a FVIIa Ki= 6.4 nM [59].

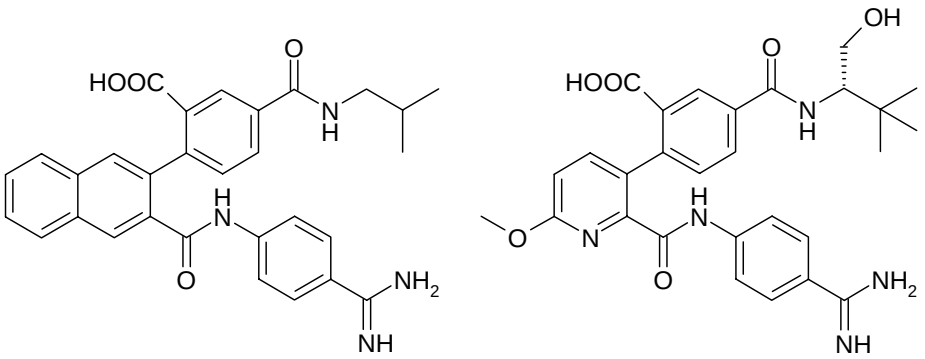

BIARYLAMIDE BASED INHIBITORS

5 **6**

1.6.5 N-(4-Amidinophenyl)-Phenylglycine Derivatives: The acylsulfonamide derivative (**7**) has a FVIIa Ki= 3 nM. Less substituted, more streamlined phenylglycine derivatives have been synthesized. The di-carboxylic acid structure shown (**8**) has a FVIIa Ki = 38.5 nM [59].

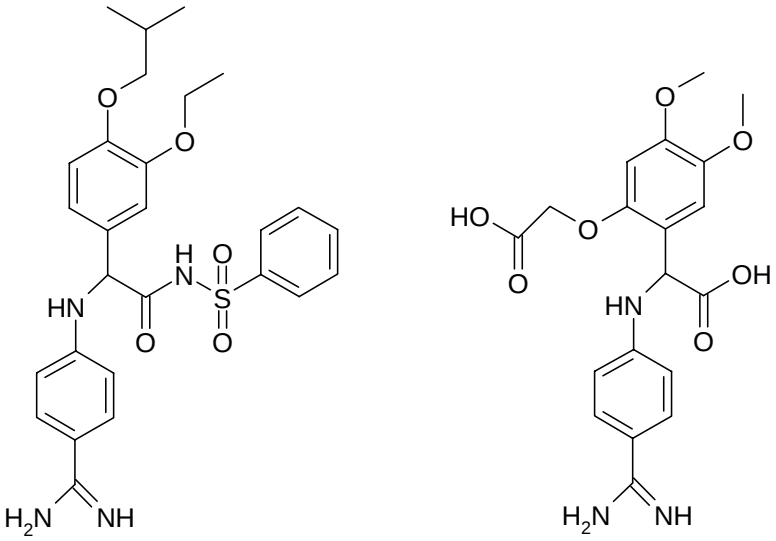

PHENYLGLYCINE BASED INHIBITORS

7 **8**

1.6.6 Pyrazinone based inhibitors: Scientists wanted to make highly selective FVIIa inhibitor that would be efficacious *in vivo* but be superior to FXa and thrombin inhibition in terms of a decreased risk of bleeding. The key to making a selective FVIIa inhibitor is to engage the Asp60 in the S2 pocket, which is unique to FVIIa [63, 64]. The S2 pocket is also more open than that in both thrombin and FXa [63, 64]. The pyrazinone core must contain a 3-amino substitution to retain a hydrogen bond with the backbone of G216. Due to the size and the electronics of the S2 pocket of FVIIa vs. thrombin, it is possible to

insert an electron donating group on the P2 phenyl ring to increase potency and selectivity. The group at the meta position is able to hydrogen bond with the Asp60. The addition of a meta carboxylic acid allows the inhibitor to engage the K192 of FVIIa while simultaneously being repelled by the E192 of thrombin. The final structure (**9**) has a FVIIa IC_{50} = 16 nM with selectivity for FVIIa over thrombin and FXa (>6000 fold) (figure 15) [63, 64]. This compound was eventually used in primates to show that FVIIa inhibition can prevent thrombosis and have a lower risk of bleeding [65].

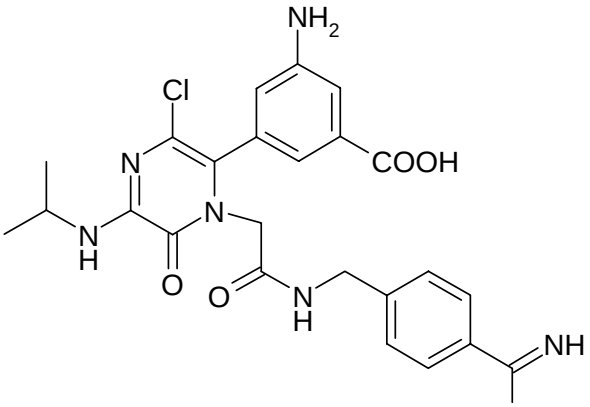

PYRAZINONE BASED INHIBITOR

9

Figure 15. Crystal structure of **9** bound in the active site of TF/VIIa complex at 2.1 Å resolution. Some important side chains of Factor VIIa are shown. The dotted white lines represent hydrogen bonds between the inhibitor and FVIIa. The *m*-amino group makes contacts in the S_2 pocket, while the carboxylic acid group interacts with the ε-amino group of Lys 60A. This image is adapted directly from [64].

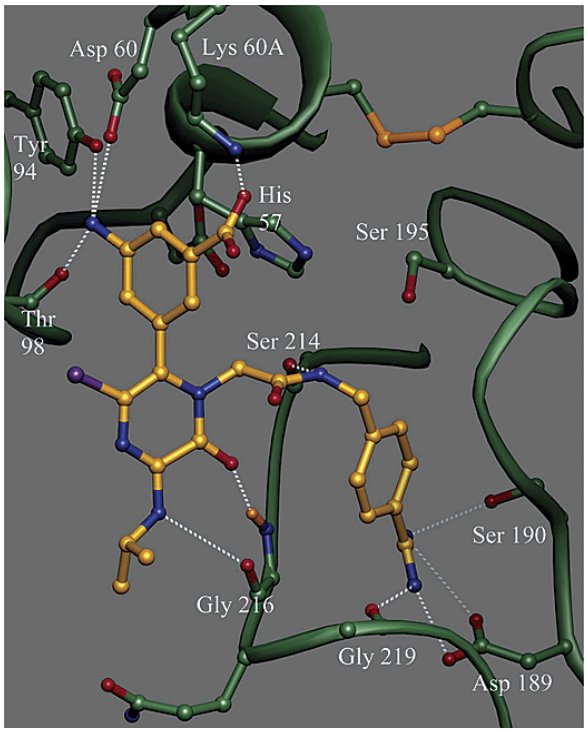

1.6.7 Pyrazinone prodrugs: The best compound in this series contains a basic benzamidine moiety which is associated with undesirable pharmacokinetics, namely poor oral activity. Two prodrugs (**10, 11**) were made of the best pyrazinone [59].

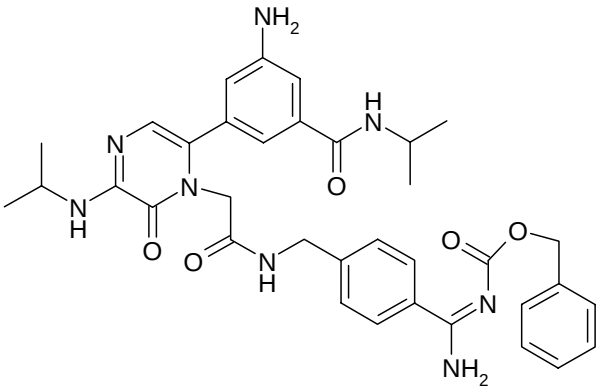

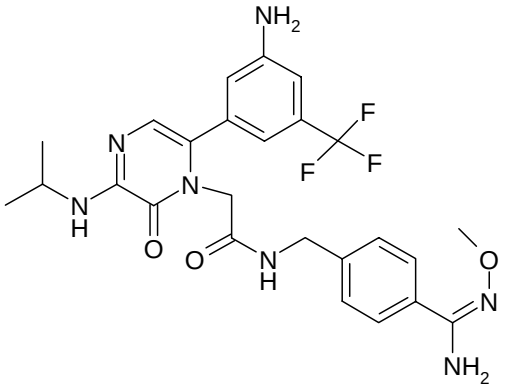

PRODRUGS OF PYRAZINONE BASED INHIBITOR

10 **11**

1.6.8 Pyridinone based inhibitor: By replacing the nitrogen at the 4 position of pyrazinone, you generate pyridinone as your core ring structure [66]. The new compound was less potent (**13**) (IC_{50} = 118 nM) due to loss of hydrogen bonding and van der Waals interactions (figure 16). Further SAR studies led to the development of a compound (**12**) with 84 nM IC_{50} against TF/FVIIa and >700 fold selectivity over thrombin and FXa [59].

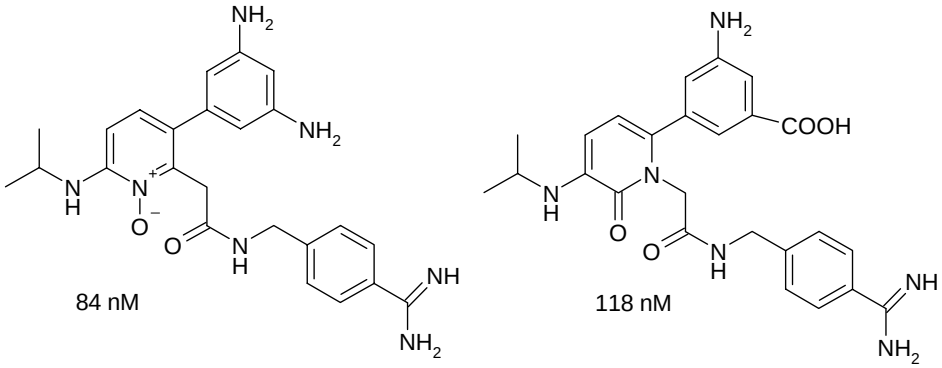

PYRIDINONE BASED INHIBITORS

12 **13**

Figure 16. Crystal structure **13** bound in the active site of TF/VIIa complex at 2.2 Å resolution. Some important amino acids in Factor VIIa are shown. The hydrogen bonds formed by the inhibitor are represented by dotted magenta lines. This image is adapted directly from [66].

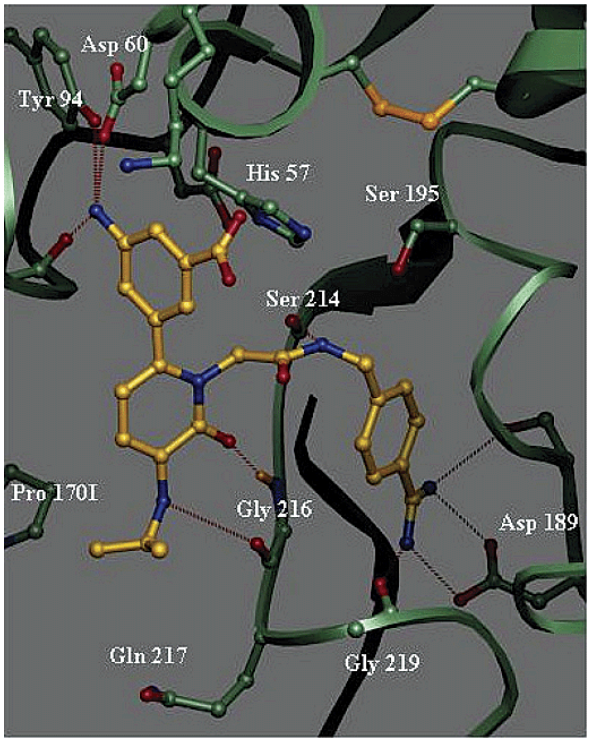

1.6.9 Naphthyl-amidine based compound: This FVIIa inhibitor (**14**) has an IC_{50} = 4 nM [59].

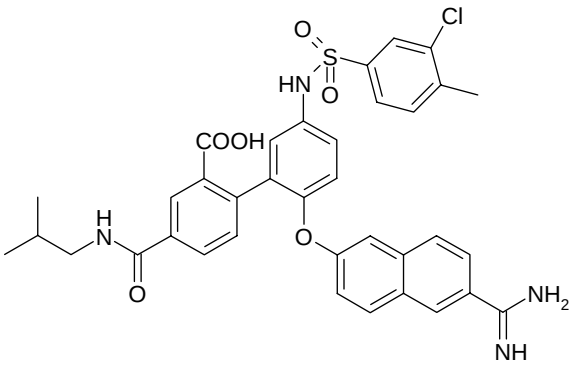

NAPHTHYL-AMIDINE BASED COMPOUND

14

1.6.10 Benzimidazole and Indole amidines: A benzimidazole based compound (**15**) had a Ki= 78 nM, but it was relatively nonspecific (figure 17). Based on modeling studies with FVIIa active site, the benzimidazole ring was exchanged for an indole ring, a carboxylic acid group was added and the amine was switched with a nitro group to design (**16**), which resulted in a Ki of 3 nM and large increase in selectivity [67].

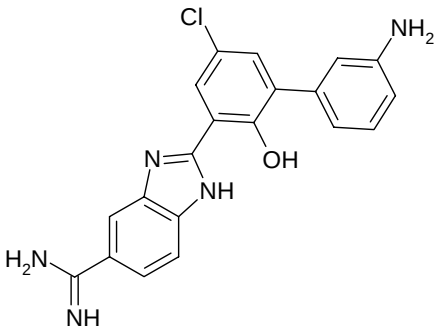

BENZIMIDAZOLE BASED INHIBITOR

15

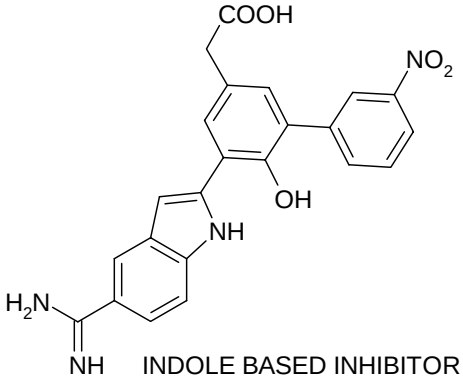

INDOLE BASED INHIBITOR

16

Figure 17. A model of **15** bound in the factor VIIa active site. This image is adapted directly from [67].

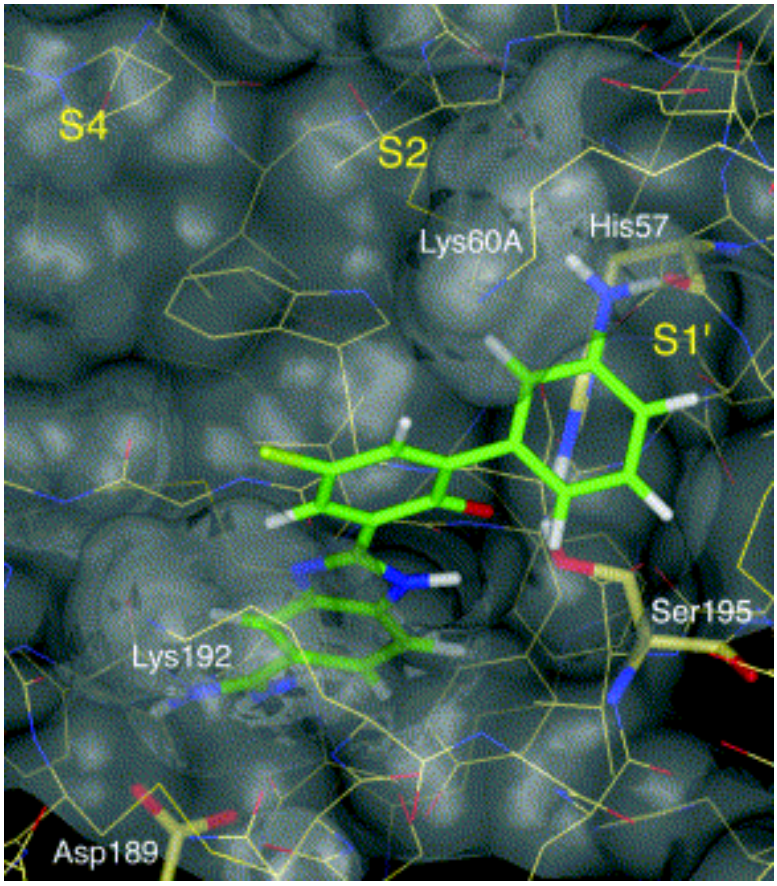

1.6.11 Amidinophenyl Urea inhibitors: The lead compounds were identified from screening. The most potent compound had a Ki = 1.9 nM but minimal selectivity (**17**). Docking studies were performed to understand the orientation of compound **17** in the FVIIa active site. The benzamidine binds in the S1 pocket, the two urea nitrogens interact with Ser195 and the other aromatic ring fits into the S2 pocket. Alpha position methylation and ring substitution decreased potency, but were able to greatly enhance selectivity [68]. Compound **18** has a FVIIa Ki = 23 nM, a thrombin Ki = 16400 nM and a

FXa Ki >10000 nM. Compound **19** has a FVIIa Ki =27 nM, a thrombin Ki >100000 nM and a FXa Ki >10000 nM.

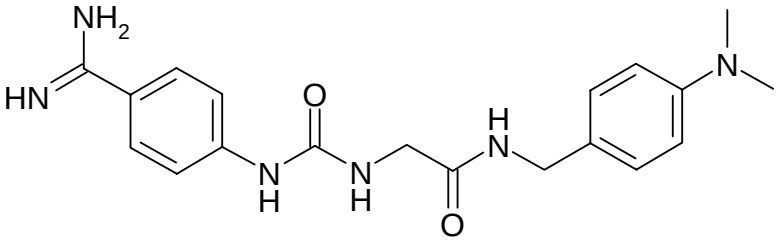

17

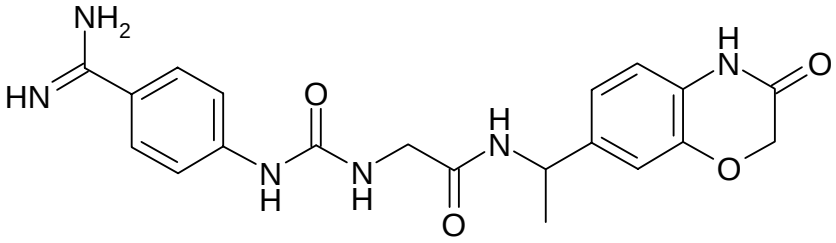

18

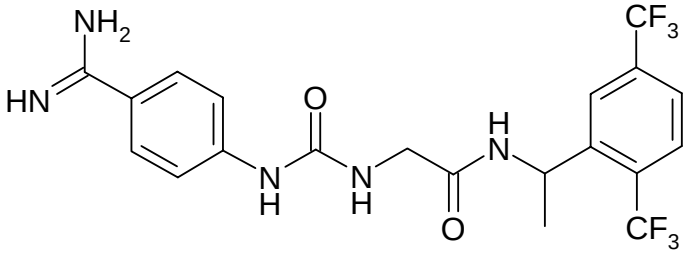

19

AMIDINOPHENYLUREA BASED INHIBITORS

1.6.12 Tifacogin: the recombinant form of TFPI. However, it differs slightly from endogenous TFPI by one additional alanine at the N terminus and the recombinant form is not glycosylated. Tifacogin (and TFPI) have a two step binding process. First, tifacogin binds to and inactivates FXa by binding to the catalytic domain. Then the TFPI/FXa complex inhibits TF-bound FVIIa [69]. Although it was believed to have potential therapeutic benefit in the treatment of sepsis [69], it has been shown not to be efficacious in sepsis [22].

1.6.13 Recombinant nematode anticoagulant protein c2 (rNAPc2): an 85 amino acid polypeptide produced by the dog hookworm, *Ancylostoma caninum*. The recombinant form is expressed in the yeast, *Pichia pastoria* [70]. NAPc2 requires two binding steps to mediate its mechanism of inhibition. NAPc2 initially binds to a noncatalytic site on factor X or factor Xa [71]. Factor Xa or factor X can be considered cofactors that are an absolute requirement before NAPc2 can bind to the FVIIa/TF complex [70]. Once bound to factor X(a), NAPc2 will bind to TF/FVIIa and form a quaternary complex [71]. The NAPc2/FX(a) complex inhibits FVIIa in the FVIIa/TF complex. This mechanism is like TFPI but different in an important way. TFPI must utilize activated factor X (FXa) because it needs to access the active site [71]. Since NAPc2 can bind both FXa and FX, this implies binding to another region, like an exosite or an extended binding site [71]. Interestingly, when FXa is part of the quaternary complex, it can still cleave small peptidyl substrates, but not prothrombin [72]. The binding of the FX(a)/NAPc2 complex to the TF/FVIIa complex is initially mediated by the interaction of the (Gla)-domain of FX and

the cell membrane [71]. The reactive portion of the rNAPc2 inserts into the catalytic site of FVIIa. This forms a reversible, competitive complex with a slow dissociation rate [71]. NAPc2 prolongs PT at concentrations that do not prolong APTT which is indicative of an anticoagulant that affects the extrinsic pathway while sparing the intrinsic pathway [73]. However, APTT is prolonged at higher concentrations because rNAPc2 has a FXa Kd= 780 pM, which sterically restricts the formation of the prothrombinase complex (Ki= 5 nM) [72]. The half-life of rNAPc2 is >50 hours, which causes concern about overdosing a patient [74]. To counteract this problem, recombinant factor VIIa has been explored as an antidote [75].

1.6.14 E-76: an 18 amino acid peptide (Ac-ALCDDPRVDRWYCQFVEG-NH_2). The precursor for E-76, E-56, was discovered using phage display of naive peptide libraries. E-76 was generated by creating partially randomized phage library based on the E-56 structure. The IC_{50} values for E-76 inhibition of factor X activation and inhibition of small molecule substrates was 1.1 nM and 7.4-9.7 nM, respectively. Like other FVIIa inhibitors, E-76 selectively prolongs PT without altering APTT. Both E-56 and E-76 bind to an allosteric site on FVIIa and noncompetitively inhibit the FVIIa active site, however the binding is Ca^{+2} dependent. E-76 has a Kd= 8.5 nM for both FVIIa and the FVIIa/TF complex, while no binding was detected for TF alone or numerous other serine proteases. This indicates a strong selectivity for FVIIa and no preference for the presence or absence of TF. This selectivity is likely achieved because serine protease active sites tend to be very similar while serine protease exosites are inherently unique because they are

responsible for determining substrate recognition and specificity. Based on crystallography and mutagenesis studies, the E-peptide exosite is described as a trough that is separate from, but close to the active site (figure 18). One of the walls that make up the exosite trough contains the Ca^{+2} binding site. This explains the Ca^{+2} requirement for E-peptide binding and inhibition. The hydrophobic face of E-76 makes contact with FVIIa while the helix located at the N-terminus interacts with the Ca^{+2} binding site. E-76 causes a conformational change in the 140s activation loop of FVIIa. This loop is involved in FX recognition and it is also located closely to the active site. It is thought that E-76 binding can inhibit FX activation by sterically impeding FX binding and by disrupting the oxyanion hole that is present in the FVIIa active site. This has been described as an allosteric "switch" mechanism of inhibition mediated by the 140s activation loop. This represents completely novel mechanism of action for the design of direct FVIIa inhibitors [76].

1.6.15 A-183 has the primary sequence EEWEVLCWTWETCER and contains one disulfide bond [77]. A-183 is a peptide based inhibitor of FVIIa that binds to a novel exosite near the active site (figure 18). This binding site has not previously been described in FVIIa or any serine protease as a substrate recognition site or an inhibitory exosite. A-183 was discovered using a peptide phage library much like E-76. This new exosite is different from the E-76 exosite. Specifically, the novel exosite is composed of the 60s loop and the C-terminus, with Trp61 and Leu251 being critical for binding. A-183 prolongs PT but not APTT, demonstrating its specificity for TF dependent clotting. The

dissociation constants for A-183 binding to FVII and FVIIa were 1.4 ± 0.1 and 2.8 ± 0.2, respectively. In the presence of tissue factor, the Kd values for TF/FVII and TF/FVIIa were 10.0 ± 1.2 and 5.5 ± 0.5, respectively. Competitive binding studies with E-76 yielded a TF/FVIIa + E-76 Kd= 5.5 ± 0.5, indicating that the A-183 and E-76 binding sites are distinct and noncontiguous. A-183 is specific for FVIIa because no binding was observed for the other nine serine proteases [78]. A-183 potently inhibits FX and FIX activation by TF/FVIIa (IC_{50}= 1.6 ± 1.2 and 3.5 ± 0.3, respectively). The Ki for FX activation is 200 pM, but its maximal inhibition of FX activation is 78 ± 3%. This incomplete inhibition of TF/FVIIa is considered desirable because it allows for the development of novel anticoagulants with an increased therapeutic window [77].

Figure 18. The various FVIIa binding sites. The distinct regions of the peptide binding exosites for A-183 (green) and E-76 (blue) are shown for FVIIa. The active site region is covalently modified with D-Phe-L-Phe-L-Arg-chloromethyl ketone (red). This image is adapted directly from [77].

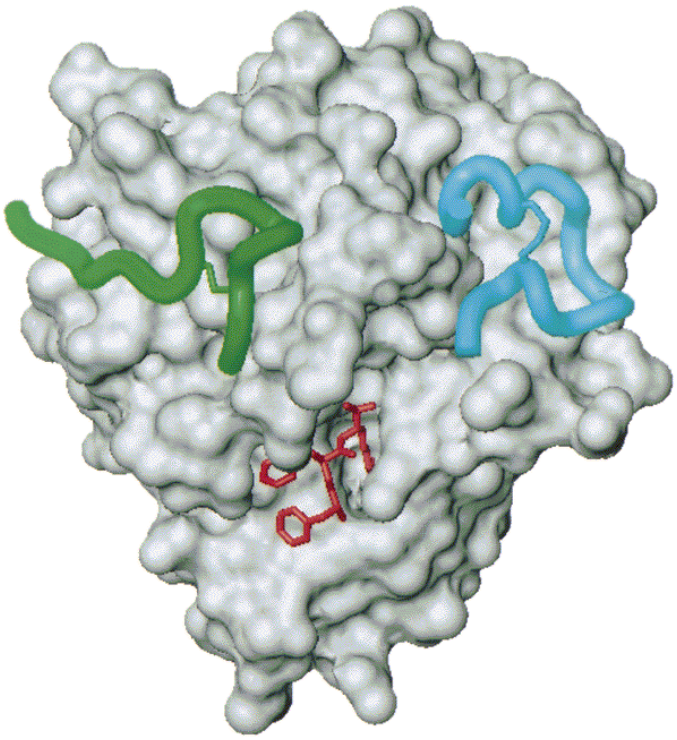

1.6.16 Inactivated FVIIa (FVIIai or FFR-FVIIa): This is a recombinant form of human FVIIa in which the active site has been covalently inactivated by the inhibitor Phe-Phe-Arg chloromethyl ketone [60]. FVIIai competes with endogenous FVIIa for the opportunity to bind with tissue factor [60].

1.6.17 Anti-TF antibodies: a monoclonal antibody that directed against an epitope that is present on both FVII and FVIIa (Corsevin M^{TM}) [60].

1.7 Inhibitors of propagation of coagulation

1.7.1 Mechanism of Action

These molecules block FIXa, FXa, or their cofactors FVIIIa or FVa, respectively. This results in a down regulation of thrombin production and a slowing of the FXa mediated feed back activation loops that result in prothrombinase complex formation as well as prothrombin activation. FXa inhibitors can influence coagulation without affecting platelet function, which is believed to decrease inappropriate bleeding side effects [61].

Direct FXa inhibitors bind to the active site. Unlike the heparin: AT complex, direct FXa inhibitors inhibit both free FXa and platelet bound FXa, which is part of the prothrombinase complex [21]. This is theorized to make them superior to indirect inhibitors. Many of the currently reported non-peptide FXa inhibitors have a dibasic functionality, which limits their oral bioavailability, but it has been shown that less basic inhibitors are also active [13].

1.7.2 Factor Xa active site

The S2 pocket is considered to be blocked by Y99 and is believed to mediate the preference of FXa for Gly substrates [79]. However, opposite the S2 is a cleft, which has an architecture that is considered specific to FXa, and is composed of E147, Q192, G218, C191 and C220 [79]. The cleft has been termed an “ester pocket” because it readily

accommodates such groups in inhibitor co-crystallization experiments. The S1 pocket contains the catalytic triad and has similar geometry to the other serine proteases and there are numerous opportunities for hydrophobic interactions as well as ionic and hydrogen bonding. Since the S1 pocket is not exclusively driven by electrostatic interactions, it is possible to use less basic, more hydrophobic moieties as inhibitors. This is important because it makes the design of orally active inhibitors possible without the use of a prodrug strategy. Compared with trypsin, the S1 pocket does contain differences that can lead to selectivity. Trypsin has a Ser 190, while FXa has an Ala at that position. This causes an enlargement of the S1 pocket in FXa. S4 pocket in FXa is a deep hydrophobic groove composed of Y99, F174 and W215 [79]. Trypsin has a different S4 pocket, which is composed of L99, Q175 and W215. These differences make the FXa groove deeper and more aromatic in nature, which is conducive for π stacking interactions with potential inhibitors. Based on experimental evidence, it has been shown that differences in the S4 pocket are more important than the S1 pocket for inhibitor design and selectivity [79]. However, both contribute significantly. Asp189 ionic interactions are possible in the S1 pocket, but not absolutely required. More important are hydrogen bonding with the carbonyl and backbone amide of G219 and hydrophobic interactions with the top of the S1 pocket. Aromatic interactions in the S4 pocket are paramount [79].

Figure 19. The structure of FXa active site. The active site residues and other key residues are displayed for reference. This image was created from the PDB file 1ezq using sybyl 7.2

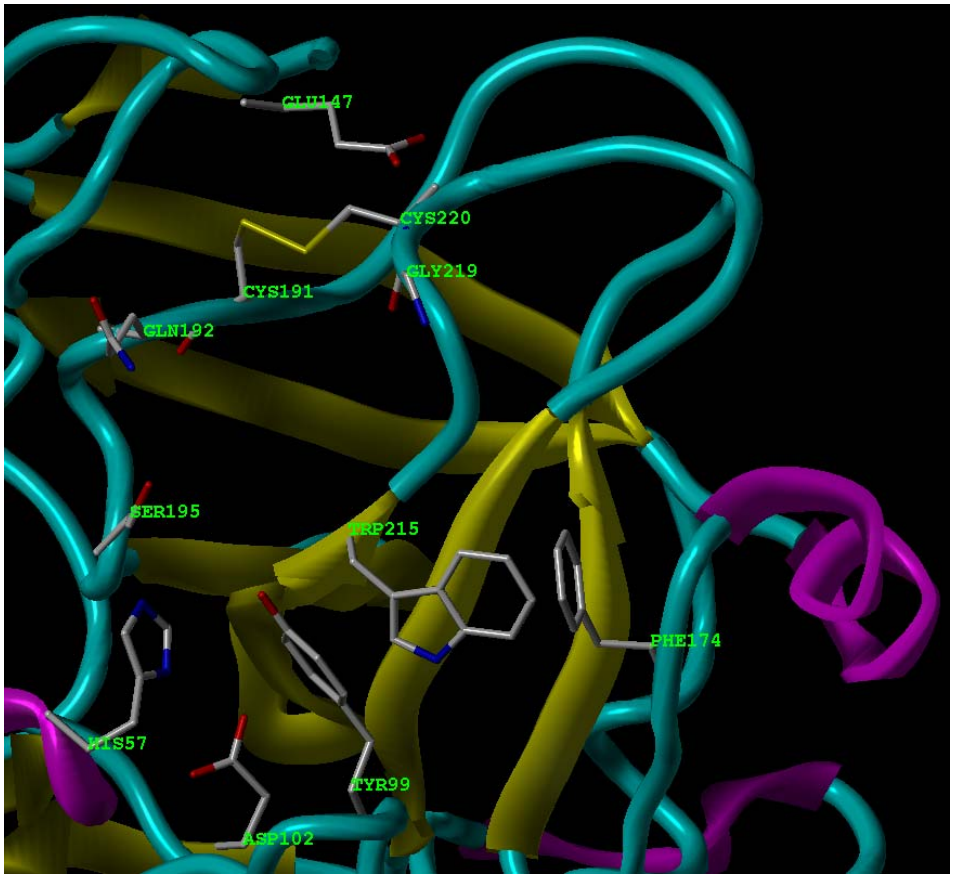

1.7.3 Benzamidine based factor Xa inhibitors

1.7.3.1 3-amidobenzyl derivatives: Although these compounds are not particularly potent (Ki ~5 μM), they are historically important because they showed for the first time that direct FXa inhibition could exhibit an anticoagulant effect [80]. These molecules contain the 3-amidobenzyl group as shown in **20**.

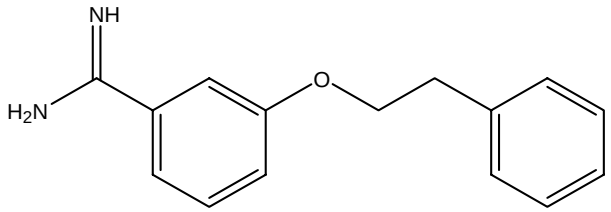

3-AMIDINOBENZYL DERVIVATIVE

20

1.7.3.2 KFA-1411: Ki = 1.7 nM and it has a 15,000-fold selective over thrombin, 3600-fold over trypsin, 80-fold selective over kallikrein and plasmin [81]. KFA-1411 is a closely related analogue of KFA-1982 and its prodrug KFA-1892, which are under further development and their structure has not yet been disclosed.

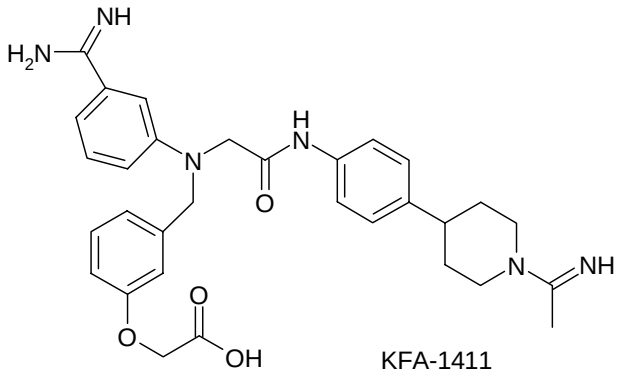

KFA-1411

21

1.7.3.3 β-amidoesters: precursors to **FXV673**, the most potent FXa inhibitor in this series. Compound **22**, has a Ki of 37 nM as a racemic mixture. The R,R stereoisomer has a Ki= 21 nM, whereas the S,S stereoisomer has a Ki= 100 nM. The benzamidine binds in the S1 pocket and the biphenyl groups bind in the S4 pocket [82]. Compound **23** has the ethyl phenyl replaced by a smaller methyl group and that produces a Ki= 5.3 nM [83]. Several different substitutions were tried on the biphenyl ring and compound **24** was observed to be both potent (FXa Ki= 1.3) and selective (thrombin Ki >4000 nM, trypsin Ki= 185 nM). Compound **25** was more potent than **24** but less selective (FXa Ki= 0.9, thrombin Ki >2920 nM, trypsin Ki= 95 nM) [84]. Compound **25** was designed to form an ionic interaction with the S4 pocket [84]. Compound **26** shows that productive S4 interactions can be achieved through hydrogen bonding (FXa Ki= 69 nM). Compound **26** has a thrombin Ki= 3950 nM and a trypsin Ki= 90 nM. The S4 pocket can also bind heteroaromatic rings [85]. **Otamixaban** (**27**) (**FXV673**, **RPR130673**) was shown to be very potent (Ki= 0.4 nM) and selective (thrombin Ki= 4000 nM, trypsin Ki= 300 nM) [82]. The binding is described as fast, tight and reversible with a >1000-fold selectivity over thrombin, activated protein C, plasmin and tissue plasminogen activator [82]. The IC_{50} = 1.38 nM against the prothrombinase complex [82]. The benzamidine group forms a hydrogen bond with the carbonyl of Gly 218 and forms ionic interaction with Asp189 (figure 20) [85]. There is hydrogen bonding between the amide linkage and amine of G218. The N-oxidepyridylphenyl group interacts with the S4 pocket by making

hydrophobic interactions [85]. It also forms a hydrogen bond between its N-oxide and a water molecule that interacts with the FXa backbone [85].

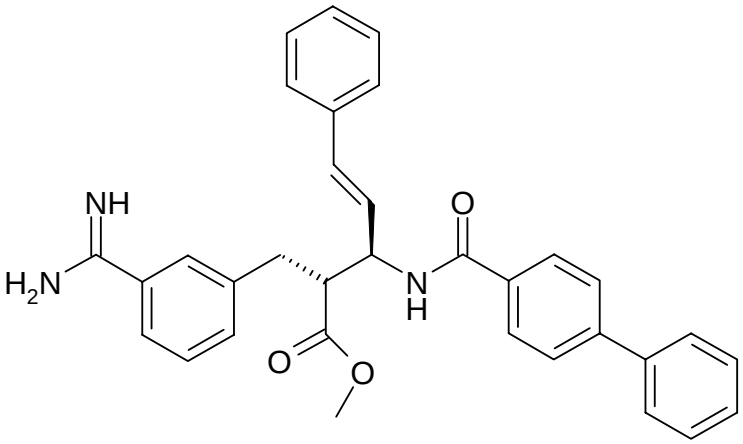

22

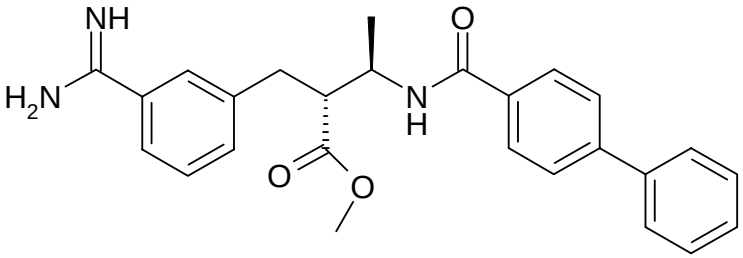

23

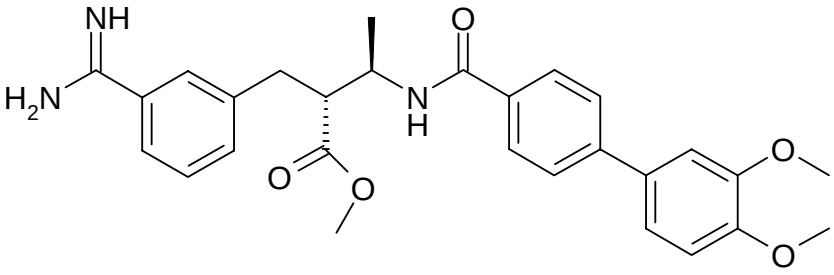

24

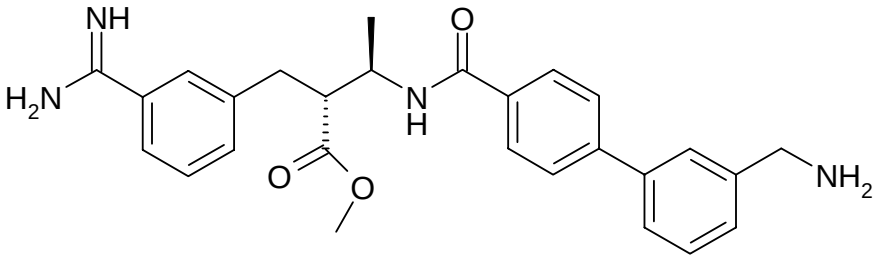

25

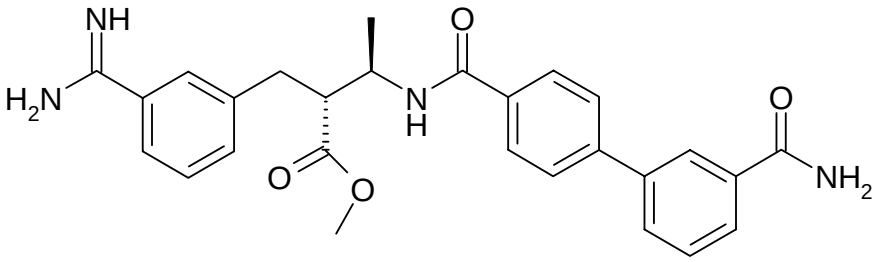

26

BETA-AMIDOESTERS (PRECURSORS TO FXV673)

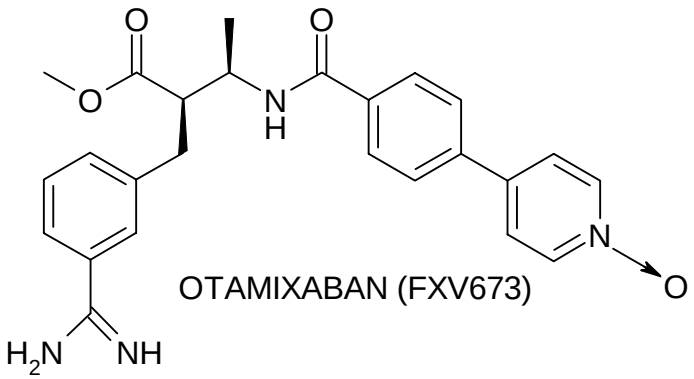

OTAMIXABAN (FXV673)

27

Figure 20. Otamixaban bound to the FXa active site. The FXa carbon atoms are shown in green, while the otamixaban carbon atoms are shown in orange. The large red spheres represent water molecules and the dashed white lines indicate various interactions. This image is adapted directly from [85].

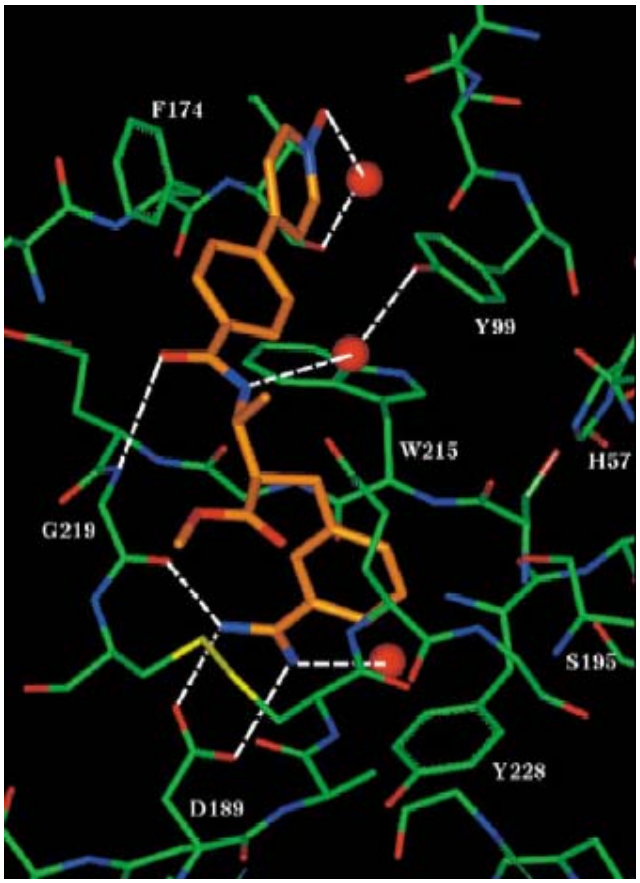

1.7.4 Hydroxylated benzamidine based factor Xa inhibitors

1.7.4.1 **ZK-807834** (**28**) is a selective FXa inhibitor (527 Da) possessing a Ki = 0.11 nM with >2500 fold selectivity against other serine proteases. ZK-807834 makes contacts with Asp189 and Ser195, as well as aromatic ring-stacking interactions with Trp215 (figures 21 and 22) [86, 87].

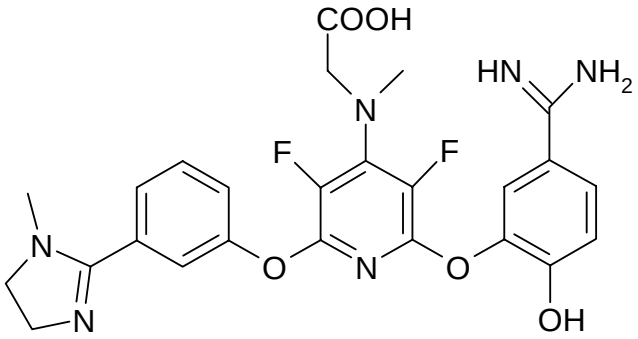

ZK-807834

28

Figure 21. Structure of **ZK-807834** demonstrating its most important interactions with factor Xa. Close contacts are indicated by thick black lines and hydrogen bonds are illustrated with dotted lines. This image is adapted directly from [87].

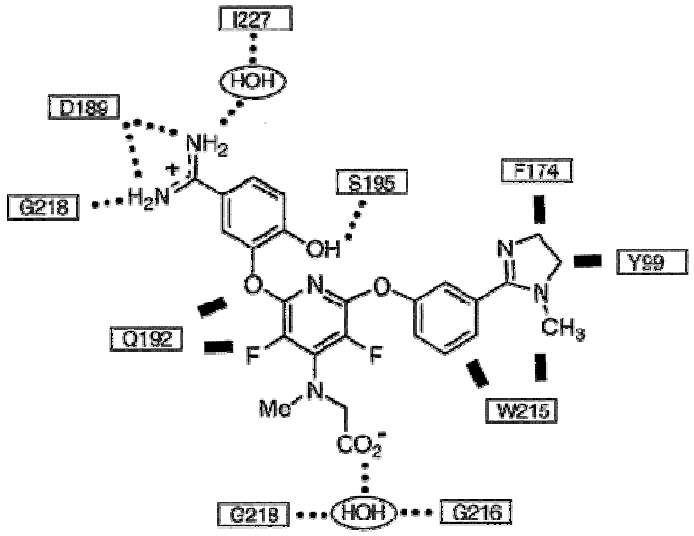

Figure 22. ZK-807834 bound in the factor Xa active site. The carbon atoms of the inhibitor are colored green. Asp189 at the bottom of the S1 pocket and Glu97 in the S4 pocket are light blue. The catalytic triad Ser195, His57, and Asp102 are orange. Residues that make up the S4 pocket (Tyr99, Phe174 and Trp215) are magenta, while hydrogen bonds are shown as dotted lines. This image is adapted directly from [87].

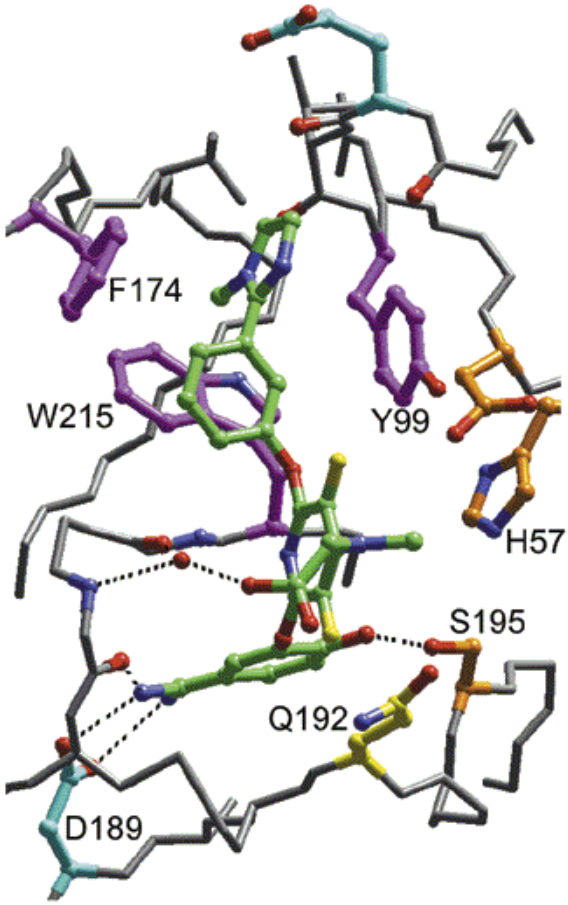

1.7.4.2 Hydroxylated amidopropylbenzamidines and Hydroxylated allyl-benzamidines: Compounds **29-34**. Addition of a hydroxyl group to compound **30** increases the potency from 1000 nM (**29**) to 88 nM (**30**) [88]. The addition of a

carboxyamide (**31**) increased the potency to 7 nM. Hydroxylated allyl-benzamidines are restricted analogues of the hydroxylated amidopropylbenzamidines. These structures gained some potency over their saturated counterparts. Compound **32** has a Ki = 51 nM compared with a Ki = 88 nM for the saturated analogue above in the hydroxylated amidopropylbenzamidine series (**30**). The most potent derivative was compound **34** with a Ki= 0.75 nM, while compound **33** had a respectable FXa Ki = 5 nM [88].

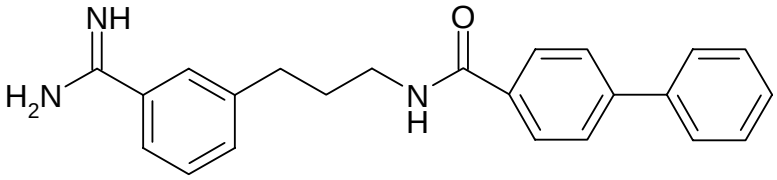

29

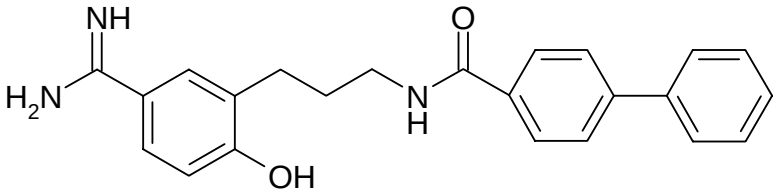

30

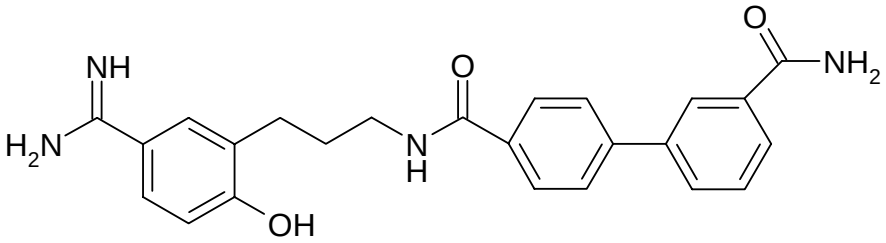

31

HYDROXYLATED AMIDOPROPYLBENZAMIDINES

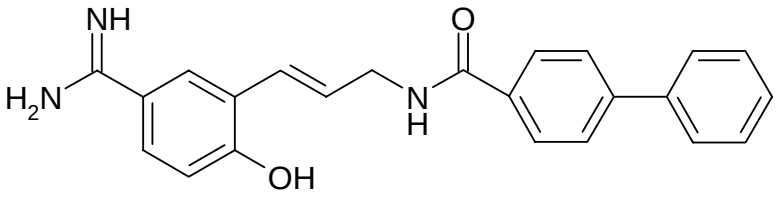

32

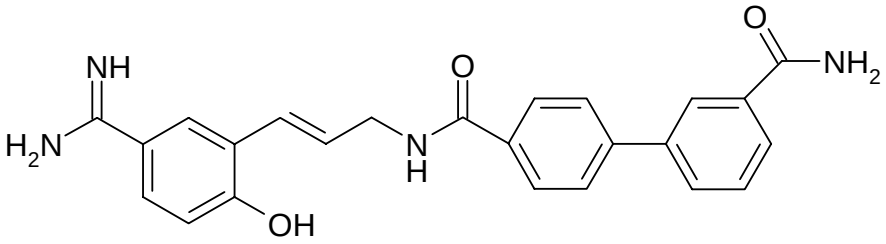

33

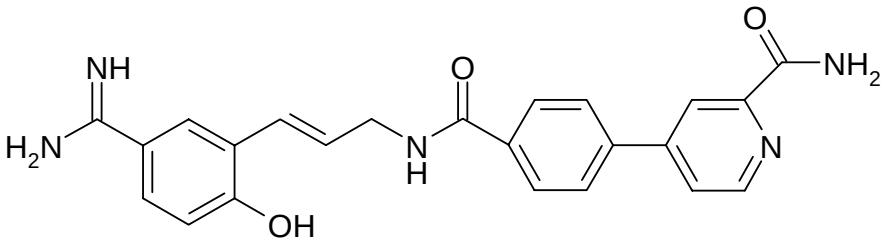

34

HYDROXYLATED ALLYL-BENZAMIDINES

1.7.5 Naphthyl-amidine based factor Xa inhibitors

1.7.5.1 DX-9065a is a 571 Da, reversible, non-peptidic Arg derivative (peptidomimetic) that targets the active site of FXa [82]. Its selectivity for FXa over thrombin is very good (Ki= 41 nM vs. >2000 μM) [81]. It inhibits free FXa, FXa in the prothrombinase complex, clot bound FXa and clot bound prothrombinase complex [89]. The naphthamidine portion binds in the S1 pocket by forming a salt bridge with Asp189.

The pyrrolidine ring binds to the S4 aryl binding site [90]. Thrombin Glu192 has a repulsive electrostatic interaction with the carbonyl group of the inhibitor, which provides the basis for selectivity [91]. Because of its three charged groups, it has poor pharmacokinetic properties [91]. It has also been determined to have undesirable cardiovascular side effects [91]. Because of these properties, DX-9065a is a parenteral agent. An oral form of DX-9065a, DU-176b, has been created but its structure remains unknown [55].

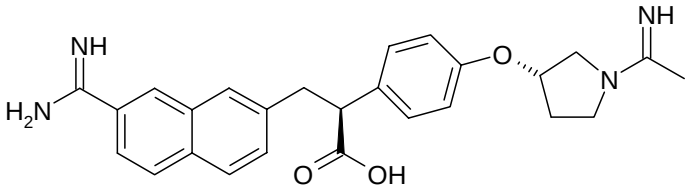

DX-9065a

35

1.7.5.2 YM-60828 (**36**) is a peptidomimetic, N-((7-amidino-2-napthyl)methyl)aniline derivative, which is selective for FXa. Lipophilic substitutions are detrimental to activity, while hydrophilic substitutions enhanced the anticoagulant effect in the prothrombin time assay. **YM-60828** is a sulphamoyelacetic derivative with a Ki = 2.3 nM. The **YM-60828** IC_{50} value for thrombin and trypsin is >100,000 nM and 216 nM, respectively [92].

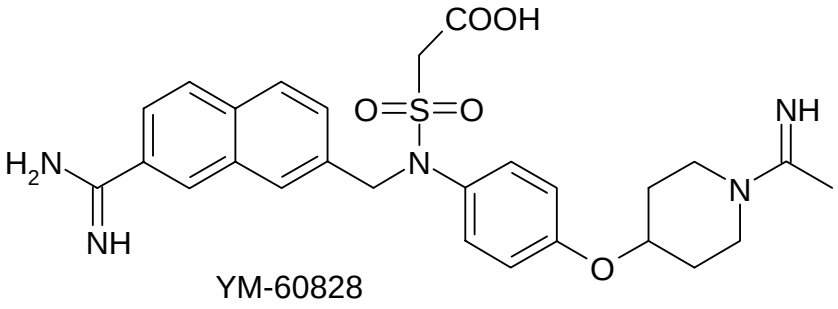

36

1.7.5.3 Benzoxazinone derivatives (**37**) is a lead compound that has been described by Millennium Pharmaceuticals, is potent against FXa (Ki= 0.7 nM) [55].

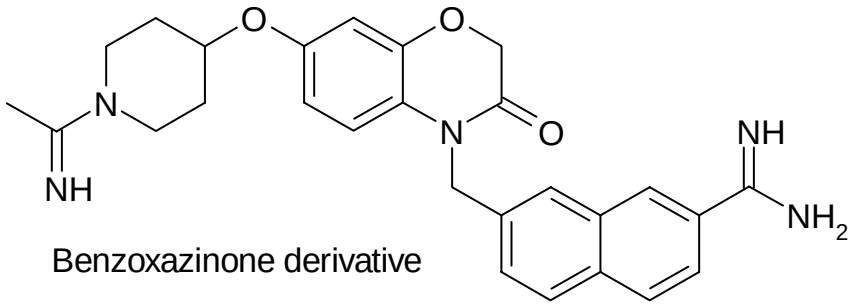

37

1.7.6 Non-amidine based factor Xa inhibitors

1.7.6.1 Rivaroxaban (BAY 59-7939) (38) is an orally available, small molecule that is a direct and selective competitive FXa inhibitor [55]. It is interesting because it does not contain an amidine group to target the enzymes active site. The FXa Ki= 0.4 nM and rivaroxaban exhibits >10,000-fold selectivity over other serine proteases. Rivaroxaban can potently inhibit the prothrombinase complex (IC_{50}= 2.1 nM) and FXa in human plasma (IC_{50}= 21 nM). Rivaroxaban is capable of doubling PT and APTT at concentrations of 0.23 μM and 0.69 μM, respectively [55].

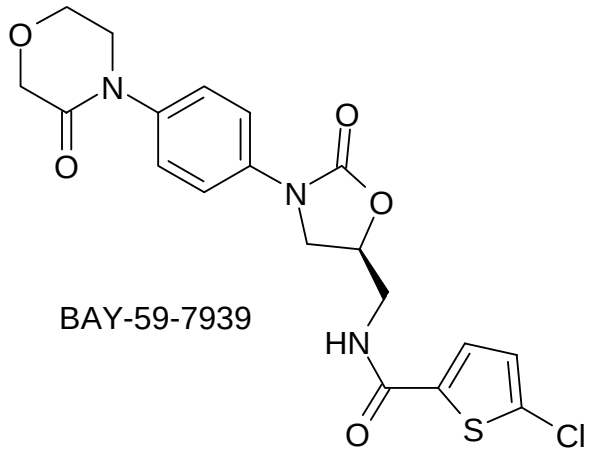

BAY-59-7939

38

1.7.6.2 **M55113**: (**39**) a potent and highly selective inhibitor of FXa (Ki = 60 nM). **39** is considered to be a peptidomimetic with structural similarities to DX-9065a (**35**) and YM-60828 (**36**) [13].

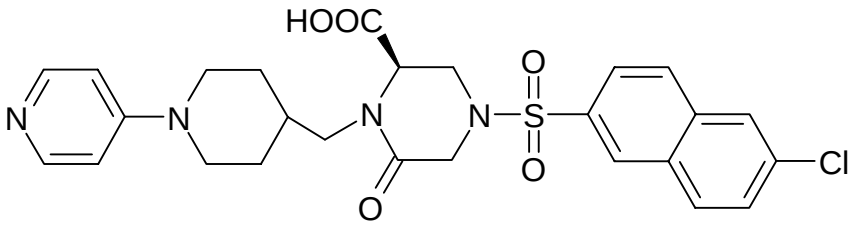

M55113

39

1.7.6.3 **LY-517717**: (**40**) This indole based compound represents a lead structure for FXa inhibitors. It is orally available, potent (Ki= 5 nM) and has a 1000-fold selectivity over the other serine proteases [93].

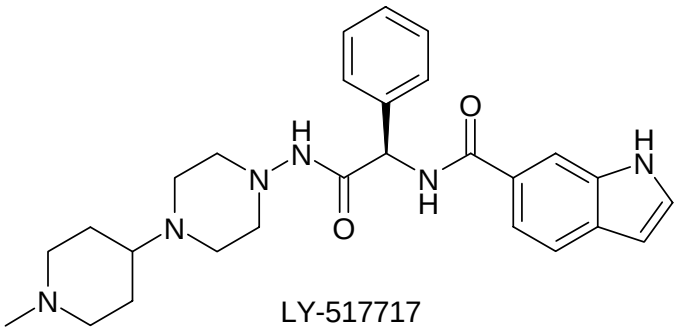

LY-517717

40

1.7.7 Non-amidine based factor Xa inhibitors developed from amidine based inhibitors

1.7.7.1 **DPC-423** (**43**) is a biphenylamine containing amide. It is an orally active, competitive, noncovalent inhibitor of FXa with a Ki= 0.15 nM [94]. The earlier compounds that lead to this structure were isoazolines derivatives with benzamidine moieties for basicity. **SF303** (**41**) is a representative structure [95]. The isoazoline core was replaced with a pyrazole to create **SN-429** (**42**) (FXa Ki= 13 pM) [94]. Modifications to **SN-429 (42**), which included poly-fluorination and the replacement of the highly basic benzamidine with benzylamine, resulted in **DPC-423** (**43**) [94]. It is considered to be selective over the other coagulation proteases but not selective for trypsin and kallikrein with Ki = ~60 nM for both enzymes [94]. **DPC-602** (**44**) is an analogue of the 3-(aminomethyl)phenylpyrazole DPC423, which was created to improve the selectivity of FXa inhibition (figure 23). By creating the 2-(aminomethyl)phenylpyrazole (**DPC-602**), a >1000-fold selectivity over the other serine proteases [96]. **Razaxban (DPC-906)** (**45**) is a synthetic, non-peptide oral FXa inhibitor. It has a molecular mass of 564.92 Da and FXa Ki= 0.19 nM [97]. This compound is considered the next generation compared to **DPC-602** (**44**) and **DPC-423** (**43**). The benzylamine has been replaced with an aminobenzisoxazole to given better selectivity over trypsin (Ki >10,000) and kallikrein (Ki >2300) while still maintaining selectivity over the coagulation proteases [97]. Modifications to the biphenylamine were also made by replacing the distal phenyl ring with a substituted imidazole.

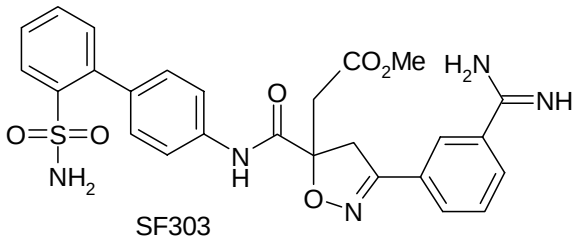

SF303

41

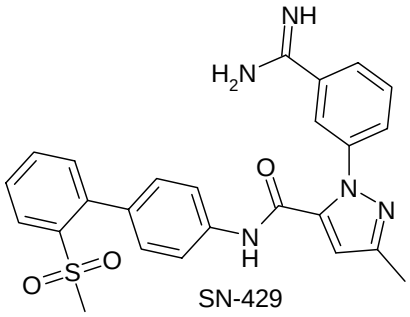

SN-429

42

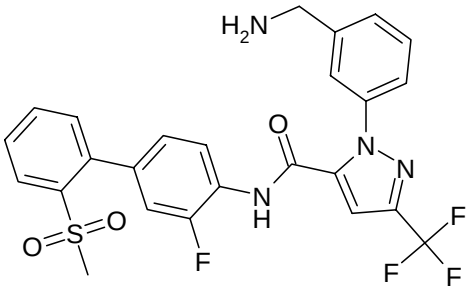

DPC-423

43

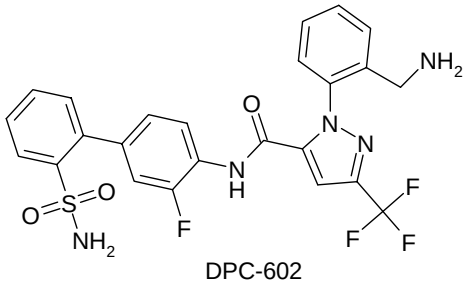

DPC-602

44

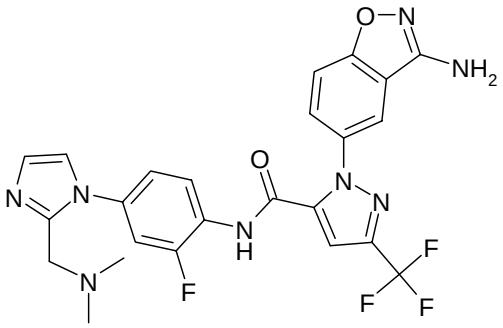

RAZAXABAN (DPC-906)

45

Figure 23. X-ray structure of **45** (razaxaban) in the factor Xa active site. The amino group formed hydrogen bonds with Asp189 (2.7 Å) and the carbonyl group of Gly218 (3.5 Å). The pyrazole N-2 nitrogen interacts with the backbone NH of Gln192 (3.4 Å) and the 5-carboxamide carbonyl interacts with the NH of Gly216 (3.0 Å). The N-3 nitrogen of the imidazole P_4 group forms a direct hydrogen bond (3.6 Å) and indirect hydrogen bonds through a water molecule (3.0 and 3.1 Å) with Glu97. This image is adapted directly from [97].

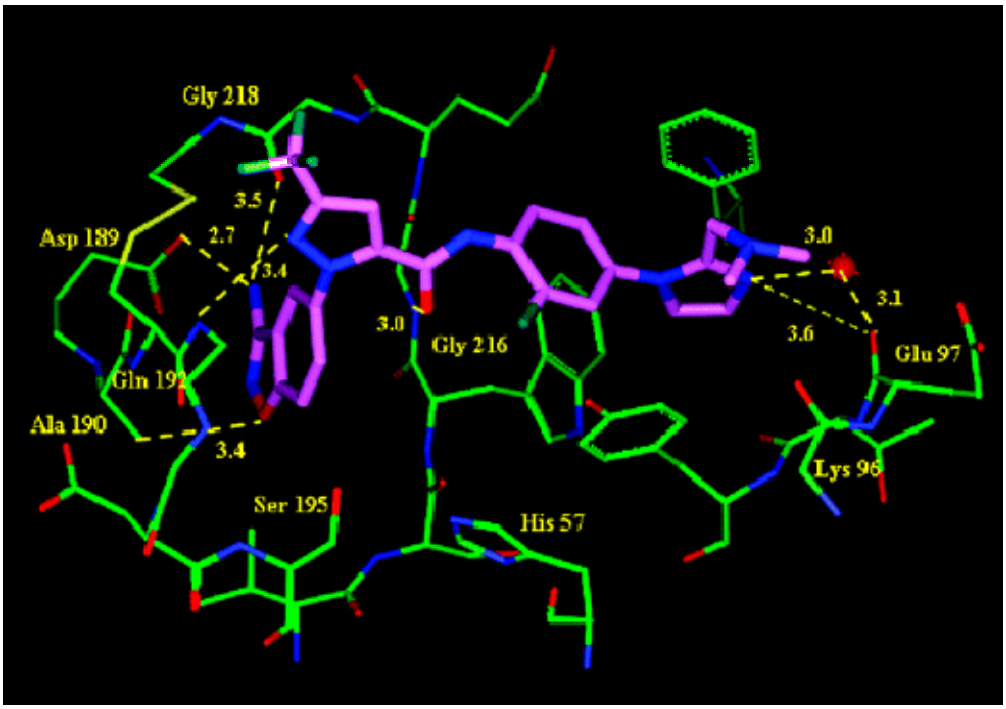

1.7.7.2 3-Sulfonamido Pyrrolidinones: The general structure of this class of molecules is as shown in figure 24. Several substitutions were made on the naphthalene ring. These substitutions were done to probe the S4 pocket to increase activity. The best compound had a 7 position methoxy group (compound **46,** Ki= 47 nM) [82]. Using compound **46**, the benzamidine was changed by incorporating heteroaromatic benzamidines to find improved activity. The 2,4 thiophene amidine (**47**) was observed to increase potency to Ki= 11 nM [82]. Methylation of the sulfonamide nitrogen atom increase potency by ~2-fold [82]. These SAR findings were combined to create compound **48** (RPR120844) [98]. It has a FXa Ki = 7 nM and good selectivity over thrombin (140-fold), trypsin (76-fold), plasmin (630-fold), t-PA (>1000-fold) and aPC (340-fold). A hydroxylated benzamidine was used to create a compound **49** with increased potency (FXa Ki = 3 nM) and good selectivity over thrombin (Ki = 206 nM), trypsin (Ki = 305 nM) [82]. Benzothiophenes were substituted in place of the naphthalene rings and shown to improve potency relative to unsubstituted napthalene. Chloro substitutions on the benzothiophene ring further improved activity. Compound **50** which is a 6-chlorobenzothiophene was the most active chloro substituted compound with a FXa Ki = 4 nM [82]. Compound **50** selectivity is excellent (thrombin Ki= 1200 nM and trypsin Ki= 1200 nM).

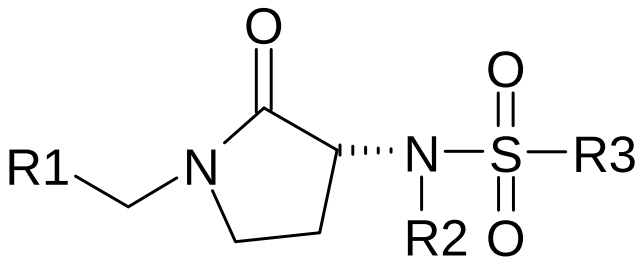

Figure 24. General structure of 3-Sulfonamido Pyrrolidinones

Other thiophenes were examined for activity. Compound **51** contained a 3-pyridylthiophene combined with a hydroxylated benzamidine. It was both potent and selective for FXa (Ki = 2 nM) (Thrombin Ki = 2800 nM and Trypsin Ki= 2900 nM) [99]. Thienopyridines were also investigated for their ability to probe the S4 pocket. The most potent of this series was compound **52** (Ki= 0.7 nM). Compound **51** was further studied (*RPR130737)* and determined to be a competitive, fast binding, reversible FXa inhibitor [99].

The benzamidine has a pKa of ~11 and that basicity limits its permeability, ultimately limiting its oral bioavailability. By cyclizing the amidine into an aminoisoquinolone, the pKa drops to ~7. When thienopyridine is added to the scaffold containing a less basic moiety, the Ki= 22 nM (**53**) [82]. When the thienopyridine is retained but the aminoisoquinolone is replaced with a 6-azaindole (**54**), a Ki= 18 nM is achieved [100].

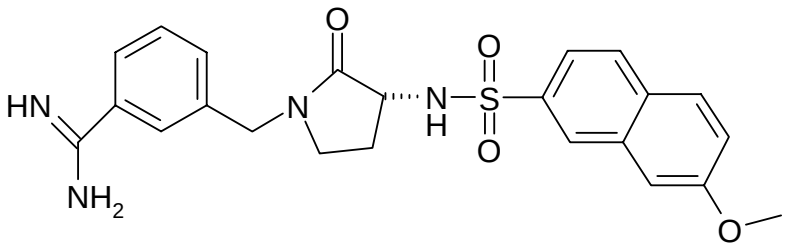

46

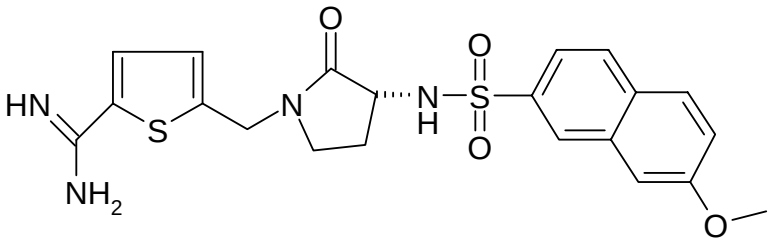

47

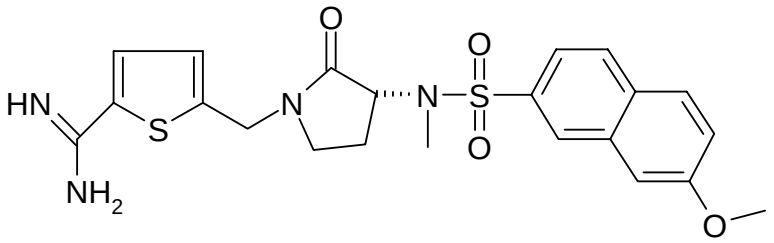

48

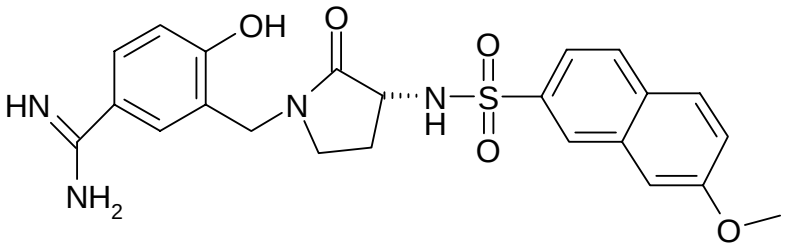

49

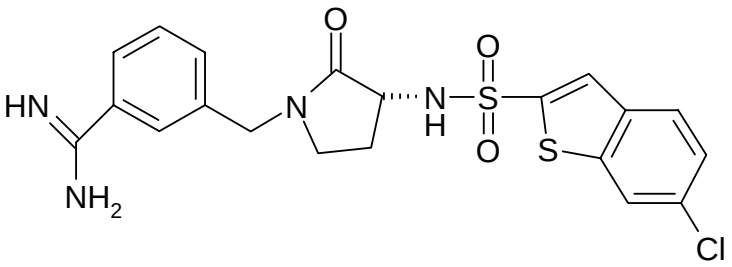

50

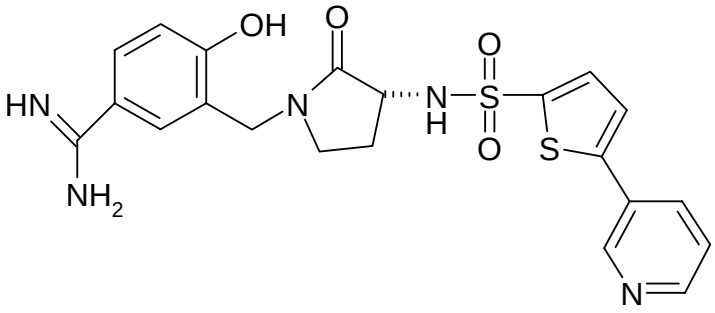

51

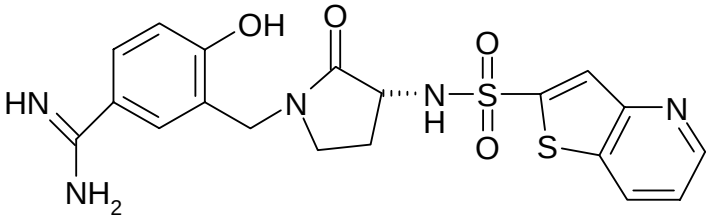

52

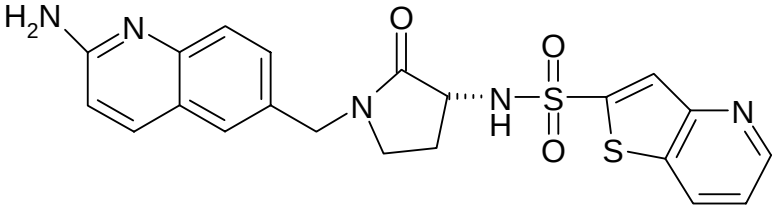

53

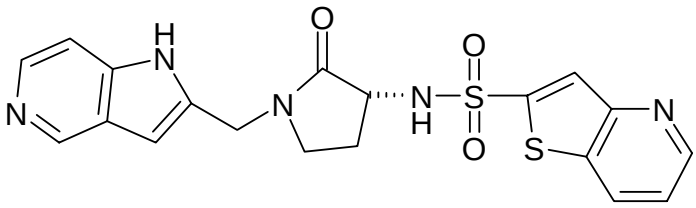

54

3-SULFONAMIDO PYRROLIDINONES

1.7.7.3 Ketopiperazine inhibitors: The meta and para benzamidines were made and the para was found to be more potent (**55** vs. **56**). The para benzamidine had a Ki= 1.3 nM and the meta benzamidine had a Ki= 18 nM [82]. Both have strong selectivity over other serine proteases. Interestingly, the crystal structure of compound **55** shows that the benzamidine moiety binds in the S4 pocket as opposed to the S1 pocket [101]. The chloro-benzothiophene group binds to the S1 pocket. Compound **57** (Ki= 1.4 nM) has an aminoisoquinolone in place of a benzaimidine moiety while compound **58** (Ki= 0.8 nM) has an aminoquinazoline. Compound **59** has a 5-azaindole as a benzamidine replacement (Ki= 4 nM). Compound **60** contains a chloro-thiophene in place of the chloro-benzothiophene and an improvement in potency is observed (Ki= 1.1 nM). Compound **60** also binds with the chloro-thiophene in the S1 pocket and the benzamidine replacement in the S4 pocket [101].

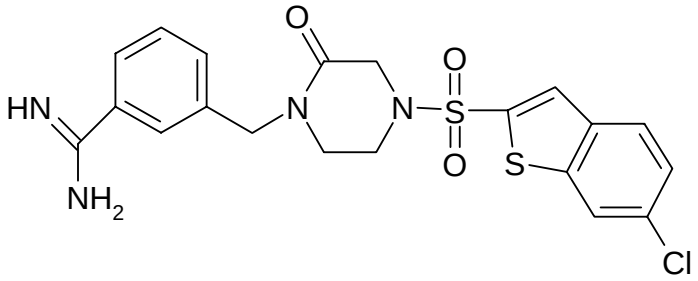

55

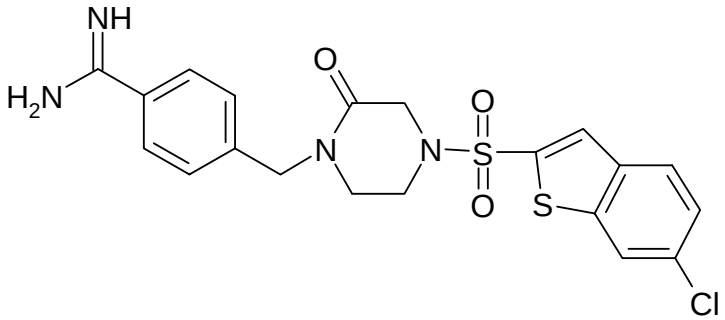

56

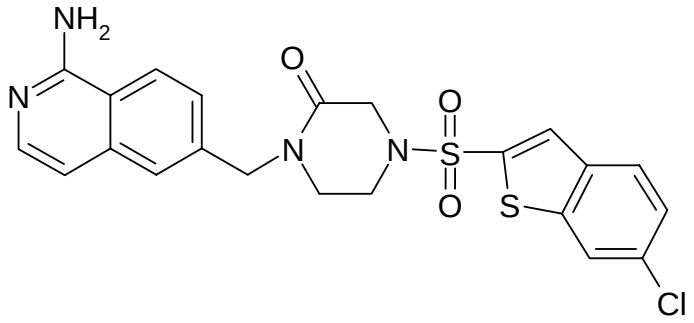

57

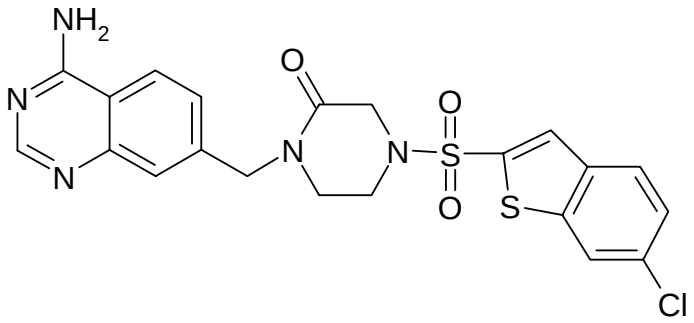

58

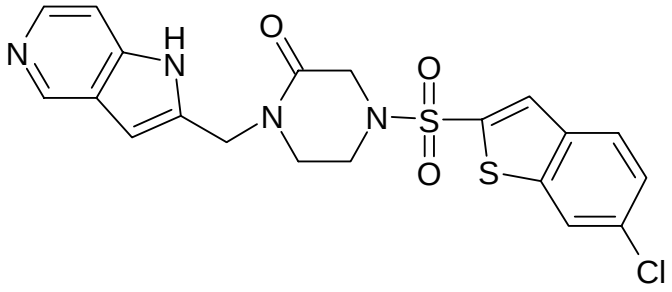

59

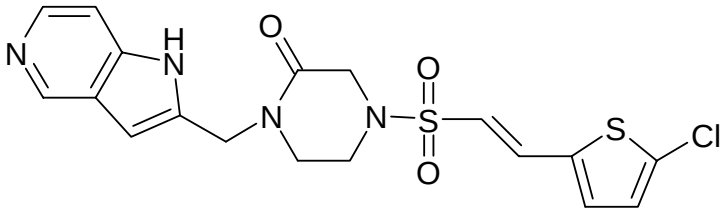

60

KETOPIPERAZINE INHIBITORS

1.7.8 Transition state FXa inhibitors

These inhibitors are based on the highly specific chromogenic FXa substrate D-Arg-Gly-Arg-pNA (S-2765) [102]. The D-Arg residue binds in the S4 pocket with the p-nitroaniline substituted Arg binding in the S1 pocket. If the p-nitroaniline is replaced by an electron withdrawing group, the catalytic serine 195 can react with the electropositive carbonyl and form a hemiketal, which can be thought of as a transition state inhibitor [103]. The first transition state inhibitors which substituted a simple hydrogen in place of p-nitroaniline was shown to have an IC_{50}= 50 nM.

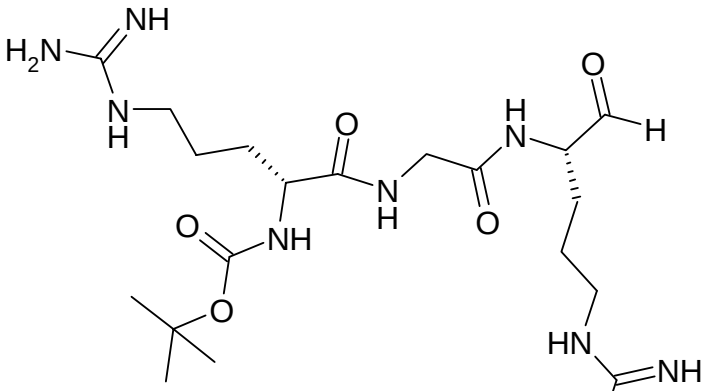

Boc-(D)-Arg-Gly-Arg

61

1.7.8.1 α-ketothiazole*:* Compound **62** was the first α-ketothiazole transition state inhibitor, D-Arg-Gly-Arg-ketothiazole. It had a FXa IC_{50}= 8nM, APC, a plasmin and t-PA IC_{50} >10 μM and a kallikrein IC_{50}= 500nM [103]. Within this series, compound **63** was considered to be the most promising. It displayed a FXa IC_{50}= < 0.5 nM and exhibited

excellent selectivity over the other serine proteases (APC IC_{50}= 6000 nM, plasmin IC_{50}= 300 nM and t-PA IC_{50}= 330 nM and kallikrein IC_{50}= 27 nM) [103]. The Ki for FXa was determined to be 13 pM and it does not exhibit slow binding kinetics [103]. The mode of binding for compound **63** is as follows: D-Arg binds in S4 making hydrophobic and ionic interactions as well as potential hydrogen bonding interactions. The other Arg can form hydrogen bonds with Asp 189 in the S1 pocket and the reactive ketone can form a reversible hemiketal with Ser195. The thiazole nitrogen is believed to hydrogen bond with His 57 [103].

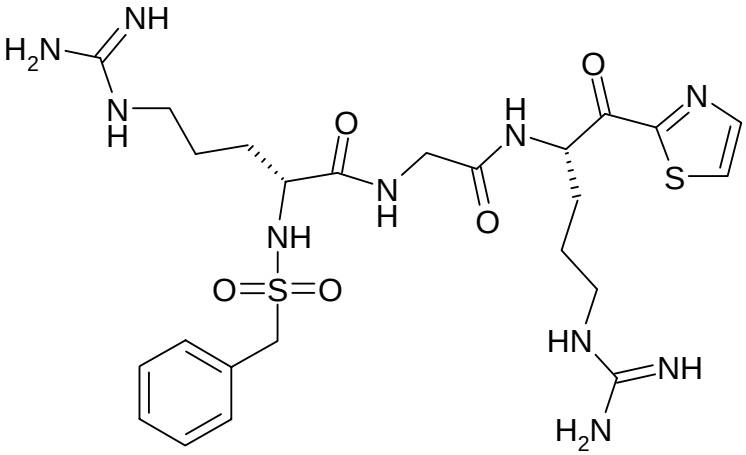

62

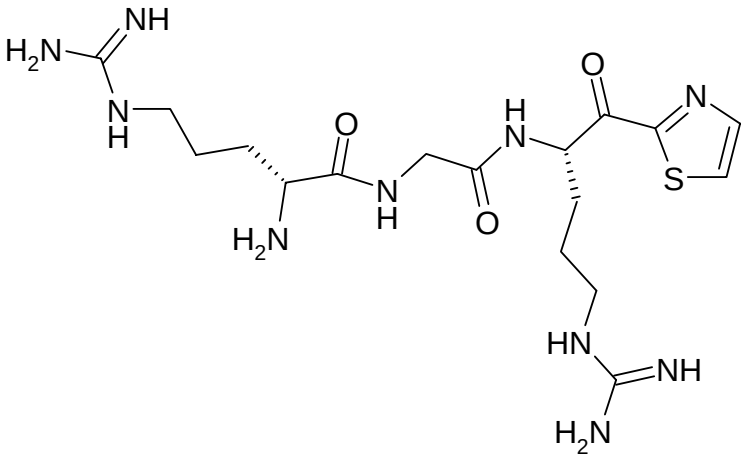

63

ALPHA-KETOTHIAZOLE INHIBITORS

Different heterocycles were tested in place of ketothiazole (compound **64** vs. **65** and **66**). There was no major difference in IC_{50} and all three were selective for FXa over thrombin. Compound **64** had a FXa IC_{50}= 1 nM, and a thrombin IC_{50}= 24000 nM. Compound **65** had a FXa IC_{50}= 2 nM and a thrombin IC_{50}= 26000 nM. Compound **V** had a FXa IC_{50}= 2 nM, and a thrombin IC_{50}= 1000 nM. The ketothiazoles were ultimately retained for synthetic and performance reasons [103]. The large hydrophobic blocking group at the N-terminus enhances FXa binding through hydrophobic interactions and decreases thrombin affinity because of thrombin's preference for a positively charged terminal amine [52]. Retention of the glycine residue affords the greatest degree of selectivity over thrombin (IC_{50}= 0.65 nM to 10000 nM) but N-alkylation with methyl, phenyl and benzyl groups also yield subnanomolar IC_{50} values [103]. Exchanging glycine with proline eliminates FXa selectivity over thrombin due to thrombin's penchant for proline substrates [52, 103].

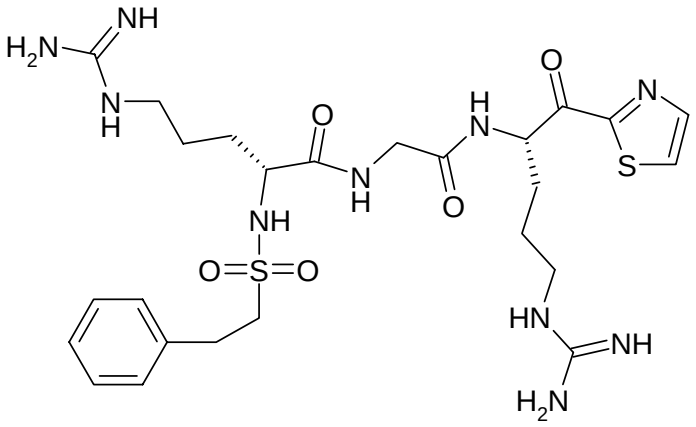

64

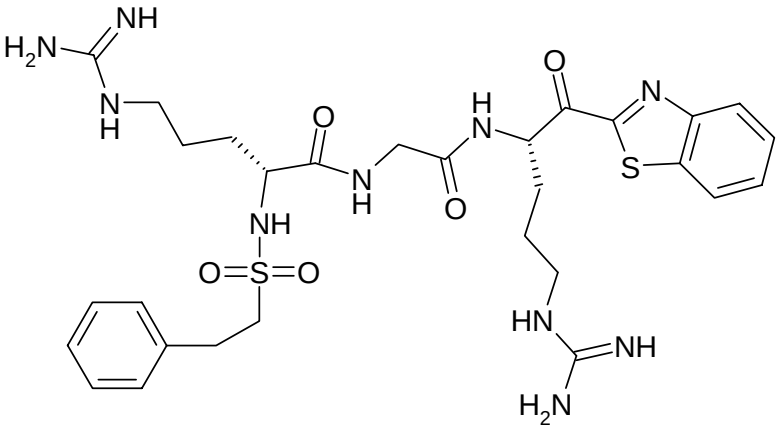

65

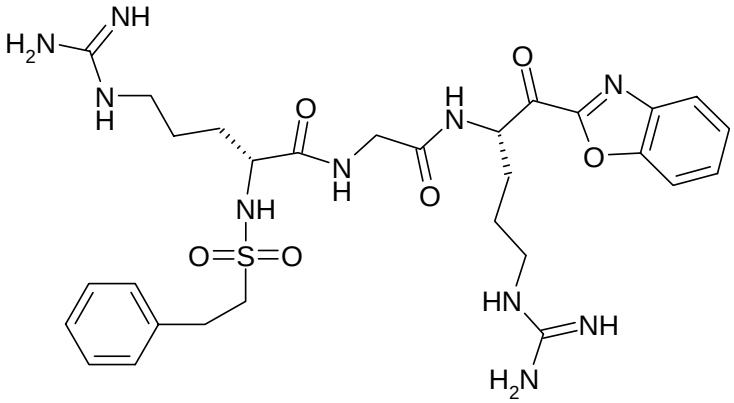

66

Despite creating potent and generally selective FXa inhibitors, due to the dibasic nature of the two Arg residues, there is no selectivity for FXa over trypsin [103]. Replacement of the S1 binding Arg with a less ionic or neutral moiety is believed to increase selectivity and potential for oral absorption. The incorporation of Trp in place of Arg yielded an inhibitor that was potent for FXa and selective over trypsin. Compound **67** has a FXa IC_{50}= 39 nM, a thrombin IC_{50}= > 500,000 nM and a trypsin IC_{50}= 180,000 nM. Replacement of the N-terminal Arg with less basic or neutral organic substituents and amino acids led to less selectivity for the other serine proteases [103].

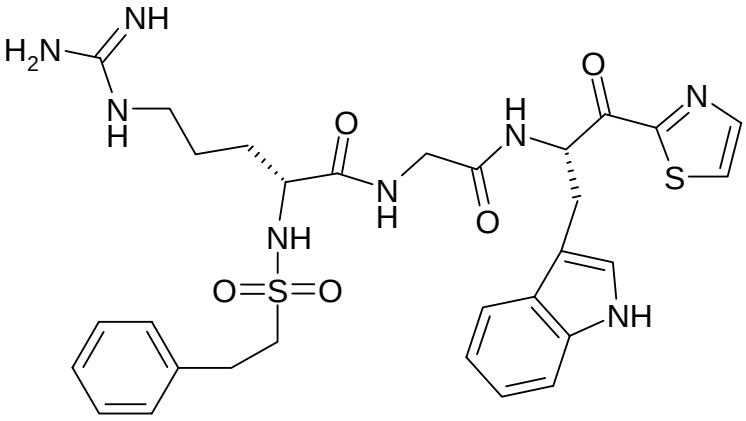

67

ALPHA-KETOTHIAZOLE INHIBITOR

1.7.8.2 α-amino lactams: Compound **68** has a FXa IC_{50}= 29 nM but a thrombin IC_{50}= 138 nM [103]. The development of compound **69** showed a decrease in potency but excellent selectivity over thrombin with a FXa IC_{50}= 65 nM and a thrombin IC_{50}= 12,000 nM [103]. Due to the difficulty in developing selectivity and the unwanted chiral center, lactams were abandoned in favor of simpler scaffolds.

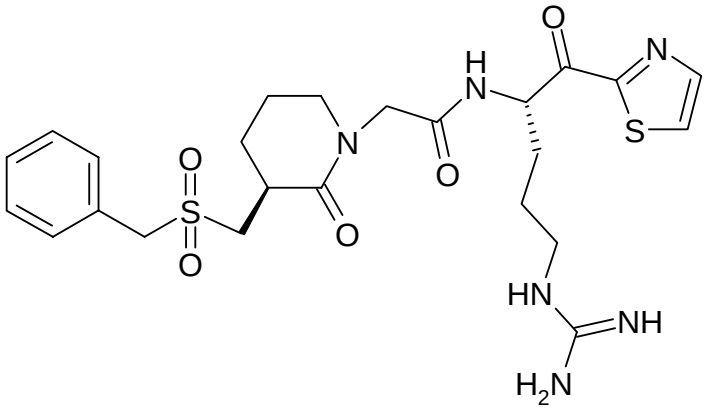

68

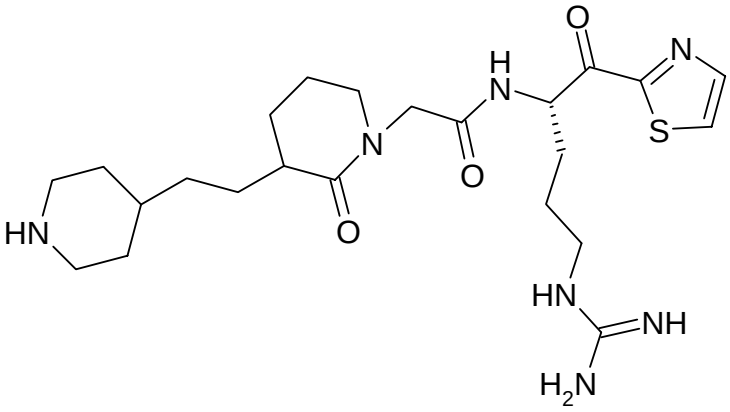

69

ALPHA-AMINO LACTAMS

1.7.8.3 Piperazinone transition state inhibitors: Compound **70** has a FXa IC_{50}= 4 nM but a thrombin IC_{50}= 400 nM. Better potency and selectivity can be achieved by benzenesulfonamide halogenation. Compound **71** has a FXa IC_{50}= 2 nM while thrombin IC_{50}= 1000 nM. Subnanomolar potency can be achieved with substituted fused bicyclic arylsulfonamides. Compound **72** has a FXa IC_{50}= 0.5 nM. All three compounds mentioned still strongly inhibit trypsin due to the S1 binding Arg residue [103].

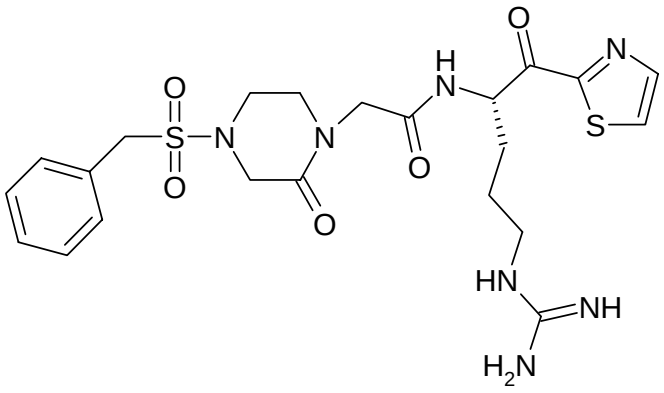

70

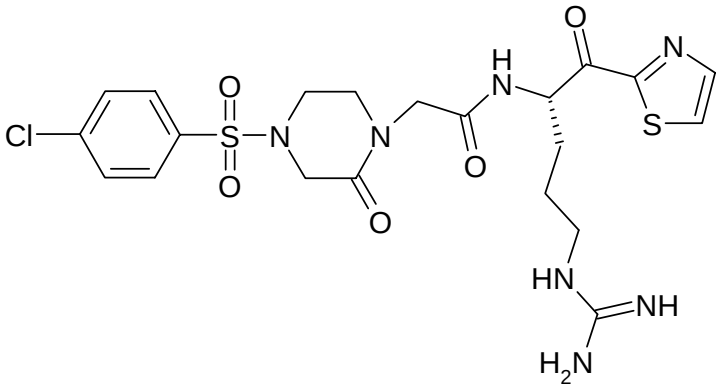

71

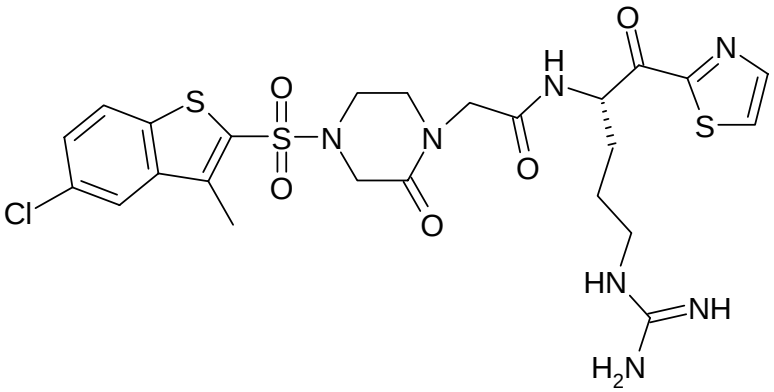

72

PIPERAZINONE INHIBITORS

1.7.9 Non-small molecule factor Xa inhibitors

1.7.9.1 Tick Anticoagulant peptide (TAP): Produced from the soft tick, *Ornithodorus moubata*, TAP is also expressed as a recombinant protein (rTAP) in yeast [104]. This 60 amino acid polypeptide (6977 Da) exists as a monomer [105]. TAP is a direct factor Xa inhibitor that is a slow, tight binding, reversible, competitive inhibitor [106]. TAP has a factor Xa Ki= 0.18 nM [107]. The binding of TAP to factor Xa is a two step process that involves both low and high affinity binding steps. The first step is the low affinity binding (Ki= 68 μM) to an exosite region that is does not effect the catalytic region of factor Xa. This step is followed by the high affinity binding (Ki= 0.3 nM) step which forms a more stable complex between enzyme and inhibitor [107]. TAP is highly selective for factor Xa over all other serine proteases (minimum 50,000-fold selectivity) [106, 107]. This is likely due to its binding of both the catalytic site as well as a unique exosite. The region of TAP that mediates the high affinity interaction by recognizing the catalytic domain of factor Xa is found in the amino terminal and there is no data showing that TAP is ever cleaved by factor Xa [108]. The other region of TAP that interacts with factor Xa are the amino acid residues found in positions 40-54. These residues share homology with a factor Xa recognition sequence found in human and bovine prothrombin. The current model is that TAP residues 40-54 are responsible for the low affinity recognition of factor Xa at an exosite. This association leads to a conformational change in TAP that promotes the interaction of the TAP amino terminus with the catalytic region of factor Xa, resulting in the formation of the high affinity complex [109]. This model is also consistent with the observation that TAP is able to inhibit the prothrombinase complex

[106, 110]. The prothrombinase Ki is a remarkable 6 pM, a 30-fold improvement over the free FXa Ki of 180 pM [110]. This great improvement in affinity for the prothrombinase complex has created speculation that TAP may also recognize factor Va [109].

1.7.9.2 **Ecotin**: regarded as the most potent reversible FXa inhibitor to date, ecotin is an 18 kDa protein expressed in the periplasm of *E. coli*. Ecotin is a potent reversible, tight binding factor Xa inhibitor (Ki= 54 pM) and it is believed to be protective against mammalian proteases that are present in the GI tract [111]. Because of this putative protective role, ecotin has mixed selectivity for FXa over other serine proteases. Ecotin does not inhibit thrombin, TF/FVIIa, FXIa, aPC, plasmin or t-PA, but it does inhibit FXIIa, plasma kallikrein, human leukocyte elastase (HLE), trypsin and chymotrypsin. In fact, ecotin is very potent against FXIIa, kallikrein and HLE (Ki< 1 nM). Ecotin is capable of forming a homodimer with a Kd= 390 nM. It has been shown that FXa slowly cleaves ecotin at the amide linkage between M84 and M85. When M84 is mutated to R or L, the subsequent ecotin mutants exhibit greater factor Xa potency (Ki= 11 pM and 21 pM, respectively). In addition to the changes in FXa potency, these mutants exhibited mixed selectivity against various serine proteases. The mutants were able to inhibit thrombin, FXIa, aPC and plasmin, whereas, wildtype ecotin could not. The mutants retained their potency towards FXIIa, kallikrein, trypsin and chymotrypsin but interestingly, they lost their potency towards HLE [111].

1.7.9.3 Antistasin: a 119 amino acid, (15-kDa) protein with 10 disulfide bridges, derived from the salivary glands of the Mexican leeches *Hementeria officinalis* and *Hementeria ghilianii* [112]. The 119 residues are separated into three domains. Residues 1-55, 56-110 and 111-119 constitute domains I, II and III respectively [113]. Domain I is the domain that directly inhibits factor Xa [114]. Although antistasin is selective for most serine proteases, it is still capable of inhibiting trypsin with nanomolar potency. Depending on the source, the reported FXa Ki= 470 -620 pM, the trypsin IC_{50}= 10 nM and the trypsin Ki= 5 nM [115]. Antistasin binding to FXa is described as reversible and tight binding [115]. The most potent synthetic peptide derived from antistasin contains the amino acids found in positions 27-49 with a 35 nM Ki against FXa [116]. Antistasin, which has an Arg residue at position 34, mediates its inhibition by mimicking a natural substrate. When Arg 34 binds in the P1 site of FXa, the amide bond directly following Arg 34 is hydrolyzed and resynthesized [115].

1.7.9.4 Therostasin: an 82 amino acid (8990 Da) polypeptide produced by the salivary glands of the Rhynchobdellid leech *Theromyzon tessulatum*. It is characterized as a direct FXa inhibitor with a FXa Ki= 34 pM, which is the most potent leech derived FXa inhibitor to-date [117]. Although it is inactive against most serine proteases, it has a trypsin Ki= 7.0 nM (> 200-fold selectivity).

1.7.9.5 Ghilianten: a ~15 kDa anticoagulant protein derived from the salivary glands of giant Amazonian leech, *Haementeria ghilianii* [118]. Ghilianten is a potent,

reversible inhibitor of FXa. The ghilianten IC_{50}= 3.1 pM for the inhibition of FXa within the prothrombinase complex [119]. Ghilianten has also been shown to have anti-metastatic properties [120].

1.7.9.6 AcAP: a nematode anticoagulant peptide from the hookworm, *Ancyclostoma caninum* [121]. It is a 8.7 kDa polypeptide with a factor Xa Ki= 323.5 pM. AcAP is capable of inhibiting the prothrombinase complex with an IC50= 336 pM. AcAP is highly selective for FXa over other serine proteases. However, at 50 nM, AcAP is capable of inhibiting the *in vitro* activity of factor XIa by 55% (compared to 98% inhibition of FXa *in vitro* activity at 50 nM). In the PT assay, AcAP was superior to both hirudin and TAP by doubling the clotting time at 35 nM compared to 410 nM and 1256 nM, respectively. In the APPT assay, AcAP was superior to TAP, but not hirudin, by doubling the clotting time at 85 nM compared to 2365 nM and 32 nM, respectively [122]. The recombinant AcAP (rAcAP) has been tested on LOX human melanoma cells and shown to be antimetastatic. These studies show that rAcAP prevents specific interactions between factor Xa and tumor cells by blocking active site mediated interactions and prothrombinsae complex activity [123].

1.7.9.7 Lefaxin: a 30 kDa protein that is produced in the salivary glands of the leech *Haementeria depressa*. Lefaxin is a direct FXa inhibitor with a Ki= 4nM. Lefaxin is also capable of inhibiting the prothrombinase complex (IC_{50}= 40 nM) [124].

1.7.10 FIXa active site

FIXa is considered to be a catalytic weakling compared to thrombin and FXa. While most serine proteases like thrombin and FXa readily cleave a variety of peptide and synthetic substrates, FIXa is considered to have poor amidolytic activity [125, 126]. The other clotting serine proteases are able to hydrolyze synthetic substrates that have a natural recognition sequence with a catalytic efficiency (k_{cat}/K_M) ranging from 10^5-10^6 M^{-1} sec^{-1} [126]. However, no synthetic substrates with a k_{cat}/K_M >103 M^{-1} sec^{-1} has been developed or discovered [125]. The S1 pocket appear geometrically similar to FXa, which is considered to be catalytically efficient, two specific residues appear to mediate a structural disadvantage to FIXa and its catalytic abilities [127]. Glu 219 is positioned at the entrance of the S1 pocket and is highly conserved in mammalian FIXa sequences, while this position is occupied by a conserved glycine residue in the other serine proteases [128]. A tyrosine residue in a segment known as the 99-loop also places steric constraints on access to the factor IXa active site. The 99-loop is on the border of the S2-S4 sites and the Y99 residue directly impinges on the S2-S4 site affecting its size and chemical nature [129]. FXa also has a Y99 but its orientation is very different [127]. In FIXa, the Y99 is able to adopt various conformations, depending on what is bound to the active site. In the relaxed state, Y99 is observed to be blocking the S2 and the S4 site [125]. This is deemed to be unsuited for proper substrate binding and efficient amidolytic activity. Rotation of Y99 to an orientation more closely resembling that of FXa is believed to be necessary for FIXa to be more catalytically competent. Even when large inhibitors are bound, the Y99 occludes the S4 pocket [127]. Based on experimental evidence, it is speculated that the binding of

FVIIIa to FIXa may indirectly reorient the 99-loop, which displaces Y99 and allows for better access to the entire FIXa active site [127]. It is this restricted active site that has made FIXa chromogenic substrate and inhibitor development so challenging.

1.7.11 FIXa inhibitors

1.7.11.1 Small molecule inhibitors of factor IXa

Since FIXa is specific to the intrinsic pathway, its inhibition can be used to reduce undesirable clotting in areas where TF is low. FIXa inhibitors are not expected to be effective in areas where TF is high. These include areas where vascular damage has occurred including wounds found at surgical sites [130]. A selective, efficacious FIXa inhibitor should be able to increase the clot time in the APTT assay at a low dose, while not affecting the clot time observed in the PT assay [131]. A group at Celera has recently screened their small molecule library to identify inhibitors of FIXa [130]. This resulted in a lead compound, a 5-amidino-benzimidazole analog (**73**), which had a 99 nM potency towards FIXa. However, it was not sufficiently active in the APTT nor did it show enough selectivity over FXa and FVIIa. They reasoned that decreasing the lipophilicity of compound **73** would enhance activity in the APTT assay [132]. They decided to exchange the phenolic ring with a heterocycle that was less lipophilic but that would not drastically alter the molecular weight. Thus, compound **74**, a hydroxyl pyrazole was designed [132]. Replacement with the 5 atom heterocycle, altered the geometry of the phenyl substituent and changed the position of hydroxyl group, yet the hydroxyl pyrazole displayed better potency towards FIXa [132] and improves its performance in the APTT assay. The Celera

group felt that by modifying the phenol to a more hydrophilic moiety, they had "improved the physicochemical properties" of the compound which "translated into better *ex vivo* efficacy" [132]. The new hydroxyl pyrazole also had increased selectivity for FIXa over the other pro-coagulant serine proteases, specifically thrombin, FXa and FVIIa [132]. The hydroxyl pyrazole was not very active in the PT assay, which is an expected and desirable trait for FIXa inhibitors. Removal of the benzimidazole moiety and replacing it with an amide linkage made the compound inactive. Removal of the amidine also eliminates activity because it is believed to interact with Asp189 located in the S1 pocket [133]. According to the authors there are at least three factors that help enhance the selectivity of compound **74**. The position of the Asp189 is almost an angstrom different between FIXa and FVIIa in the S1 pocket of the active site. This makes the FIXa S1 pocket bigger, which allows compound **74** to bind deeper in the pocket. Also, in FIXa, Phe41 is closer to the S1 pocket than it is in FVIIa. This puts the Phe41 in closer proximity to the terminal phenyl group. The angle between the amido-benzimidazole moiety and the phenyl ring is greater when connected by a 5 member ring as compared to the 6 member ring. This gives the structure a more linear look. The two unique architectural features of the FIXa active site along with the more linear inhibitor appear to allow for deeper binding in the pocket, increased potency and increases selectivity [132]. This hydroxyl pyrazole offers a promising scaffold from which to make analogs that are both selective and efficacious for FIXa.

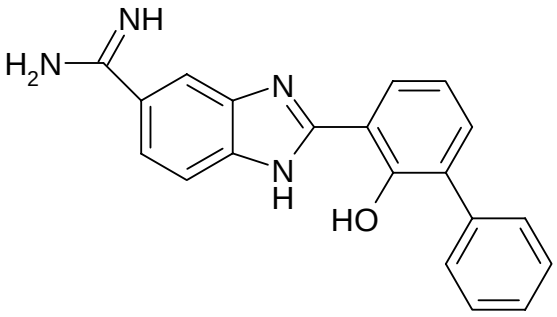

73

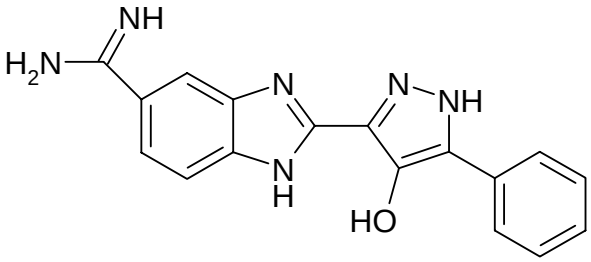

74

FACTOR IXa INHIBITORS

1.7.11.2 Non-small molecule inhibitors of factor IXa

Prolixin-S is an anticoagulant heme protein (19,992 Da) that is expressed in the salivary glands of the kissing bug (a blood sucking insect), *Rhodnius prolixus*. Prolixin-S is a specific inhibitor of intrinsic pathway because it prolongs APTT but not PT. More specifically, prolixin-S inhibits factor IXa and prevents activation of FX in presence of Ca^{2+} and phospholipids. However, the presence or absence of FVIIIa had no effect on prolixin-S inhibition of FIXa. The prolixin-S IC_{50} for the inhibition of the factor X activation complex in the presence and absence of FVIIIa is ~1.75 μM (~35 μg/ml) in both cases. Prolixin-S does not affect the amidolytic activity of FIXa. Prolixin-S is believed to block the interaction between FIXa and factor X on the phospholipid surface [134].

1.8 Inhibitors of fibrin formation

Direct thrombin inhibitors (DTIs) prevent thrombin from interacting effectively with its substrates. Thrombin inhibitors prevent fibrin formation, block thrombin-mediated feedback activation of FV, FVIII, XIII and FXI, attenuate thrombin induced platelet aggregation, block activation of protein C and many other functions of thrombin [37].

1.8.1 Requirements for good DTI

-***Low Ki***. If the potency is too low, then the DTI will be ineffective. However, if the Ki is too low then other problems can arise (*e.g.* as observed with the tight binding inhibitor, hirudin).

- ***Needs to be selective for thrombin***. This is typically most difficult for trypsin. However, some advocate the concept that less specific, dual coagulation protease inhibitors would be potentially superior.

-***Needs to be orally bioavailable***. There are several effective parenteral anticoagulants (heparin, LMWH, hirudin, argatroban) but only one orally active anticoagulant has been approved in the U.S (warfarin).

-***Balanced lipophilicity:hydrophilicity***. If the DTI is too hydrophobic then increased plasma protein binding will be problematic [135].

-***Need avoid hepatobiliary excretion*** [135]. This can typically be accomplished by enhancing the hydrophobicity of the drug. This is especially important because issues with hepatotoxicity (e.g. Ximelagatran caused liver toxicity which ended its bid to replace warfarin as the oral anticoagulant of choice) [135].

1.8.2 DTI advantages

It is expected that DTIs will produce a more predictable anticoagulant response, because assuming that lipophilicity is not excessive, DTIs will not bind plasma proteins. [136]. DTIs do not need the assistance of endogenous cofactors such as heparin cofactor II or antithrombin, and they are able to inhibit free thrombin as well as fibrin-bound thrombin [136]. DTIs can also inhibit the effects of thrombin on platelets like thrombin-induced platelet aggregation. DTIs do not bind PF4 [136] and do not induce autoimmune thrombocytopenia like heparin [37]. Thrombin has also been implicated in promoting tumor growth and DTIs may represent an adjuvant therapy [137].

1.8.3 Thrombin active site

Thrombin is a serine protease and is considered to be a trypsin-like member of the broader chymotrypsin family (figures 25-28). Similar to trypsin, thrombin has a preference for substrates that have a positively charged amino acid in the P1-position, the N-terminal residue constituting the scissile bond. The structural basis for this preference comes from the Asp189 residue that lines the bottom of the S1 pocket and makes electrostatic interactions with cationic substrates [138]. The specificity pocket (S1), which houses the catalytic triad, has very similar geometry to the other known serine proteases like trypsin and chymotrypsin. The catalytic triad is composed of Ser195-His57-Asp102 [139]. The S2 pocket is described as "much more encapsulated and hydrophobic than that of trypsin" [57]. With respect to the S3 pocket, thrombin is considered to be more acidic then most serine proteases because it contains a Glu at position 192. The S4-subsite is

composed of W215, I174, E217 and has a very different architecture compared to trypsin [57]. Additionally, the S4 pocket has a preference for an aliphatic group, while proline binds best in the S2 pocket and Arg is preferred in the S1 pocket [138]. Early studies showed that the tripeptide, Arg-Pro-Phe, was a high affinity peptide for thrombin and imitated many natural substrate interactions. The Arg residue binds at the P1 position, while the Pro occupies position P2 in the narrow active site cleft. Phe makes aromatic interactions in a manner similar to natural substrate residues found in the P4 position. However, this tripeptide makes no other interactions due to its length [140]. Thrombin has many roles in coagulation, and therefore many substrates. In order to appropriately coordinate all of these tasks, thrombin relies on subtle structural differences in its tertiary structure to facilitate proper substrate recognition and discourage improper substrate recognition [140].

One obvious region of the thrombin tertiary structure that confers substrate selectivity are the residues immediately surrounding the catalytic triad in the active site. Some of the first crystallographers to study thrombin describe its active site as "a deep, narrow canyon" because of its deep narrow cleft that must be traversed to access the catalytic serine [57]. The two sides of the canyon are insertion loops known as the 60-loop and the γ-insertion loop. The amino acids that form the "rims" of the active site cleft are overwhelmingly hydrophobic. Based on the secondary and tertiary structure of these loops, they are able to restrict substrate access to the catalytic serine and confer selectivity. The unique 60-loop (Leu60, Tyr60A-Thr60I) is considered to be hydrophobic and rigid due to the type of residues present and the two consecutive prolines, respectively. The complete

sequence of the loop is LYPPWDKNFT [140]. This loop will favorably interact with hydrophobic residues that are located N-terminally to the P1 position, while interaction with hydrophilic residues will be selected against. Unlike trypsin, which is considered to have a more open active site, Tyr60A-Trp60D imposes great steric hindrance and is likely responsible for limiting thrombin's active site accessibility to substrates and inhibitors alike [57]. The γ-insertion loop (Thr147, Trp147A-Val147F) is considered to be more hydrophilic and more flexible then the 60-loop. The residues that make up this loop are TWTANV [140]. The γ-insertion loop also plays a role in substrate specificity because it partially occludes the active site [140]. The γ-insertion loop interacts with the substrate amino acids that are located C-terminally to the P1 position.

Figure 25. An illustration of thrombin showing its binding sites.

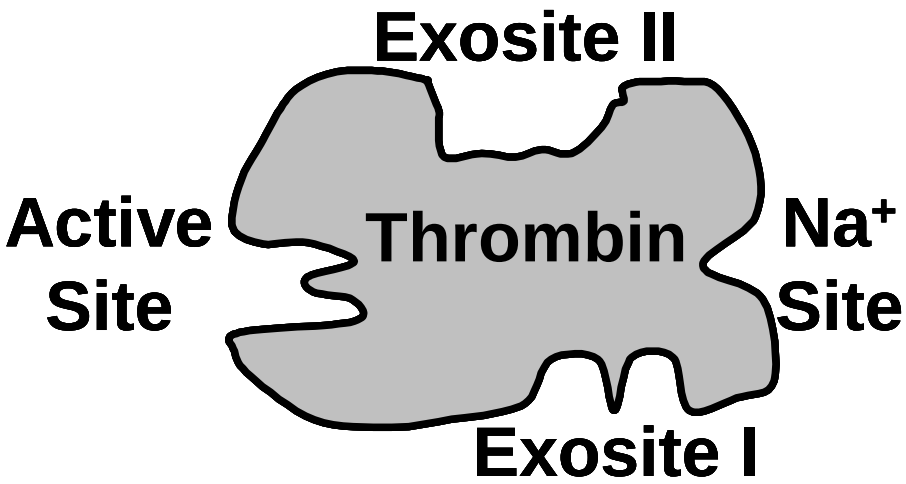

Figure 26. The structure of thrombin. The active site residues are displayed for reference. This image was created from the PDB file 1XMN using sybyl 7.2.

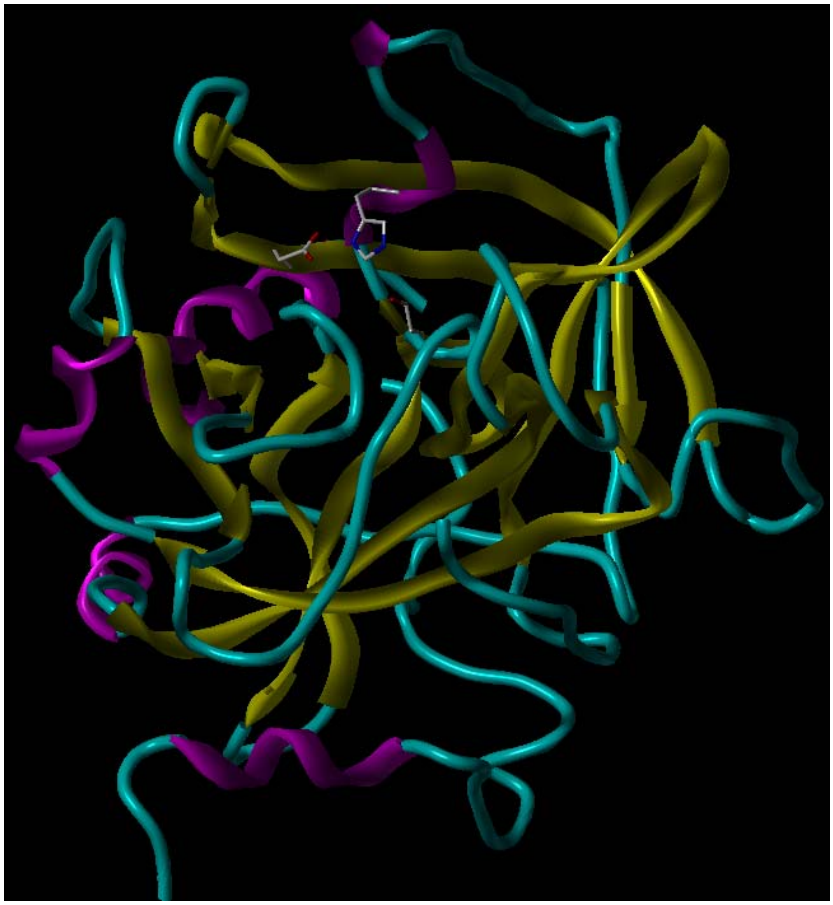

Figure 27. The structure of the thrombin active site. The active site residues and other important residues are displayed for reference. This image was created from the PDB file 1XMN using sybyl 7.2.

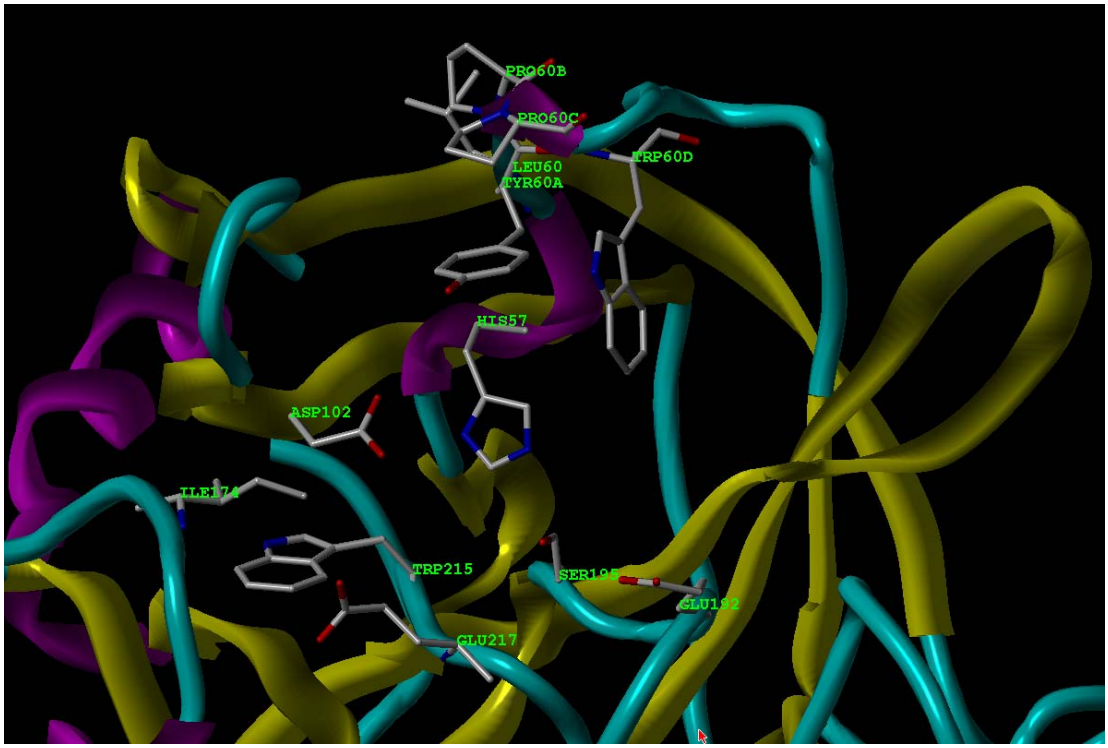

Figure 28. Thrombin surface electron density map with electrostatic potentials. The more basic the protein surface, the more red that area appears. The active site, both exosites, the Na+ binding site, the 60-loop and γ-loop are all labeled. This image was created from the PDB file 1XMN using sybyl 7.2.

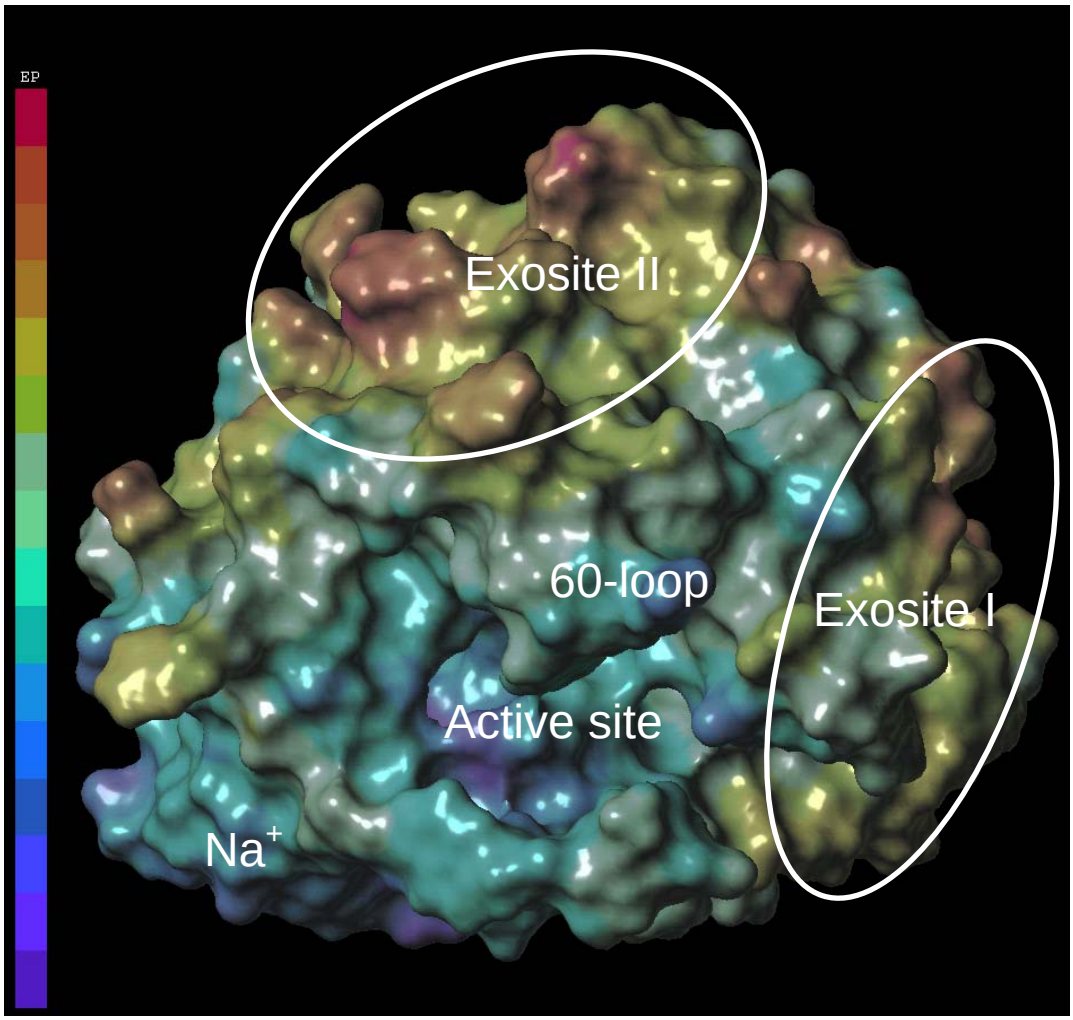

1.8.4 Thrombin anion-binding exosites and ligand interactions

The active site is not the only region on thrombin that is capable of mediating substrate selectivity. Thrombin possesses two exosites that also make specific interactions with various substrates. Exosite I is composed of a cluster of positively charged (basic) amino acids and is also known as the fibrinogen recognition site. The residues that constitute exosite I are Lys21, Arg62, Arg68, Arg70, Tyr71, Arg73, Lys106 and Lys107 [138]. Exosite I can interact with substrate residues that are on the P2 side of the cleavable amide bond. Exosite II (or heparin binding domain) is more basic then exosite I. This highly cationic domain makes exosite II the region on thrombin that polyanionic heparin binds during the formation of the ternary AT:heparin:thrombin inhibitory complex. The primary residues in exosite II are Arg89, Arg98, Arg245, Lys248 and Lys252 [138]. Thrombin substrate selectivity is dictated by a combination of necessary active site and exosite interactions. These interactions and steric barriers are the gatekeepers to the catalytic serine and prevent thrombin from behaving as a promiscuous protease. If a putative substrate fails to make the necessary interactions then amide hydrolysis will not occur. All known natural substrates of thrombin engage at least one of the two exosites, while some substrates require both [140].

Fibrinogen is an inactive procoagulant structural protein that is converted to fibrin by thrombin. Fibrinogen makes contacts with thrombin's active site and exosite I with μM affinity [141]. Because of the importance of exosite I in fibrinogen recognition, exosite I is also commonly referred to as the fibrinogen binding domain. The residues that are involved in fibrinogen binding to thrombin are K36, R67, H71, R73, Y76, R77a, K81,

K109 and K110 of exosite I. Additionally, residues near the Na^+ binding site, the 60 loop and the active site are involved in fibrinogen recognition [141]. Exosite I has also been shown to be necessary for the recognition of protease activated receptors (PAR 1 and PAR 4) [142], cofactors FV and FVIII [143], thrombomodulin [144], GPIbα [145], the serpin heparin cofactor II (HCII) [146] and hirudin [147]. Specifically, the C-terminal segment of hirudin makes contact with thrombin exosite I. Of the 17 side chains in the C-terminus, 12 of the side chains make hydrophobic or ionic interactions with thrombin (figures 8 and 9). The electrostatic interactions are h-Glu49 with Lys60f and Arg35, h-His51 with Glu39, h-Asp55 with Arg73 and Lys149E, h-Glu58 with Arg77A, h-Glu65 and the C-terminus with Lys36 [39]. Heparin makes its nonspecific, electrostatic interactions with exosite II of thrombin (figures 29-31). It has been determined that heparin binds to exosite II by making ionic interactions (in order of importance) with R93, K236, K240, R101 and R 233 [148]. Additionally, exosite II is involved in the recognition of FV and FVIII [143], GPIbα [149] and the anticoagulant leech protein, haemadin [150].

1.8.5 Sodium binding site on thrombin

Thrombin is allosterically regulated by a small Na^+ binding surface exposed loop. Thrombin has superior catalytic properties in the presence of Na^+ compared to the absence of Na^+. The carbonyl oxygen atoms of Tyr190, Arg233 and Lys236 directly coordinate with Na+. Additionally, Asp199, Glu229, Asp234 and Tyr237 have been energetically linked to Na^+ binding [151].

Figure 29. Illustration showing heparin binding to exosite II of thrombin.

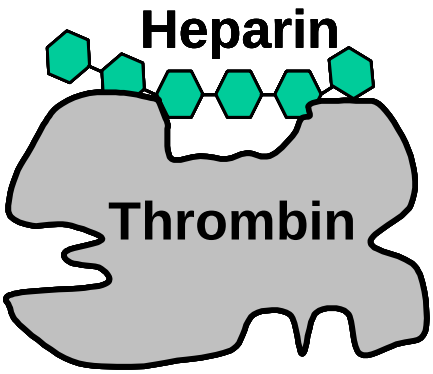

Figure 30. A mixed rendering including the ribbon structure of thrombin with the exosite II residues displayed for reference. This image was created from the PDB file 1XMN using sybyl 7.2.

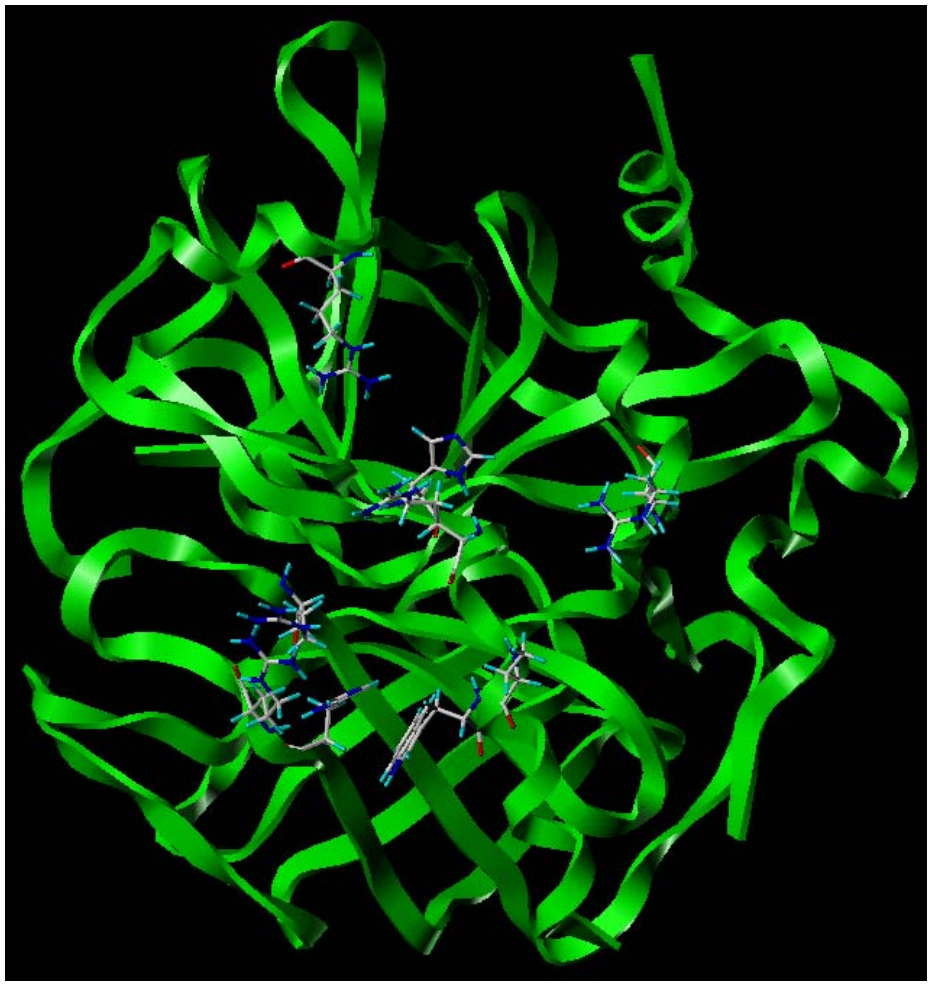

Figure 31. A model of heparin octasaccharide bound to thrombin exosite II. The surface exposed electron density of thrombin with calculated electrostatic potentials are shown. The more red the color, the more electropositive the region is. This image was created from the PDB file 1XMN using sybyl 7.2.

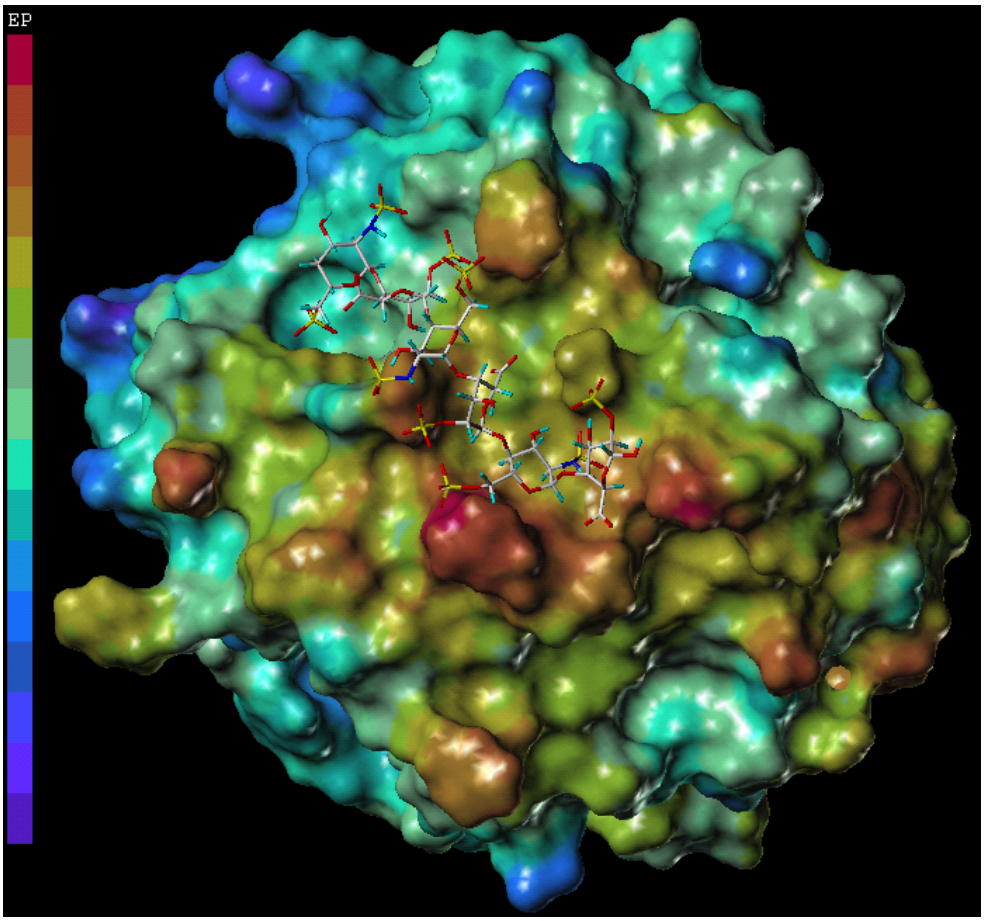

Figure 32. Thrombin surface electron density map with electrostatic potentials. The more basic the protein surface, the more red that area appears. The active site, both exosites, the 60-loop and γ-loop are all labeled. This image was created from the PDB file 1XMN using sybyl 7.2.

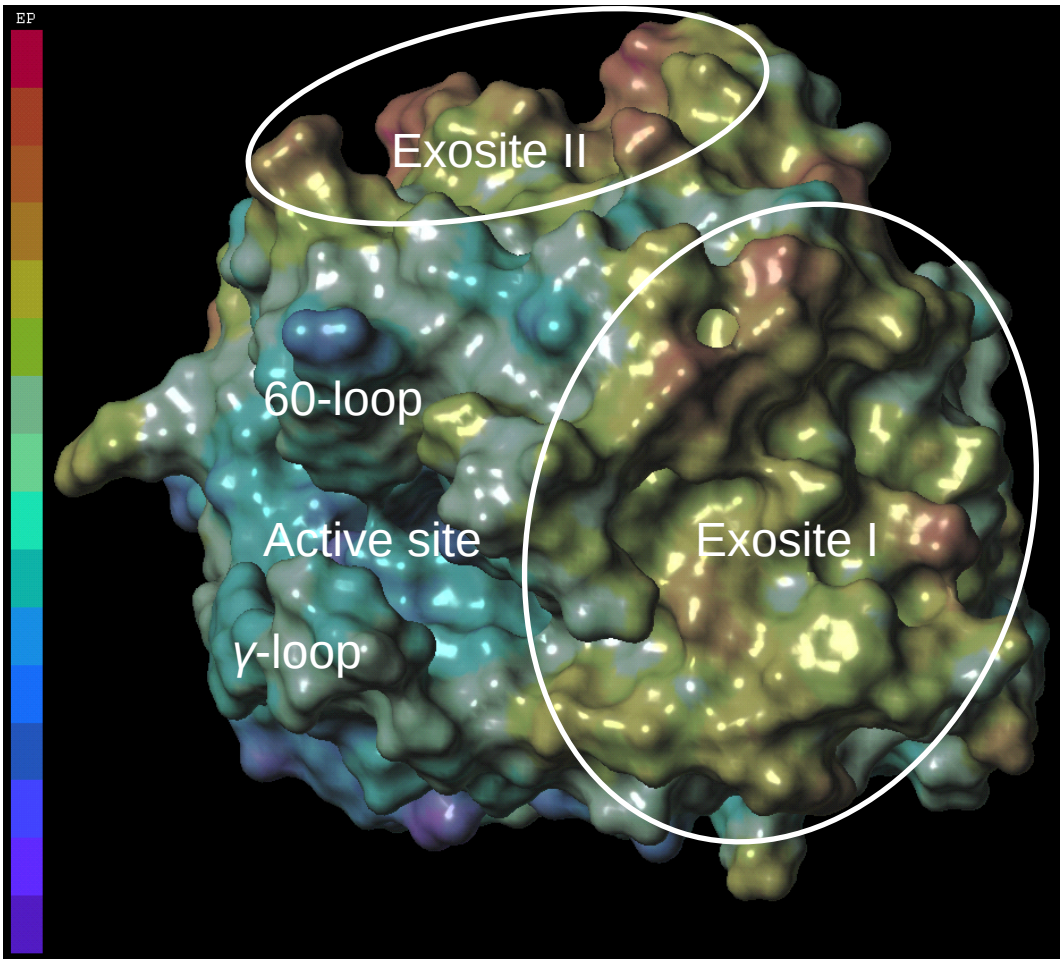

Figure 33. Thrombin surface electron density map with electrostatic potentials. The more basic the protein surface, the more red that area appears. The active site, both exosites, the 60-loop and γ-loop are all labeled. This image was created from the PDB file 1XMN using sybyl 7.2.

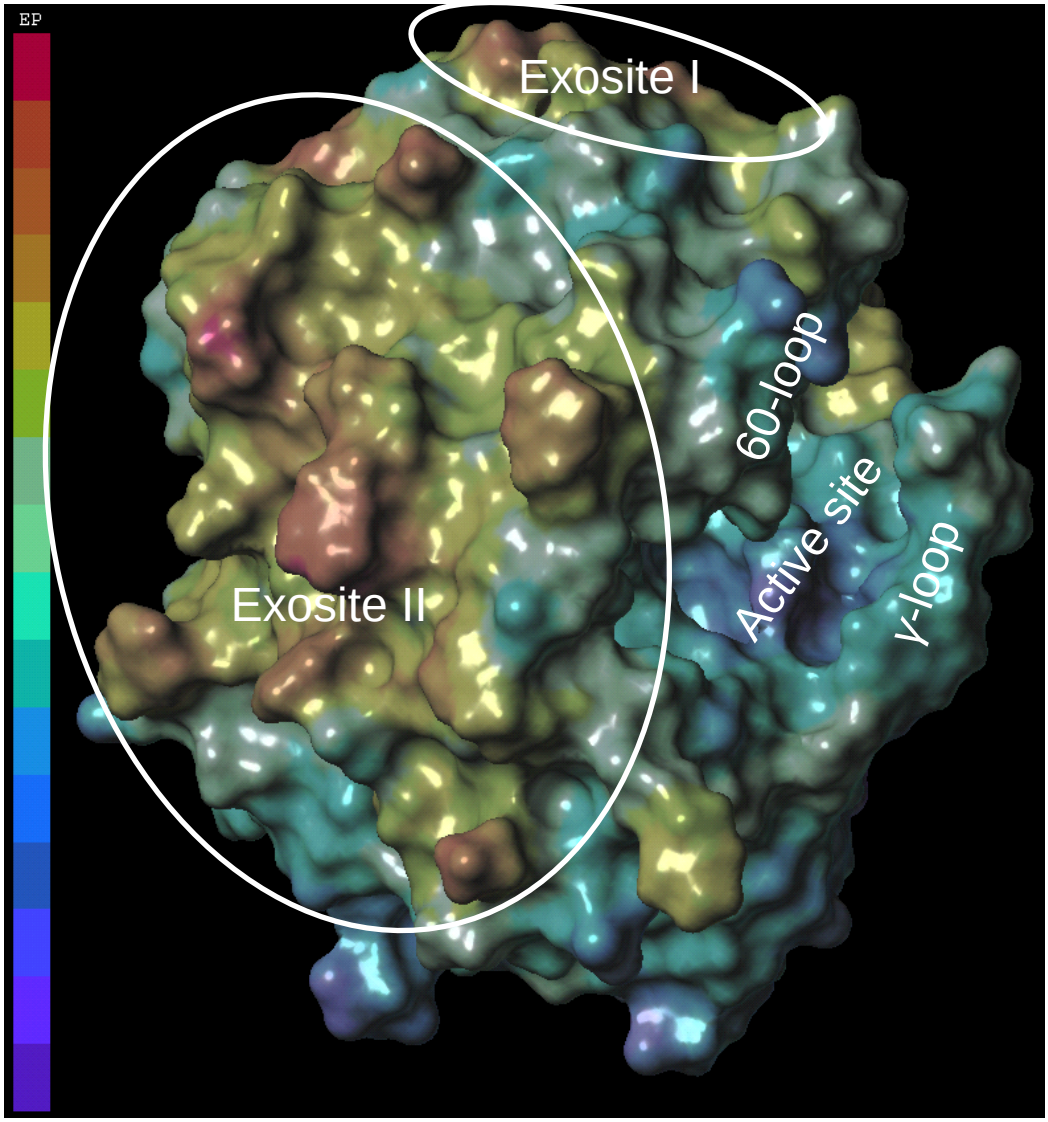

1.9 Thrombin inhibition

An observation was made that fibrinopeptide A and certain tripeptide fragments could inhibit thrombin [135]. This discovery represented the first lead compounds in the development of direct thrombin inhibitors.

1.9.1 Arginine derivatives as inhibitors of thrombin

1.9.1.1 D-Phe-Pro-Arg-chloroketone (PPACK) (**75**) is a selective, covalent inhibitor of thrombin, which contains an Arg residue at the P1 position (figure 34) [152]. The nucelophilic Ser195 of thrombin attacks the electropositive carbon adjacent to the chlorine atom forming a covalent bond. Thrombin selectivity is mediated by the tripeptide sequence, which is the same sequence that thrombin recognizes in fibrinopeptide A.

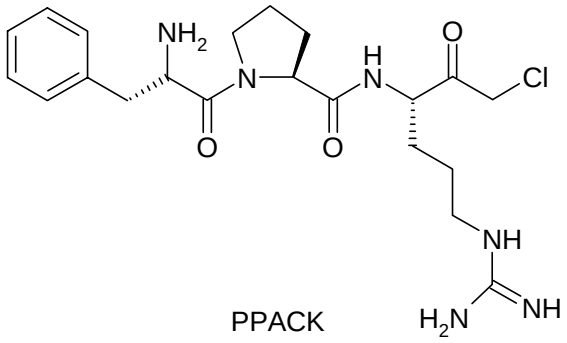

PPACK

75

Figure 34. PPACK bound to thrombin. PPACK is shown as a ball and stick model. Ser195 and His57 are also shown. This image was created from the PDB file 1PPB and sybyl 7.2.

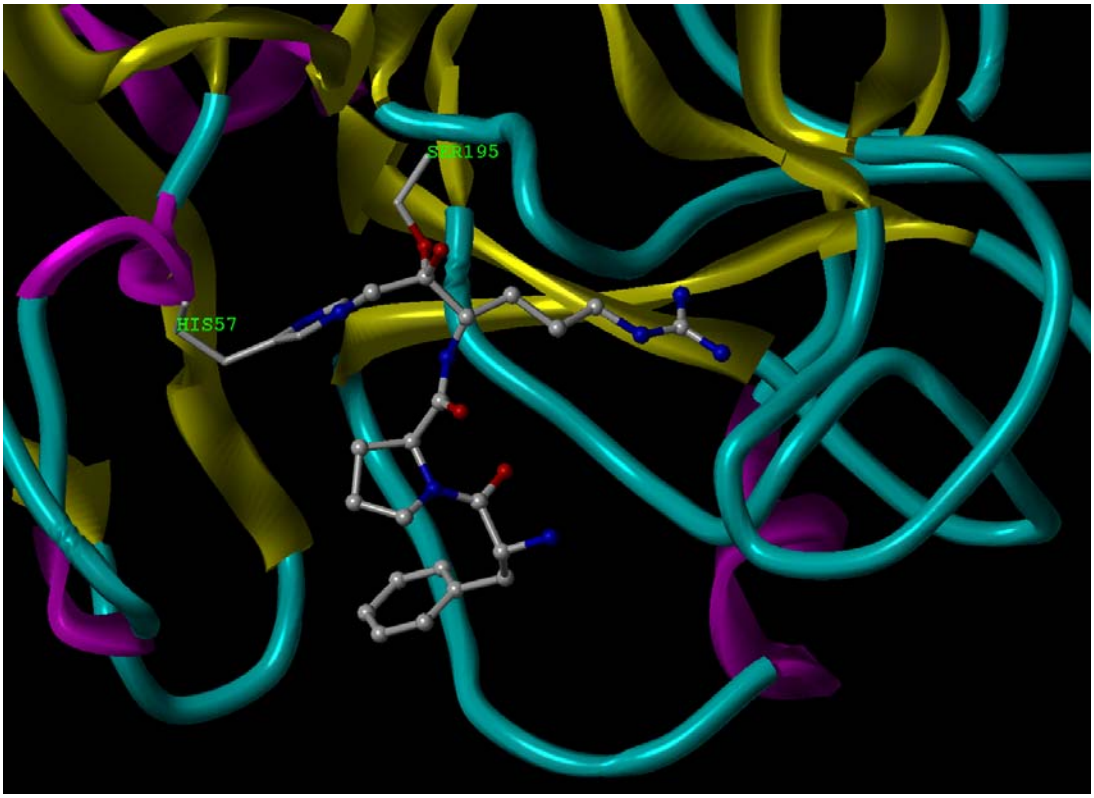

1.9.1.2 **DUP 714**: (**76**) a covalent thrombin inhibitor with a Ki= 41 pM [153].

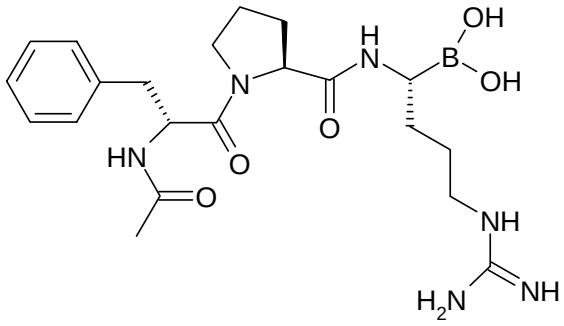

DUP 714

76

1.9.1.3 **Cyclotheonamide A:** (**77**) This natural product was isolated form a marine sea sponge (genus *Theonella*). It is a macrocyclic peptide with a thrombin Ki= 180 nM, however it is more potent against trypsin and streptokinase (Ki= 23 and 35 nM, respectively) [154]. The β diketone forms a hemiketal with Ser195 of thrombin. Despite the lack of selectivity, this represents a great lead compound.

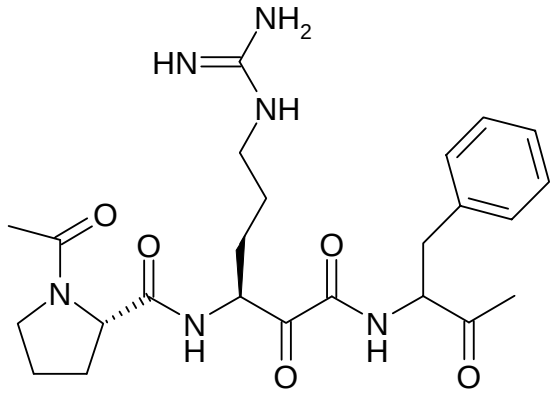

CYCLOTHEONAMIDE

77

1.9.1.4 Derivatives of cyclotheonamide (77)

Table 1. Derivatives of cyclotheonamide (**77**) [135].

Derivatives of cyclotheonamide (**77**)				
Name	#	Structure	Thrombin Ki (nM)	Trypsin Ki (μM)
L-370518	78	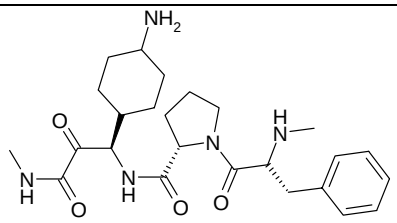	0.5	1.15
L-372460	79	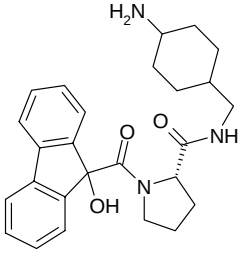	1.5	0.86
Derivative of L-372460	80	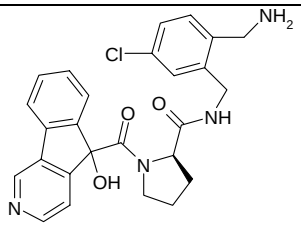	0.4	N/A
L-374087	81	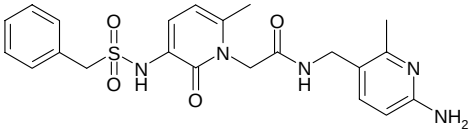	0.5	3.2
L-375378	82	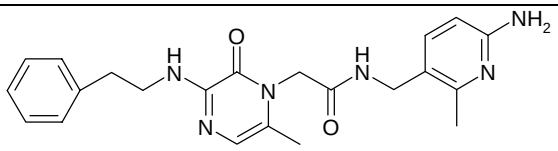	0.8	1.8

1.9.2 Amidine and guanidine based inhibitors of thrombin

1.9.2.1 Dabigatran etexilate (BIBR-1048) (**84**): it is the orally active prodrug form of Dabigatran (BIBR-953) (**83**) [155]. It is converted by esterases to dabigatran. Dabigatran (**83**) is a competitive, reversible inhibitor of thrombin (figure 35) [37]. Its thrombin Ki= 4.5 nM and its trypsin Ki= 50 nM, which is more selective then melagatran [155]. It represents a unique class of compounds based on a 1,2,5-trisubstituted benzimidazole core scaffold [156]. Dabigatran (**83**) is a zwitterion that is protected at both ionizable sites by lipophilic groups which are capable of being hydrolyzed [156].

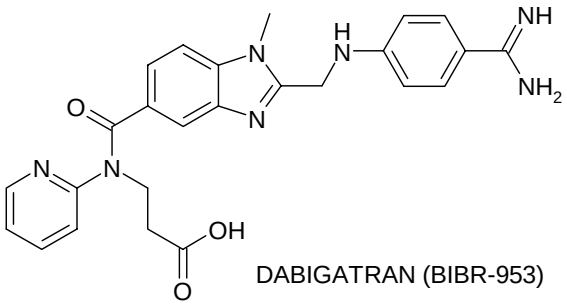

DABIGATRAN (BIBR-953)

83

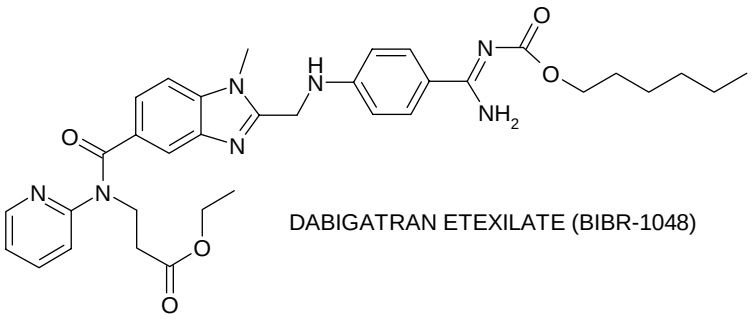

DABIGATRAN ETEXILATE (BIBR-1048)

84

Figure 35. Structure of compound **83** bound to the thrombin active site. The lipophilic potential is mapped on the protein surface. This image is adapted directly from [156].

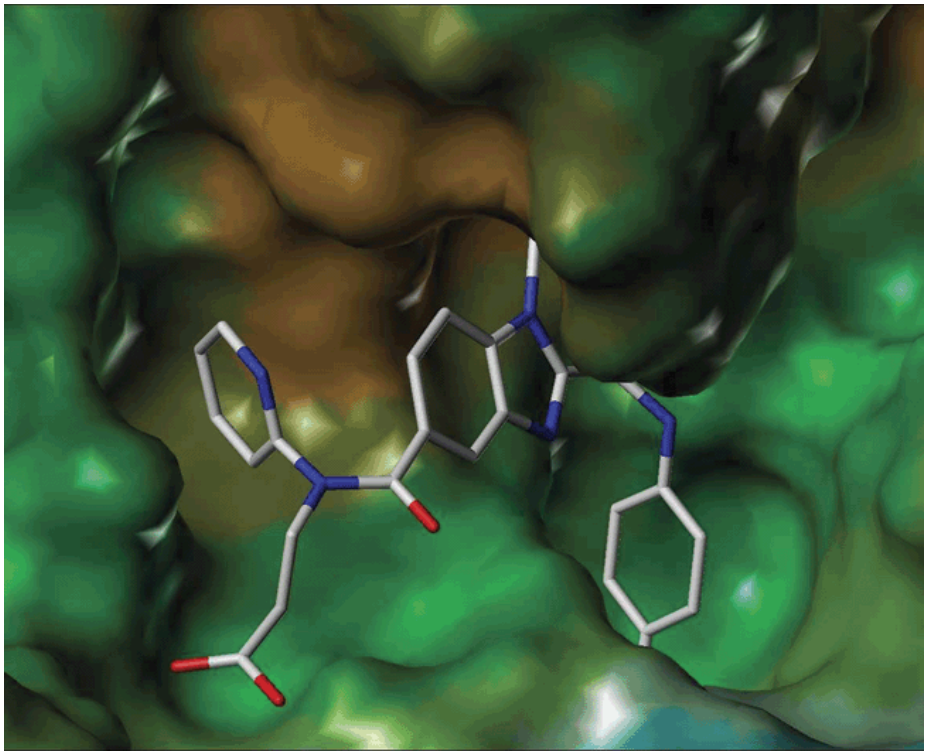

1.9.2.2 **LB-30812**: (**85**) With a Ki= 3 pM, it is the most potent synthetic inhibitor to-date. It is highly selective, but only has moderate oral activity [135].

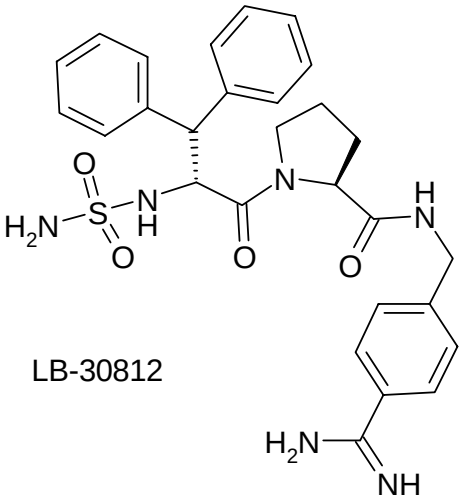

85

1.9.2.3 **Oxyguanidines:** compound **86**, thrombin Ki= 11.9 nM. Compound **87**, thrombin Ki= 4 nM. Both compounds have high plasma protein binding [157].

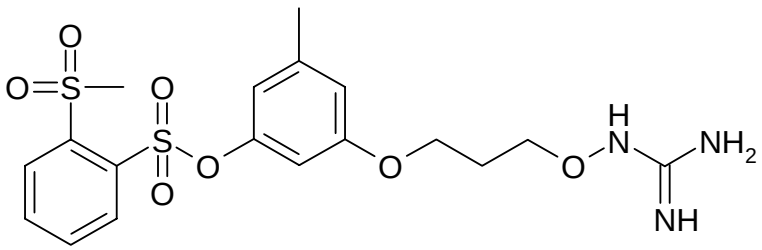

86

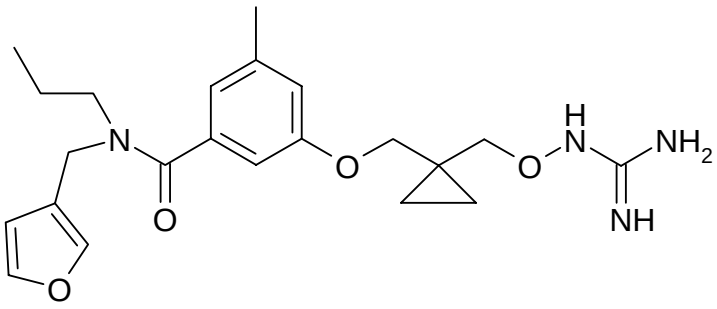

87

OXYGUANIDINES

1.9.2.4 Metal chelators: this compound (**88**) is an amidino-benzimidazoles derivative. It has a thrombin Ki= 5.6 nM in presence of Zn^{2+} and a Ki= 2.3 µM in the absence of Zn^{2+} [158, 159]. Zn^{2+} coordinates with His57 and Ser195 of thrombin and the two benzimidazoles of the chelator (figure 36).

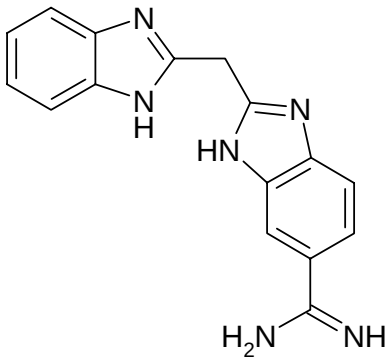

METAL CHELATOR

88

Figure 36. Zn^{2+} coordinates with His57 and Ser195 of thrombin and the two benzimidazoles of the chelator. The structure of the chelator shown is similar to **88** and binds in a manner analogous to **88**. This image is adapted directly from [159].

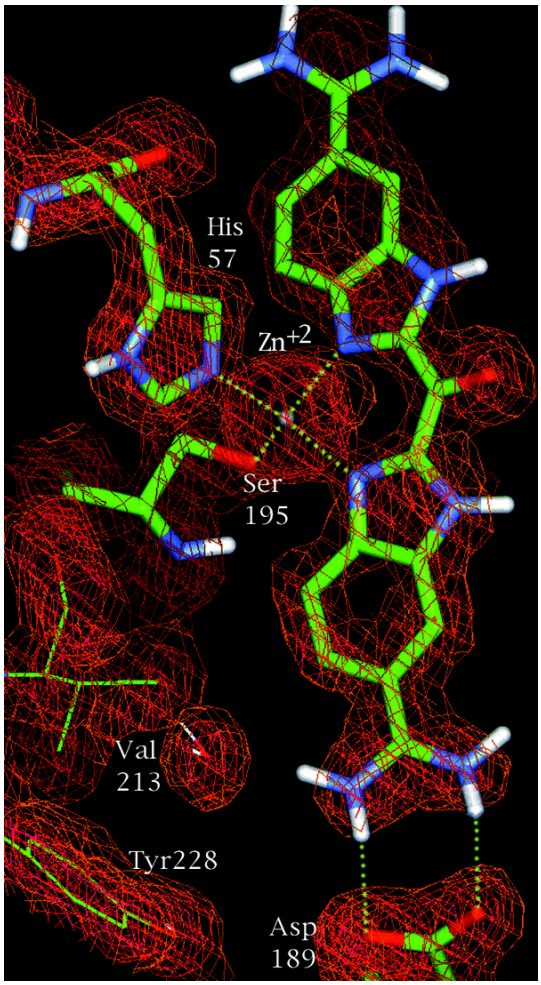

1.9.3 Non-amidine based inhibitors of thrombin

1.9.3.1 SSR-182289 (90): its design is based on the argatroban (**1**) structure. It is characterized as an oral, competitive, reversible thrombin inhibitor [160]. Compound **90** not a prodrug and its oral bioavailability is due to its 3-amino-pyridine moiety (pK_a close to 7.5) [160]. It has good selectivity, thrombin Ki= 31 nM, while the trypsin Ki= 54μM. It is also selective towards the other serine protease inhibitors including FXa (Ki= 167 μM). All of the Ki values for FVIIa, FIXa, plasmin, urokinase, tPA, kallikrein and aPC exceed 250 μM [160].

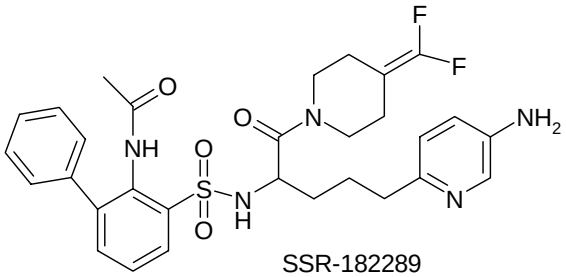

SSR-182289

90

1.9.3.2 TRI50c (91): it is a derivative of DUP 714 (**76**). Its thrombin Ki= 9 nM. Its trypsin Ki= 1 μM and it exhibits even better selectivity versus the other serine proteases [161].

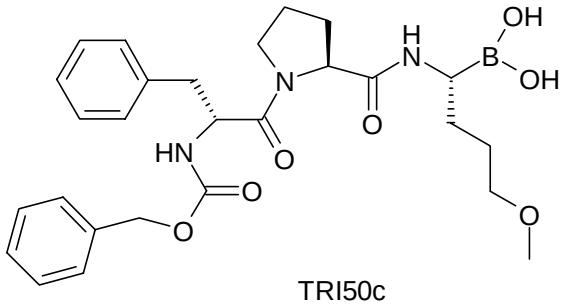

TRI50c

91

1.9.3.3 LB-30057 (92): This DTI is a tripeptide mimic that contains a less basic group at the P1 position. The amidrazonophenylalanine group confers better orally bioavailability over more basic moieties [162]. The thrombin Ki= 0.38 nM and it is considered to be selective [135]. Additional testing showed that an ortho substituted fluorine on the amidrazonophenylalanine ring improved oral activity [162].

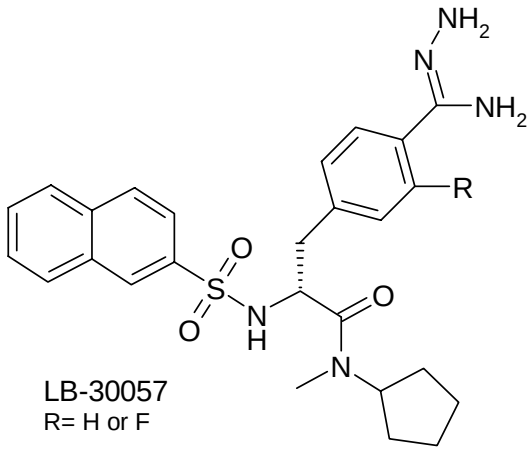

92

1.9.3.4 LB-30870 (**93**): it is a derivative of LB-30812 (**85**) with good oral activity. It contains a 2,5-thienylamidine as a less basic P1 moiety and also has a carboxylic acid. Although it is less basic than other moieties, it is still able to form strong ionic interactions with Asp189 (figure 37). It has a thrombin Ki= 15 pM and a trypsin Ki= 300 pM [163].

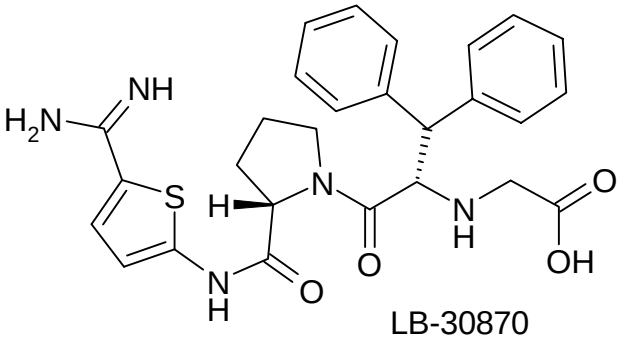

LB-30870

93

Figure 37. Compound **93** is bound to thrombin in a surface representation. The diphenyl moiety fits in the P4 site. Oxygen atoms are shown in red, nitrogen atoms are shown in blue, sulfur is shown in yellow and carbons are shown in either green or dark-gray. This image is adapted directly from [163].

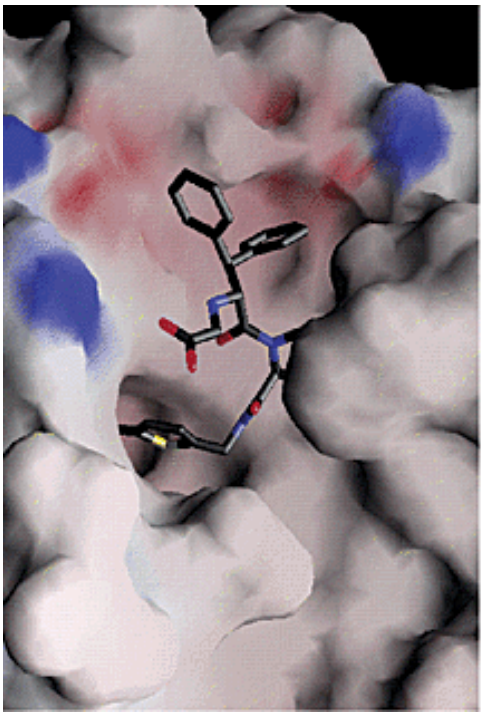

1.9.3.5 **N-oxide derivatives**: In compound **94**, fluorine was placed on the benzylamide which yielded a Ki for thrombin of 2.3 nM. It also has better solubility and improved oral activity [164]. Compound **95**, with an N-oxide on central ring, yielded a thrombin Ki= 3.2 nM [165].

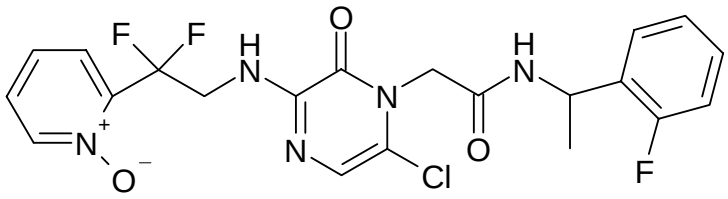

94

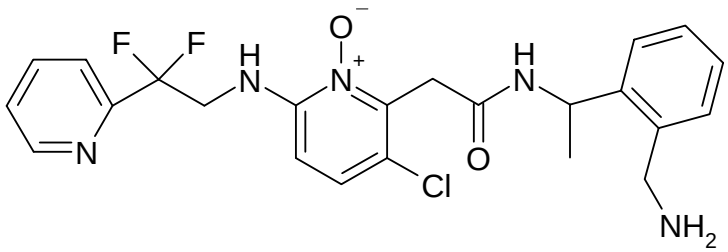

95

N-OXIDE DERIVATIVES

1.9.16 Non-small molecule inhibitors of thrombin

1.9.16.1 **Theromin**: described as the most potent thrombin inhibitor to date. It is produced by the Rhynchobdellid leech *Theromyzon tessulatum* (also produces Therostasin) as a homodimer (14.5 kDa) composed of 67 amino acids, 16 of which are Cys. Theromin is specific for thrombin and shows no activity against other serine proteases. The thrombin

Ki= 12 ± 5 fM [166]. This is superior to the thrombin Ki for hirudin and Haemadin (21 fM and 99 fM, respectively) [167]. Although dimerization is required for maximal activity, individual monomers are capable of inhibiting thrombin.

1.9.16.2 Haemadin: a slow, tight binding thrombin inhibitor (~5 kDa) produced by the Indian leech, *Haemadipsa sylvestris*. Haemadin is selective for thrombin over other serine proteases. The thrombin Ki= 99 ± 26 fM for native haemadin. Recombinant haemadin has also been produced and the thrombin Ki is comparable (Ki= 210 ± 62 fM) [167]. Structural studies demonstrate that haemadin binds to both the active site and exosite II (figures 38 and 39) [150].

Figure 38. Haemadin (green) bound to thrombin. This image was created from the PDB file 1e0f using sybyl 7.2.

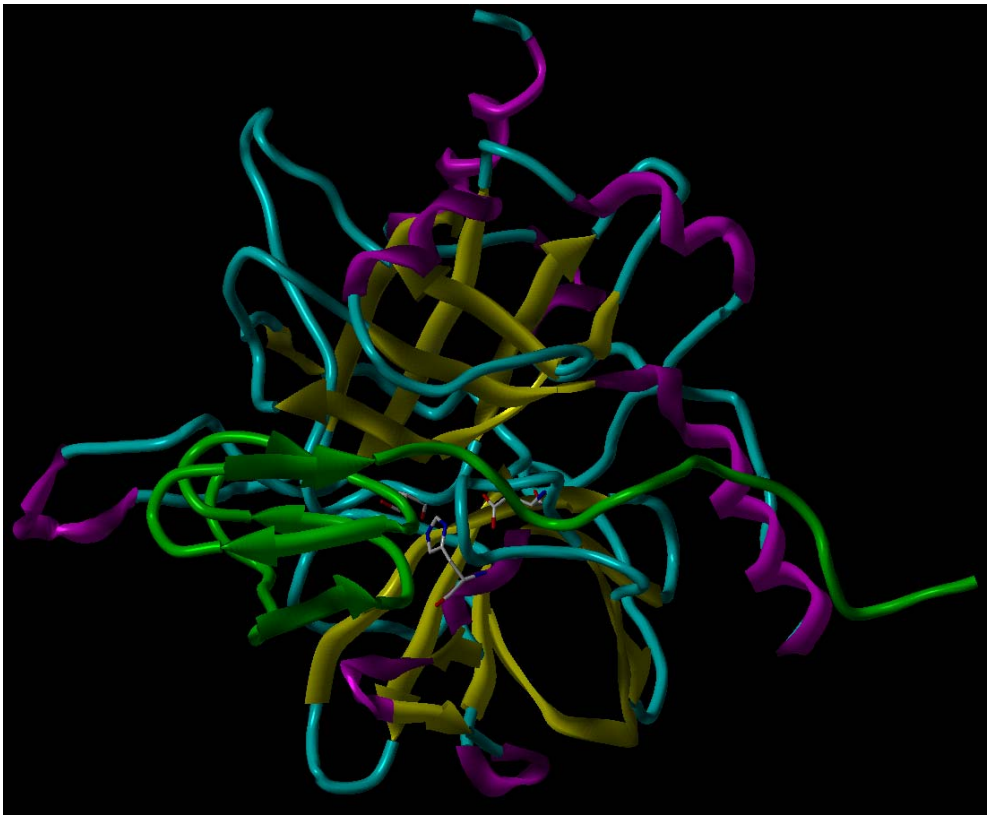

Figure 39. Haemadin (green) bound to thrombin. This image was created from the PDB file 1e0f using sybyl 7.2.

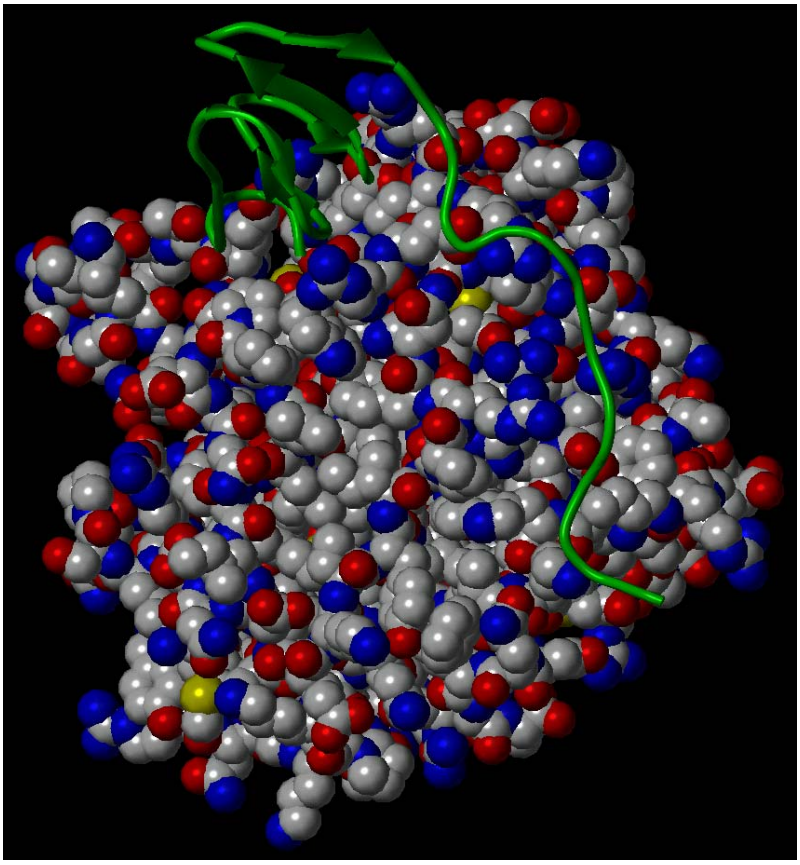

1.9.16.3 Bufrudin: an anticoagulant protein (~7 kDa) derived from the salivary glands of the Asian leech, *Hirudinaria manillensis*. Bufrudin is a potent, direct thrombin inhibitor with some homology to hirudin. The N-terminal proteolytic fragment composed of residues 1-47 is responsible for the thrombin inhibitory activity [118, 168].

1.9.16.4 Triabin: a 142 residue (~17 kDa) anticoagulant protein derived from the saliva of the insect, *Triatoma pallidipennis*. Recombinant triabin has been expressed in E. coli as well a baculovirus/insect system [169]. Triabin is a thrombin inhibitor that forms a noncovalent complex with thrombin, which leads to inhibition of thrombin-induced platelet aggregation and a prolongation of both thrombin clotting time and APTT. The triabin platelet aggregation IC_{50}= 2.6 nM, which was more potent than hirulog and the synthetic active site inhibitor, α-NAPAP (IC_{50}= 280 nM and 21 nM, respectively) [170]. The amidolytic activity of small peptide substrates by thrombin is not inhibited by triabin. Furthermore, triabin inhibits the cleavage of thrombin by trypsin and inhibits the effects of thrombomodulin on thrombin. These results suggest that triabin interacts with exosite I of thrombin and not the active site. Triabin potently inhibits the thrombin mediated fibrinogen conversion to fibrin (Ki= 3 pM) [169]. Triabin inhibited thrombin mediated arterial relaxation with an IC_{50}= 3.2 nM, which compared favorably with hirudin (IC_{50}= 1.5 nM) [170]. Structurally, triabin is a single domain protein consisting of an eight-stranded β-barrel [171]. The center of the barrel houses a hydrophobic core that also has a cluster of residues that form several salt bridges. The majority of the triabin, thrombin exosite I interactions are hydrophobic in nature. The side chain of thrombin Arg77 reaches into the hydrophobic core and makes ionic interactions with two of the triabin amino acids. It is clear from the crystal structure that triabin does not interfere with the active site of thrombin and exclusively occupies the exosite region, consistent with the previous experimental results [171].

1.9.16.5 Bothrojaracin: an anticoagulant protein produced by the venomous South American snake, *Bothrops jararaca*. It has a molecular weight of ~27 kDa and is composed of two polypeptide chains (15 and 13 kDa) that are connected via a disulfide linkage. Bothrojaracin is a thrombin inhibitor that forms a noncovalent complex with thrombin by interacting with both exosite I and II. This complex does not disturb or occlude the active site because small peptide substrates can still be hydrolyzed. Depending on the thrombin concentration, bothrojaracin is capable of potently inhibiting thrombin-induced platelet aggregation (IC_{50} values range from 1-20 nM). Bothrojaracin is able to prolong fibrinogen clotting time. This is due to the ability of bothrojaracin to potently compete with fibrin(ogen) for exosite I (Ki= 15 nM). Additionally, bothrojaracin is able to inhibit thrombin binding to thrombomodulin by 87% and subsequently, bothrojaracin decreases the rate of protein C activation by thrombin. Bothrojaracin is also capable of competing with hirudin for exosite I, indicating its potent nature [172]. The thrombin Kd= 0.62 ± 0.2 nM for bothrojaracin and the C-terminal hirudin peptide (exosite I specific ligand) is capable of inhibiting this interaction (Ki= 50 ± 16 nM). One isoform of thrombin, known as γ-thrombin, is characterized by having a disrupted exosite I due to controlled proteolysis by trypsin. The γ-thrombin Kd= 0.30 ± 0.07 μM for bothrojaracin. This is substantially greater than the α-thrombin dissociation constant, indicating the importance of exosite I in thrombin recognition by bothrojaracin. However, this Kd clearly indicates that additional areas of thrombin are involved in bothrojaracin binding. Bothrojaracin is able to decrease the rate of heparin mediated antithrombin inhibition of α- and γ-thrombin, but it has no effect on the antithrombin inhibition of α- and γ-thrombin in

the absence of heparin. The presence of heparin or prothrombin fragment 2, both exosite II ligands, inhibited the binding of bothrojaracin to α- and γ-thrombin. These three experiments taken together indicate that bothrojaracin also binds to exosite II in addition to exosite I. Bothrojaracin is also able to bind to prothrombin with a Kd= 31 ± 14 nM. This interaction does not require Ca^{2+} and it is inhibited by heparin, indicating that bothrojaracin binding to prothrombin is exosite II mediated. Additionally, bothrojaracin is able to inhibit clot bound thrombin. Bothrojaracin was able to inhibit clot-induced platelet activation with an IC_{50}= 35 nM [173].

1.9.16.6 Rhodniin: a thrombin inhibitor (103 amino acid residues, ~11 kDa) that is produced by the insect, *Rhodnius prolixus* [174]. Rhodniin is a two domain protein that can be expressed in a recombinant form by *E. Coli*. The thrombin Ki for rhodniin and recombinant rhodniin is 203 ± 87 fM and 172 ± 52 fM, respectively. The crystal structure of recombinant rhodniin and bovine thrombin shows that the N-terminal rhodniin domain binds to the active site of thrombin in a substrate-like manner. The reactive site loop of the N-terminal domain (Cys6-Arg14) binds in the thrombin active site, with the His10 residue binding in the S1 pocket by making hydrogen bonds and ionic interactions with Asp189 and Glu192. This appears to be the first example of a His residue acting as a P1 residue [175]. The scissile peptide bond is His10-Ala11 of rhodniin and it appears to remain intact in the thrombin complex. The His10 carbonyl is located in the oxyanion hole and makes hydrogen bond interactions with the backbone nitrogens of Gly193 and Ser195. The C-

terminal domain of rhodniin binds to exosite I through numerous electrostatic interactions [175].

1.10 Dual serine protease inhibitors

The notion of inhibiting multiple steps in the process of coagulation has been employed by blood sucking animals for millions of years. The medicinal leech, *Hirudo medicinalis*, produces the potent thrombin inhibitor hirudin as well as a prostaglandin-like compound that inhibits platelet aggregation [61]. The soft tick *Ornithordus moubata* produces three anticoagulants, ornithodrin, TAP and moubatin, which inhibit thrombin, FXa and platelet aggregation, respectively [61]. Strong evolutionary pressure has been placed on a blood sucking species' ability to thwart the procoagulant systems of its host. It seems logical that perhaps the best way to anticoagulate blood in patients, is to use dual inhibitors of coagulation. A dual inhibitor of coagulation would be a single synthetic molecule or natural product that is capable of inhibiting two of the serine proteases of the coagulation cascade. The alternative to this would be the separate development of two selective serine protease inhibitors that are co-administered. This is obviously not as cost effective because of the need for individual preclinical and clinical studies as well as combined studies [61]. Dual inhibitors are already being used in anticoagulation as well as in the treatment of cardiovascular and renal pathologies. Unfractionated heparin (UFH) is capable of inhibiting both thrombin and FXa by activating antithrombin [61]. A class of drugs known as vasopeptidase inhibitors are dual inhibitors that act on both the

angiotensin-converting enzyme (ACE) and neutral endopeptidase, which are used to treat diseases of the cardiovascular and renal systems [176].

1.10.1 Dual thrombin and FXa inhibitors

These inhibitors block preexisting thrombin as well as prevent the formation of new thrombin. The thrombin active site is larger and more hydrophobic, than the FXa active site. Yet, both enzymes have similar S1 pockets and their difference in specificity is best determined by their S2 pockets. Thrombin has a YPPW loop that is compact and rigid, which creates a small hydrophobic pocket [57], while the S2 site of FXa is blocked by Y99, which prevents bulky groups from binding that location [177]. The S3 pockets for both enzymes accommodate hydrophobic bulk, while in terms of ionic character; only the S3 pocket of FXa has some electronegative groups. Thus, FXa inhibitors that contain both hydrophobic and cationic substituents fit in the S3 binding pocket [92, 129]. Because, trypsin has an active site that is more accommodating than thrombin selectivity of dual thrombin/FXa inhibitors over trypsin is a major challenge.

1.10.1.1 1-methylbenzimidazole compounds:

1.10.1.1.1 ***BIBM1015*** (**96**): Thrombin Ki= 20 nM, FXa Ki= 15 nM, trypsin Ki= 102 nM [178].

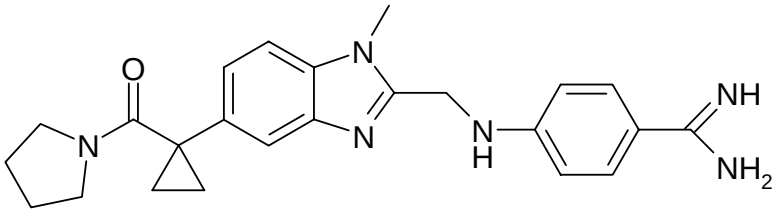

BIBM1015

96

1.10.1.1.2 ***BIBR830ZW*** (**97**)*:* Thrombin Ki= 4.8 nM, FXa Ki= 160 nM [61].

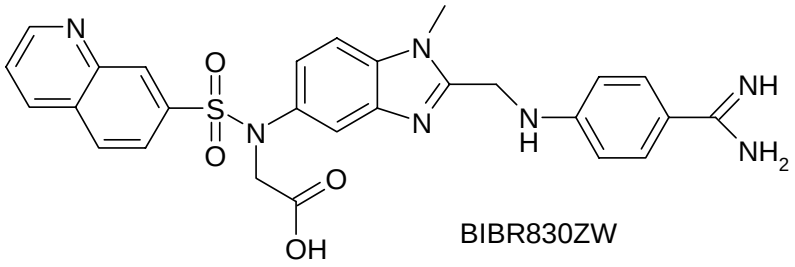

BIBR830ZW

97

1.10.1.2 1,2,5-trisubstitiuted benzimidazole scaffold:

***1.10.1.2.1 BIBR 953* (98):** Thrombin Ki= 4.5 nM, FXa Ki= 3760 nM. By adding bulk to the S1 position, FXa activity is removed while thrombin potency is retained [156].

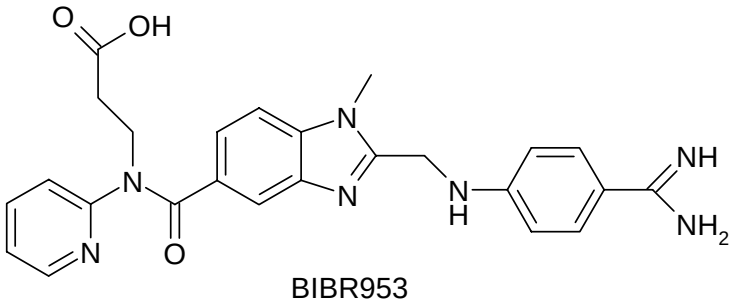

BIBR953

98

1.10.1.3 Oxazolpyridine series (**99**): Thrombin Ki= 0.04 nM, FXa Ki= 3.9 nM, low oral activity [179].

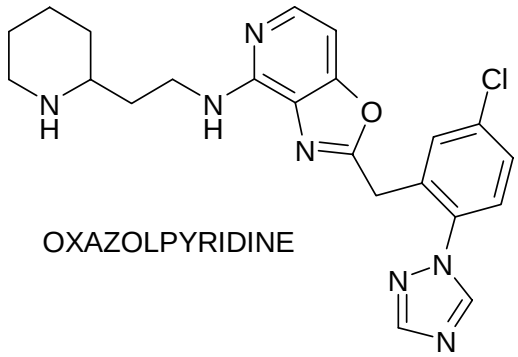

OXAZOLPYRIDINE

99

1.10.2 Dual FVIIa and FXa inhibitors

The greatest difficulty for making these inhibitors is that trypsin is less specific than the coagulation proteases, primarily because of its larger active site [59]. Amplification is a major component of the coagulation cascade, so it is logical to design compounds that inhibit more than one enzyme. Specifically, it is better to inhibit the enzymes that are directly linked to each other within the cascade [61]. The S1 pockets of all three enzymes are similar in shape but differences are also present. FVIIa has a S190 while thrombin and FXa have A190 [129, 178]. The greatest variation is in the S2 pocket. FVIIa has a small cavity in S2 while FXa is blocked by Y99 and thrombin has partial blockage by L99. The transition between S2 and S3 is well defined in FVIIa [180]. By inhibiting enzymes earlier in the pathway, clot formation can be prevented with the bleeding risks associated with thrombin inhibition.

1.10.2.1 2'-sulfamoyl and 2'-methylsulfamoyl substituted biphenyl group series:

These compounds contain a benzamidine moiety, a linker and a biphenyl moiety. The best compound is compound **100**, with a factor VIIa and factor Xa IC_{50} value of 13 nM and 20 nM, respectively [61]. Compound **100** has a 2-phenylacetamide linker and a 2'-sulfamoyl as the biphenyl. The best 2'-methylsulfamoyl of this series is compound **101** with a factor VIIa and factor Xa IC_{50} value of 46 nM and 110 nM, respectively. Compound **102** has 2'-methylsulfamoyl but the benzamidine is replaced by neutral p-chlorophenyl [61]. This is to improve pharmacokinetics since the benzamidine leads to poor oral bioavailability. The FVIIa and FXa IC_{50} values for this compound are 65 nM and 86 nM, respectively.

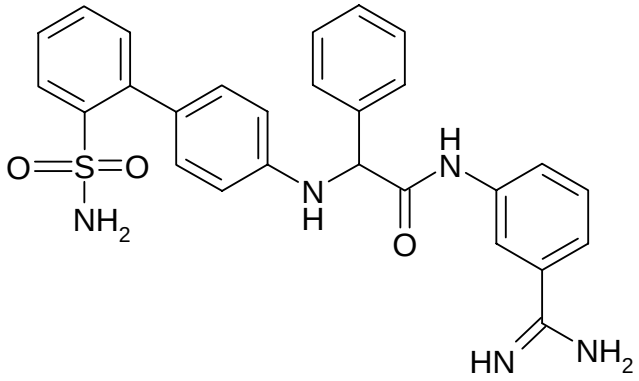

100

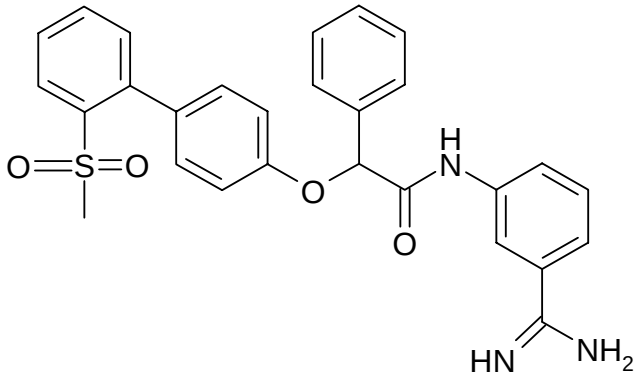

101

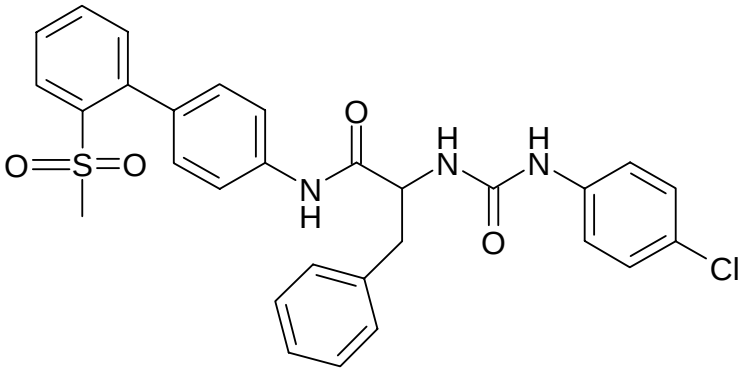

102

1.10.2.2 Morpholin-4-ylphenyl (103): FVIIa IC_{50}= 22 nM, FXa IC_{50}= 34 nM. [61].

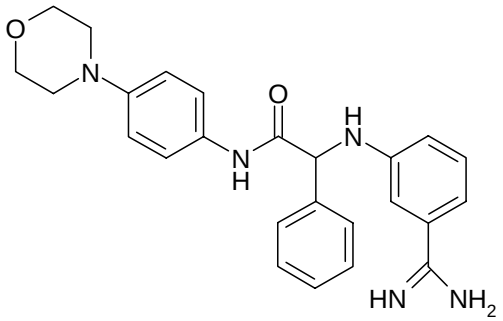

MORPHOLIN-4-YLPHENYL

103

1.10.2.3 2-oxo-piperidin-1-ylphenyl (104): FVIIa IC_{50}= 14 nM, FXa IC_{50}= 32 nM. [61].

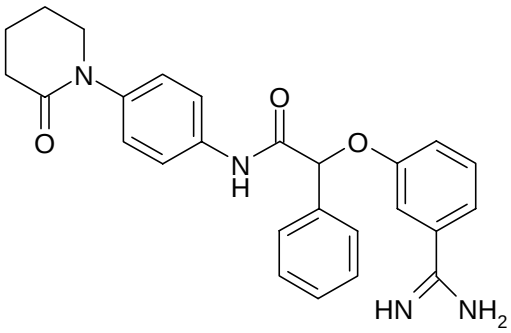

2-OXO-PIPERIDIN-1-YLPHENYL

104

1.10.2.4 2-oxo-pyrolidin-1-ylphenyl (105): FVIIa IC_{50}= 65 nM, FXa IC_{50}= 39 nM. [61].

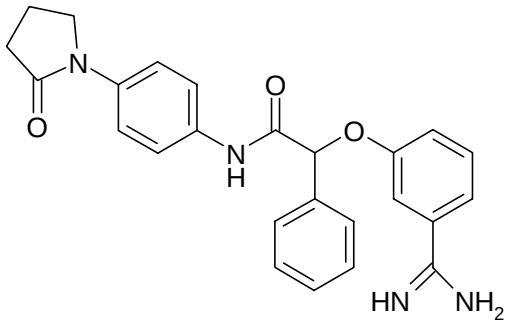

2-OXO-PYROLIDIN-1-YLPHENYL

105

1.10.2.5 Semicarbazide derivatives: Additional structural modifications found that semicarbazide derivatives were also equipotent [59]. Compound **106** has a factor VIIa and factor Xa IC_{50} value of 9.8 nM and 16 nM, respectively. Compound **107** has a factor VIIa and factor Xa IC_{50} value of 5.1 nM and 8.6 nM, respectively.

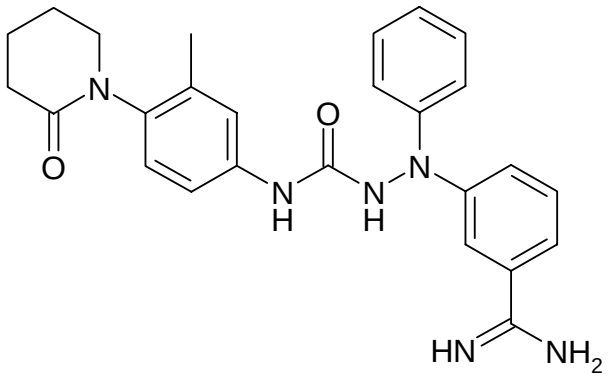

106

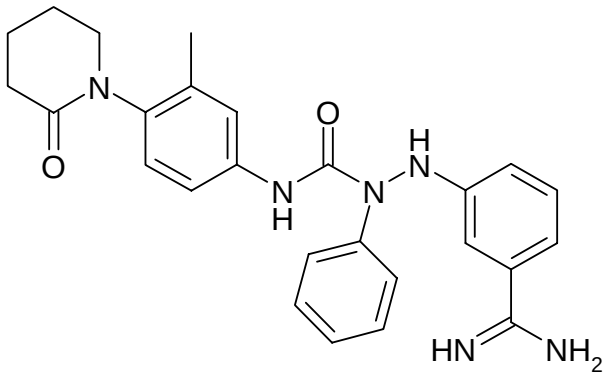

107

SEMICARBAZIDE DERIVATIVES

1.10.2.6 5-aminoindole series: Compound **108** has better selectivity for other serine proteases but compound **109** is more potent for FXa. The affinity values for compound **108** are FVIIa Ki = 3 nM and FXa Ki = 60 nM. The affinity values for compound **109** are FVIIa Ki = 3 nM and FXa Ki = 15 nM [61].

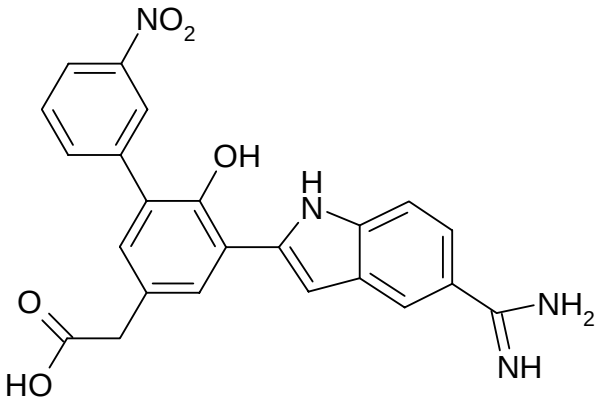

108

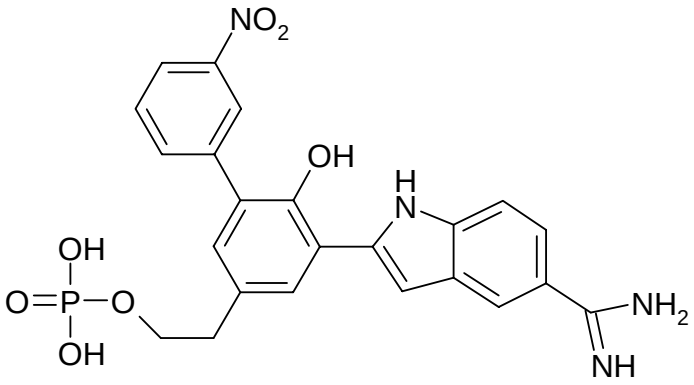

109

5-AMINOINDOLE SERIES

1.10.2.7 Carbohydrate derivative (110): These structures contain two benzamidine rings connected by a carbohydrate linker. It is able to inhibit both proteases but the linker must be attached at both meta positions in order to achieve nanomolar potency [59]. The most potent structure has a factor VIIa and factor Xa IC_{50} value of 100 nM and 150 nM, respectively.

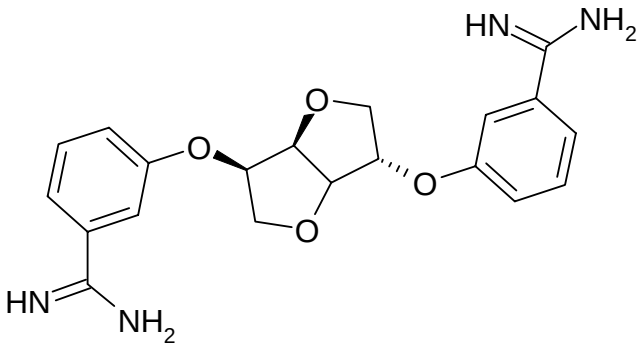

CARBOHYDRATE DERIVATIVE

110

1.10.2.8 Neutral/less basic inhibitors: Instead of making a benzamidine prodrug, it is possible to change to a less basic or neutral group but still achieve active site directed inhibition [59]. The best example of these compounds (**111**) has a factor VIIa and factor Xa IC_{50} value of 99 nM and 58 nM, respectively.

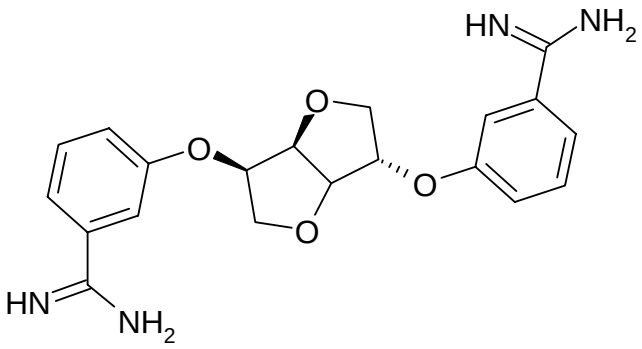

CARBOHYDRATE DERIVATIVE

111

1.10.3 Dual FVIIa and thrombin inhibitors

This unique inhibitor, dysinosin A (**112**), is a natural product derived from a marine sponge (family *Dysideidae*). Its FVIIa Ki= 108 nM and Thrombin Ki= 452 nM [181]. The guanidine moiety occupies the S1 pocket.

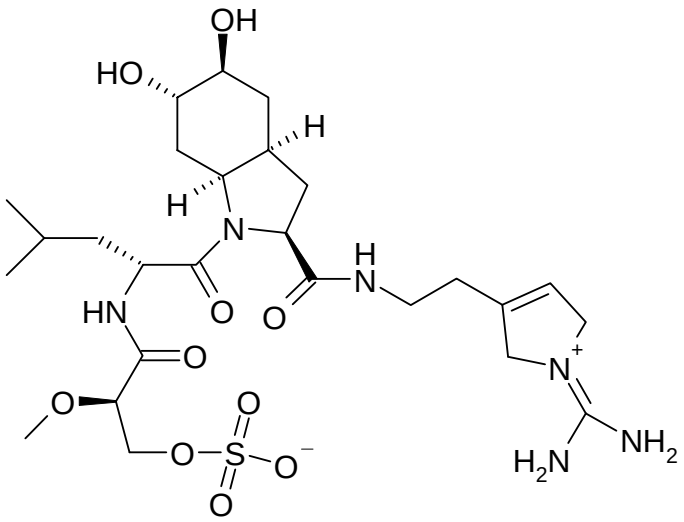

DYSINOSIN A

112

1.10.4 Dual inhibitors of FIXa and FXa

These inhibitors will effectively block the intrinsic cascade while leaving the extrinsic cascade intact. An initial screen identified an amidinoindole inhibitor (**113**) with a FIXa Ki = 66 nM and a FXa Ki = 0.63 nM [182].

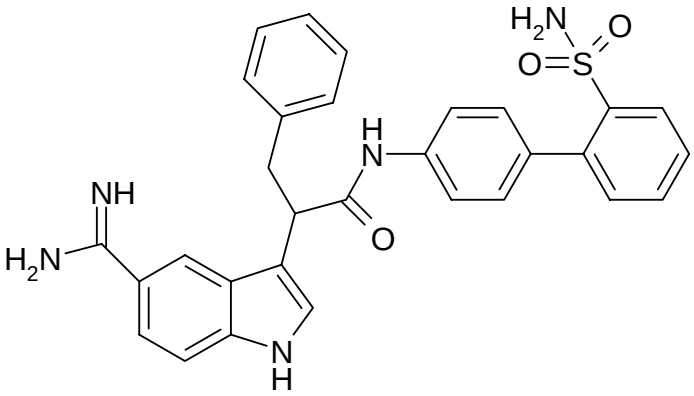

DUAL FIXa/FXa LEAD COMPOUND

113

From this lead (**113**), a series of 5-amidino-benzo[*b*]thiophene compounds were synthesized (**114**). Based on docking studies, the 5-amidinoindole did not fit well into the FIXa active site while it fit extremely well into FXa. The 5-amidinoindole group forms a hydrogen bond with Ser195 in FXa but not FIXa. The hydrogen bond with Ser195 is responsible for the 1000-fold difference in the initial lead structure. The introduction of a 5-benzo[*b*]thiophene group eliminates that specific hydrogen bond in FXa and the potency becomes more equivalent [182]. For **114**, the Ki for FIXa becomes 74 nM and the Ki for FXa becomes 47 nM.

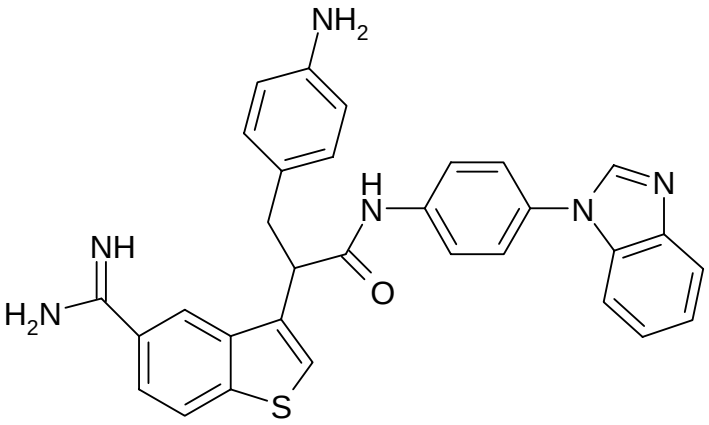

5-AMIDINOBENZO[*b*]THIOPHENE

114

Chapter 2: Rationale

2.1 Background

The clinical prevalence of thrombosis in several medical conditions creates a market for anticoagulants, which reached around $4 billion worldwide in 2004 [183]. Thrombotic disorders are the underlying cause of 38% of all non-communicable disease-related deaths worldwide [184]. Examples of these disorders include pulmonary embolism, deep-vein thrombosis, disseminated intravascular coagulation, acute myocardial infarction, unstable angina, cerebrovascular thrombosis, and others. Approximately 576,000 new cases of deep vein thrombosis (DVT) and pulmonary embolism (PE), two common thrombotic conditions, occur in the U.S. every year [185]. Additionally, thrombotic disorders are ~3 times more likely in people with cancer [186]. Anticoagulant drugs are used in the treatment and prevention of thromboembolic disorders. The most widely used anticoagulants today include the heparins (unfractionated heparin and low molecular weight heparin) and the coumarins (warfarin). The anticoagulant, unfractionated heparin (UFH), mediates its effect by accelerating the inactivation of thrombin and FXa, in the presence of antithrombin [187]. Low-molecular-weight heparins (LMWHs), introduced in the mid-1990s, have reduced side-effects, yet are still associated with risk of bleeding, variable patient responses and heparin-induced thrombocytopenia (HIT) [56]. Recently, the design of a five residue pentasaccharide, fondaparinux, which displays absence of HIT and

minimal bleeding, has been approved for use in patients [188]. Yet, the therapy is not cost-effective because fondaparinux synthesis is elaborate, laborious and low yielding. Newer anticoagulant agents have been introduced, including the hirudins (lepirudin, desirudin and bivalirudin), the pentasaccharides (fondaparinux and idraparinux), and the peptidomimetic small molecules (argatroban, dabigatran, ximelagatran, razaxaban and DX9065a) [21]. However, these new anticoagulation therapies are hindered by a significant number of adverse reactions including enhanced bleeding risk, immunological reaction, genetic variation in metabolism, food or drug interactions and liver toxicity. In addition, problems such as patient-to-patient response variability, narrow therapeutic index, inadequate duration of action, poor oral bioavailability, the need for frequent coagulation monitoring, and high cost to benefit ratio further complicate their effective use in the treatment of thrombotic conditions. We reasoned that to reduce the problems associated with the current anticoagulation therapy, molecules with a radically different structure from all the current agents (the heparins, warfarins, hirudins, and the peptidomimetics) need to be discovered. This idea is based on the concept that structure dictates function. The structure of the anticoagulant mediates its interaction with its appropriate drug target. Three such examples are heparin, hirudin and argatroban. Heparin contains a pentasaccharide sequence, which binds and activates antithrombin. Hirudin has a highly evolved tertiary structure that specifically interacts with the active site and exosite I of thrombin. Argatroban (**1**) has an Arg residue side chain that anchors it in the thrombin active site. However, the structure of an anticoagulant also mediates undesirable interactions, causing the drug's side effect profile and dictating its route of administration.

Heparin's structural heterogeneity causes variable inter- and intra-patient responses because each dose is structurally different from every other dose (like a snowflake) [56]. Heparin's nonspecific binding to platelet factor 4 (PF4) creates an antigenic epitope that induces an immunologic response resulting in the formation of antibodies against the complex. This in turn causes HIT [189]. Hirudin's highly evolved tertiary structure binds so tightly to thrombin that is essentially irreversible and can not be displaced by an antidote, leading to an increased bleeding risk [38]. Since it is a foreign peptide, it is extremely immunogenic [38]. Argatroban's Arg side chain has a high pKa, which means it will be ionized in the GI tract and therefore not orally bioavailable [45]. To design better, more cost-effective, and possibly orally active anticoagulants, we looked for chemical structures that would be structurally different from all current anticoagulants, easily synthesized and amendable to prodrug design.

2.2 New antithrombin-based anticoagulants

Over the last three decades, major effort has focused on discovering anticoagulants that are heparin-based derivatives. These include natural polysaccharides, synthetically modified heparins and synthetic oligosaccharides [187]. Our laboratory has advanced the concept that non-heparin molecules, which are synthetic and sulfated, may be designed to function as activators of antithrombin [190-192]. This work has led to the design of highly sulfated bicyclic-unicyclic molecules, which activate antithrombin and accelerated inhibition of FXa [190-192]. These molecules are attractive because they are not polysaccharide-based and they utilize conformational activation of antithrombin as the mechanism of activation.

Our laboratory reasoned that antithrombin activation should also be possible with non-sulfated molecules based only on carboxylic acid groups. As a proof of the principle, linear polyacrylic acids (PAA) (**115**) were found to bind antithrombin and significantly accelerate the inhibition of FXa and thrombin. PAAs are simple, linear, organic polymers containing only one functional group, the carboxylic acid moiety [193, 194]. They bear no structural resemblance to heparin and do not contain sulfate groups. A specific advantage of the carboxylic acid group is its feasibility of conversion to a prodrug form for oral delivery. Yet, PAAs bind antithrombin with poor affinities under physiological conditions, which precludes their use as anticoagulants [193, 194].

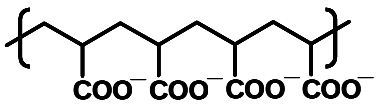

	M_R	Monomers
PAA1500	1,500 Da	~21-mer
PAA2280	2,280 Da	~32-mer
PAA3450	3,450 Da	~48-mer
PAA6200	6,200 Da	~86-mer

115

2.3 Sulfated Dehydropolymers (DHPs)

The absence of non-ionic binding forces in antithrombin-PAA interactions results in weak binding under physiological conditions and their ability to chelate of Ca^{+2} ions nullifies their anticoagulant activity in APTT assays [193, 194]. Thus, we sought a scaffold with carboxylate and sulfate groups that 1) can bind to antithrombin, FXa and thrombin 2) that does not chelate Ca^{+2} ions; 3) that shows non-ionic binding in addition to electrostatic binding; and 4) that are amenable to structural modifications for introducing oral activity in the future. Our rationale was that appropriate positioning of carboxylate and sulfate groups should not favor Ca^{+2} binding, should favor tight binding to antithrombin and should afford orally active synthetic prodrugs.

Dehydropolymers (DHPs), from cinnamic acid derivatives meet the above criteria. Synthesis of these polymers was inspired by the biosynthesis of lignin, an abundant natural plant product assembled through enzymatic-oxidative coupling of phenyl-propenoid radicals. DHPs, the synthetic *in vitro* version of natural lignins, are assembled through horseradish peroxidase catalyzed coupling of cinnamyl radicals [195-197]. Furthermore, the intermonomeric linkages of DHPs have been structurally characterized [198-199].

To design better, more cost-effective, and possibly orally active anticoagulants, we have synthesized a new class of anticoagulant molecules using a chemo-enzymatic approach. Synthetic lignins, referred to as DHPs, are obtained using enzymatic coupling of cinnamyl radicals and can possess several different inter-monomer linkages. In addition to micro-heterogeneity, the free radical coupling mechanism generates polydispersity within the DHP mixture. These variations introduce significant structural diversity, which is necessary for rapid scaffold evaluation. Our DHPs were prepared through peroxidase-catalyzed oxidative coupling of the commercially available 4-hydroxycinnamic acids, caffeic acid (CA), ferulic acid (FA) and sinapic acid (SA) (**116**). We have discovered that chemo-enzymatically synthesized lignins, represented by three sulfated dehydropolymer (DHP) molecules, named **CDs**, **FDs** and **SDs**, possess extremely interesting anticoagulant properties and a novel mechanism of action.

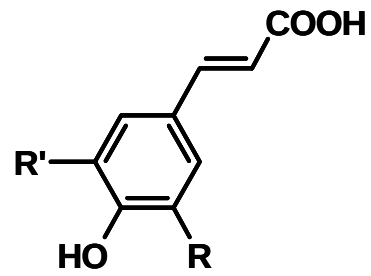

CA: R = OH; R' = H
FA: R = OMe; R' = H
SA: R = OMe; R' = OMe

116

These DHPs are designed to mimic heparin. The oligomeric and polyanionic nature of individual DHP molecules, as well as the polydispersity and micro-heterogeneity present in a DHP mixture is similar to that of heparin. The ability of 4-hydroxycinnamic acids to accept sulfate groups made them especially desirable for designing heparin mimics. Heparin is a series of six-membered rings, linked into a polymer and then it is enzymatically modified (sulfates added). DHPs are created by enzyme mediated free radical coupling, followed by chemical modification (sulfates added). The aromatic ring in a cinnamic acid is approximately the same size as a heparin monomer. However, DHPs have a planar geometry while carbohydrates have various conformations. Furthermore, the intermonomeric linkages between cinnamic acid monomers are slightly longer than the linkages in heparin. The cinnamic acid backbone is substantially more hydrophobic in comparison to the carbohydrate backbone of heparin. The chapters that follow detail the synthesis, structural characterization, mechanism of action, *in vitro* and *ex vivo* potency of our novel, sulfated DHPs. Thus, these molecules were synthesized and studied for anticoagulant properties.

Chapter 3: Novel Chemo-Enzymatic Oligomers of Cinnamic Acids as Direct and Indirect Inhibitors of Coagulation Proteinases

3.1 ABSTRACT

Thrombin and factor Xa, two important procoagulant enzymes, have been prime targets for regulation of clotting through the direct and indirect mechanism of inhibition. Our efforts on exploiting the indirect mechanism led us to study a carboxylic acid-based scaffold, which displayed major acceleration in the inhibition of these enzymes [193, 194]. This work advances the study to chemo-enzymatically prepared oligomers of 4-hydroxycinnamic acids, DHPs, which display interesting anticoagulant properties. Oligomers, ranging in size from tetramers to pentadecamers, were prepared through peroxidase-catalyzed oxidative coupling of caffeic, ferulic and sinapic acids, and sulfated using triethylamine–sulfur trioxide complex. Chromatographic, spectroscopic, and elemental studies suggest that the DHPs are heterogeneous, polydisperse preparations composed of inter-monomer linkages similar to those found in natural lignins. Measurement of activated thromboplastin and prothrombin time indicates that both the sulfated and unsulfated derivatives of the DHPs display anticoagulant activity, which is dramatically higher than the reference polyacrylic acids. More interestingly, this activity approaches that of low-molecular-weight heparin with the sulfated derivative showing ~2–3-fold greater potency than the unsulfated parent. Studies on the inhibition of factor Xa and

thrombin indicate that the oligomers exert their anticoagulant effect through both direct and indirect inhibition mechanisms. This dual inhibition property of 4-hydroxycinnamic acid-based DHP oligomers is the first example in inhibitors of coagulation. This work puts forward a novel, non-heparin structure, which may be exploited for the design of potent, dual action inhibitors of coagulation through combinatorial virtual screening on a library of DHP oligomers.

3.2 INTRODUCTION

Thrombin and factor Xa, two critical enzymes of the coagulation cascade, have been targets of anticoagulation drug design for a long time [189]. Both enzymes can be inhibited directly or indirectly. Traditional anticoagulants, including heparin, low-molecular-weight heparin (LMWH) and warfarin, are indirect inhibitors, which mediate their effects through an intermediary co-factor, such as antithrombin or vitamin K. For the past 7 decades these indirect inhibitors have been the mainstay of anticoagulant therapy. Yet, they suffer from several limitations, such as enhanced bleeding risk, unpredictable response, heparin-induced thrombocytopenia and lack of inhibition of clot-bound thrombin.

In contrast to indirect inhibition, direct inhibition of thrombin and factor Xa has been thought to be a better alternative, which promises to offer the important advantage of inhibition of both circulating and clot-bound thrombin. A prototypic member in this class of inhibitors is hirudin, which targets the active-site and exosite I of thrombin, and several derivatives of this peptide are now clinically available [37]. Intensive efforts are also being made to develop the first orally bio-available direct thrombin inhibitor. These are small

molecule pro-drugs that target the active site of these enzymes. However, challenges with these molecules include establishing enzyme binding affinity that is not associated with excessive bleeding, achieving inhibition of both clot-bound and unbound proteinases, and avoiding liver toxicity [37].

The traditional anticoagulant, heparin or LMWH, is an anticoagulant of choice because of its good efficacy and easy availability. It is a linear co-polymer of glucosamine (GlcN*p*) and iduronic acid (IdoA*p*) residues linked in a 1→4 manner [27]. Yet, heparin is a complex, heterogeneous, polydisperse molecule. Further, the high sulfation level of heparin generates massive negative charge density, thereby introducing an ability to bind to a large number of proteins in the plasma [29], a probable cause for its some of its side-effects.

To reduce the limitations of heparin therapy, we have focused on designing scaffolds that possess much lower anionic character, have more hydrophobic nature, and yet retain the function of heparin [190-194]. In the process, we have designed some small sulfated flavonoids that utilize the antithrombin conformational activation mechanism for factor Xa inhibition [190-192] and have studied polymers of acrylic acid that utilize the bridging mechanism for inhibiting thrombin [193, 194]. While our sulfated flavonoids displayed some 20-fold acceleration, polyacrylic acids (PAAs) displayed a massive 300–1,100-fold acceleration in antithrombin-dependent inhibition of factor Xa and thrombin. Yet, PAAs were not likely to be useful as anticoagulants because of their poor antithrombin binding affinity and ability to chelate Ca^{2+} ions under physiological conditions [194]. We reasoned that both these problems could be addressed simultaneously

through the introduction of two features – a more rigid hydrophobic backbone and some sulfate groups – in the PAA scaffold.

Scaffolds of the size of heparin (or LMWH) that simultaneously possess these two properties are difficult to find. Other than natural polysaccharides, only a couple of natural macromolecular structures are known – condensed tannins and lignins – that could possibly be simultaneously hydrophobic and anionic. Whereas condensed tannins, or proanthocyanidins [200, 201] are polymers of either flavan-3-ol, or flavan-4-ol, or flavan-3,4-diol monomers, lignins are polymers of phenylpropanoid monomers [202, 203]. The presence of aromatic skeleton and phenolic, as well alcoholic, groups in both these structures ensures a combination of hydrophobic and anionic character.

We chose to explore lignin derivatives in view of the considerable literature available on the chemo-enzymatic synthesis of lignins [195, 204]. Synthetic lignins, also called dehydrogenation polymers (DHPs), are prepared from cinnamyl alcohol monomers using oxidative radical coupling and possess at least four types of inter-monomer linkages, including β-*O*-4 and β-5 (figure 40, page 164). These variations introduce significant heterogeneity and complexity in the macromolecule, thereby generating high structural diversity necessary for rapid evaluation of structures.

We describe our initial results with oligomers of cinnamic acid as novel coagulation inhibitors. The DHP oligomers were prepared in good yields through chemo-enzymatic oxidative coupling of 4-hydroxycinnamic acids [204, 205]. The DHPs prolong activated thromboplastin and prothrombin time, APTT and PT respectively, with approximately equal potency as LMWH. Preliminary studies suggest that the DHPs inhibit

factor Xa and thrombin in an antithrombin –dependent and –independent manner suggesting an interesting dual inhibition approach. While in depth studies are necessary to understand specific structural and mechanistic aspects of these DHPs, our results put forward a potent, non-heparin structures, the 'lignin carboxylates', for rational, anticoagulant drug design.

3.3 RESULTS

3.3.1 Synthesis of Dehydrogenation Polymers

Three cinnamic acid derivatives, caffeic acid, ferulic acid and sinapic acid, were chosen for homo-polymerization primarily due to their ability to hydrogen bond, form ionic interactions and undergo sulfation. HRP–catalyzed oxidation of these monomers generates radical intermediates, especially I_1 and I_2 (figure 40), which couple with monomers to give β-*O*-4- and β-5-linked dimeric units. These units undergo chain extension with radicals, such as I_1 and I_2, to give DHPs. Simultaneously, side reactions, such as decarboxylation, may occur to give variant oligomers. The DHPs were judged to be heterogeneous through size-exclusion and reverse-phase chromatographies (not shown).

To determine the average molecular weight of these polymers, we synthesized their acetylated derivatives CD_{AC}, FD_{AC} and SD_{AC} and utilized non-aqueous SEC, a technique found useful for lignins and cinnamyl alcohol-based DHPs [206]. CD_{AC} and SD_{AC} gave comparable SEC chromatograms, while FD_{AC} displayed a significant shift toward higher molecular weight species (Figure 42, page 166). The peak-average molecular weight (M_P) of acetylated CD, FD and SD was found to be 1,180, 2,480 and 1,190 Da, respectively,

while the number-average molecular weight (M_N) was 880, 1,870, and 1,020 Da, respectively, suggesting unsymmetrical distribution of higher and lower molecular weight chains. The weight-average molecular weight (M_W) was found to be 2,800, 3,650, and 2,990 Da, respectively, indicating that on average these oligomers are reasonably similar. Yet, the proportion of smaller chains is higher for both CD_{AC} and SD_{AC} than for FD_{AC}. Using the molecular weight of acetylated monomers, the average oligomer is estimated to be between 4–13-mer for CD, 8–15-mer for FD, and 4–11-mer for SD.

The DHPs were sulfated using $Et_3N{:}SO_3$ complex under conditions established earlier to obtain sulfated oligomers CD_S, FD_S and SD_S [192]. In this reaction, free phenolic and alcoholic groups are converted into organic sulfate groups resulting in an anionic oligomer. To assess the level of sulfation in these oligomers, elemental composition was determined. The C, H, and O composition of CD was found to be similar to SD, while that of FD, especially in the proportion of carbon, is significantly different (Table 2, page 157-158). Likewise, CD_S and SD_S compositions are similar, and unlike that of FD_S. Calculation of the elemental composition of these oligomers assuming a homogeneous decamer with β-*O*-4 inter-monomer linkage indicates striking similarity to the observed composition for FD and FD_S oligomers. In contrast, the observed composition for the other two DHP derivatives does not match the homogeneous decamer calculation (Table 2, page 157-158). This suggests greater proportion of structurally similar oligomers in FD and FD_S preparations, while CD and SD (also CD_S and SD_S) are expected to be more heterogeneous. The sulfur proportion in the sulfated DHPs remains fairly consistent in the range of 4.4 to 5.3 %, which corresponds to the presence of nearly 1 sulfate group every

2.5–3.3 monomers. Among the three derivatives, FD_S is the least sulfated preparation (Table 2, page 157-158).

An important question to address with regard to these heterogeneous and polydisperse oligomers was the ease and reproducibility of their synthesis. In multiple attempts on a several different scales (up to a gram of the oligomer), the polydispersity of samples as judged by SEC remained consistent suggesting a fairly reproducible process. In addition, the two-step synthesis is a controlled oligomerization process with greater than 60% isolated yield.

3.3.2 Characterization of Dehydrogenation Polymers (DHPs)

The IR spectra of sulfated and unsulfated DHPs (Figure 43, page 167) show the presence of aromatic structures (1,550 cm^{-1}), as expected. In addition, sulfated DHPs show peaks at 1,080 and 1,110 cm^{-1} characteristic of sulfate stretches. The ^{1}H NMR spectra of DHPs show the presence of broad peaks indicating polydispersity (not shown). In contrast, quantitative ^{13}C NMR spectra, recorded with inverse gated decoupling sequence, are more revealing (Figure 43, page 167). The ^{13}C NMR spectra of dehydro-dimers and -trimers of cinnamic acid derivatives as well as lignin samples suggests that the 165 – 172 ppm signals belong to carbonyl carbon of carboxylic acid, the 110 – 150 ppm signals belong to aromatic and vinylic carbons, the 65 – 100 ppm signals are due to alkoxy carbons C_α and C_β, while the signal between 56 – 60 ppm is because of the $–OCH_3$ group. Yet, significant differences exist between the oligomers. For example, whereas C_α and C_β peaks are prominent in the 65 – 110 ppm region for SD and CD (Fig. 43A and 43C, page 167), they

are nearly absent in this region for FD (Figure 43B, page 167). In addition, the carbonyl carbon intensities for SD and CD are ~25% and 10% lower than that for FD, respectively. Thus, two of the common side-reactions in oxidative coupling – decarboxylation of –COOH groups followed by reaction with a phenoxy radical – seem to have occurred less for FD. Although some decarboxylation is noticeable for CD, the presence of a prominent signal at 68 ppm and the much lower dispersion in the aromatic region indicative of minimal vinylic composition suggests greater possibility of several different types of inter-monomeric linkages (Figure 40, page 164). In contrast, ^{13}C NMR studies, in combination with elemental analysis, suggest that oligomer FD consists primarily of inter-monomeric linkages of β-*O*-4 type.

Mass spectrometry is an important technique used in elucidation of fine structure of polyphenol polymers, although the heterogeneity and complexity of these molecules presents a formidable challenge [207]. Attempts to identify higher oligomeric chains have not yielded much success because of instability of the polyphenolic structure even under mild ionization conditions, such as ESI [207]. We explored the applicability of MS to these 4-hydroxycinnamic acid oligomers to possibly identify the inter-monomer linkages and confirm the spectroscopic results. The ESI-MS spectrum of FD in the negative ion mode is shown in Figure 44A (page 168). Mass peaks were observed primarily in the region 150 – 400 m/z, yet, smaller peaks were observable between 400 and 700 m/z (inset in Figure 44A, page 168). Mass peaks at *p1* (681 m/z), *p2* (637 m/z) and *p3* (593 m/z) can be ascribed to singly charged tetramers of FD that have sequentially lost 2, 3 and 4 carboxylic acid moieties, respectively, while those at 533, 489, and 445 m/z (peaks *p4*, *p5*,

and *p6*) most likely arise due to a singly-charged trimer that has lost 1 through 3 CO_2, respectively (Figure 44B, page 168). Likewise, peaks *p7* (385), *p8* (341) and *p9* (297) are due to $[M_2]^{-1}$, $[M_2\text{-}CO_2]^{-1}$ and $[M_2\text{-}2CO_2]^{-1}$ mass fragments, while *p10* (193) is the singly-charged ferulic acid monomer. This analysis supports the result that HRP-catalyzed oxidative coupling of FD gives β-*O*-4-type inter-ferulic acid linkages with the presence of vinylic double bonds in the oligomer (Figure. 44B, page 168). Yet, this interpretation does not completely exclude other inter-monomer linkages, which may be present in smaller proportion as can be noted from the large number of as yet uncharacterized peaks in the ESI-MS.

A final point regarding the structure of our DHPs is that current spectroscopic data is insufficient to make definite stereochemical interpretation regarding olefinic linkages as well as substitution at the C_β position (Figure 40, page 164). The biosynthesis of lignins is largely considered to be achiral [205] and hence, we speculate that multiple isomers are present in the mixture of our oligomers.

3.3.3 Prolongation of Clotting Time

Prothrombin and activated partial thromboplastin time (PT and APTT) reflect the activity of the extrinsic and intrinsic pathways of coagulation and thus, are measures of the anticoagulation state of the plasma. PT and APTT were measured with citrated human plasma at six to eight concentrations of unsulfated and sulfated DHPs, while PAA, (+)-CS and LMWH (Figure 41, page 165) served as reference molecules. All samples showed considerable concentration-dependent prolongation of clotting time (Figure 45, page 169)

characterized by a rapid increase in time to clot. The anticoagulant activity is typically defined in terms of the concentration of the anticoagulant needed for doubling the normal plasma clotting time. A 2-fold increase in prothrombin time required plasma concentration of unsulfated DHPs in the range of 98–212 μg/mL (Table 3, page 159-160). This concentration decreased to 42–105 μg/mL, or nearly 2–3-fold lower, for sulfated DHPs. In contrast, for the reference molecules PAA and (+)-CS, a massive 4259 and 927 μg/mL concentration was required to achieve doubling of PT, while for a LMWH (from Sigma) 142 μg/mL was sufficient.

In a similar manner, doubling of APTT required ~25–40 μg/mL and ~13–23 μg/mL of unsulfated and sulfated DHPs, respectively. In contrast, the LMWH brought about 2×APTT at 5.9 μg/mL. These results suggest that unsulfated DHPs are less potent than their sulfated counterparts. In addition, a trend is discernible. Except for APTT with unsulfated DHPs, CD appears to be consistently more potent than FD, which in turn is better than SD and this trend holds for their sulfated derivatives.

Assuming homogeneous CD, FD and SD preparations with M_W of 2,800, 3,650, and 2,990 Da, respectively (Table 2, page 157-158), ~35–71 μM and ~15–35 μM of unsulfated and sulfated oligomers, respectively, would be needed for 2×PT. These concentrations change to 9–11 μM and 5–8 μM, respectively, for a doubling of APTT. In comparison, a homogeneous chain of PAA (M_W 2280 Da) will have to be present at 1870 μM for 2×PT, or at nearly 25–125-fold higher level over DHPs. For our small molecule reference, (+)-CS, ~1140 and 350 μM will be needed for doubling of PT and APTT,

respectively, which represents ~16–76-fold and ~32–70-fold higher levels than DHPs. But more importantly, the LMWH (M_W = 5,060 Da) gives values of 28 μM and 1.2 μM for 2×PT and 2×APTT, respectively. Thus, the concentration of DHPs, especially sulfated DHPs, required to double PT are similar to LMWH, while for doubling of APTT ~3–10-fold more sulfated DHPs are required.

3.3.4 Direct and Indirect Inhibition of Coagulation Proteinases

To investigate whether our DHPs affect proteolytic activities of coagulation proteinases present in plasma, of which factor Xa and thrombin are probably the most important, we measured residual enzymatic activity of the two enzymes following incubation for a defined time period with varying concentrations of DHPs in the presence and absence of antithrombin. The proteinase activity was determined under pseudo-first order conditions in a spectrophotometric assay using chromogenic substrates Spectrozyme FXa and TH for factor Xa and thrombin, respectively. As the concentration of DHP increases the residual proteinase activity decreases in a sigmoidal manner (Figure 46, page 170), which can be fit to a standard dose-dependence equation to derive the IC_{50} values (Table 3, page 159-160).

All unsulfated DHPs studied inhibited both factor Xa and thrombin in the absence of antithrombin with an IC_{50} value in the range of 0.2–2.8 μg/mL or 0.06–0.90 μM (Figure 46, Table 3, pages 170 and 159-160, respectively). CD was found to be ~5–7-fold more effective than FD and SD. The direct inhibitory activity of the DHPs increases significantly on sulfation with IC_{50} values in the range of 0.07–0.84 μg/mL or 20–250 nM. This suggests that sulfation of all three oligomers improves direct inhibition of both factor

Xa and thrombin nearly 3–4-fold. In contrast, PAA displayed no direct factor Xa or thrombin inhibitory activity in the presence of buffer containing $CaCl_2$ (Table 3, page 159-160).

Indirect inhibition by sulfated DHPs in the presence of antithrombin yields IC_{50} values of 60–140 nM (0.19 – 0.56 μg/mL) against factor Xa and 50–80 nM (0.16–0.31 μg/mL) against thrombin (Table 3, page 159-160). Although these activities indicate good indirect inhibition potency of the sulfated DHPs, closer inspection of the data indicates some differences and complexities. The IC_{50} value decreases ~2-fold for SD_S in the presence of antithrombin from that in its absence. The decrease in IC_{50} suggests that the indirect and direct inhibition pathway complement each other for SD_S. In contrast, the IC_{50} value increases ~2–3-fold for CD_S and FD_S in the presence of antithrombin from that in its absence (Table 3, page 159-160). Thus, for CD_S and FD_S the two pathways appear to either compete with each other or induce side-reactions that prevent additive effects (see Discussion section). These mixed inhibition results indicate interesting differences between these three apparently similar oligomers.

An important difference elucidated in these studies is the level of enzyme inhibition induced with each oligomer. Figure 7 shows that the relative residual proteinase activity decreases to a minimum of ~50%, ~38% and ~0% for factor Xa, while it reaches ~30%, ~18% and ~0% for thrombin in the presence of SD, SD_S and SD_S + AT, respectively. Similar results were also achieved with CD and FD oligomers (not shown). This suggests that even at high enough concentration of unsulfated and sulfated oligomers 100% inhibition of both factor Xa and thrombin was difficult to achieve. In contrast, the

inhibition was consistently complete in the presence of antithrombin for all three oligomers. Thus, the presence of antithrombin, or indirect pathway, greatly aided inhibition of both factor Xa and thrombin.

3.4 DISCUSSION

The template-driven acceleration in antithrombin inhibition of pro-coagulant proteinases, especially thrombin, is extremely attractive because it does not depend on the serpin conformational change phenomenon that is so critically dependent on the structure of the activator [208]. This led to our studies with the carboxylic acid-based scaffold, PAA, which displayed phenomenal acceleration in inhibition, but at physiologically prohibitive concentrations [193-194]. To capitalize on this observation, we sought to introduce two types of functional groups – hydrophobic (–Ar structure) and hydrogen bonds (–OH) – while retaining carboxylic acid (–COOH) groups, so as to enhance the anticoagulant activity.

Macromolecules that satisfy this criteria are difficult to find, except perhaps for synthetic lignins, the so-called DHPs [205]. However, natural lignins do not contain carboxylic acid moieties. Synthetic lignins containing carboxylic acid groups have been obtained, yet molecules longer than trimers have not been synthesized to-date [204]. We utilized HRP-catalyzed oxidative coupling conditions, such as high reactant concentrations and controlled gradual addition of the oxidant, which reduce chain termination, to obtain oligomers with average molecular weight between 800 and 3,500 Da. This corresponds to

a size range of tetramers to pentadecamers. This is the first time that higher order oligomers of –COOH containing DHPs have been synthesized.

Detailed characterization of all possible inter-monomeric linkages in these DHPs is difficult, yet the ESI-MS spectrum of FD indicates the presence of at least one type of linkage, the β-*O*-4-type (Figure 44, page 168). This is likely to be the major linkage in FD with other linkages, such as β-5, β-β and 5-5 also present to some extent. In addition, it is likely that not all carboxylic acid groups are retained during oligomerization, as suggested by the ^{13}C NMR spectrum (Figure 43, page 167), due to the competing decarboxylation reaction. Finally, a number of chiral centers are being generated in oxidative β-5 and β-β coupling, which are likely formed without any stereochemical control [209]. Thus, despite the apparent simplicity of ESI-MS spectrum (Figure 44, page 168) the composite structure of FD, and of CD and SD too, is likely to be complex. This structural complexity is expected to be retained in sulfated DHPs.

The presence of so many structures in a single preparation of DHPs is both a blessing and a curse. While heterogeneity and polydispersity imply that reliable, discrete structural information on molecules that possess activity is difficult, they also afford an essentially high-throughput screening of a large library, which in this case is combinatorial because of the nearly random coupling of radicals (Figure 40, page 164). For this work in which the objective was on arriving at effective structure(s), rather than coming up with detailed structural sequence of a potent molecule, screening such a library was especially advantageous. This library represents a group of structures – the 'lignin carboxylates' – because each molecule herein contains the fundamental lignin structure, an aromatic ring, a

three-carbon unit and some –OH groups, with a high probability of possessing carboxylic acid groups.

The anticoagulant properties, assessed under *in vitro* conditions using PT and APTT assays, suggest that all DHPs studied, sulfated and unsulfated, were fairly potent. In addition, the potency of these DHPs was dramatically greater than our reference polymer, PAA (Table 3, page 159-160), suggesting that our reasoning based on first principles – hydrophobicity and anionic character – appears to have succeeded. More importantly, the results indicate that unsulfated CD, FD and SD were similar in potency to a LMWH in PT assays. This result is striking considering that LMWHs are currently being used in the clinic. More experiments are needed to better understand the anticoagulant efficacy of our DHPs.

In contrast to unsulfated DHPs, their sulfated counterparts were nearly 1.4–3.4-fold more effective than LMWH in PT assays (Table 3, page 159-160). In APTT assays, the unsulfated DHPs were 4.2–6.7-fold weaker than LMWH, while the sulfated DHPs were 2.2–3.8-fold less effective. Thus, sulfation enhanced the anticoagulation potency of DHPs. Overall, both sulfated and unsulfated DHPs are more effective at prolonging the APTT than the PT (Figure 45, Table 3, pages 169 and 159-160, respectively). LMWH also behaves in a similar fashion. This suggests that DHPs affect the intrinsic pathway of coagulation more than the extrinsic pathway, similar to LMWHs.

Among the six DHPs studied, the anticoagulant potency followed an order CD_S > FD_S > SD_S ≅ CD. Although it is difficult to derive precise structural information, it is tempting to suggest that the order of potency possibly follows the number of anionic group

density in these oligomers. Yet, calculations using the sulfate content (Table 2, page 157-158) and carbonyl carbon intensities (Figure 43, page 167) reveal that the negative charge ($–COO^-$ and $–OSO_3^-$) density follows the order $CD_S = FD_S > SD_S > CD$. Further, although the anticoagulant activity of CD_S is similar to that of LMWH, its charge density is significantly lower [27, 29]. Thus, while the negative groups are important for enhancing activity, they are by no means the only determinant of anticoagulant activity.

With respect to structural diversity of these preparations, SD is the least diverse because of the presence of two methoxy groups in the aromatic ring, which reduce the formation of 5-5 and β-5 linkages. In contrast, CD with one hydroxyl group, which encourages such linkages, is the most diverse [205]. Thus, it is likely that an optimal combination of structural diversity and anionic character generates the anticoagulant property in these DHPs.

Mechanistic differences between DHPs and LMWH are revealed in experiments on direct and indirect inhibition of thrombin and factor Xa (Figure 46, Table 3, pages 170 and 159-160, respectively). All DHPs, sulfated and unsulfated, inhibited the hydrolysis of an appropriate chromogenic substrate by both factor Xa and thrombin directly in the absence of antithrombin! This is quite an un-expected result considering that PAA does not display this behavior. It is likely that the significant hydrophobic character of these DHPs is the origin for this direct inhibition effect.

The IC_{50} values of these effects were ~4–135-fold below the lowest concentration necessary for a 2-fold increase in APTT suggesting that direct inhibition of these proteinases is most probably a relevant mechanism of action of these anticoagulants. As

observed in clotting time assays, sulfated DHPs were more effective at inhibiting both proteinases than unsulfated counterpart by a factor of ~2.6–9.7-fold. Likewise, CD and CD_S were better anticoagulants than the other two DHPs in these assays and probably for the same reasons of structural diversity and charge density.

Inhibition of thrombin and factor Xa with DHPs in the presence of antithrombin exhibited greater complexity. While the IC_{50} value against thrombin and factor Xa improved nearly 2-fold for SD_S, it worsened 2–3-fold for CD_S and FD_S. Indirect inhibition of thrombin and factor Xa with these anticoagulants is a complex process because of two simultaneous processes – direct and basal inhibition. Thus, indirect inhibition is an additive function of the two processes. A pathway that competes with the indirect effect and reduces its efficiency is the substrate pathway [187]. This substrate pathway regenerates a fully active enzyme from the covalent antithrombin–enzyme complex, thereby raising the stoichiometry of inhibition [187]. It is possible that some molecules present in heterogeneous CD_S and FD_S preparations introduce the substrate pathway component, thereby decreasing the overall efficacy of inhibition in the presence of antithrombin.

At a molar level, comparison of the IC_{50} value in the presence of antithrombin (indirect inhibition) suggests that DHPs are 8–20-fold weaker factor Xa inhibitors and 24–38-fold weaker thrombin inhibitors than LMWH (Table 3, page 159-160). The proportions do not change much for direct inhibition of these two enzymes (~5–35-fold against FXa and 10–48-fold against thrombin). This observation suggests that although DHPs can utilize the antithrombin-dependent (indirect) pathway, the antithrombin-independent (direct) pathway is the major contributor to overall proteinase inhibition.

With the limited knowledge we have on these novel oligomers at the present time, it remains to be determined whether this represents a significant divergence from the effect of traditional anticoagulant, LMWH, which is known to predominantly utilize the indirect pathway [209]. Recent studies suggest that LMWH may also function through inhibition of intrinsic tenase complex, which is independent of antithrombin [210]. Likewise, heparin is known to interact with an exosite on factor IXa, which plays an important role in antithrombin-independent inhibition of intrinsic tenase [211].

Although the heterogeneous and polydisperse nature of these DHP oligomers suggest an intrinsic difficulty of deriving useful structural information for rational design of advanced molecules, the results present a wealth of opportunities. The molecules present in the mixture have a common structure, the 'lignin carboxylate'. Assuming that a decamer is the minimal size necessary for anticoagulant function, a combinatorial virtual library can be prepared with the type of monomer, e.g., CA, FA and SA (Figure 40, page 164), and inter-monomer linkages, e.g., β-*O*-4, β-5, β-β and 5-5, as variables. A simple calculation shows that 262,144 different decamer structures are possible for each monomer from these four inter-monomer linkages. This library size is well within the reach of virtual screening techniques. Thus, our current 'structure(s)' search is expected to generate some novel first generation structures for traditional organic synthesis and biochemical evaluation.

In conclusion, preliminary results suggests that our chemo-enzymatically prepared structurally complex DHPs from 4-hydroxycinnamic acids display interesting anticoagulant activities with the potency of CD_S resembling LMW heparin *in vitro* plasma clotting time assays. In addition, the anticoagulant function appears to originate from both

antithrombin-dependent and –independent mechanisms with the indirect pathway appearing to be the major contributor. This dual inhibition property of our DHP oligomers is the first example in inhibitors of coagulation. Yet, detailed mechanistic studies are necessary to better understand the mode of action of these novel oligomers. These molecules are structurally unlike the highly sulfated polysaccharide scaffold of heparins and are readily obtained in few steps. This work puts forward novel, non-heparin structure(s), which may be exploited for the design of potent, dual action inhibitors of coagulation through combinatorial virtual screening on a library of DHP oligomers.

3.5 EXPERIMENTAL

3.5.1 Proteins and Chemicals

Horseradish peroxidase (HRP) with activity of 250-330 units/mg was from Sigma (St. Louis, MO). Human antithrombin (AT) was from Molecular Innovations (Southfield, MI) and proteinases, factor Xa and thrombin, were from Haematologic Technologies (Essex Junction, VT). Stock solutions of proteins were prepared in 20 mM sodium phosphate buffer, pH 7.4, containing 100 mM NaCl (AT and thrombin) or 5 mM MES buffer, pH 6.0 (factor Xa). Chromogenic substrates Spectrozyme TH and Spectrozyme FXa were from American Diagnostica (Greenwich, CT). Citrated human plasma for coagulation time assays was purchased from Valley Biomedical (Winchester, VA). Thromboplastin and ellagic acid were obtained from Fisher Diagnostics (Middletown, VA). LMWH (M_W = 5,060 Da), 30% hydrogen peroxide, sinapic acid (SA), ferulic acid (FA) and caffeic acid (CA) were from Sigma (St. Louis, MO). PAA2280 was from American Polymer Standards

(Mentor, OH), while (+)-CS (Fig. 2) was prepared as described earlier [190-192]. All other chemicals were analytical reagent grade from either Aldrich Chemicals (Milwaukee, WI) or Fisher (Pittsburgh, PA) and used without further purification.

3.5.2 Oxidative Coupling and Sulfation of 4-Hydroxycinnamic Acid Derivatives

The dehydrogenation polymers (DHP) were prepared by the slow addition of a phenylpropenoid precursor and H_2O_2 to a solution of horseradish peroxidase (HRP) [195]. Briefly, 4-hydroxycinnamic acid precursor (25 mM) in 10 mM sodium phosphate buffer, pH 8.0, (200 mL) and H_2O_2 (75 mM) in the same buffer (100 mL) were simultaneously added drop-wise over a 5 h period to a stirring solution of HRP (10 mg) in the sodium phosphate buffer (50 mL) at room temperature in dark. Three additional aliquots H_2O_2 (75 mM) were added over the next 72 h while monitoring the polymerization using analytical size-exclusion chromatography (SEC). At the end of nearly 80 hours, the solution was freeze-dried, the solid re-dissolved in deionized water, and the solution filtered repeatedly through a molecular membrane (Amicon YM5K) to remove salts and low molecular weight material. The final solution was washed with ether and lyophilized to give a dark brown powder, the sodium salt of the DHP. The synthetic DHPs were sulfated with triethylamine-sulfur trioxide complex [192]. Briefly, the lyophilized DHP sample (500 mg) was dissolved in dry DMF (50 mL) containing triethylamine – sulfur trioxide complex (1 g) and stirred for 24 h at 60°C. After the removal of most of the DMF *in vacuo*, the remaining product was taken up in 30% aqueous sodium acetate, the sodium salt

precipitated using ~10 volume of cold ethanol. The precipitated product was further purified with dialysis using Amicon 10K cutoff dialysis membrane.

3.5.3 Characterization of DHPs

Elemental analysis of DHP samples was obtained from Atlantic Microlabs (Norcross, GA). Infrared spectra were recorded on a Thermo Nicolet Avatar 360 FT-IR spectrophotometer (Somerset, NJ) with DHP samples in KBr pellets. The molecular weights of acetylated DHPs were determined using a Phenogel 500Å non-aqueous size-exclusion column (300 × 7.8 mm, Phenomenex, Torrance, CA). Acetylation of DHPs was performed using a standard Ac_2O-pyridine (1:1) mixture for 24 h at room temperature. Acetylated DHPs were eluted with THF at 0.75 mL/min and detected at 280 nm. Polystyrene samples (450–7,600 Da) from American Polymer Standards, Mentor, OH were used as standards. Number average molecular weights (M_N) and weight average molecular weights (M_W) were calculated by dividing the base of each peak into 10 equal intervals. The peak heights at each of these points were determined using CLASS VP (Shimadzu) software and the molecular weights at these points obtained from a standard curve. The M_N and M_W values were then calculated using standard equations. For ^1H and ^{13}C NMR spectroscopy, 5–20% (w/v) solutions of dry DHPs in DMSO-d_6 were prepared. The spectra were recorded on a Gemini 300 spectrometer (Varian, Palo Alto, CA) at 298 K (^1H) or 323 K (^{13}C). Quantitative analysis of ^{13}C signal intensities was performed using inverse gated decoupling sequence with a 10 s relaxation delay and an acquisition time of 1.7 s. Nearly 25,000 to 40,000 scans were acquired for signal integration. Mass spectrometry was

performed on sulfated and unsulfated DHP samples using a Micromass ZMD4000 single quadrupole mass spectrometer with ESI ionization probe operating in negative ion mode (Waters Corp., Milford, MA). The samples, dissolved in acetonitrile containing formic acid (5% v/v), were infused at 10 μL/min and optimized MS ionization conditions were employed. The source block temperature and the probe temperature were held at 100 and 120 ^{O}C, respectively. Corona and cone voltages of 2.69 kV and 161 V were selected following optimization. The desolvation nitrogen flow was 500 L/hour. Mass spectra were acquired in the mass range from 110 to 1000 daltons at 400 amu/sec.

3.5.4 Prothrombin Time and Activated Partial Thromboplastin Time

Clotting time was determined in a standard 1-stage recalcification assay with a BBL Fibrosystem fibrometer (Becton-Dickinson, Sparles, MD). For PT assays, thromboplastin was reconstituted according to manufacturer's directions and warmed to 37°C. A 10 μL sample of the DHP, to give the desired concentration, was brought up to 100 μL with citrated human plasma, incubated for 30 s at 37 ^{O}C following by addition of 200 μL pre-warmed thromboplastin. Clotting time in the absence of an anticoagulant was determined using 10 μL deionized water. For APTT assay, 10 μL DHP sample was mixed with 90 μL citrated human plasma and 100 μL of pre-warmed APTT reagent (0.2% ellagic acid). After incubation for 220 s, clotting was initiated by adding 100 μL of 25 mM $CaCl_2$ (37 ^{O}C) and time to clot noted. Each clotting assay was performed in duplicate or triplicate. The data

were fit to a quadratic function, which was used to determine the concentration of DHP (or the reference molecules) necessary to double the clotting time, 2×APTT or 2×PT.

3.5.5 Proteinase Inhibition

Both direct and indirect inhibition of thrombin and factor Xa by sulfated and unsulfated DHPs was determined through a chromogenic substrate hydrolysis assay. A 10 μL sample of DHP at concentrations ranging from 0.035 to 10,000 μg/mL was diluted with 885 μL of 20 mM Tris-HCl buffer, pH 7.4, containing 100 mM NaCl, 2.5 mM $CaCl_2$ and 0.1 % PEG8000 at room temperature in polyethylene glycol-coated polystyrene cuvettes, followed by addition of 5 μL of proteinase solution to give 4 nM thrombin or factor Xa. After 10 min of incubation at room temperature, 100 μL of 1 mM chromogenic substrate was added (Spectrozyme FXa for factor Xa and Spectrozyme TH for thrombin) and the residual proteinase activity was determined from the initial rate of increase in absorbance at 405 nm. Relative residual proteinase activity at each concentration was calculated using the proteinase activity measured under otherwise identical conditions, except for the absence of DHP. Indirect inhibition of thrombin and factor Xa using antithrombin-sulfated DHP complex was performed in the presence of 100 nM and 200 nM antithrombin for inhibition, respectively, in an otherwise identical manner. The sigmoidal dose-dependence of residual proteinase activity was fitted with a logistic function of the form $f(x) = Y_O + (1—Y_O)/(1+([DHP]_O/IC_{50})^{HS})$, where Y_O is the lower threshold level of the inhibitory activity and HS is the Hill-slope.

Table 2. Average molecular weight, elemental composition and sulfate density of DHPs from cinnamic acid derivatives.

[a] Average molecular weight was obtained through non-aqueous SEC on the acetylated derivatives, CD_{AC}, FD_{AC}, and SD_{AC}, using polystyrene as standards. The error in determination of these numbers is less than 10% (see Methods). [b] Peak-average molecular weight. [c] Number-average molecular weight. [d] Weight-average molecular weight. [e] Size of an average oligomer. [f] Analysis was performed on unsulfated or sulfated DHPs, and not on acetylated DHPs. [g] Average number of sulfates per monomeric unit was calculated from elemental sulfur composition and the size of an average unsulfated oligomer. [h] numbers in brackets shows the predicted composition of a homogeneous β-*O*-4-linked decamer of appropriate DHP. [i] not determined.

DHP	*Average Molecular Weight*[a]				*Elemental Composition*[f]			*Sulfates per Unit*[g]	
	M_P[b]	M_N[c]	M_W[d]	*Size*[e]	*C*	*H*	*O*	*S*	
	(Da)	*(Da)*	*(Da)*		*(%)*	*(%)*	*(%)*	*(%)*	
CD	1,180	880	2,800	5–13	54.8 (61.0)[h]	3.5 (3.0)	39.2 (36.0)	-	-
FD	2,480	1,870	3,650	8–15	61.9 (62.8)	4.3 (3.8)	33.6 (33.4)	-	-
SD	1,190	1,020	2,990	4–11	55.8 (59.7)	4.2 (4.2)	38.0 (36.1)	-	-
CD_S	-[i]	-	-	-	46.1 (49.6)	4.0 (2.2)	36.7 (38.1)	5.3 (5.9)	~0.40
FD_S	-	-	-	-	52.4 (54.1)	4.6 (3.1)	35.1 (35.3)	4.4 (4.3)	~0.30
SD_S	-	-	-	-	45.8 (50.4)	4.0 (3.4)	39.0 (37.8)	4.5 (4.9)	~0.38

Table 3. Anticoagulation effect of DHPs from 4-hydroxycinnamic acids.

[a] PT and APTT values were deduced *in vitro* human plasma experiments where the clot initiator is either thromboplastin or ellagic acid, respectively. Experiments were performed in duplicate or triplicate (see Methods). Errors represent ± 1 S. E. [b] IC_{50} values were determined through direct inhibition of thrombin or factor Xa using a chromogenic substrate hydrolysis assay (see Methods). [c] S.E. ±1 [d] Not determined. [e] No inhibition was observed in buffer containing Ca^{2+} at concentrations lower than 4560 µg/mL. [f] Experiment performed only once.

DHP	*Clotting Time*[a]		IC_{50}[b]			
	2×PT	*2×APTT*	*fXa*	*fXa w/ AT*	*T*	*T w/ AT*
	(μg/mL)	*(μg/mL)*	*(μg/mL)*	*(μg/mL)*	*(μg/mL)*	*(μg/mL)*
CD	98.1 ± 0.7	24.9 ± 2.3	0.4 ± 0.1[c]	-[d]	0.19 ± 0.03	-
FD	161.3 ± 2.7	39.5 ± 0.8	2.7 ± 0.3	-	1.16± 0.06	-
SD	212.0 ± 2.9	32.1 ± 1.5	2.8 ± 0.9	-	1.00 ± 0.04	-
CD_S	42.1 ± 0.3	13.0 ±5.0	0.11 ± 0.01	0.19 ± 0.01	0.07 ± 0.01	0.20 ± 0.02
FD_S	63.4 ± 0.1	18.3 ± 1.9	0.32 ± 0.04	0.56 ± 0.02	0.12 ± 0.01	0.31 ± 0.02
SD_S	104.6 ± 3.9	22.6 ± 1.1	0.84 ± 0.08	0.37 ± 0.01	0.33 ± 0.01	0.16 ± 0.01
LMWH	142.1 ± 3.6	5.9 ± 3.0	-	0.037± 0.003	-	0.011 ± 0.001
PAA	4259 ± 40	-[d]	No Inh.[e]	No Inh.	No Inh.	No Inh.
(+)-CS	927[f]	284[f]	-[d]	-	-	-

Figure Legends

Figure 40. Chemo-enzymatic synthesis of 4-hydroxycinnamic acid-based dehydropolymers (DHPs), CD, FD and SD. Horseradish peroxidase (HRP)-catalyzed oxidative coupling of caffeic acid (CA), ferulic acid (FA) or sinapic acid (SA), in the presence of H_2O_2 generates oligomers of size 4–15 units, which are sulfated with $Et_3N{:}SO_3$ complex to give sulfated DHPs. Phenolic oxidation can generate four types of radical intermediates, of which typically intermediates I_1 and I_2 couple with starting material to give oligomers with different types of inter-monomeric linkages. The most common linkages formed include β-*O*-4 and β-5. Other less common linkages include β-β, 5-5 and 5-*O*-4, for which oligomerization tends to arrest chain growth [205]. The length of the chain greatly depends on the conditions of oligomerization.

Figure 41. Structures of reference compounds, low molecular weight heparin (LMWH), polyacrylic acid (PAA), and (+)-catechin sulfate ((+)-CS). The average molecular weights (M_W) for polymers LMWH and PAA are as specified, whereas (+)-CS has a molecular weight of 814 Da. LMWH is a heterogeneous mixture of oligosaccharide chains, in which the uronic acid can be iduronic or glucuronic acid, while the glucosamine can be *N*-sulfated or *N*-acetylated (R = $–SO_3^-$ or $–COCH_3$). The 2-, 3-, and 6-positions of saccharide residues can be either sulfated or unsulfated (X, Y and Z = –H or $–SO_3^-$).

Figure 42. Non-aqueous size exclusion chromatography of acetylated DHPs. Analytical SEC was performed with ~100-150 μg of CD_{AC} (·····), FD_{AC} (—) and SD_{AC} (—) oligomers using dry THF as the mobile phase at 0.75 mL/min. Each chromatogram is scaled to the highest peak intensity (set to 100%). The time of monomer elution is indicated.

Figure 43. Quantitative ^{13}C NMR spectra of DHPs, SD (A), FD (B) and CD (C) in DMSO-d_6 obtained using inverse gated decoupling pulse sequence. Four regions are apparent, the carboxylic acid region between 160–170 ppm, the aromatic and vinylic peaks between 100–160 ppm, the α and β-carbons of alkoxy groups between 70–100 ppm, and the methoxy groups at 56 ppm. Solvent signal is observed at ~40 ppm. Note the variation in intensity of carboxylic acid carbon at ~165 ppm and the significant difference in signal composition between the three oligomers. D) shows the fingerprint region in the IR spectrum of FD (light line) and FD_S (dark line) in KBr pellets. Sulfate stretches in FD_S are observed at 1080 and 1110 cm^{-1}.

Figure 44. ESI-MS of FD oligomer through direct infusion of the oligomer (A) and mass analysis of peaks *p1* through *p6* using β-*O*-4 inter-monomeric linkages (B). Peaks merge into the background above 700 amu. A majority of the significant peaks, especially in the higher mass range, can be explained on the basis of a mono-charged molecular ion, which has lost 1 through 3 CO_2 units.

Figure 45. Prolongation of clotting time as a function of SD (closed circles) and SD_S concentrations (open circles) in either prothrombin time assay (A) or the activated partial thromboplastin time assay (B). The solid lines are trend lines, and not exponential fits. Error bars in the range of symbol size have been omitted. In both assay, sulfation of DHP enhanced the anticoagulant activity of oligomer. See experimental section for details.

Figure 46. Inhibition of the blood coagulation proteases factor Xa (A) and thrombin (B) by dehydrogenation polymers from sinapic acid: SD (●), SD_S (■) and SD_S in the presence of antithrombin (▼). The inhibition of thrombin and factor Xa by sulfated and unsulfated DHPs was determined through a chromogenic substrate hydrolysis assay. Compared to its unsulfated counterpart, the sulfated DHP was found to be better in inhibiting the procoagulant proteinases. See text for details.

Figure 40

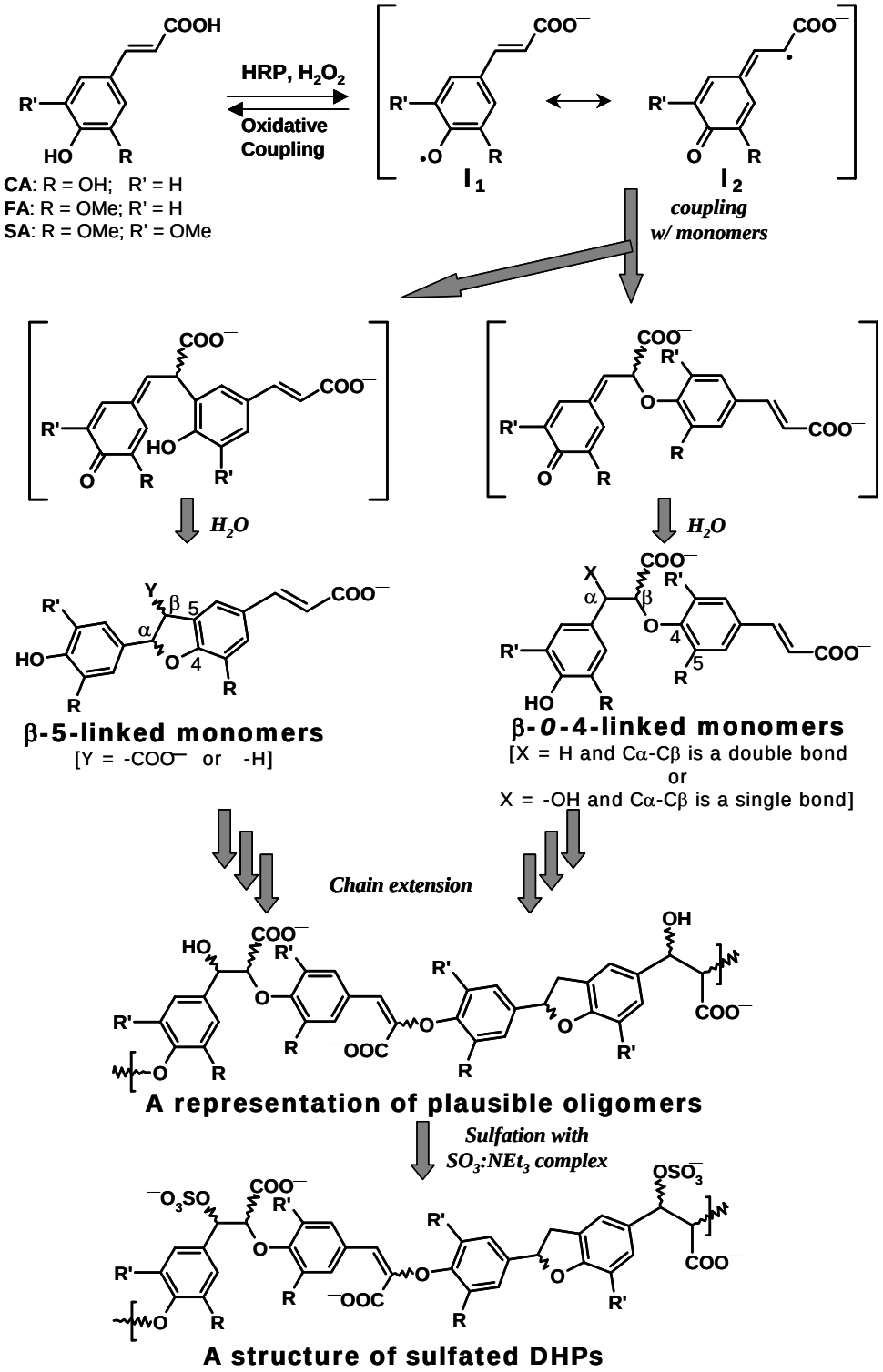

Figure 41

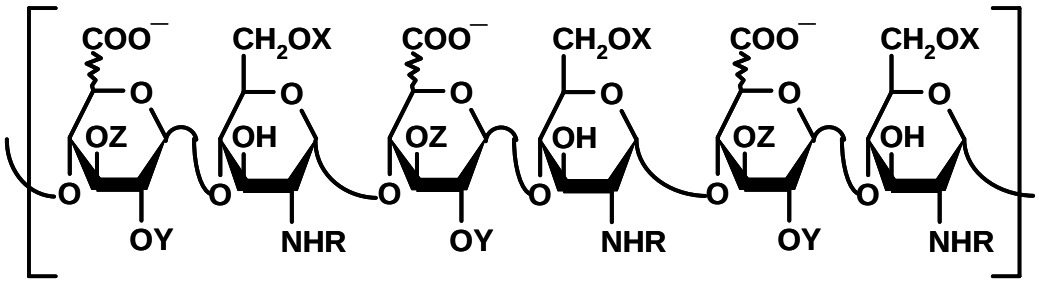

LMWH (M_W = 5,060 Da)
R = $-SO_3^-$ or $-COCH_3$
X, Y and Z = –H or $-SO_3^-$

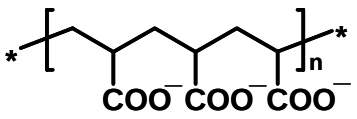

PAA (M_W = 2,280 Da)

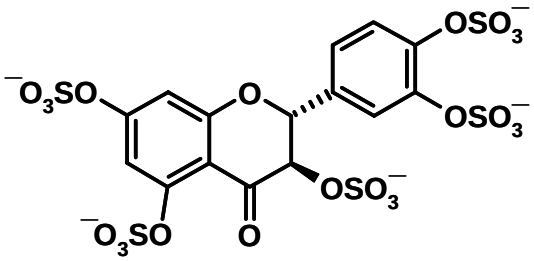

(+)-CS

Figure 42

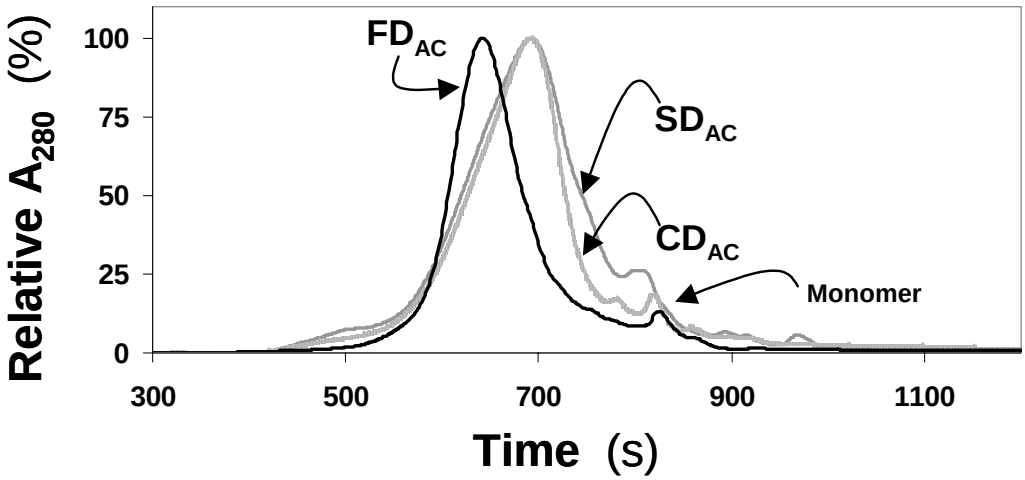

Figure 43

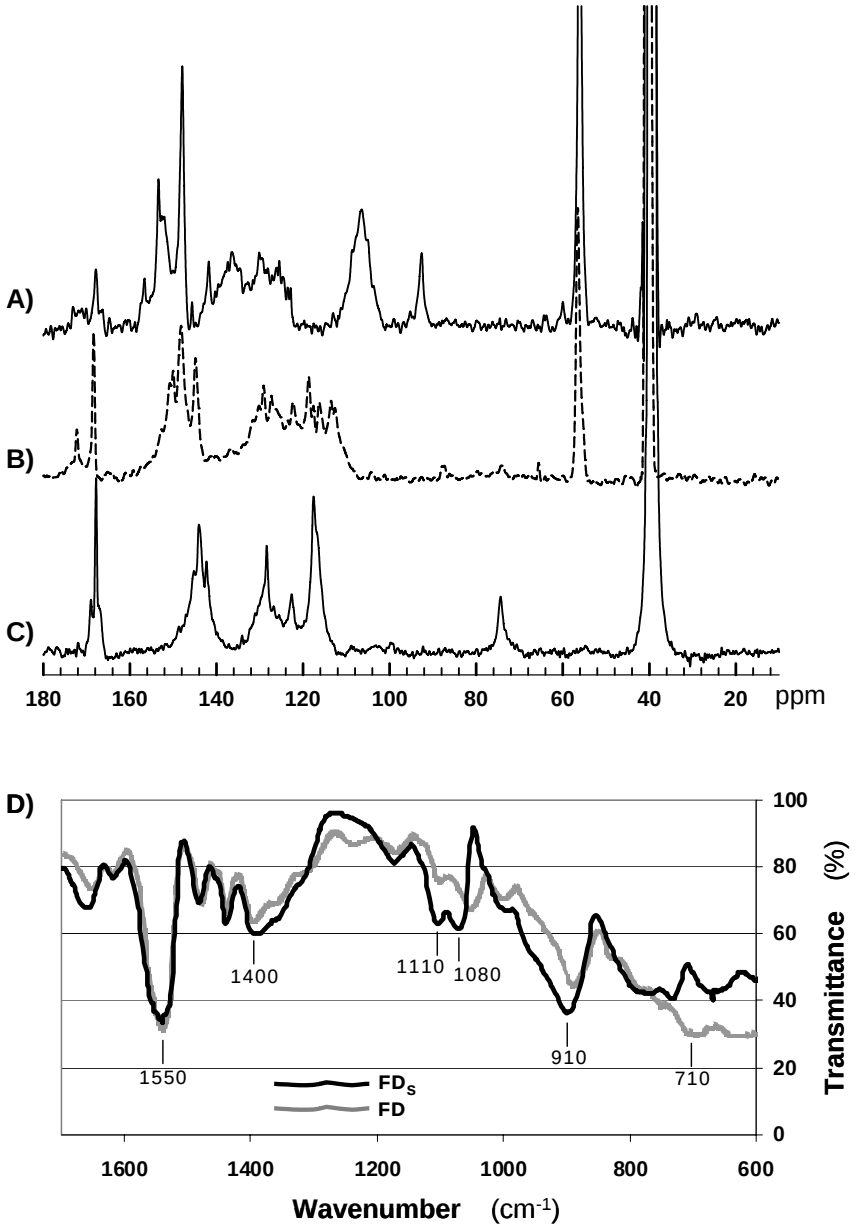

Figure 44

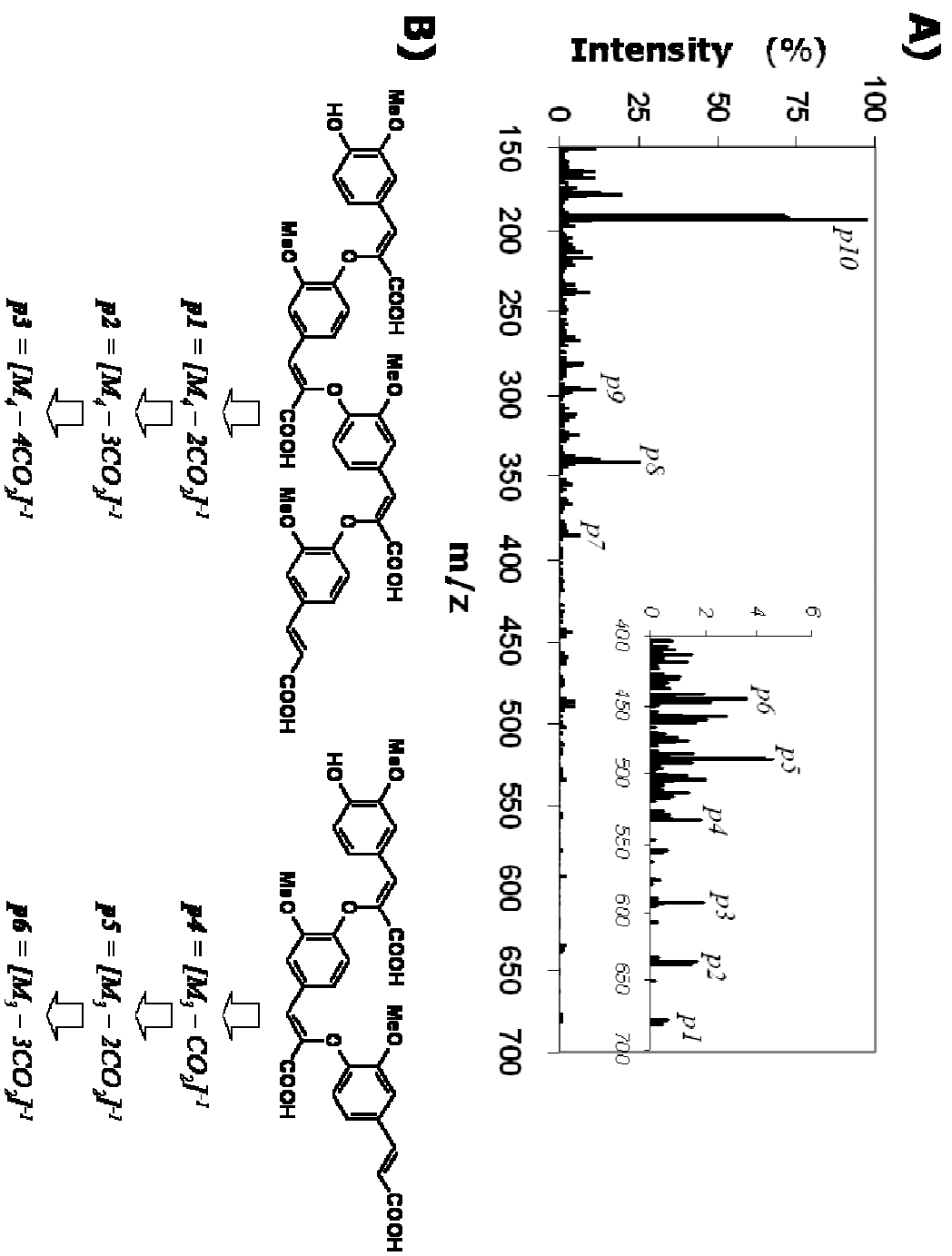

Figure 45

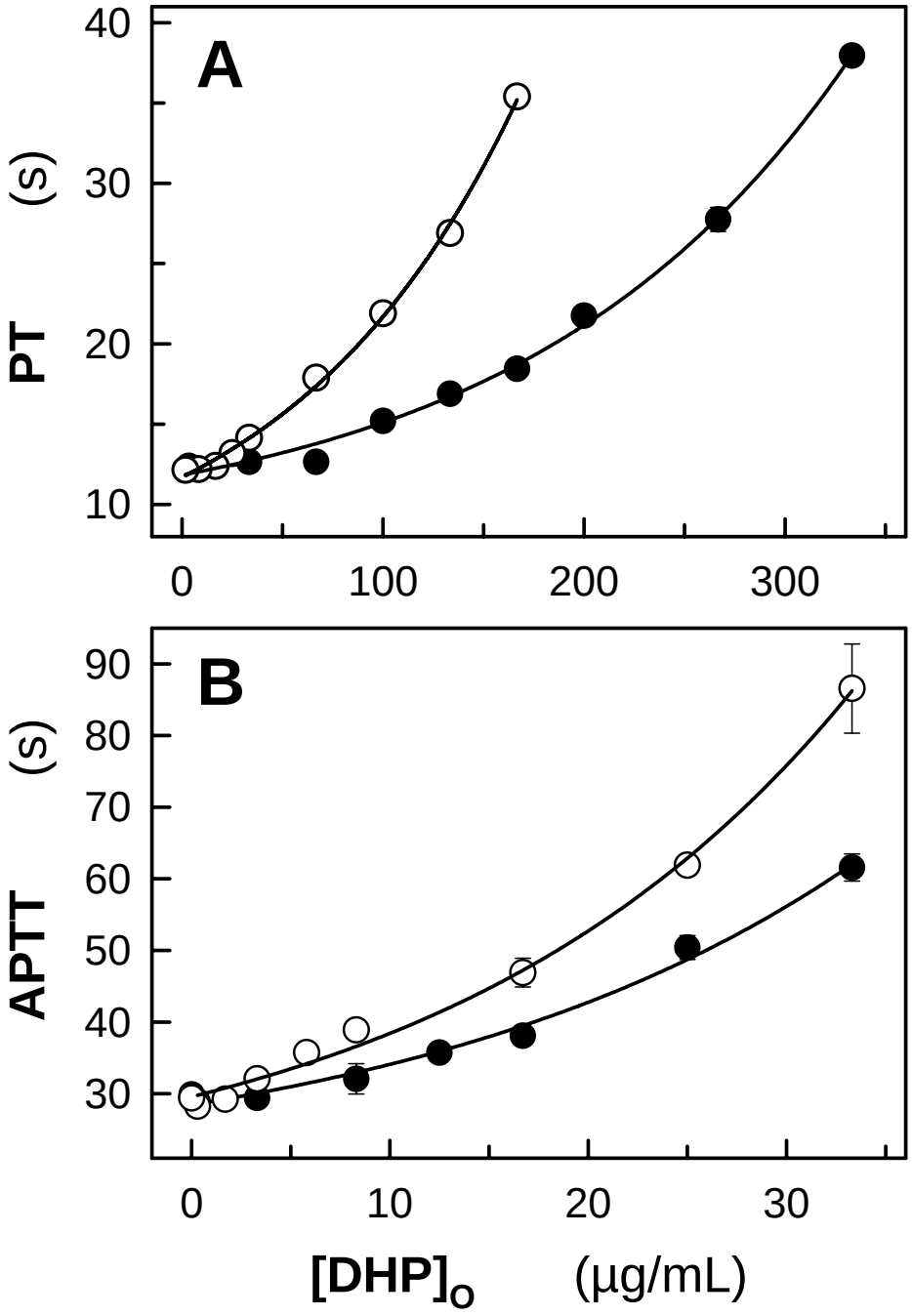

Figure 46

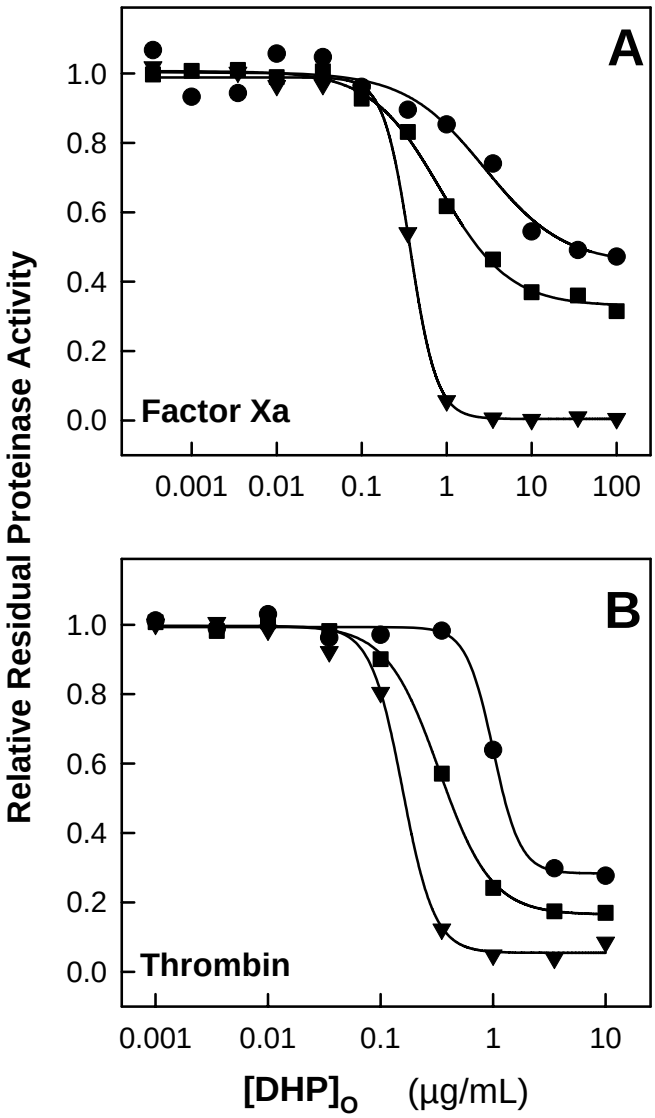

Chapter 4: Characterization of the Anticoagulation Profile of Novel, Synthetic, Sulfated Dehydropolymers of 4-Hydroxycinnamic Acids in Plasma and Blood

4.1 Abstract

Background- Recently, we designed sulfated dehydropolymers (DHPs) of 4-hydroxycinnamic acids that displayed interesting anticoagulant properties [212]. Sulfated DHPs are structurally completely different from all the current clinically used anticoagulants and represent a new class of coagulation inhibitors. ***Objective***- To elucidate the anticoagulant potential of sulfated DHPs in plasma and blood. ***Methods***- Clotting time assays, thrombin generation assay, thromboelastography and haemostasis analysis system were used to evaluate the anticoagulant potential. ***Results***- Sulfated DHPs prolong prothrombin and activated partial thromboplastin times at concentrations comparable to the clinically used low molecular weight heparin, enoxaparin. Studies in human plasma and whole blood show that sulfated DHPs possess an anticoagulation profile similar to enoxaparin, the clinically used LMWH, except for the concentration range at which they are effective. Thrombogenesis studies in plasma indicate that sulfated DHPs are less potent than enoxaparin by a factor of 7–16-fold, while whole blood studies using thromboelastography and Hemostasis Analysis System indicate that they are 17–140-fold less potent. ***Conclusion***- In combination, the results demonstrate that the first generation

sulfated DHPs compare well with enoxaparin and represent potent novel molecules for further rational modifications.

4.2 Introduction

Thrombin and factor Xa (FXa), two key serine proteases of the coagulation cascade, have been the target of rational design of coagulation inhibitors [21]. Both proteases can be targeted through either direct or indirect inhibition pathway. Direct inhibitors include hirudin, argatroban ximelagatran and others, while heparin and its derivatives utilize the indirect pathway.

The commonly used anticoagulant heparin works through antithrombin, a plasma serine proteinase inhibitor (serpin) and a major regulator of clotting. Heparin greatly enhances the rate of antithrombin inhibition of thrombin, FXa and factor IXa (FIXa) under physiological conditions, which forms the basis for its clinical use for the past eight decades [213]. Yet, heparin suffers from several limitations including enhanced risk for bleeding, variable patient response, heparin-induced thrombocytopenia and the inability to inhibit clot-bound thrombin [214]. Low molecular weight heparins (LMWHs), derivatives of heparin with reduced polymeric length, and fondaparinux, a specific sequence of five saccharide residues (Figure. 47A, page 192), have been introduced in the past two decades as better mimics of heparin. Yet, these newer anticoagulants still possess enhanced bleeding risk and are unable to inhibit clot-bound thrombin [215, 216].

Arguable, the problems of heparin therapy arguably arise from the structure of heparin. Heparin is a linear, co-polymer of glucosamine and uronic acid residues that are decorated with a large number of sulfate groups generating a highly anionic polymer. The average molecular weight of full-length heparin is ~15,000 Da implying the presence of ~65–85 negative charges on average on a single chain [187]. In addition to this polyanionic character, heparin biosynthesis results in millions of sequences that differ from each other in the placement of sulfate groups, thereby generating considerable heterogeneity in each preparation of the anticoagulant. Both these structural features introduce a large number of interactions with plasma proteins and cells [29], which likely induce many of heparin's adverse effects.

Apart from the indirectly acting anticoagulants, several direct inhibitors have been put forward such as argatroban, ximelagatran and dabigatran for thrombin and, DX9065a and razaxaban for factor Xa. Structurally, most direct inhibitors of thrombin (DTIs) and factor Xa contain a guanidine or an amidine group that mimic the critical arginine residue at the P-1 site of the proteinase recognition sequence [13]. DTIs and factor Xa inhibitors form a major class of clotting regulators that are considered to be superior to heparins primarily because of the expectation that they can inhibit both circulating and clot-bound enzymes. Yet, challenges exist in the development of these inhibitors including establishing enzyme-binding affinity that is not associated with excessive bleeding and avoiding liver toxicity [37].

Mechanistically, the direct and indirect inhibitors utilize different pathways of inhibition. While heparins require antithrombin to mediate their effect, the direct inhibitors

of thrombin and FXa either bind the active site or an exosite on the enzyme to reduce its proteolytic activity [13]. In principle, these pathways are complementary and, although no molecule can simultaneously utilize both the direct and indirect pathways, the design of such dual inhibitors is expected to greatly advance current anticoagulant therapy.

We reasoned that reducing heparin's high negative charge density would reduce its adverse effects. At the same time, enhancing heparin's hydrophobic character would introduce greater specificity of action. Thus we designed sulfated dehydropolymers (DHPs) of 4-hydroxycinammic acids (Figure 47B, page 192). These designed molecules were prepared in a simple, two-step chemo-enzymatic process involving enzymatic coupling of 4-hydroxycinnamic acids followed by the chemical sulfation of the resulting DHPs [212]. Preliminary studies with the sulfated DHPs suggested the presence of potent anticoagulant activity arising from a possible dual mechanism of factor Xa and thrombin inhibition. Such dual mechanism of inhibition (indirect and direct) has not been observed earlier for any anticoagulant. In addition to this unique mechanistic feature, sulfated DHPs are also structurally unique. DHPs possess a scaffold unlike any other class of anticoagulants investigated to-date, including the heparins, the coumarins, the hirudins and the peptidomimetics.

Although much work remains to be performed regarding the detailed mechanism of action of these sulfated DHPs, establishing the viability of these molecules as anticoagulants of interest is important. In this paper, we report on the performance of our sulfated DHPs in several *in vitro* and *ex vivo* systems including activated partial thromboplastin time (APTT), prothrombin time (PT), thromboelastography (TEG®) and

Hemostasis Analysis System (HAS™). Our studies in human plasma and citrated whole blood show that the sulfated DHPs, which represent only the first generation design in the category of non-polysaccharide heparin mimics, compare favorably with the clinically used anticoagulant, enoxaparin.

4.3 Materials and Methods

4.3.1 Proteins, Chemicals and Coagulation Assay Conditions

Sulfated DHPs, CDSO3, FDSO3 and SDSO3 (Fig. 47B, page 192) were prepared in two steps from 4-hydroxycinnamic acid monomers, caffeic acid, ferulic acid and sinapic acid, as described previously [212]. Stock solutions of sulfated DHPs were prepared in deionized water and stored at $-80^{O}C$. Chromogenic substrate Spectrozyme TH was purchased from American Diagnostica (Greenwich, CT). Citrated human plasma for coagulation time assays was purchased from Valley Biomedical (Winchester, VA). Activated partial thromboplastin time reagent containing ellagic acid (APTT-LS), thromboplastin-D and 25 mM $CaCl_2$ for plasma assays were obtained from Fisher Diagnostics (Middletown, VA). Thromboelastograph® Coagulation Analyzer 5000 (TEG®), disposable cups and pins, and 200 mM stock $CaCl_2$ for blood assays were obtained from Haemoscope Corporation (Niles, IL). LMWH (M_W 5,060 Da) was purchased from Sigma (St. Louis, MO), while enoxaparin (M_W 4,500 Da) was from Aventis Pharmaceuticals. All other chemicals were analytical reagent grade from either Sigma Chemicals (St. Louis, MO) or Fisher (Pittsburgh, PA) and used as obtained.

4.3.2 Prothrombin Time and Activated Partial Thromboplastin Time

Clotting time was determined in a standard 1-stage recalcification assay with a BBL Fibrosystem fibrometer (Becton-Dickinson, Sparles, MD). For PT and APTT assays, the reagents were pre-warmed to 37°C. For PT assays, 10 µL sulfated DHP (or the reference molecule) was mixed with 90 µL of citrated human plasma, incubated for 30 s at 37 ^{O}C followed by addition of 200 µL pre-warmed thromboplastin. For APTT assays, 10 µL DHP was mixed with 90 µL citrated human plasma and 100 µL 0.2% ellagic acid. After incubation for 220 s, clotting was initiated by adding 100 µL of 25 mM $CaCl_2$. Each experiment was performed at least twice. The averaged data was fitted by a quadratic equation to calculate the concentration of the anticoagulant necessary to double the clotting time (2×APTT or 2×PT).

4.3.3 Inhibition of Thrombin Generation in Plasma by Sulfated DHPs

A 650 µL aliquot of freshly thawed human plasma was co-incubated with 10 µL sulfated DHP (or the reference molecule) and 200 µL APTT-LS reagent at 37°C for 5 minutes. Following incubation, 850 µL of this sample was transferred to a PEG 20000-coated polystyrene cuvette. Clotting was quickly initiated by adding 50 µL of 2 mM Spectrozyme TH and 200 µl 25 mM $CaCl_2$ [217]. Plasma thrombin activity was continuously monitored from the sigmoidal increase in absorbance at 405 nm, which was followed until a plateau was reached to measure the lag time and the slope of the thrombin 'explosion' phase.

4.3.4 Thromboelastograph (TEG®) Analysis of Clot Formation in the Presence of DHPs

The TEG® assays were performed essentially as reported earlier [218]. Briefly, the assays were initiated by transferring 20 µL of 200 mM $CaCl_2$ into the Haemoscope™ disposable cup, oscillating through 4^0 45' angle at 0.1 Hz, followed by the addition of a mixture of 340 µL of sodium citrated whole blood containing 10 µL sulfated DHP or dH_2O (control) at 37 ^OC. This recalcification initiates clot formation in the TEG® coagulation analyzer, which operates until all necessary data collection (R, K, α and MA) is completed in an automated manner.

4.3.5 Hemostasis Analysis System (HAS™) Analysis of Clot Formation in the Presence of Sulfated DHPs.

Analysis of platelet function and clot structure was performed using the HAS™ (Hemodyne, Inc., Richmond, VA). A mixture of 700 µl of citrated whole blood and 10 µl sulfated DHP or dH_2O (control) was co-incubated at room temperature for 5 minutes and then 700 µl was placed in a disposable cup. To initiate clotting, 50 µl of 150 mM $CaCl_2$ was added to 700 µl of the blood – DHP mixture to give a final $CaCl_2$ concentration of 10 mM, while the cone was simultaneously lowered into the recalcified blood sample. As the clotting proceeds, platelets attach to both surfaces generating tension within the fibrin meshwork. This tension is measured with a displacement transducer in terms of platelet contractile force (PCF). The onset of PCF is a measure of thrombin generation time (TGT),

while clot elastic modulus (CEM) is the ratio of the applied force (stress) by the transducer to the measured displacement (strain). The HAS^{TM} system operates in an automated manner until all data is collected.

4.4 RESULTS

4.4.1 Effect of Sulfated DHPs on Clotting Times

PT and APTT are commonly used to assess the coagulation status of human plasma [131]. Whereas PT is an indicator of the extrinsic pathway, APTT indicates the status of the intrinsic pathway, although some overlap cannot be avoided due to the interconnectivity of the pathways. Previously we have reported our preliminary results on the effect of the sulfated DHPs in these assays [212]. We have now extended these results and added the clinically used LMWH, enoxaparin, as a reference. Briefly, all three sulfated DHPs exhibited a significant concentration-dependent prolongation of clotting time in both the assays (not shown). A typical parameter for describing anticoagulant activity in these assays is the concentration of the anticoagulant needed for doubling the normal plasma clotting time (2×PT or 2×APTT). The 2×PT value for sulfated DHPs ranged from 13.1–33.3 μM, while that for enoxaparin was 75.3 μM suggesting 2.3–5.7-fold better PT activity for the DHPs (Table 4, page 187). The doubling of APTT required 2.9–6.4 μM concentration of the three sulfated DHPs, while enoxaparin required 1.2 μM. This indicates that the sulfated DHPs are ~2.4–5.3-fold weaker anticoagulants in the APTT assay as compared to enoxaparin and the order of activity is CDSO3 > FDSO3 > SDSO3 (Table 4, page 187).

4.4.2 Effect of Sulfated DHPs on Thrombogenesis in Normal Human Plasma

Thrombin amplifies its own production. An effective anticoagulant is expected to decrease thrombogenesis by delaying this amplification [217, 218]. To characterize the ability of sulfated DHPs to inhibit thrombogenesis in human plasma, we utilized an *in vitro* absorbance assay based on the thrombin-specific chromogenic substrate, Spectrozyme TH. The thrombin generation profile was sigmoidal as expected (Figure 48, page 193) [217]. The lag phase of the profile, during which thrombin levels increase in a slow, linear fashion, corresponds to the accumulation of the upstream coagulation factors that are required for amplification of the dormant thrombin response (see Inset to Figure 48, page 193). The next phase involves a rapid growth in thrombin activity, called 'explosion', which is quantified by the slope of the vertical segment of the sigmoidal profile. In the final phase, a clot forms as thrombin levels reach a maximum.

Inhibitors of thrombin are expected to increase the lag time and decrease the thrombin 'explosion' slope [218-220]. All three DHPs prolonged the lag time as well as reduced the slope corresponding to thrombin 'explosion' in a dose-dependent manner (Figure 48, page 193). These profiles were similar to enoxaparin, although the effective concentration ranges were different. Thus, sulfated DHPs rapidly inhibit basal activation of pro-thrombin as well as significantly reduce the positive feedback effects of thrombin.

To compare the efficacies, the dependence of lag time (Figure 48B, page 193) and thrombin 'explosion' slope (Fig. 48C, page 193) on the concentration of the anticoagulants was plotted. A rapid increase in lag time and decrease in 'explosion' slope with the

increase in the concentration of sulfated DHPs was evident. These profiles were also similar to those obtained for enoxaparin. As a comparative measure, the concentration of the anticoagulant required to extend the lag time to twice the normal, uninhibited value (70 sec) was calculated. This concentration was found to be 5.0, 10.2 and 11.6 μM for CDSO3, FDSO3, and SDSO3, while for enoxaparin it was 0.7 μM (Figure 49B, page 194). Thus, with respect to the inhibition of initial thrombin synthesis in human plasma, DHPs are less potent than enoxaparin by a factor of 7.1–16.6-fold. For comparing the potency in reducing thrombin amplification, the concentration of the three sulfated DHPs that results in a 50% decrease in the 'explosion' slope was calculated. This concentration was found to be 5.9, 10.1, and 14.5 μM for CDSO3, FDSO3 and SDSO3, respectively, while it was 0.8 μM for enoxaparin. These results parallel the lag time results and show that sulfated DHPs are only 7.3–18.1-fold weaker than enoxaparin in inhibiting the strong positive feedback process of thrombin.

4.4.3 Effect of Sulfated DHPs on Whole Blood Clotting as Evaluated by Thromboelastography

The study on thrombin generation in plasma primarily describes the inhibition phenomenon prior to clot formation. However, clot is a dynamic system that matures and evolves as clotting proceeds. More specifically, it is a complex process of thrombin-mediated fibrin formation that involves many other components, e.g., platelets. To determine whether sulfated DHPs differ from enoxaparin in whole blood, we employed

thromboelastography (TEG®), a technique used routinely in clinical settings as well as for following anticoagulation with LMWHs [221-223].

TEG® measures various responses of a formed clot to shearing force. In this technique, a pin is inserted into an oscillating cup containing whole blood. As fibrin polymerizes, the pin starts to move with the oscillating cup and the movement of the pin is recorded as amplitude, which in time reaches maximum amplitude (MA) (Figure 49A, page 194). The stronger the clot, the more the pin moves with the cup and the higher the MA. Shear elastic modulus strength (G), a measure of clot stiffness, is calculated from MA. Additionally reaction time R and angle α (Figure 49A, page 194) are also obtained in a TEG® experiment. R is the time required for the appearance of the first detectable signal of 2mm in amplitude and is interpreted as the time required for the initial fibrin formation. Angle α is the acute angle in degrees between an extension of the R tracing and the tangent of the maximum slope produced by the TEG® tracing during clot stiffening. Angle α is a measure of the rate of formation of three-dimensional fibrin network. Parameters that affect MA include fibrin concentration and structure, concentration and functional state of platelets, deficiency of coagulation factors and presence of clotting inhibitors [224].

All three sulfated DHPs affect R, α, MA and G parameters in a dose-dependent manner (Table 5, page 188). For example, as the concentration of CDSO3 increases from 0 μM to 24.3 μM, R increases from 7.0 to 21.5 min. This effect parallels the time to clot results obtained in the plasma assay. Likewise, sulfated DHPs lower the value of angle α from 59° for normal blood to 13.5–17° at the highest concentrations studied. This indicates

that the kinetics of fibrin polymerization and networking is significantly retarded by the presence of sulfated DHPs. Enoxaparin exhibits similar characteristics, except that it is 23–51-fold more potent than sulfated DHPs when comparisons are made at doubling the R value from its value in the absence of any anticoagulants (not shown). Likewise, enoxaparin is 17–32-fold and 18–37-fold more potent when comparisons are made for a 50% reduction in the angle α and shear elastic modulus G, respectively (Figure 49B, page 194).

4.4.4 Effect of Sulfated DHPs on Whole Blood Coagulation as Evaluated by Hemostasis Analysis System.

To further compare the whole blood anticoagulant potential of the sulfated DHPs with enoxaparin, we performed an *ex-vivo* study using HAS™, which measures the forces generated by platelets within a clot [225]. In this technique, the clot is allowed to form between a temperature-controlled lower surface (cup) and a parallel upper surface (cone). As the clot grows, it attaches to both the surfaces pulling the fibrin strands inward. This pull is measured by a displacement transducer, which produces an electrical signal on the cone proportional to the amount of force generated by the platelets. HAS™ also provides detailed information on clot structure through the measurement of clot elastic modulus (CEM), which is the ratio of stress induced by platelets to strain arising from the change in clot thickness [226]. PCF is observed to increase as soon as thrombin is formed suggesting that appearance of PCF can be used as surrogate marker for TGT (described above), the time required for production of thrombin following initiation of clotting [225].

In addition to its dependence on thrombin, PCF is sensitive to platelet number, platelet metabolic status, presence of thrombin inhibitors and degree of GPIIb/IIIa exposure [222, 227-229]. Likewise, CEM is a complex parameter that is sensitive to changes in clot structure, fibrinogen concentration, the rate of thrombin generation and red blood cell flexibility, while TGT is sensitive to clotting factor deficiencies, antithrombin concentration and presence of anticoagulants. Low PCF and low CEM coupled with a prolonged TGT are associated with increased bleeding risk, while elevated PCF and CEM paired with a decreased TGT are associated with thrombotic disease states.

All three DHPs affect TGT, PCF and CEM parameters in a dose-dependent manner (Table 6, page 189). For example, as the concentration of FDSO3 increases from 0 to 23.8 μM, the TGT value increases from 235 seconds to 465 seconds (Figure 50A, page 195). This effect parallels the results obtained in the plasma thrombogenesis assay and TEG®. More importantly, the presence of sulfated DHPs in blood decreases PCF from 7.6 Kdynes to 2.4–1.2 Kdynes at 14–37 μM (Figure 50B, page 195), while enoxaparin induces a PCF of 0.9 Kdynes at 0.44 μM. When comparisons are made for a 50% reduction in PCF, enoxaparin is 63–140-fold more potent. Likewise, sulfated DHPs decrease CEM from 21.6 Kdynes/cm^2 for normal blood to 4.5–1.3 Kdynes/cm^2 at the highest concentrations studied. Comparison of CEM values indicates that enoxaparin is 43–90-fold more potent than sulfated DHPs (Figure 50C, page 195). These results confirm that sulfated DHPs behave in a manner similar to enoxaparin, except for the concentration at which these are effective.

4.5 DISCUSSION

Sulfated DHPs studied here are structurally unlike heparin and its derivatives including LMWHs, fondaparinux and idraparinux. Whereas heparin possesses a polysaccharide scaffold, DHPs are based on a 4-hydroxycinnamic acid scaffold. Earlier work suggests that sulfated DHPs contain an average of 0.8–0.9 anionic (sulfate and carboxylate) groups per repeating unit [212], while for heparins this number is ~2.6 [230]. Additionally, sulfated DHPs contain multiple aromatic rings, which are completely absent in heparin. These structural features introduce considerable hydrophobicity in sulfated DHPs in comparison to heparin.

Sulfated DHPs are also completely different from any of the clinically used anticoagulants including hirudin, bivalirudin, argatroban, dabigatran and ximelagatran. Whereas the peptides or peptidomimetics utilize positively charged groups, e.g. arginine or an arginine-mimic, to target the active site of pro-coagulant proteinases, sulfated DHPs are devoid of any positively charged group. Thus, sulfated DHPs represent a structurally distinct class of molecules.

On a mechanistic front, sulfated DHPs appeared to display a novel mechanism of anticoagulation. Preliminary investigations suggested that sulfated DHPs preferred to inhibit thrombin and factor Xa directly, although indirect mechanism through antithrombin could not be ruled out completely [212]. This was striking considering that sulfated DHPs were originally designed to mimic the function of heparin. Considering that these novel anticoagulants are negatively charged molecules, it can be inferred that direct inhibition of

thrombin and factor Xa does not arise from an active site competition, but possibly from an allosteric inhibition mechanism.

Given the unique structural and mechanistic features of sulfated DHPs, we sought to investigate the comparative anticoagulant potency of these molecules. The work presented here shows that in the PT assay, the three sulfated DHPs are effective at concentrations in the range of enoxaparin, while in the APTT assay they are only 2–6-fold weaker. Interestingly, despite major structural differences, both sulfated DHPs and enoxaparin prolong APTT better than PT. This suggests that the DHPs affect the intrinsic pathway of coagulation more than the extrinsic pathway. Finally, the anticoagulant potency among the sulfated DHPs followed the order of CDSO3 > FDSO3 > SDSO3 indicating a significant dependence of activity on structure.

All three sulfated DHPs inhibit the initial activation of prothrombin to thrombin in human plasma and also slow down the process of thrombin 'explosion' suggesting that the new molecules possess properties characteristic of an anticoagulant. Initial thrombin formation is slowed because the sulfated DHPs are inhibiting upstream enzymes, especially factor Xa, while the rate of thrombin 'explosion' is significantly reduced due to direct thrombin inhibition. Likewise, in whole blood all three sulfated DHPs increased the R time, while decreasing α, MA and G in the TEG® study. The three sulfated DHPs are also able to decrease CEM and PCF, and increase TGT in HAS™ experiments. Overall, in both human plasma and whole blood, CDSO3 displays the best anticoagulant profile followed by FDSO3 and SDSO3, a trend noted consistently in current studies.

Comparison of the efficacy shows that in plasma, sulfated DHPs are 3–6-fold and 7–18-fold less active than enoxaparin in the APTT and thrombin generation assays, respectively. Studies in whole blood show that sulfated DHPs are 17–51-fold and 43–140-fold less active than enoxaparin in TEG® and HAS™ assays, respectively. The precise origin of the significant difference between plasma and whole blood efficacies of sulfated DHPs is not clear and represents an important area to address in future design. Yet, except for the efficacy, the DHPs display inhibitory profiles similar to enoxaparin in the assays studied here. It is interesting that although sulfated DHPs and enoxaparin display different structures and mechanism of action, they exhibit similar anticoagulation profiles at significantly different concentrations. Further, the result that structurally-related DHPs possess significant differences in their anticoagulant potential bodes well for future improvement. These results suggest that sulfated DHPs are novel and interesting first generation anticoagulants from which advanced molecules should be possible to design through structural modifications. More studies are necessary to further understand similarities and differences, especially whether the DHPs can inhibit clot-bound thrombin, a desirable property found to be absent in LMWHs. Finally, toxicity studies are desirable to assess whether current sulfated DHPs induce adverse effects at the concentrations required for anticoagulant effect.

4.6 Tables

Table 4. Effect of DHPs and enoxaparin on human plasma clotting times.

	Concentration (μM)	
	2 × PT[a]	***2 × APTT***[b]
FDSO3	16.6 ± 1.7	4.1 ± 0.4
SDSO3	33.3 ± 3.0	6.4 ± 1.2
Enoxaparin	75.3 ± 2.0	1.2 ± 1.1
CDSO3	13.1 ± 1.3	2.9 ± 0.8

[a]The normal human plasma PT was found to be 12.2 sec. [b] The uninhibited human plasma APTT was 29.5 sec.

Table 5. Parameters obtained from thromboelastograph (TEG®) study of sulfated DHPs and enoxaparin in human whole blood.[a]

	$[DHP]_O$	*TEG® Parameters*[a]			
		R[b]	***α***[c]	***MA***[d]	***G***[e]
	(μM)	*(min)*	*(degrees)*	*(mm)*	*(Dynes/cm²)*
No Anticoagulant	0	7.0	59.0	56.5	6456.5
CDSO3	8.1	7.0	49.5	56.5	6494.5
	16.2	10.5	38.0	47.0	4434.0
	20.3	19	27.0	40.0	3333.5
	24.3	21.5	15.0	29.5	2092.0
FDSO3	6.5	7.0	60.0	55.0	6111.0
	13.0	11.5	43.5	48.5	4708.5
	19.6	13.5	34.5	44.0	3928.5
	26.1	14.0	22.5	36.5	2874.0
	32.7	19.0	13.5	27.5	1896.5
SDSO3	22.8	8.5	50.5	51.5	5309.5
	38.0	13.0	26	43	3772.0
	45.6	21.0	17.0	32.5	2407.5
Enoxaparin	0.3	8	49	51	5204.0
	0.44	9.5	39.5	51	5204.0
	0.6	11.5	43.0	47.0	4434.0
	0.75	14.0	41.0	46	4259.5
	0.89	17.0	36.5	47.0	4434.0
	1.0	17.0	31.5	42.0	3620.5

[a]TEG parameters were obtained in an automated manner from the TEG® coagulation analyzer. See Experimental Procedures for a description of the setup. [b]Reaction time R is the time interval between the initiation of coagulation and the appearance of first detectable signal of no less than 2 mm in amplitude. [c]Angle α is the acute angle in degrees between an extension of the R value tracing and the tangent of the maximum slope produced by the TEG® tracing. [d]Maximum amplitude (MA) is the maximum distance the pin of TEG® moves at the end. [e]The shear elastic modulus strength (G) is a calculated parameter (G = 5000×MA / (100 – MA) and is a measure of clot strength.

Table 6. HAS™ parameters for sulfated DHPs and enoxaparin in human whole blood.[a]

	$[DHP]_o$	*HAS™ Parameters*[a]		
		TGT[b]	***PCF***[c]	***CEM***[d]
	(μM)	*(min:sec)*	*(Kdynes)*	*(Kdynes/cm²)*
No Anticoagulant	0	3:55	7.6	21.6
CDSO3	8.0	3:24	6.8	18.7
	10.0	3:43	5.1	14.2
	12.0	5:55	3.5	9.4
	14.0	9:14	2.4	4.5
FDSO3	9.5	5:12	6.5	19.5
	12.7	5:25	4.9	13.5
	15.9	5:45	4.1	10.2
	23.8	7:45	2.2	3.9
SDSO3	14.8	3:35	6.5	17.8
	18.5	4:24	5.7	14.8
	27.8	6:55	3.2	7.0
	37.0	13:00	1.2	1.3
Enoxaparin	0.146	5:15	5.3	15.1
	0.218	9:05	3.6	12.7
	0.346	11:00	2.8	8.5
	0.437	12:45	0.9	2.9

[a]HAS™ parameters were obtained in an automated manner from the Hemostasis Analysis System. See Experimental Procedures for a description of the setup. [b]Thrombin generation time is the time interval between the initiation of coagulation and the onset of detectable platelet contractile force. [c]Platelet contractile force describes the forces generated by platelets during clot retraction. [d]Clot elastic modulus is the ratio of the applied force (stress) to the measured displacement of the clot.

4.7 FIGURE LEGENDS

Figure 47. Structures of heparins (A) and sulfated DHPs (B). A) Fondaparinux is based on heparin pentasaccharide, while heparin and LMWHs are polydisperse, heterogeneous mixture of polysaccharide chains (M_R ~13,000 and ~4,000 Da, respectively) arising due to variations in X, Y, Z and R groups. B) Sulfated DHPs possess a radically different structure from the heparins (and other anticoagulants) and are synthesized in two steps from the corresponding 4-hydroxycinnamic acid monomers, caffeic acid (CA), ferulic acid (FA) or sinapic acid (SA). The M_R of the sulfated DHPs is in the range of 3,000–4,000 Da. Linkages, β-*O*-4 and β-5, are commonly present in sulfated DHPs (shown as shaded ovals).

Figure 48. A) Inhibition of thrombin generation in human plasma by CDSO3 in the range of 0 to 20 μM. Inset diagram shows three parameters – lag time, slope of thrombin explosion, and clot time – typically derived from the thrombin generation curve. B) and C) show the dependence of thrombin generation lag time and slope, respectively, on anticoagulant concentration. Solid lines represent trend lines used to obtain the concentration of anticoagulant necessary for doubling of lag time and 50% decrease in slope value.

Figure 49. Comparison of the effect of sulfated DHPs and enoxaparin on clot formation in whole blood using TEG®. Inset in (A) shows a typical thromboelastogram expected of any anticoagulant. MA, R, α and G are parameters obtained from TEG® analysis. See Methods for details. (B) shows the variation in G as a function of concentration of the sulfated DHPs and enoxaparin. Solid lines are trend lines (not regression fits) from which concentration of anticoagulant needed to reduce shear elastic modulus G by 50% (shown as shaded line) of the starting value was derived.

Figure 50. Comparison of the effect of sulfated DHPs and enoxaparin on platelet function in whole blood using HAS™. A) shows selected HAS™ profiles obtained with FDSO3, B) and C) show the variation in PCF and CEM, respectively, as a function of concentration of the sulfated DHPs and enoxaparin. Solid lines are trend lines from which the concentration of anticoagulant needed to reduce PCF or CEM by 50% (shaded line) of the starting value was derived.

Figure 47

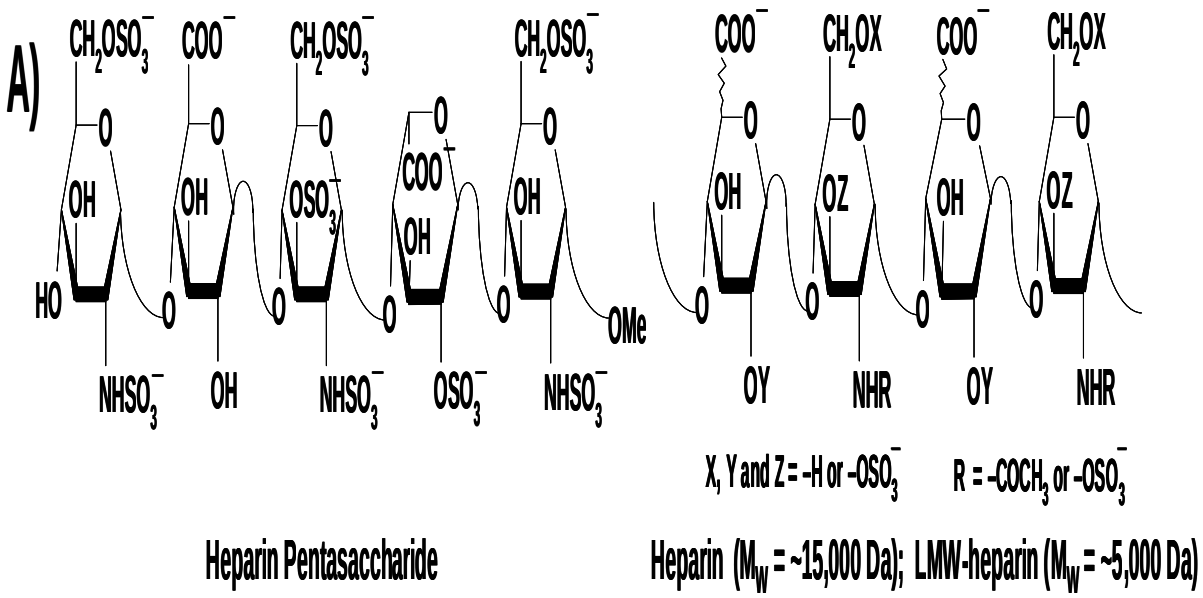

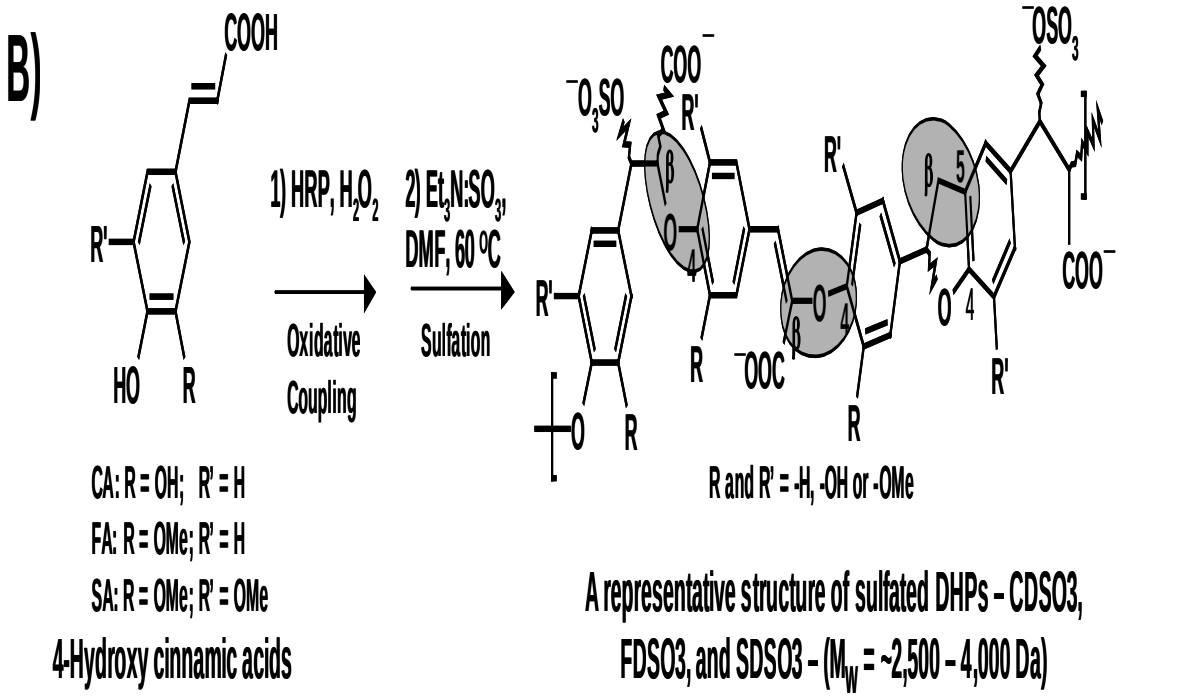

Figure 48

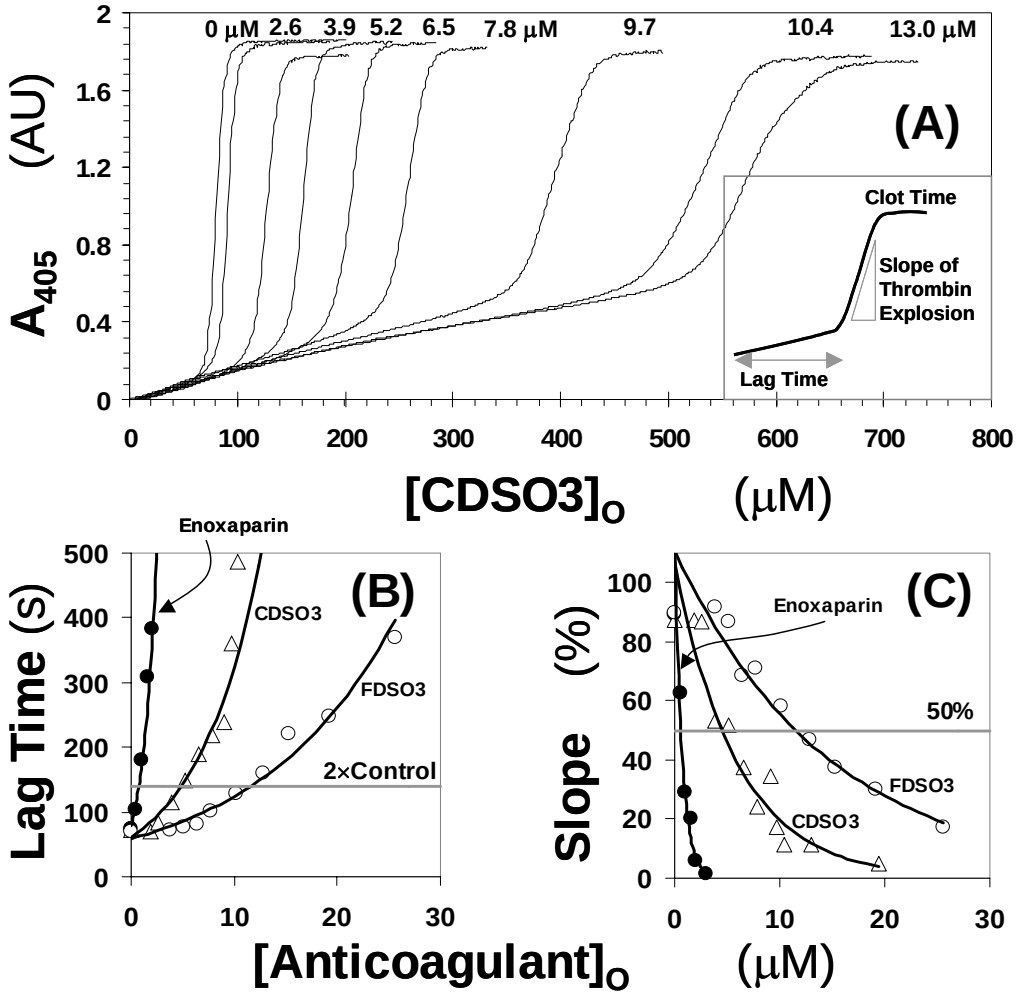

Figure 49

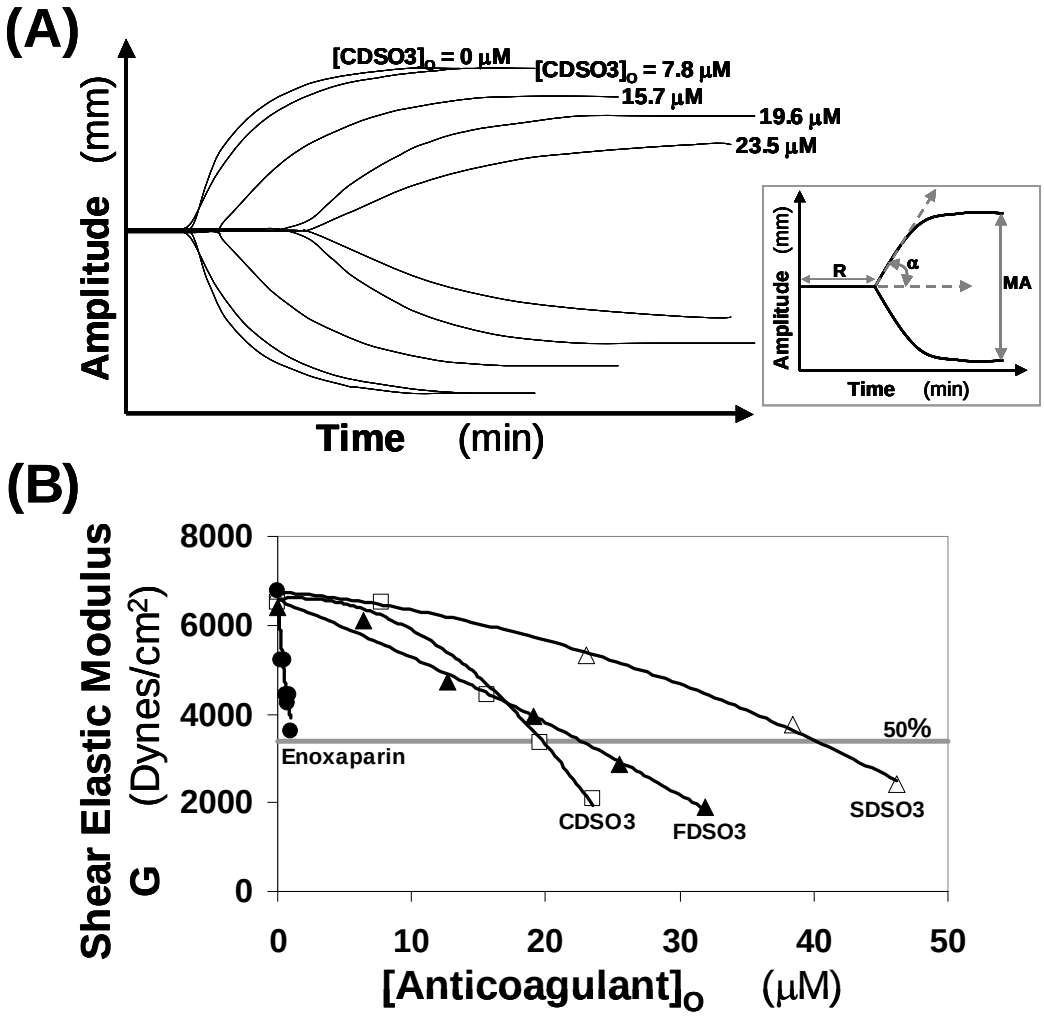

Figure 50

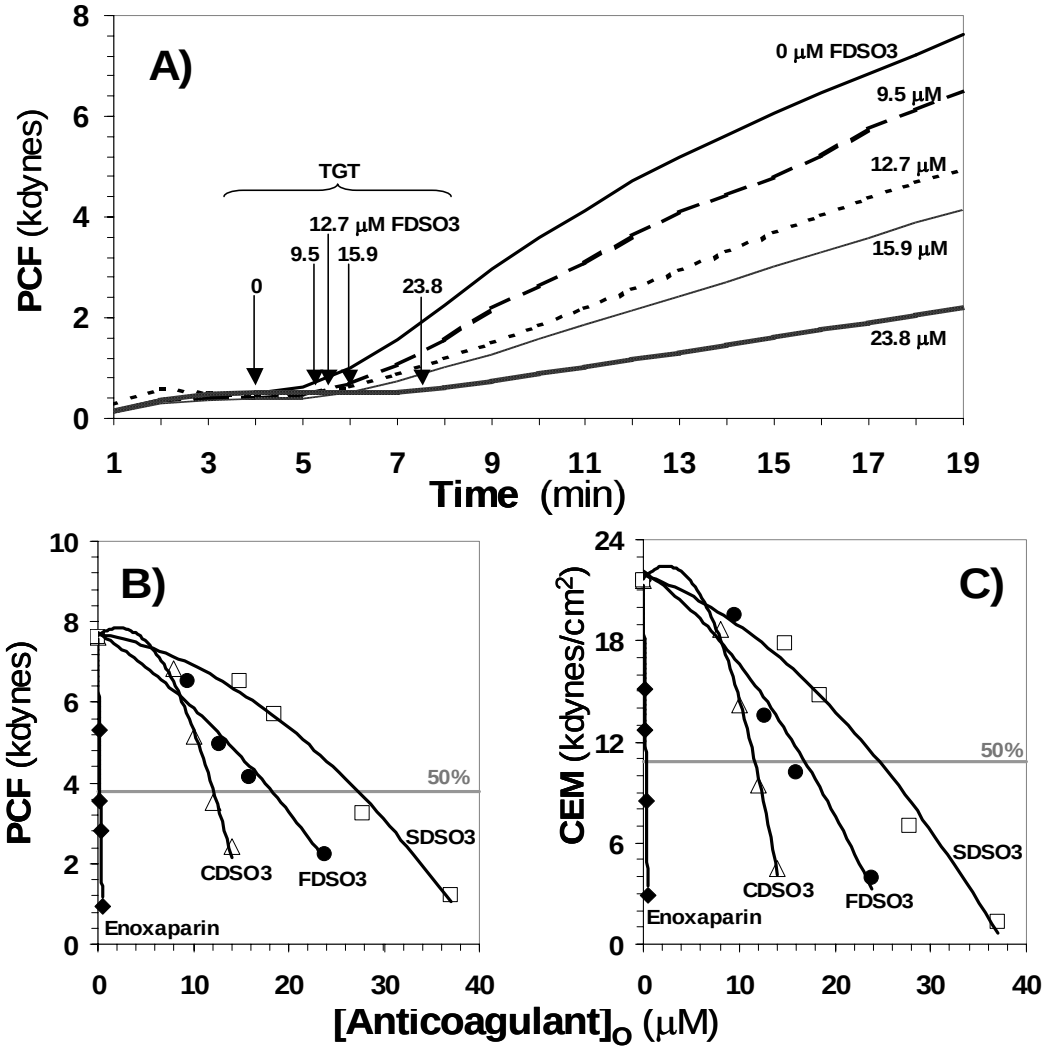

Chapter 5: A Novel Allosteric Pathway of Thrombin Inhibition
EXOSITE II MEDIATED POTENT INHIBITION OF THROMBIN BY CHEMO-ENZYMATIC, SULFATED DEHYDROPOLYMERS OF 4-HYDROXYCINNAMIC ACIDS

5.1 Abstract

Thrombin and factor Xa, two important pro-coagulant proteinases, can be regulated through direct and indirect inhibition mechanisms. Recently, we designed sulfated dehydropolymers (DHPs) of 4-hydroxycinnamic acids that displayed interesting anticoagulant properties [212]. To better understand their mechanism of action, we studied the inhibition of thrombin, factor Xa, factor IXa, and factor VIIa in the presence (indirect) and absence (direct) of antithrombin by CDSO3, FDSO3 and SDSO3, three analogs of sulfated DHPs. CDSO3 and FDSO3 displayed a 2–3-fold preference for direct inhibition of thrombin over factor Xa, while this preference for inhibiting thrombin over factor IXa and factor VIIa increases to 17–187-fold and >815-fold, respectively, suggesting a high level of specificity. Whereas CDSO3 and FDSO3 prefer the direct pathway for inhibiting thrombin and factor Xa, the indirect pathway is preferred for inhibition of factor IXa. Although structurally related to CDSO3 and FDSO3, SDSO3 inhibits all four enzymes primarily through the indirect inhibition mechanism. Competitive binding studies with a thrombin-specific chromogenic substrate, a fluorescein-labeled hirudin peptide, bovine heparin, enoxaparin, and a heparin octasaccharide suggest that CDSO3 preferentially binds in or near anion-binding exosite II of thrombin. Studies of the hydrolysis of H-D-

hexahydrotyrosol-Ala-Arg-*p*-nitroanilide indicate that CDSO3 inhibits thrombin through allosteric disruption of the catalytic apparatus, specifically through the catalytic step. Overall, sulfated DHPs appear to be the first molecules that bind primarily in the region defined by exosite II and allosterically induce thrombin inhibition. The molecules are radically different in structure from all the current clinically used anticoagulants and thus, represent a novel class of potent dual thrombin and factor Xa inhibitors.

5.2 Introduction

The coagulation cascade is composed of two intertwined pathways, called the extrinsic and the intrinsic pathways, which operate in a highly complex, but tightly-regulated, manner to bring about controlled formation of the fibrin polymer. Several enzymes participate in this process, including factor IXa and factor VIIa, which belong to the intrinsic and extrinsic pathways, respectively, and thrombin and factor Xa, which belong to the common pathway. The cascade is regulated by several proteins present naturally in the plasma, of which antithrombin is a major regulator.

Antithrombin, a member of the serpin (serine proteinase inhibitor) family of proteins, primarily inhibits thrombin, factor Xa, and factor IXa, while also possibly inhibiting several other enzymes to a lesser extent. Yet, antithrombin is a rather poor inhibitor of these pro-coagulant enzymes and requires the presence of heparin to exhibit its anticoagulant potential. Heparin is a highly sulfated, polysaccharide that greatly enhances the rate of antithrombin inhibition of thrombin, factor Xa and factor IXa under

physiological conditions. This acceleration is the primary reason for heparin's continued use as an effective anticoagulant for the past eight decades. Yet, heparin suffers from several limitations including enhanced risk for bleeding, variable patient response, heparin-induced thrombocytopenia and the inability to inhibit clot-bound thrombin [21]. Low molecular weight heparins (LMWHs), derivatives of heparin with reduced polymeric length, and fondaparinux, a specific sequence of five saccharide residues (Figure 47A, page 192), have been introduced in the past decade as better mimics of full-length heparin. These new anticoagulants still possess risk for bleeding and are unable to inhibit clot-bound thrombin [21].

A major reason for the limitations of heparin therapy is its high negative charge density. Heparin (and LMWH) is a linear, co-polymer of glucosamine and uronic acid residues that are decorated with a large number of sulfate groups generating a complex, heterogeneous, polyanionic macromolecule (Figure 47A, page 192). This highly polyanionic polymer is capable of interacting with a large number of plasma proteins and cells, which likely induce many of the adverse effects of heparin [29].

Apart from the indirectly acting heparins, several direct inhibitors have been put forward including argatroban, ximelagatran, and dabigatran for thrombin and, DX9065a and razaxaban for factor Xa [37]. Structurally, most direct inhibitors of thrombin (DTIs) and factor Xa contain a guanidine or an amidine group that mimic the critical arginine residue at the P-1 site of the proteinase recognition sequence [13]. DTIs and direct factor Xa inhibitors form major classes of clotting regulators that are considered to be superior to heparins primarily because of the expectation that they are likely to inhibit both circulating

and clot-bound enzymes. Yet, challenges exist in the development of these inhibitors including establishing enzyme-binding affinity that is not associated with excessive bleeding and avoiding liver toxicity [37].

Mechanistically, the direct and indirect anticoagulants utilize different pathways of inhibition. While heparins require antithrombin to mediate their effect, DTIs and direct factor Xa inhibitors either bind in the active site or to an exosite on the enzyme to inhibit its proteolytic function [13]. With a goal of developing dual inhibitors of factor Xa and thrombin that are less polyanionic and more hydrophobic than heparins, we designed sulfated dehydropolymers (DHPs) (Figure 47, page 192). Three sulfated DHPs – CDSO3, FDSO3 and SDSO3 – were prepared in a simple, two-step chemo-enzymatic process involving horseradish peroxidase catalyzed oligomerization of 4-hydroxycinnamic acid monomers followed by the chemical sulfation of the resulting DHPs with triethylamine-sulfur trioxide complex [212]. Preliminary studies suggested that the chemo-enzymatic sulfated DHPs were potent anticoagulants *in vitro*. The sulfated DHPs prolonged activated partial thromboplastin time and prothrombin time at concentrations equivalent to LMWH. The studies also suggested that CDSO3, FDSO3 and SDSO3 inhibited factor Xa and thrombin in an antithrombin–dependent as well as independent manner suggesting a potentially novel mode of inhibition [212].

In this chapter, we report that CDSO3, FDSO3, and SDSO3 possess high selectivity for inhibiting thrombin and factor Xa over other enzymes of the coagulation cascade; CDSO3 inhibits thrombin through allosteric disruption of its catalytic apparatus; and preferentially binds the enzyme in or near the region formed by anion-binding exosite

II. Sulfated DHPs appear to be the first molecules that induce inhibition of pro-coagulant proteinases, thrombin and factor Xa, through exosite II. Our work suggests that sulfated DHPs are structurally, functionally and mechanistically a very interesting class of molecules that may lead to novel anticoagulants.

5.3 EXPERIMENTAL PROCEDURES

5.3.1 Proteins and Chemicals

Sulfated dehydropolymers CDSO3, FDSO3 and SDSO3 (Figure 47B, page 192) were prepared in two steps from 4-hydroxycinnamic acid monomers, caffeic acid (CA), ferulic acid (FA) and sinapic acid (SA) using chemo-enzymatic synthesis described by Monien *et al* [212]. Human antithrombin (AT) was purchased from Molecular Innovations (Southfield, MI), while the human plasma proteinases, factor VIIa, factor IXa, factor Xa and α-thrombin, were purchased from Haematologic Technologies (Essex Junction, VT) and used as such. Stock solutions of proteins were prepared in 20 mM sodium phosphate buffer, pH 7.4, containing 100 mM NaCl and 2.5 mM $CaCl_2$ (AT and thrombin) or 5 mM MES buffer, pH 6.0 (factor Xa). Factor VIIa stock solutions of proteins were prepared in 25 mM HEPES buffer, pH 7.4, containing 100 mM NaCl and 5 mM $CaCl_2$, while factor IXa stock solutions were prepared in 5 mM MES buffer, pH 5.5 containing 150 mM NaCl. Chromogenic substrates Spectrozyme TH (H-*D*-hexahydrotyrosol-Ala-Arg-*p*-nitroanilide), Spectrozyme FXa (Methoxycarbonyl-*D*-cyclohexylglycyl-Gyl-Arg-*p*-nitroanilide), Spectrozyme FIXa (*D*-Leu-Phe-Gly-Arg-*p*-nitroanilide) and Spectrozyme FVIIa (methanesulphonyl-*D*-cyclohexylalanyl-butyl-Arg-*p*-nitroanilide) were purchased from

American Diagnostica (Greenwich, CT). A low molecular weight heparin (M_W 5,060 Da) used in plasma assays was purchased from Sigma (St. Louis, MO), while enoxaparin (M_W 4,500 Da, from Aventis Pharmaceuticals) and fondaparinux (M_W 1,727 Da, from GlaxoSmithKline) were pharmaceutical grade. Heparin octasaccharide H8 was from Dextra Laboratories (Reading, UK). Thrombin substrate *p*-nitrophenyl-*p'*-guanidinobenzoate (NPGB) and active site fluorophore *p*-aminobenzamidine (PABA) were purchased from Sigma Chemicals (St. Louis, MO) and used as such. Tyr63-sulfated hirudin-(54-65) labeled with 5-(carboxy)fluorescein ([5F]-Hir[54-65](SO_3^-)) was prepared as described earlier [209]. All other chemicals were analytical reagent grade from either Sigma Chemicals (St. Louis, MO) or Fisher (Pittsburgh, PA) and used without further purification.

5.3.2 Physico-chemical Properties of CDSO3, FDSO3 and SDSO3

The weight average molecular weight (M_W) of the unsulfated parent dehydropolymers CD, FD and SD were determined by Monien *et al.* [212] using non-aqueous size-exclusion chromatography (Table 7, page 220). The M_W values suggest that an average of 12.7, 15.5, and 14.4 monomer units are present in CD, FD and SD, respectively. Sulfate composition of the sulfated DHPs was determined by elemental analysis and found to be 0.40, 0.30 and 0.38 sulfate groups per monomer unit [212]. This implies that an average of 5.1, 4.7, and 5.5 sulfate groups per average DHP chain are present in CDSO3, FDSO3, and SDSO3, respectively. Thus, the M_W value of the sulfated DHPs was calculated to be 3320, 4120, and 3550 Da for CDSO3, FDSO3, and SDSO3, respectively (Table 7, page 220).

5.3.3 Direct and Indirect Inhibition of Coagulation Proteinases

Both direct and indirect inhibition of thrombin, factor Xa, factor IXa, and FVIIa by sulfated DHPs was determined by chromogenic substrate hydrolysis assays [211, 213, 231, 232]. For these assays, 10 µL DHP at concentrations ranging from 0.035 to 10,000 µg/mL was diluted with 930 µL of the appropriate buffer in PEG 20,000-coated polystyrene cuvettes. The buffers used in these experiments include 20 mM Tris-HCl buffer, pH 7.4, containing 100 mM NaCl, 2.5 mM $CaCl_2$ and 0.1 % polyethylene glycol (PEG) 8000 for thrombin and factor Xa; 100 mM HEPES buffer, pH 8, containing 100 mM NaCl and 10 mM $CaCl_2$ for factor IXa [231]; and 25 mM HEPES buffer, pH 7.4, containing 100 mM NaCl and 5 mM $CaCl_2$ for factor VIIa [232]. Following the preparation of the sulfated DHP solution, 10 µL of the proteinase solution was added to give 1 to 10 nM initial enzyme concentration and the cuvette incubated for 10 minutes. Thrombin, factor Xa and factor VIIa assays were incubated at 25°C, while factor IXa assays were incubated at 20°C. Following incubation, 50 µL of 2 mM chromogenic substrate, Spectrozyme TH, FXa, FVIIa or Spectrozyme FIXa, was rapidly added and the residual enzyme activity was determined from the initial rate of increase in absorbance at 405 nm. Relative residual proteinase activity at each concentration was calculated using the activity measured under otherwise identical conditions, except for the absence of the sulfated DHP. Indirect inhibition of thrombin by sulfated DHPs was performed at a fixed 100 nM concentration of antithrombin, while for indirect inhibition of factors VIIa, IXa and Xa a 200 nM concentration of the serpin was used. Except for the presence of antithrombin, the indirect

inhibition assays were performed in an otherwise identical manner to the direct inhibition assays. Logistic equation I was used to fit the dose-dependence of residual proteinase activity to obtain IC_{50}.

$$Y = Y_O + \frac{Y_M - Y_O}{1 + 10^{(\log IC_{50} - [DHP]_O)HS}} \qquad \textbf{Eq. I}$$

In this equation Y is the fractional residual proteinase activity, Y_M and Y_O are the maximum and minimum possible values of the proteinase activity, IC_{50} is the concentration of the inhibitor that results in 50% inhibition of enzyme activity, and HS is the Hill slope.

5.3.4 Michaelis-Menten Kinetics of Spectrozyme TH Hydrolysis by Thrombin in the Presence of CDSO3

The initial rate of Spectrozyme TH hydrolysis by 1 nM thrombin was monitored from the linear increase in absorbance at 405 nm corresponding to less than 10% consumption of the substrate. The initial rate was measured as a function of various concentrations of the substrate (0.2 to 20 μM) in the presence of fixed concentration of CDSO3 (10–100 nM) in 20 mM Tris-HCl buffer, pH 7.4, containing 100 mM NaCl, 2.5 mM $CaCl_2$ and 0.1 % PEG8000 at 25 ^{O}C. The data was fitted by the Michaelis-Menten equation to determine $K_{M,app}$ and V_{MAX}. To calculate k_{CAT} from V_{MAX}, active site titration of thrombin with NPGB was performed, according to the reported procedure [233], and the change in extinction co-efficient of 9920 $M^{-1}cm^{-1}$ [234, 235] was used for the release of *p*-nitroaniline.

5.3.5 Michaelis-Menten Kinetics of Spectrozyme TH Hydrolysis by Thrombin in the Presence of [5F]-Hir[54-65](SO_3^-)

The initial rate of Spectrozyme TH hydrolysis by 1 nM thrombin was monitored from the linear increase in absorbance at 405 nm corresponding to less than 10% consumption of the substrate. The initial rate was measured as a function of various concentrations of the substrate (0.4 to 20 μM) in the presence of fixed concentration of [5F]-Hir[54-65](SO_3^-) (8.6–103.2 nM) in 20 mM Tris-HCl buffer, pH 7.4, containing 100 mM NaCl, 2.5 mM $CaCl_2$ and 0.1 % PEG8000 at 25 ^{O}C. The data were analyzed as described above.

5.3.6 Competitive Binding Studies with [5F]-Hir[54-65](SO_3^-), an Exosite I ligand

CDSO3-dependent thrombin inhibition studies in the presence of [5F]-Hir[54-65](SO_3^-) were performed in a manner similar to that described above for direct thrombin inhibition using the chromogenic substrate hydrolysis assay. A 950 μL solution containing CDSO3, [5F]-Hir[54-65](SO_3^-) and thrombin, each at their required concentrations, in 20 mM Tris-HCl buffer, pH 7.4, containing 100 mM NaCl, 2.5 mM $CaCl_2$ and 0.1 % PEG 8000 was incubated at 25 ^{O}C in PEG 20,000-coated polystyrene cuvettes for 10 minutes. Following incubation, 50 μL of 2 mM Spectrozyme TH was added and the initial change in absorbance at 405 measured. A 4 nM concentration of thrombin was found to give sufficient signal at various concentrations of the fluorescent peptide for reproducible results. The dose-dependence of the fractional residual proteinase activity at each concentration of the competitor was fitted by equation **I** to obtain the apparent

concentration of CDSO3 required to reduce thrombin activity to 50% of its initial value ($IC_{50,app}$).

5.3.7 Competitive Binding Studies with Anion-Binding Exosite II Ligands

Exosite II competition experiments were performed in a manner similar to that described above, except for the presence exosite II competitors. Briefly, residual thrombin activity was measured in a spectrophotometric assay following 10 minute incubation of CDSO3, exosite II competitor and thrombin, each at the required concentration, in 20 mM Tris-HCl buffer, pH 7.4, as described above. Exosite II competitor ligands included bovine heparin, enoxaparin and H8. The M_W of bovine heparin and enoxaparin were assumed to be 15000 and 4500 Da, respectively, as reported in the literature [209, 236]. The dose-dependence of the fractional residual proteinase activity at each concentration of the competitor was fitted by equation I to obtain $IC_{50,app}$. The affinities of bovine heparin, enoxaparin and H8 for thrombin under the conditions utilized for inhibition experiments were measured spectrofluorometrically using *p*-aminobenzamidine (PABA), as reporter of interaction following published procedures [237]. The interaction of exosite II GAG ligands with thrombin–PABA complex results in a saturable quenching in fluorescence at 370 nm (~16 %, λ_{EX} = 345 nm), which can be fitted by the quadratic binding equation to derive the K_D for the interaction.

5.4 RESULTS

5.4.1 Structure of Sulfated Dehydropolymers (DHPs)

The sulfated DHP molecules studied in this work were prepared chemo-enzymatically in two steps from 4-hydroxy cinnamic acid monomers, caffeic acid, ferulic acid and sinapic (Figure 47B, page 192). Horseradish peroxidase-catalyzed oxidative coupling followed by sulfation of the available hydroxyl and phenolic groups gives the corresponding sulfated DHPs, CDSO3, FDSO3, and SDSO3, in reproducibly good yields [212]. Overall, these sulfated DHPs are a mixture of many oligomeric species that range in size from 4–15 monomer units and contain several inter-monomer linkages, including β-*O*-4, β -5, β - β and 5-5. Of these, β -*O*-4 and β -5 linkages form the major proportion (Figure 47B, page 192), except for SDSO3 (see below).

Although heparins and sulfated DHPs belong to structurally distinct class of molecules, with respect to the properties of polydispersity and microheterogeneity, they have much in common. Each preparation of both these types of molecules contains numerous sequences possessing different chain lengths and fine structure. Yet, the level of sulfation in the sulfated DHPs is significantly lower than that found in heparins. Whereas the three sulfated DHPs studied here have an average of 1 sulfate group for every 2–3 monomer residues, heparins possess an average of 2–2.5 sulfate groups for every disaccharide (Table 7, page 220). More importantly, the backbone of sulfated DHPs is composed of a number of aromatic rings, a feature completely absent in heparin. Thus, the sulfated DHPs are significantly more hydrophobic than heparins, while heparins have significantly more anionic character. Finally, whereas unfractionated heparin with a M_W of

~15,000 Da is considerably larger, sulfated DHPs (~2500–4000 Da) are comparable to enoxaparin (4,500 Da) and fondaparinux (~1,700 Da) (Table 7, page 220).

Although all three sulfated DHPs possess several types of inter-monomer linkages, structural constraints in the SA monomer do not allow the formation of 5-5 and β-5 inter-monomer linkages in the oligomer [212]. Thus, the predominant inter-monomeric linkage in SDSO3 is β-*O*-4 with some proportion of β-β. This implies that the SDSO3 dehydropolymer is structurally more homogeneous, or less diverse, than CDSO3 and FDSO3.

5.4.2 Sulfated DHPs Inhibit Factor Xa and Thrombin in the Presence and Absence of Antithrombin

To understand the origin of the anticoagulant activity of sulfated DHPs, we previously performed some initial studies on direct and indirect inhibition of factor Xa and thrombin, two key enzymes of the coagulation cascade [212]. These studies have been extended and compared with two clinically used anticoagulants, enoxaparin and fondaparinux. Inhibition of these enzymes was studied by measuring the residual enzyme activity following incubation with sulfated DHPs under pseudo-first order conditions for a fixed time in the presence and absence of a fixed concentration of human plasma antithrombin. The residual enzyme activity was measured by spectrophotometric determination of the initial rate of hydrolysis of chromogenic substrate. Enoxaparin (and a LMWH from Sigma) was used as a reference for both factor Xa and thrombin, while fondaparinux served as an additional reference for factor Xa.

As the concentration of the sulfated DHP was increased, the residual factor Xa or thrombin activity in the absence of antithrombin progressively decreased (Figure 51, page 228). In striking contrast, enoxaparin and fondaparinux displayed no inhibition even at concentrations higher than 100 μM (not shown). The decrease in activity was fitted by the logistic dose–response equation I to derive the IC_{50} value, the concentration of the inhibitor that results in 50% reduction in enzyme activity (Table 8, page 221-222). The three sulfated DHPs inhibited factor Xa and thrombin with IC_{50} values in the range of 34–244 nM and 18–94 nM, respectively (Figure 51, Table 8). Of the three sulfated DHPs, CDSO3 and FDSO3 are nearly 3.2–7.2-fold better than SDSO3. This suggests that the sulfated DHPs studied here are potent direct inhibitors of factor Xa and thrombin.

A decrease in enzyme activity with increasing concentrations of the sulfated DHPs was also observed in the presence of antithrombin (Figure 51, page 228). These indirect inhibition curves yielded IC_{50} values of 53–133 nM against factor Xa. In contrast, enoxaparin, a LMWH (from Sigma) and fondaparinux displayed IC_{50} values of 3.4, 6.9 and 1.9 nM, respectively (Table 8, page 221-222). This suggests that the sulfated DHPs are approximately 28–70-fold weaker inhibitors of factor Xa in the presence of antithrombin than the three reference molecules. Likewise, the IC_{50} values for indirect inhibition of thrombin by sulfated DHPs were found to be in the range of 45–71 nM, approximately 24–37-fold lower than that for enoxaparin and a Sigma LMWH (Table 8, page 221-222).

A closer look at the data highlights differences in the enzyme inhibition by the sulfated DHPs. Both CDSO3 and FDSO3 are better at inhibiting factor Xa and thrombin directly in comparison to that in the presence of antithrombin. Whereas the IC_{50} value

against factor Xa increases 1.6–2.9-fold for CDSO3 and FDSO3 in the presence of antithrombin as compared to that in its absence, for SDSO3 the IC_{50} value decreases ~2.5-fold. Although the indirect and direct inhibition pathways are expected to complement each other, it appears that the antithrombin-mediated pathway is a competing side reaction for CDSO3 and FDSO3, but not for SDSO3. It is possible that antithrombin competes with thrombin (and factor Xa) for CDSO3 and FDSO3, but possesses relatively weaker inhibition properties in complex with the DHPs, thereby reducing the concentration of free sulfated DHPs for direct reaction with thrombin (or factor Xa). More work is needed to clarify the proportion of contribution of the indirect pathway to the overall process of inhibition by CDSO3 and FDSO3. Yet, the current work indicates that CDSO3 and FDSO3 prefer to inhibit thrombin and factor Xa through the direct pathway, while SDSO3 appears to utilize both pathways for thrombin and factor Xa inhibition.

5.4.3 Effect of Sulfated DHPs on the Direct and Indirect Inhibition of Factor IXa and Factor VIIa

To determine whether the sulfated DHPs inhibit other enzymes of the coagulation cascade, we studied direct and indirect inhibition of factor IXa and factor VIIa, enzymes of the intrinsic and extrinsic pathways, respectively. The inhibition was studied in a manner similar to that reported in the literature, except for the presence of sulfated DHPs (or reference compound) in the reaction mixture [231, 232]. In the absence of antithrombin, CDSO3 and FDSO3 inhibited factor IXa with IC_{50} values of 3.4 and 0.5 μM, while inhibition of factor VIIa was not detectable (Table 8, page 221-222). Likewise, in the

direct inhibition assay SDSO3 was essentially inactive against both factor IXa and factor VIIa (Figure 52, page 229). These results suggest that CDSO3 and FDSO3 are better direct inhibitors of factor Xa and thrombin with 7–99-fold and 17–187-fold, respectively, higher selectivity over factor IXa. The level of specificity of direct inhibition against factor VIIa is even greater (>319-fold).

In the presence of antithrombin, all three sulfated DHPs displayed reasonably good inhibition of factor IXa with IC_{50} values in the range of 0.6–4.1 μM, while enoxaparin showed an IC_{50} value of 56 nM indicating a 11–73-fold greater potency (Table 8, page 221-222). Against factor VIIa, the presence of antithrombin did not induce any inhibition with CDSO3 and FDSO3 (Table 8, page 221-222). Together, these results suggest that CDSO3 and FDSO3 are better inhibitors of factor Xa and thrombin in the presence of antithrombin than factor IXa by a factor of 4.5–78-fold and 8–78-fold, respectively. This specificity of indirect inhibition increases much more when compared to factor VIIa (>178).

As an indirect inhibitor, SDSO3 displayed fairly potent inhibition of factor VIIa with an IC_{50} value of 356 nM (Figure 52, Table 8). In comparison, the enoxaparin–antithrombin complex was completely inactive against factor VIIa even at concentrations as high as 222 μM. This result suggests that SDSO3 induces antithrombin to become a better inhibitor of factor VIIa. Overall, SDSO3 is the only sulfated DHP studied that inhibits all four enzymes with good to reasonable potency in the presence of antithrombin (Table 8). Thus, SDSO3 appears capable of utilizing both the direct and indirect inhibition pathways.

5.4.4 CDSO3 Inhibits Thrombin by Disrupting its Catalytic Apparatus

To understand the molecular basis for sulfated DHPs inhibiting thrombin, we studied the Michaelis-Menten kinetics of Spectrozyme TH hydrolysis at pH 7.4 and 25 ^{O}C in the presence of CDSO3, a representative sulfated DHP. Plots of the initial rates *versus* Spectrozyme TH concentration were hyperbolic, as expected (Figure 53, page 230), from which the apparent Michaelis constant ($K_{M,app}$) and maximal velocity of the reaction (V_{MAX}) were derived (Table 9, page 223). The results show that although the concentration of CDSO3 increased from 0 nM to 300 nM, the $K_{M,app}$ value remained essentially invariant in the range of 2.2 to 0.9 μM. This suggests that the presence of CDSO3 does not much affect the binding of the chromogenic substrate to the active site of the enzyme. In contrast, the V_{MAX} value decreased steadily from a high of 21.5 mAbsU/min in the absence of CDSO3 to a low of 9.5 mAbsU/min at 300 nM CDSO3 (Figure 53, Table 9) corresponding to a decrease in k_{CAT} value from 36.1 to 16.0 s^{-1}, respectively. Thus, the presence of CDSO3 brings about structural changes in the active site of thrombin, which do not alter the formation of the thrombin–Spectrozyme TH Michaelis complex, but significantly reduce the rate of conversion of the complex into products.

5.4.5 CDSO3 Does Not Interact with Thrombin in the Anion-Binding Exosite I

To test whether CDSO3 binds in the anion-binding exosite I, we sought to measure the effect of a hirudin-based peptide, [5F]-Hir[54-65](SO_3^-), on the IC_{50} value of CDSO3-inhibition of thrombin. Previous studies indicate that [5F]-Hir[54-65](SO_3^-) binds thrombin

with 28 nM affinity in exosite I with 1:1 stoichiometry [238]. However, the effect of this exosite I ligand on the catalytic apparatus of thrombin was not clear. Literature reports on studies with the parent Hir[54-65](SO_3^-), which is also known to bind in exosite I of thrombin, show that the k_{CAT}/K_M value increases or decreases approximately 2-fold depending on the type of chromogenic substrate [144]. Thus, we first determined the effect of [5F]-Hir[54-65](SO_3^-) on the thrombin hydrolysis of Spectrozyme TH using the standard Michaelis-Menten conditions at pH 7.4. As the concentration of the exosite I ligand was increased to 103.6 nM, the K_M remained essentially constant in the range of 1.2 to 1.7 μM, while the V_{MAX} increased steadily from 18.7 to 31.1 mAbs/min (Figure 54, Table 10). This suggested that [5F]-Hir[54-65](SO_3^-) increased the catalytic efficiency of Spectrozyme TH hydrolysis arising specifically from a k_{CAT} effect.

The [5F]-Hir[54-65](SO_3^-)-dependent enhancement and the CDSO3-dependent reduction in rate of Spectrozyme TH hydrolysis (k_{CAT}) afforded a fine experimental setup to study competition between these two ligands. Thus, we measured the IC_{50} values of thrombin inhibition by CDSO3 in the presence of the dodecapeptide over a concentration range up to 3.7-fold higher than the K_D of the thrombin-[5F]-Hir[54-65](SO_3^-) complex [209]. The $IC_{50,app}$ values were measured in the standard dose-response assay, which we had used to detect thrombin inhibition. Figure 54B (page 231) shows the change in the dose-response profile of CDSO3 inhibiting thrombin in the presence of [5F]-Hir[54-65](SO_3^-) at pH 7.4 and 25 ^{O}C. As the concentration of the dodecapeptide was increased from 0 to 103.6 nM, $IC_{50,app}$ increased from 28 to 57.8 nM (Table 10, page 224). This represents a 2.1-fold change in $IC_{50,app}$ value for a 3.7-fold increase in concentration over

the K_D of the exosite I competitor. Additionally, the change in $IC_{50,app}$ value appears to be not linear with the concentration of [5F]-Hir[54-65](SO_3^-). For example, the $IC_{50,app}$ value increases ~1.7-fold at 8.6 nM dodecapeptide ($0.3\times K_D$), which is followed by much slower increases (Table 10, page 224). These small changes suggest that that the interaction of [5F]-Hir[54-65](SO_3^-) with thrombin does not affect CDSO3 inhibition of thrombin to a significant extent. Thus, it appears that CDSO3 does not preferentially bind thrombin in anion-binding exosite I.

5.4.6 CDSO3 Interacts with Thrombin in or Near Anion-Binding Exosite II

To assess whether CDSO3 binds in the region formed by anion-binding exosite II of thrombin, we resorted to the enzyme inhibition assay described above. Exosite II ligands, bovine heparin, enoxaparin and heparin octasaccharide H8, did not affect the proteolytic activity of thrombin (not shown), while CDSO3 is a potent inhibitor. Thus, if CDSO3 binds in or near the GAG binding site, its inhibition potency is expected to decrease as a function of the concentration of the GAG competitor. Figure 55A (page 232) shows the change in the dose-response curve of CDSO3 inhibiting thrombin in the presence of H8 at pH 7.4 and 25 ^{O}C. As the concentration of H8 was increased to 26.3 μM, the IC_{50} value of thrombin inhibition increases from 28 to 414 nM (Table 11, page 225). Less dramatic, but significant, changes in dose-response profiles were also observed for bovine heparin and enoxaparin (not shown), corresponding to increases in apparent IC_{50} values (Table 11), suggesting that all three GAG ligands compete with CDSO3.

A more quantitative test of competitive binding is the Dixon-Webb relationship (**Eq. II**), which predicts the effect of competition on a measured parameter, e.g., K_D or IC_{50}. In this equation, K_{GAG} is the dissociation constant of thrombin–GAG (bovine heparin, H8 or enoxaparin) interaction.

$$IC_{50,app} = IC_{50}(1 + \frac{[GAG]_O}{K_{GAG}}) \qquad \textbf{Eq. II}$$

The equilibrium dissociation constants (K_{GAG}) of bovine heparin, enoxaparin and H8 were determined independently by fluorescence titration with the active site probe, PABA, and found to be 15.6±3.1 μM, 6.6±0.5 μM and 11.3±1.4 μM, respectively, under otherwise identical conditions (not shown). Using K_{GAG} and Dixon-Webb equation II, the $IC_{50,app}$ values for CDSO3 inhibition of thrombin in the presence of H8, bovine heparin and enoxaparin were calculated (Table 11, page 225). Figure 55B (page 232) shows a comparison of the observed and predicted $IC_{50,app}$. While the measured $IC_{50,app}$ values are higher than those predicted for H8 competition, while the correspondence is better for competition with bovine heparin. For enoxaparin, equation II predicts a weaker competitive effect than that observed (Table 11). Yet, the competitive effect of all three exosite II ligands is much greater than that observed for exosite I ligand. The precise origin of the more-than-predicted competitive effect of exosite II ligands is difficult to pinpoint at this time given the heterogeneity of CDSO3 preparation, however the results support the notion that CDSO3 binds thrombin in or near anion-binding exosite II.

5.5 DISCUSSION

A fundamental objective in designing sulfated DHPs was to significantly reduce the highly polyanionic nature of heparin that is arguably the origin of most of its adverse effects, yet effectively mimic its anticoagulant action. This is a major challenge considering that work performed in the past 30 years has not been able to put forward a single new heparin mimic, which is not a saccharide derivative. In fact, the new structures put forward in this category are all heparin derivatives, e.g., LMWH, fondaparinux or idraparinux [187].

Whereas heparin possesses a hydrophilic polysaccharide scaffold, sulfated DHPs are based on the hydrophobic 'lignin' scaffold. Natural lignins are plant constituents made up of phenylpropanoid monomers that offer the capability of introducing a limited number of sulfate groups [239]. We reasoned that introducing carboxylate groups in the basic lignin scaffold will offer an avenue in the future of being able to introduce oral bioavailability through the traditional carboxylic acid ester-based pro-drug approach. Structural studies performed earlier suggested that the sulfated DHPs are hydrophobic molecules containing an average of 0.8–0.9 anionic (sulfate and carboxylate) groups per monomer [212], while for heparins this number is approximately 1.78 (Table 7, page 220). Thus, the sulfated DHPs studied here are structurally unlike heparin (or heparin derivatives). In fact, these molecules are completely different from the anticoagulants used in the clinic, or currently being evaluated for clinical use, including hirudin, bivalirudin, argatroban, dabigatran and ximelagatran.

Previous work indicated that sulfated DHPs prolong plasma clotting times with potency in the range of LMWHs [212]. Among the three sulfated DHPs, CDSO3 was found to possess superior anticoagulant activity over FDSO3, which in turn was more potent than SDSO3. Current work reveals the basis of this anticoagulant action, while also uncovering interesting similarities and differences. The three sulfated DHPs inhibit two critical enzymes of the coagulation cascade, factor Xa and thrombin. Interestingly, the sulfated DHPs inhibit these enzymes in the absence of antithrombin (Figure 51, Table 8). This represents a major departure from the expected mechanism of action because the sulfated DHPs were designed to mimic heparin function. The nanomolar IC_{50} values of the sulfated DHPs suggest highly potent inhibition. This unexpected observation implies that sulfated DHPs are perhaps the first molecules outside of the peptides or peptidomimetics that show direct inhibition of thrombin and factor Xa [13, 37].

The two most active sulfated DHPs, CDSO3 and FDSO3 display a 1.9–2.6-fold preference for direct inhibition of thrombin over factor Xa (Table 8, page 221-222). This preference for directly inhibiting thrombin increases 17–187-fold and >815-fold over factor IXa and factor VIIa, respectively. Thus, CDSO3 and FDSO3 selectively inhibit thrombin (and factor Xa) utilizing the direct inhibition pathway. In contrast, SDSO3 is better at inhibiting thrombin and factor Xa through the indirect pathway in comparison to the direct pathway by 2.1- and 2.5-fold, respectively. In terms of the preference of its target in the presence of antithrombin, SDSO3 inhibits thrombin nearly 2.1-fold better than factor Xa, while it prefers thrombin over factor IXa and VIIa by a factor of ~44- and 8-fold,

respectively. These results indicate considerable selectivity in the indirect inhibition of thrombin and factor Xa by SDSO3.

The 2.0 and 0.35 μM IC_{50} values of SDSO3 against factor IXa and VIIa in the presence of antithrombin indicate considerable potency arising from this interesting sulfated DHP. In fact, perhaps the most interesting property of SDSO3 appears to be factor VIIa inhibition. It is the only molecule studied here that exhibits indirect factor VIIa inhibition. Alternatively, SDSO3 is able to induce antithrombin to inhibit factor VIIa, while enoxaparin (and CDSO3 or FDSO3) fails miserably under similar conditions. The molecular basis for this induction of antithrombin action is unclear at present, but perhaps represents a new opportunity for designing selective factor VIIa inhibitors.

Comparison of the IC_{50} values in indirect assays reveals that the sulfated DHPs are 22–70-fold weaker than the clinically used anticoagulants, enoxaparin and fondaparinux. Considering that sulfated DHPs represent only the first attempt at designing a novel non-heparin-like structure that exhibits anticoagulation, this potency is remarkable. Also of interest is the observation that in presence of antithrombin, SDSO3 exhibits reasonably good inhibition of all four pro-coagulant enzymes studied here. Thus, considering that SDSO3 is also a direct inhibitor of thrombin and factor Xa, it appears that this sulfated DHP can utilize both pathways of enzyme inhibition. This observation, if rigorously found to be true, would represent the first example of an anticoagulant possessing a dual mechanism.

All three sulfated DHPs are heterogeneous species and it is difficult to pinpoint structural features that govern anticoagulant action at this time. Just as a specific five-

residue sequence in heparin was found to be the basis of nearly all anticoagulant activity, it is likely that specific structure(s) in CDSO3 and FDSO3 exist that possess(es) nearly all the direct inhibition activity of the heterogeneous preparations. The observation that thrombin and factor Xa are preferentially inhibited suggests that specific structural features in CDSO3 and FDSO3 may be involved in this recognition.

Competitive binding studies with exosite I and exosite II ligands indicate that CDSO3 primarily binds in or near the region formed by exosite II. An important point to recall is that CDSO3 is a heterogeneous anionic molecule implying that certain sequences in CDSO3 may be still be interacting with exosite I of thrombin. However, the competitive binding data suggest that such an interaction with exosite I is likely to be of lower affinity. Studies on the hydrolysis of Spectrozyme TH indicate that CDSO3 disrupts the catalytic apparatus without binding to the active site. Thus, CDSO3 is an allosteric inhibitor of thrombin function. Although FDSO3 and SDSO3 differ from CDSO3 in terms of the fine structure, their overall similarity suggests that these oligomers may also bind thrombin exosite II. In a similar manner, these sulfated DHPs may be interacting with factor Xa in its anion-binding exosite II, which is known to recognize GAG ligands with an affinity similar to thrombin [240]. A supporting evidence for exosite II recognition is the observation that, unlike thrombin, exosite I in factor Xa is not an anion-binding site, but a cation-binding site [241].

Exosite II binding of CDSO3 also partially explains the observed weak direct inhibition of factor IXa and essentially no inhibition of factor VIIa. Factor IXa is known to possess a heparin-binding exosite II [213, 231], analogous to thrombin, which is likely to

be the CDSO3 recognition site. However, differences in the structures of exosite II in thrombin and factor IXa may introduce differences in the binding affinities of the sulfated DHPs. Finally, factor VIIa is not known to possess an anion-binding region, similar to exosite II of thrombin, explaining the lack of inhibition induced by CDSO3.

Exosite II in thrombin is known to bind GAGs and haemadin [140]. GAG binding to thrombin is non-specific, not high-affinity and non-inhibitory [237, 242]. On the other hand, haemadin is a peptide that binds thrombin with nM affinity, inhibits its proteolytic activity, but also binds in the active site [150]. Thus, our work puts forward perhaps the first organic molecules that primarily recognize anion-binding exosite II of thrombin (and possibly factor Xa) with nM potency and induce inhibition.

In conclusion, our work demonstrates that chemo-enzymatically prepared sulfated DHPs display interesting anticoagulant properties. The anticoagulant potency of the sulfated DHPs compares favorably to the clinically used anticoagulants, enoxaparin and fondaparinux. Whereas CDSO3 and FDSO3 preferentially utilize the antithrombin-independent (direct) pathway, structurally related SDSO3 can also utilize the antithrombin-dependent (indirect) pathway. All three novel anticoagulants selectively inhibit thrombin and factor Xa of the coagulation cascade through an interaction with anion-binding exosite II that allosterically disrupts the catalytic apparatus of the enzyme. This represents a novel mechanism of thrombin (and factor Xa) inhibition. Sulfated DHP molecules possess a novel structural scaffold, which is completely different from all the current clinically used anticoagulants, including the heparins, coumarins, hirudins and arginine-peptidomimetics.

Thus, sulfated DHPs represent a novel class of potent dual factor Xa and thrombin inhibitors.

5.6 Tables

Table 7. Physical properties of DHPs from cinnamic acid derivatives.

	Range of Oligomer Chain Length[a]	*Weight Average Oligomer Size*[b]	*Sulfate Groups per Monomer*[c]	*Calculated* M_W[d]
				(*Da*)
CDSO3	5 – 13	12.7	0.40	~3,320
FDSO3	8 – 15	15.5	0.30	~4,120
SDSO3	4 – 11	14.4	0.38	~3,550
Enoxaparin	6 – 27[e]	12.6	1.14[e]	~3,800[e]
Heparin	10 – 80[e]	~40	1.28[f]	~13,000

[a]Taken from [212]. [b]Size obtained by dividing the average molecular weight by the molecular weight of acetylated monomers, caffeic acid (221 Da), ferulic acid (235 Da) and sinapic acid (208 Da). [c]Average number of sulfates per monomeric unit was obtained from elemental sulfur composition [212]. [d]Calculated using the formula M_W = (M_W of unsulfated DHP) + 102 × (average oligomer size) × (sulfate groups per oligomer). M_W of unsulfated DHPs was previously obtained using non-aqueous SEC and found to be 2,800 Da (CD), 3,650 (FD), and 2,990 (SD). [e]Taken from [230]. [f]Derived from [237].

Table 8. IC_{50} values for sulfated DHPs, enoxaparin, fondaparinux and a LMWH (Sigma) inhibiting coagulation enzymes in the presence and absence of antithrombin.

[a]The IC_{50} values for direct and indirect inhibition of factor Xa, thrombin, factor IXa and factor VIIa were determined at pH 7.4 and 25 ^{O}C in appropriate buffers through spectrophotometric measurement of residual proteinase activity following incubation of the enzyme and the inhibitors for a fixed time period of 10 minutes. [b]Errors represent ± 2 S. E. [c]An estimated value based on the highest concentration of the anticoagulant used in the experiment. [d]No inhibition was observed.

	IC_{50} (nM)[a]							
	Thrombin		*Factor Xa*		*Factor IXa*		*Factor VIIa*	
	Direct	*Indirect*	*Direct*	*Indirect*	*Direct*	*Indirect*	*Direct*	*Indirect*
CDSO3	18 ± 2[b]	53 ± 6	34 ± 5	53 ± 4	3380 ± 64	4111 ± 446	>29,000[c]	>29,000
FDSO3	29 ± 2	71 ± 6	74 ± 8	133 ± 6	492 ± 16	593 ± 10	>23,640	>23,640
SDSO3	94 ± 4	45 ± 4	244 ± 28	97 ± 16	>28500	2004 ± 20	>28,500	356 ± 14
Enoxaparin	>222,222	1.9 ± 0.0	No Inh.[d]	3.4 ± 0.0	No Inh.[d]	56 ± 6	—	>222,222
Fondaparinux	—	—	—	1.9 ± 0.0	—	—	—	—
Sigma LMWH	—	2.2 ± 0.0	—	6.9 ± 0.0	—	—	—	—

Table 9. Hydrolysis of Spectrozyme TH by human α-thrombin in the presence of CDSO3.

$[\mathbf{CDSO3}]_O$	K_M	$k_{CAT}{}^a$
(nM)	*(μM)*	*(s^{-1})*
0	2.2 ± 0.2[b]	36.1 ± 1.2[c]
10.5	1.1 ± 0.1	28.2 ± 0.8
30	1.4 ± 0.1	25.9 ± 0.3
105	1.3 ± 0.1	19.2 ± 0.7
300	0.9 ± 0.1	16.0 ± 0.3

[a]obtained from V_{MAX} as described in 'Experimental Procedures'. [b]Error represents ±1 S.E. [c]Error represents ±2 S.E.

Table 10. Michaelis-Menten parameters for Spectrozyme TH hydrolysis and CDSO3-dependent thrombin inhibition parameters in the presence [5F]-Hir[54-65](SO_3^-).

$[5F\text{-}Hir[54\text{-}65](SO_3^-)]_O$	K_M	k_{CAT}	$IC_{50,app}$ [b]
(nM)	*(μM)*	*(s^{-1})*	*(nM)*
0	1.7±0.2[c]	31.4±0.8	28.0±0.4
8.6	1.5±0.1	39.5±1.0	48.4±0.6
25.8	1.2±0.1	43.3±0.8	46.8±0.6
51.6	1.3±0.1	46.0±1.3	50.2±0.6
103.6	1.5±0.1	52.2±1.2	57.8±0.8

[a] K_M and k_{CAT} values of Spectrozyme TH substrate hydrolysis by thrombin in the presence of [5F]-Hir[54-65](SO_3^-) were measured as described in 'Experimental Procedures'. [b] $IC_{50,app}$ values of CDSO3 inhibition of thrombin in the presence of [5F]-Hir[54-65](SO_3^-) were measured as described in 'Experimental Procedures'. [c] Error represents ± 2 S.E.

Table 11. Inhibition of human α-thrombin with CDSO3 in the presence of exosite II ligands.[a]

Exosite II ligand	[Ligand]$_O$ (μM)	$IC_{50,app}$ (nM)	
		Measured	***Dixon-Webb Predicted***
Octasaccharide H8	0	28 ± 4[b]	28
	0.255	112 ± 12	29
	3.0	203 ± 10	35
	26.3	414 ± 20	93
Bovine Heparin	0	28 ± 2	29
	4.2	44 ± 1	37
	12.8	50 ± 2	53
	25.0	67 ± 1	75
	42.6	71 ± 2	108
Enoxaparin	20.0	348 ± 10	113

[a]Inhibition of thrombin by CDSO3 in the presence of exosite II ligands was studied as described in 'Experimental Procedures'. [b]Error represents ±2 S.E.

5.7 FIGURE LEGENDS

Figure 51 Direct and indirect inhibition of factor Xa (A) and thrombin (B) by CDSO3. The inhibition of thrombin and factor Xa by CDSO3 in the presence (open triangles) and absence (closed triangles) of antithrombin as described under 'Experimental Procedures'. Indirect inhibition of factor Xa with enoxaparin (closed circles) and fondaparinux (open diamonds) and that of thrombin with enoxaparin (closed circles) is shown for comparative purposes. Solid lines represent dose-response fits to the data to obtain values of IC_{50}.

Figure 52 Direct and indirect inhibition of factor IXa (A) and factor VIIa (B) by SDSO3. The inhibition of factor IXa and factor VIIa by SDSO3 in the presence (open triangles) and absence (closed triangles) of antithrombin as described in 'Experimental Procedures'. Indirect inhibition of both enzymes with enoxaparin (closed circles) is shown for comparative purposes. Solid lines represent dose-response fits to the data to obtain IC_{50}.

Figure 53 Michaelis-Menten kinetics of Spectrozyme TH hydrolysis by thrombin in the presence of CDSO3. The initial rate of hydrolysis at various substrate concentrations was measured in pH 7.4 buffer as described in 'Experimental Procedures'. The concentrations of CDSO3 chosen for study include 0 (◊), 10 (▲), 20 (○), 29 (♦) and 100 nM (□). Solid lines represent non-linear regressional fits to the data by the Michaelis-Menten equation.

Figure 54 A) Influence of [5F]-Hir[54-65](SO_3^-) on the hydrolysis of Spectrozyme TH by thrombin. The Michaelis-Menten kinetics of Spectrozyme TH hydrolysis by thrombin in the presence of 0 (□), 8.6 (♦), 25.8 (○), 51.6 (▲) and 103.6 nM (◊) [5F]-Hir[54-65](SO_3^-) was studied at pH 7.4 and 25 ^{O}C. Solid lines represents non-linear regressional fits to the data by Michaelis-Menten equation. B) Competitive effect of [5F]-Hir[54-65](SO_3^-) on the inhibition of thrombin by CDSO3. Thrombin inhibition by CDSO3 in the presence of [5F]-Hir[54-65](SO_3^-) was determined spectrophotometrically through the Spectrozyme TH hydrolysis assay at pH 7.4 and 25 ^{O}C. Solid lines represent fits by the dose-response equation to obtain $IC_{50,app}$, as described in 'Experimental Procedures'.

Figure 55. A) Competitive direct inhibition of thrombin by CDSO3 in the presence of heparin octasaccharide H8. The inhibition of thrombin by CDSO3 in the presence of H8 was determined spectrophotometrically through the Spectrozyme TH hydrolysis assay at pH 7.4 and 25 ^{O}C. Solid lines represent fits by the dose-response equation to obtain $IC_{50,app}$, as described in 'Experimental Procedures'. The concentrations of H8 chosen for study include 0 (♦), 0.26 (Δ), 3.0 (●) and 26.3 μM (□). B) Comparison of the predicted and experimentally measured IC_{50} values of CDSO3 inhibition of thrombin in the presence of H8 and bovine heparin. Open bars represent the measured values, while closed bars are the values predicted using Dixon-Webb equation II. Error bars show ±2 S.E.

Figure 51.

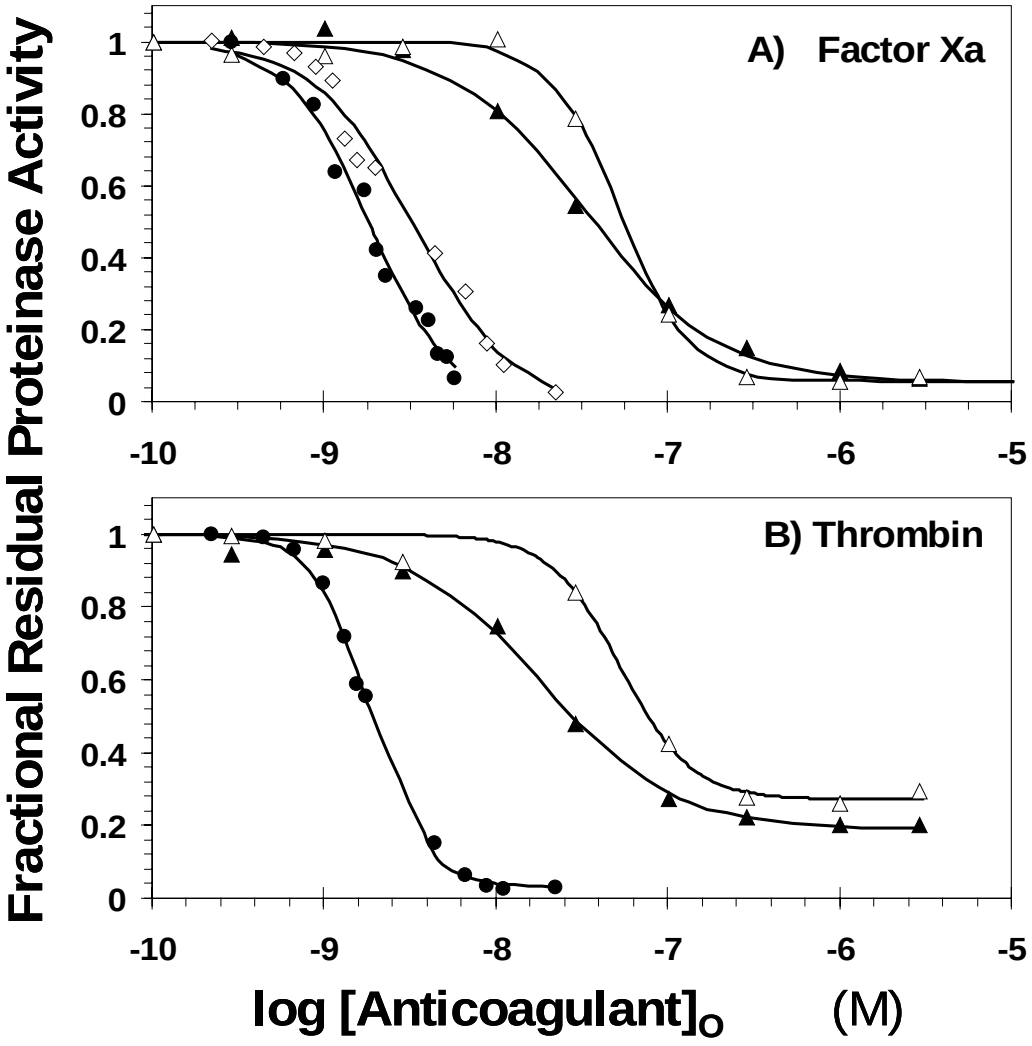

Figure 52.

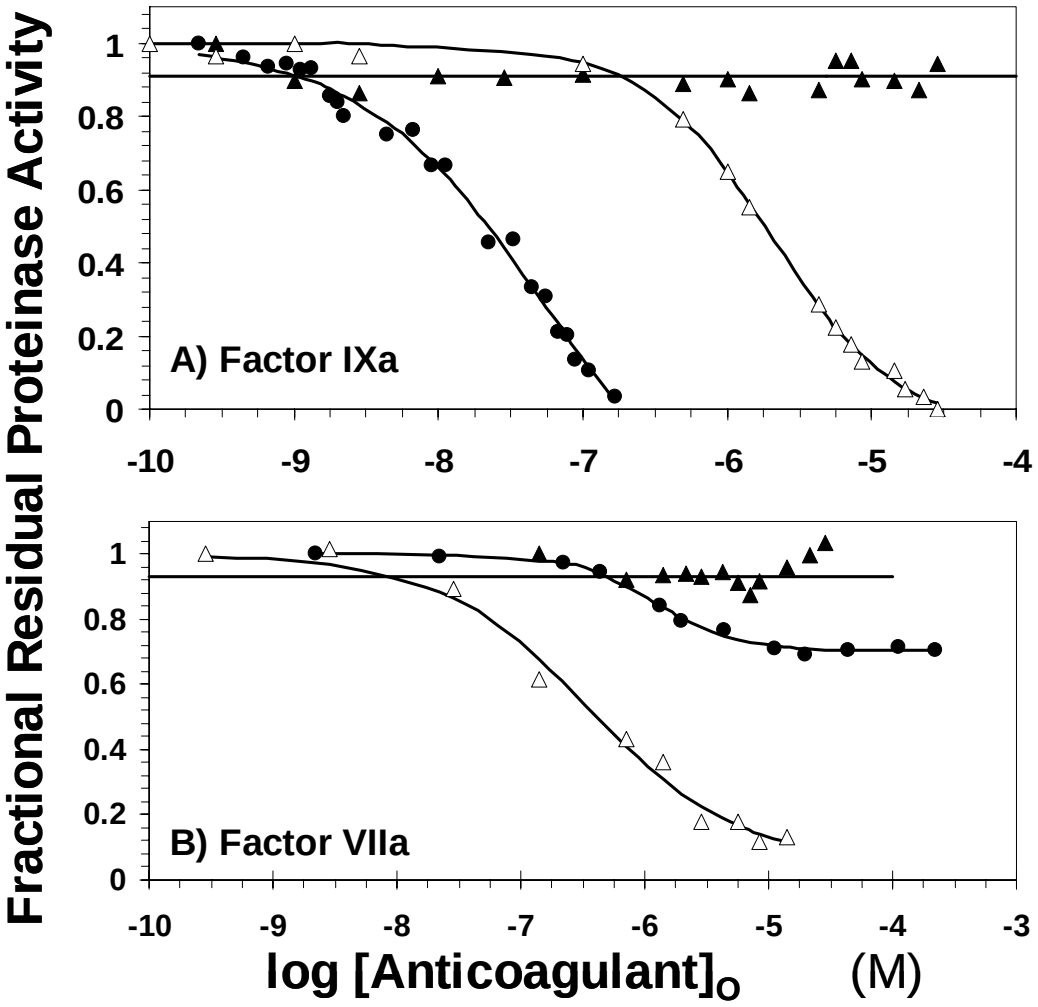

Figure 53.

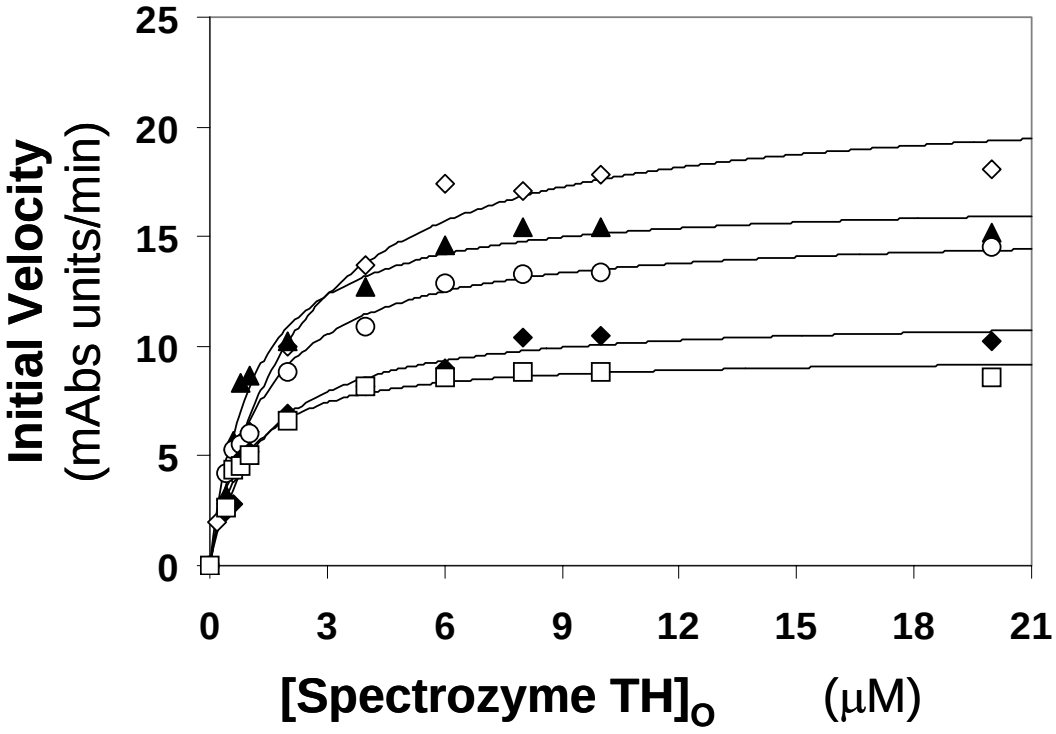

Figure 54.

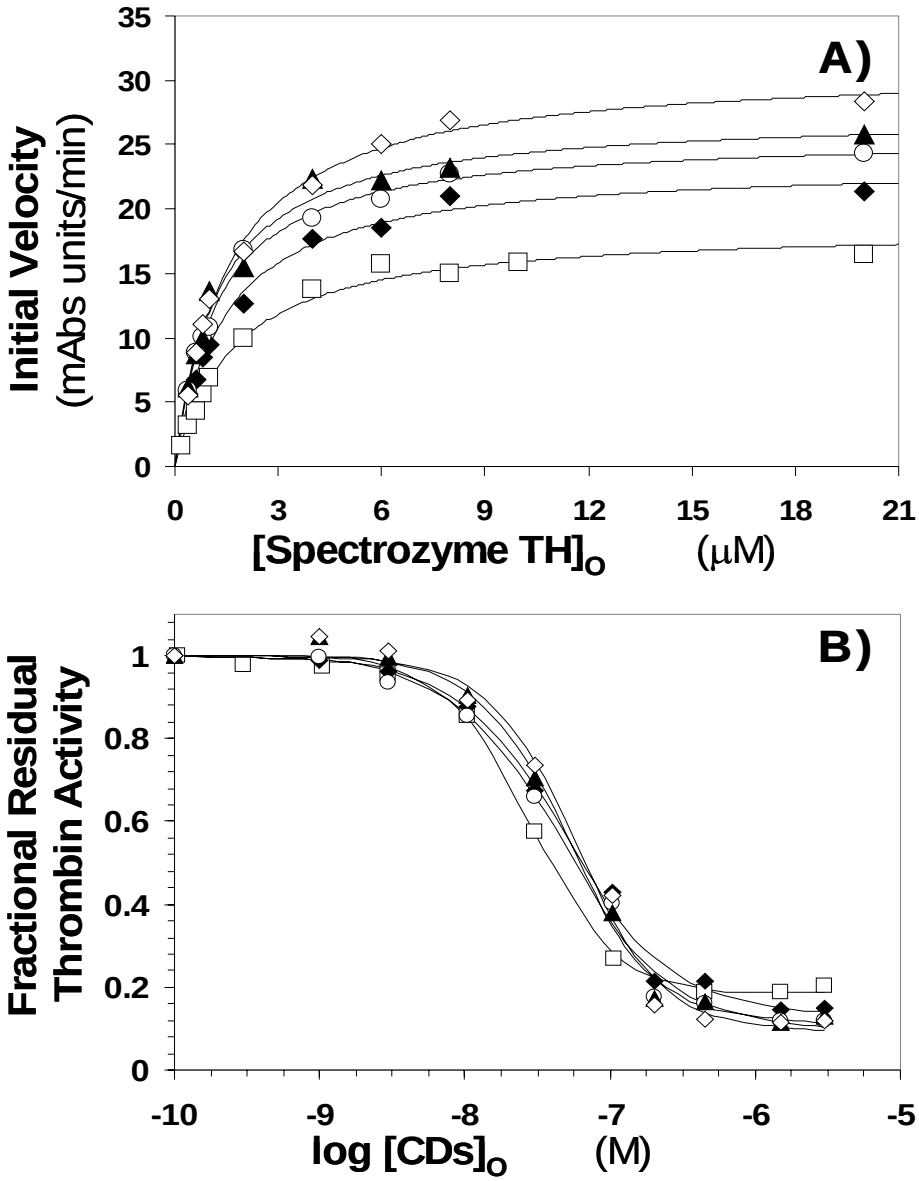

Figure 55.

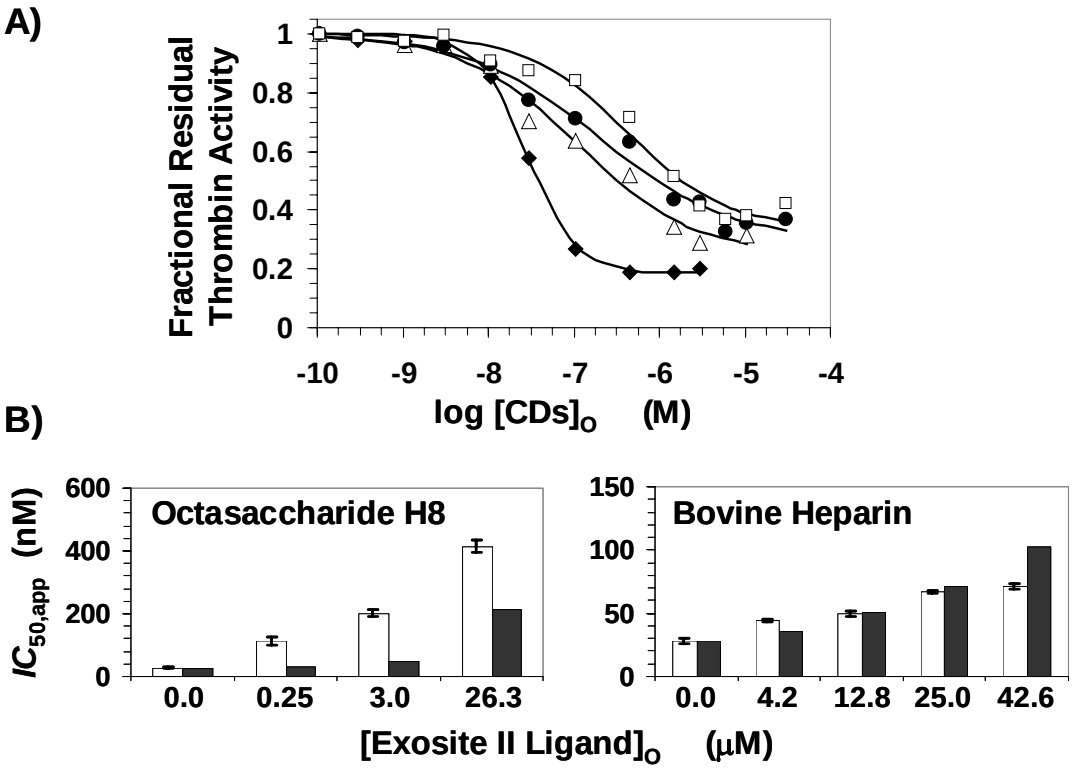

Chapter 6: Additional Biochemical Studies

6.1 Introduction

To-date, we have determined that our sulfated DHPs possess potent anticoagulant activity. They can be easily synthesized in a simple two-step chemo-enzymatic process from commercially available starting materials (4-hydroxycinnamic monomers) [212, chapter 3]. Additionally, some information about oligomer chain length, intermonomeric linkage, molecular weight and % sulfation has been determined [212, chapter 3]. They exhibit similar potency to LMWHs in both APTT and PT [212, chapter 3]. All three DHPs exhibit nanomolar potency against thrombin and factor Xa in an antithrombin dependent and independent manner [212, chapter 3]. CDs and FDs appear to function better as direct inhibitors, while the AT dependent pathway appears to be detrimental to activity. In contrast, the potency of SDs increases in the presence of AT, while it retains fairly potent direct inhibition property. All three DHPs exhibit selective direct inhibition of thrombin and factor Xa over FIXa and FVIIa [chapter 5]. Interestingly, SDs is completely inactive as a FIXa and FVIIa direct inhibitor, but is able to activate AT and inhibit both proteases [chapter 4]. CDs was found to be a non-competitive, allosteric direct inhibitor of thrombin. Even more exciting was that CDs mediates its inhibition through exosite II [chapter 5], a property not known to be present in any known direct thrombin inhibitor. It is likely that FDs and SDs exhibit similar biochemical behavior, although this needs to be

rigorously demonstrated. These exciting results are the impetus for our continued interest in these novel compounds. This chapter details the experiments we have performed to further elucidate the unique biochemical properties of DHPs.

6.2 Molecular mechanism of action of CDs, FDs and SDs

Several questions arise with respect to anticoagulant action of the sulfated DHPs:

1. What is the affinity of CDs, FDs, and SDs for thrombin, factor Xa, and antithrombin?
2. Where do they bind?
3. Is there a structural dependence in the extent of allosteric modulation induced by CDs, FDs and SDs?
4. What is the nature of the interaction (ionic or non-ionic) with antithrombin, thrombin and factor Xa?
5. Why does the presence of antithrombin reduce the potency of CDs and FDs (and enhance that of SDs)?
6. What is their kinetic mechanism of binding (one-step or multi-step)?
7. Are there any specific structure(s) in sulfated DHPs that recognize thrombin/factor Xa and antithrombin? If so, what the proportion of these specific structures in the preparation of these novel anticoagulants?
8. Do these molecules allosterically modulate binding of other ligands (exosite I/II ligands and Na^+)?
9. Do these molecules inhibit thrombin in the clot-bound form?
10. Can we enhance the potency of sulfated DHPs?

We have only just begun to address and answer some of these questions. The remainder of this chapter is focused on the results that we have collected pertaining to the various questions. The studies that have been performed versus those that have not, does not necessarily reflect the importance of any one set of experiments over another, but rather, what we were able to do with the time and resources available.

6.3 What is the affinity of CDs, FDs and SDs for antithrombin?

We have previously used a fluorescence-based approach for deducing the antithrombin binding affinity of saccharides and organic ligands [190, 191, 193, 194]. Our approach relied on the change in fluorescence of an external probe TNS (λ_{EM} = 432 nm) on interaction of organic ligands with antithrombin. In the current approach, we have used a more direct method of intrinsic tryptophan fluorescence change, which has been used previously to study AT:heparin interactions [243].

6.3.1 Methods

Antithrombin-DHP (or heparin) equilibrium binding titrations

All experiments were conducted at 25º C, ionic strength 0.15, pH 7.4 in acrylic cuvettes. The buffer contains 20 mM sodium phosphate, 100 mM NaCl, 0.1 mM EDTA and 0.1% polyethylene glycol 8000. The final concentration of antithrombin was 88 nM in the buffer above (final volume of 900 µl). DHPs (or other ligands) were added in 1 µl increments. DHPs were prepared as described earlier [212]. Fondaparinux (GlaxcoSmithKline) and heparin (Sigma) were purchased and used as obtained. The

samples were excited at λ_{EX} = 280 nm and the interaction was monitored at λ_{EX} = 340 nm [243].

6.3.2 Results

Antithrombin-DHP (or heparin) equilibrium binding titrations

Table 12. Dissociation constants for DHPs and heparins binding to AT. K_D values are an average of three titrations experiments.

AT ligand	K_D (nM) ± std. dev.
Heparin	1052 ± 122
Fondaparinux	65 ± 10
CDs	382 ± 13
FDs	2052 ± 157
SDs	2580 ± 370

Figure 56. Antithrombin-fondaparinux equilibrium binding titration.

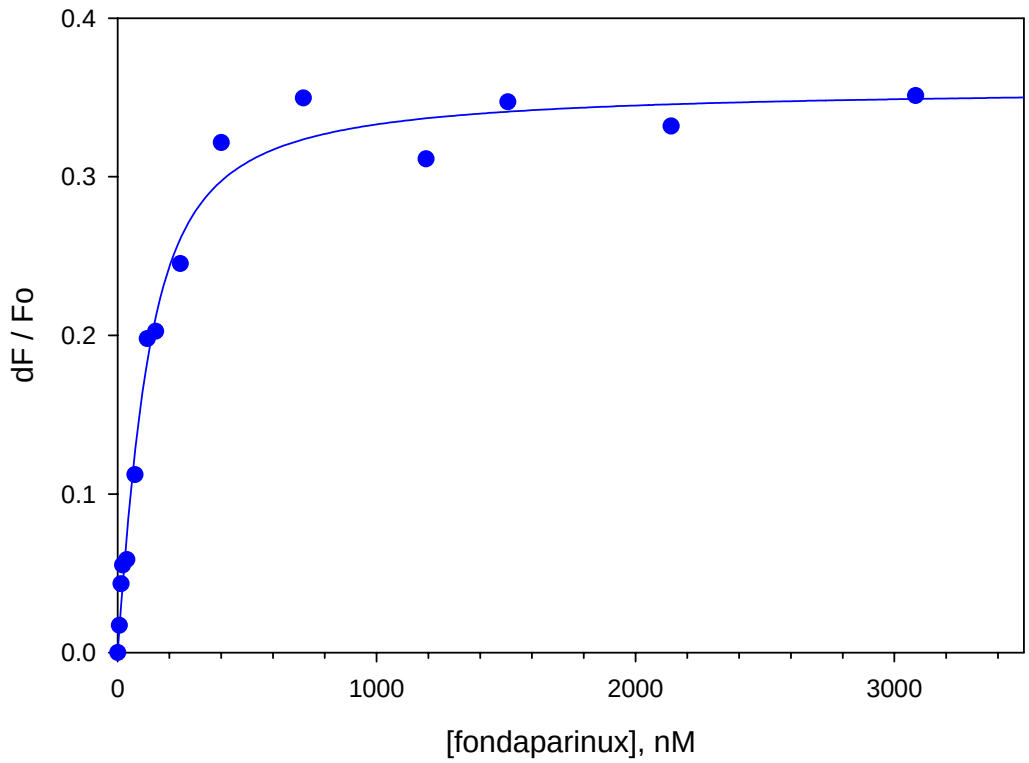

Figure 57. Antithrombin-heparin equilibrium binding titrations.

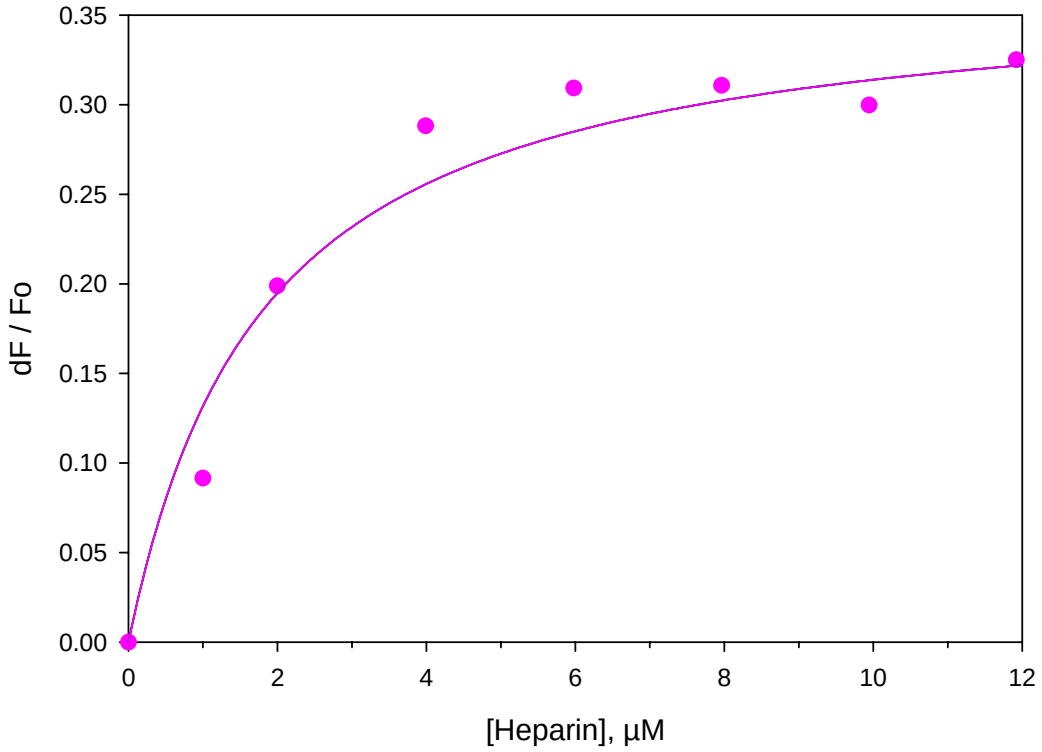

Figure 58. Antithrombin-DHP equilibrium binding titrations (**CDs, FDs and SDs**).

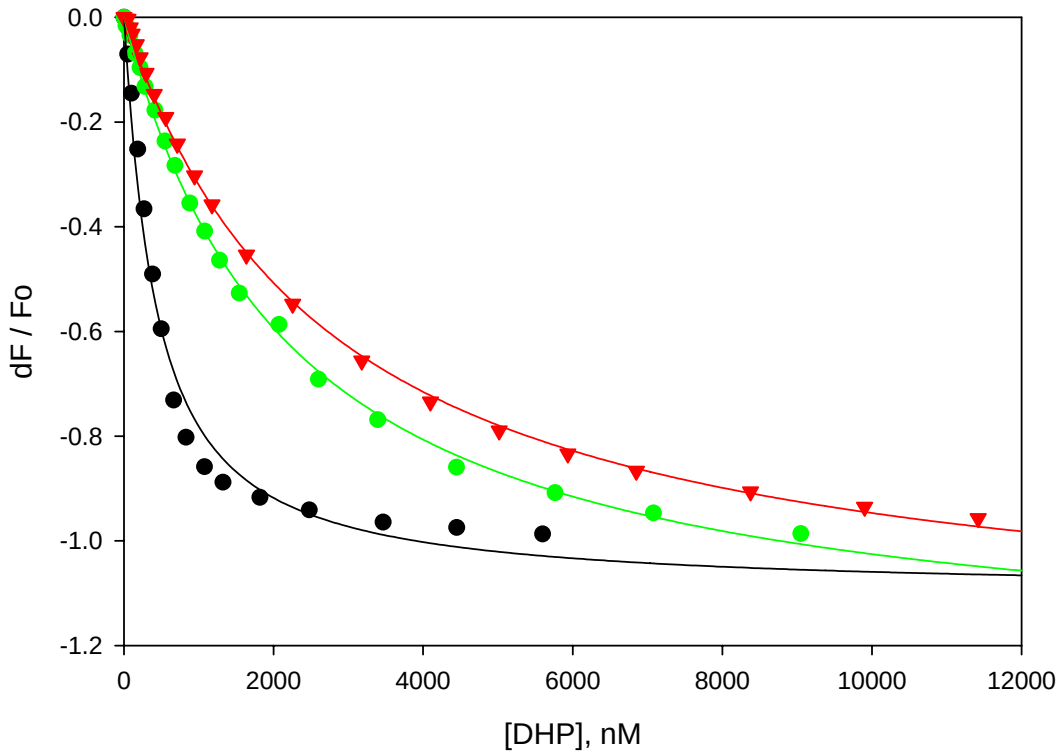

6.3.3 Discussion

Antithrombin-DHP (or heparin) equilibrium binding titrations

Heparin and fondaparinux binding to antithrombin is well characterized [211]. Fondaparinux binds to the pentasaccharide-binding site (PBS) on AT. Heparin, which contains the pentasaccharide sequence within its long carbohydrate chain, binds to the PBS as well as the adjacent extended heparin binding sequence (EHBS). Our K_D values for heparin (~1 μM) and fondaparinux (65 nM) are consistent with previously published data [211, 245], indicating that our experimental system is working properly. When

saccharides bind AT, there is generally a 30-35% increase in fluorescent signal (figures 56 and 57). When our DHPs bind to AT, there is a dose dependent decrease fluorescence that drops to baseline fluorescence. One possible explanation for this behavior is that DHPs induce a conformational change in the inhibitor, although it is appears to be different from that induced by saccharide ligands. This hypothesis requires a rigorous test.

Prior attempts to make small molecule antithrombin activators yielded AT K_D values of ~20-80 μM, which exhibited marginal activation and anticoagulant potency [190-192]. Our sulfated DHPs exhibit AT K_D values in the range of 0.38-2.5 μM and are potent anticoagulants. These AT K_D vales are superior or equivalent to that of heparin and bind AT ~6-40-fold less than fondaparinux. This is a significant result because no non-carbohydrate molecules have been designed that bind as tightly to AT as sulfated DHPs.

6.4 Where do sulfated DHPs bind on antithrombin?

SDs is more potent in the presence of antithrombin and appears to bind and activate antithrombin (chapter 3, chapter 5, [212]). CDs and FDs are less potent in the presence of antihrombin indicating that these molecules bind AT in a manner that less or nonproductive for anticoagulation (chapter 3, chapter 5, [212]). Based on these findings, it is important to determine where these DHPs bind on antithrombin. By performing competitive binding studies with full-length heparin, heparin pentasaccharide and (-) epicatechin sulfate (-ECS), the DHP:AT binding site can be determined. Full-length heparin binds in the PBS and the EHBS, fondaparinux binds exclusively in the PBS, while (-) epicatechin sulfate bind in the EHBS [191]. Competitive binding studies with

antithrombin will also utilize the intrinsic tryptophan fluorescence-based approach as discussed above [243].

6.4.1 Methods

Antithrombin competitive binding studies

Binding experiments were conducted at 25º C, ionic strength 0.15, pH 7.4 in acrylic cuvettes. The buffer contains 20 mM sodium phosphate, 100 mM NaCl, 0.1 mM EDTA and 0.1% polyethylene glycol 8000. The AT competitor along with antithrombin (final concentration 88 nM) are coincubated for 2 minutes in the buffer described above (final volume of 900 µl). DHPs were added in 1 µl increments. The samples were excited at λ_{EX} = 280 nm and λ_{EX} = 340 nm [243]. The competitors used were heparin (Sigma), fondaparinux and (-)-epicatechin sulfate. The K_D value reported for (-)epicatechin sulfate – antithrombin interaction is ~16 µM [191].

6.4.2 Results

Antithrombin-DHP competitive binding studies

Table 13. Dissociation constants for CDs binding to antithrombin in the presence of various competitors.

Competitor	Concentration	K_D (nM) ± std. dev
Control		382 ± 13
Heparin (Sigma)	1 μM	1050 ± 45
	2 μM	1460 ± 226
	8 μM	2540 ± 516
	16 μM	3223 ± 436
Fondaparinux	64 nM	637 ± 99
	128 nM	819 ± 108
	321 nM	935 ± 67
(-) Epicatechin sulfate	16 μM	503 ± 11
	166 μM	653 ± 54
	332 μM	851 ± 9

Figure 59. Competitive binding between heparin and CDs for antithrombin. This is a representative figure for all the antithrombin-DHP competitive binding experiments.

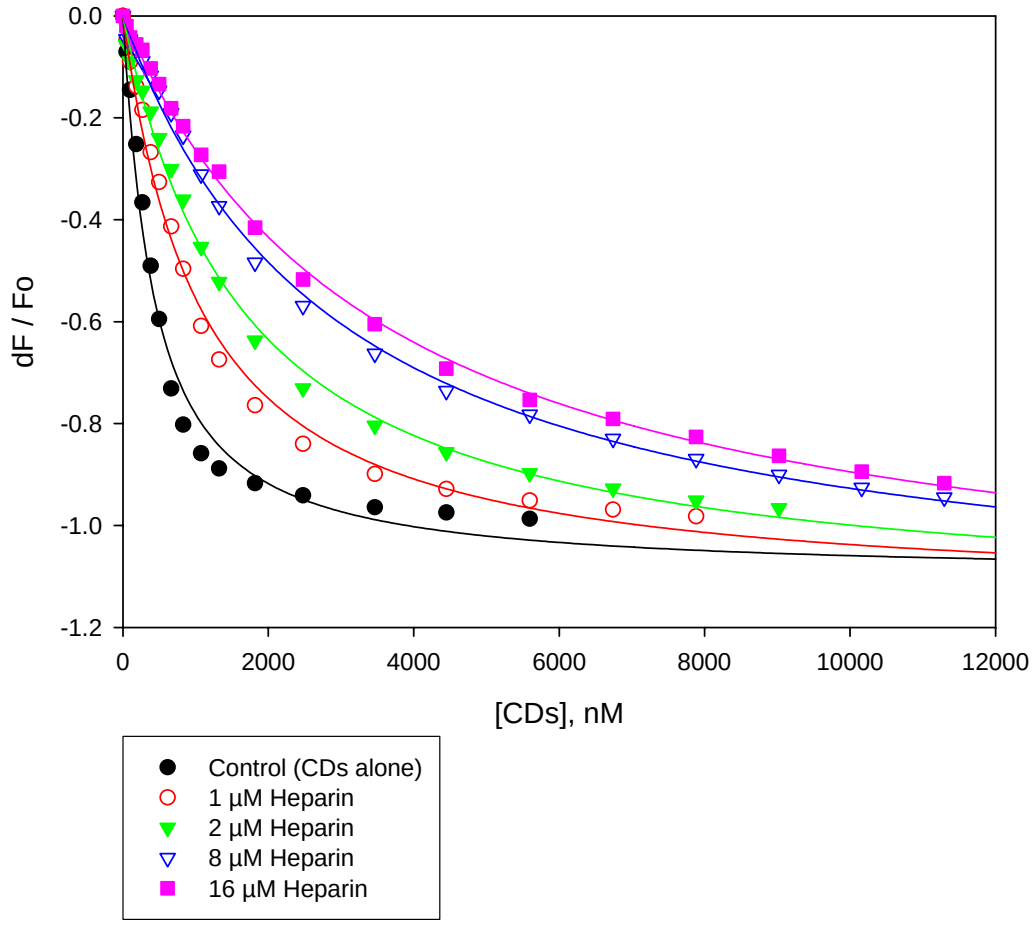

Table 14. Dissociation constants for FDs binding to antithrombin in the presence of various competitors.

Competitor	Concentration	K_D (nM) ± std. dev
Control		2052 ± 1157
Heparin (Sigma)	0.5 µM	4214 ± 659
	1 µM	4339 ± 267
	2 µM	5140 ± 162
	8 µM	7219 ± 813
Fondaparinux	64 nM	3378 ± 217
	128 nM	4121 ± 96
	321 nM	5107 ± 182
(-) Epicatechin sulfate	16 µM	2320 ± 56
	67 µM	2216 ± 209
	166 µM	2383 ± 65
	332 µM	2086 ± 57

Table 15. Dissociation constants for SDs binding to antithrombin in the presence of various competitors.

Competitor	Concentration	K_D (nM) ± std. dev
Control		2579 ± 370
Heparin (Sigma)	0.5 µM	5376 ± 218
	1 µM	5628 ± 535
	2 µM	7451 ± 671
	8 µM	9089 ± 84
Fondaparinux	64 nM	4186 ± 233
	128 nM	5980 ± 795
	321 nM	7424 ± 400
(-) Epicatechin sulfate	16 µM	3071 ± 170
	67 µM	3815 ± 318
	166 µM	4348 ± 309
	332 µM	4579 ± 492

6.4.3 Discussion

The presence of full-length heparin increased the AT K_D values for all three DHPs. Therefore, all three DHPs bind to all or some portion of the heparin bind site on AT (PBS + EHBS). To refine the location of DHP binding, fondaparinux and -ECS were used. For all three DHPs, fondaparinux increased the AT:DHP K_D in a dose-dependent manner. Therefore, all three DHPs bind in the pentasaccharide-bind site of AT (PBS). When competitive binding studies were done in the presence of -ECS, both the CDs and SDs AT K_D values increased in a dose dependent manner, indicating that these molecules also bind the EHBS. Interestingly, even at 20 times the K_D of (-)-ECS – antithrombin interaction (332 μM), no significant increase in the K_D of FDs:AT interaction was observed. This result appears to suggest that FDs does not utilize the EHBS and is selective for the PBS, although this conclusion needs to be rigorously established using additional EHBS and PBS binding site competitors. Overall, these results are exciting because prior attempts to make non-carbohydrate anticoagulants that bound AT yielded weak activators, which only bound to the EHBS [190-192]. Based on these competitive bind studies, CDs appears to bind in a manner similar to full-length heparin but with tighter binding (~2.5-fold tighter), while SDs also appears to bind in a manner similar to full-length heparin but with slightly weaker binding (~2.5-fold weaker). FDs appears to bind in a selective manner similar to fondaparinux, but ~40-fold weaker. It is interesting to note that FDs binds AT only ~2-fold weaker than heparin.

6.5 What is the nature of the antithrombin-DHP interaction (ionic or non-ionic)?

The hydrophobic nature of the backbone of our sulfated DHPs suggests a strong possibility of significant non-ionic interactions with antithrombin. This is tested by measuring the K_D of DHP:AT interaction at several ionic strengths. As the ionic strength of the solution increases, it becomes more difficult for the DHP and AT to form ionic interactions, which will cause an increase in the K_D value. The extent to which the K_D values increase from one ionic strength to the next depends on the relative contributions of ionic and non-ionic binding. Equation **III** was found to be useful for segregating the protein–heparin interaction into ionic and non-ionic components. Therefore, equation **III**, will be used for our sulfated DHPs [194, 191, 237, 245]. In the equation below, the $K_{D,OBS}$ is the observed K_D value, the $K_{D,NIO}$ is the nonionic K_D values, Ψ is a screening constant and γ is the number of ion pair interactions. Although this approach is likely to succeed, it is important to remember that sulfated DHPs may not resemble an infinite chain of negative charges. To date, only the ionic/non-ionic interaction experiments have been done between AT and the DHPs.

Figure 60. Equation **III**

$$\log K_{D,OBS} = \log K_{D,NIO} + \Psi\gamma \log[Na^+]$$

6.5.1 Methods for salt-dependent AT-DHP equilibrium binding titrations

Titrations were conducted at 25º C (298 K), pH 7.4 in acrylic cuvettes. The buffer contains 20 mM sodium phosphate, varying concentrations of NaCl, 0.1 mM EDTA and 0.1% polyethylene glycol 8000. Four NaCl concentrations were tested (21 mM, 100 mM, 200 mM and 500 mM). The final concentration of antithrombin was 88 nM in the buffer above (final volume of 900 µl). DHPs (or other ligands) were added in 1 µl increments. The samples were excited at λ_{EX} = 280 nm and λ_{EX} = 340 nm [243]. Future studies will also use the same buffers described above, but at pH= 6.0. The equations provided on each salt dependence graph (figures 65-67) correlate to equation **III** above. The slope corresponds to $\Psi\gamma$ and the Y-intercept value corresponds to the log $K_{D,\ NIO}$. Using those values, one can calculate the ΔG^{o}_{Ionic} and $\Delta G^{o}_{Non\text{-}ionic}$ (equations **IV** and **V**, respectively), which quantifies that nature of the interaction between protein and ligand (ionic vs. non-ionic for the DHP:AT interaction).

Figure 61. Equations **IV** and **V**, where R=1.987 and T= temperature in Kelvin

$$\Delta G^{o}_{Ionic} = -2.303*R*T*\Psi\gamma*\log [Na^{+}] \qquad \textbf{IV}$$

$$\Delta G^{o}_{Non\text{-}ionic} = -2.303*R*T*\log K_{D,\ NIO} \qquad \textbf{V}$$

6.5.2 Results for the salt-dependent AT-DHP equilibrium binding titrations

Table 16. Variables for equation III derived from salt-dependent AT-DHP studies

DHP	Slope ($\Psi\gamma$)	log $K_{D, NIO}$	γ	$K_{D, NIO}$ (μM)
CDs	1.0973	-5.2583	1.3	5.5
FDs	0.6492	-4.9938	0.81	10.1
SDs	0.7893	-4.8337	0.98	14.6

Table 17. The relative contributions of ionic and non-ionic interactions in AT-DHP binding.

DHP	ΔG^{o}_{Ionic} (kcal/mol)	$\Delta G^{o}_{Non\text{-}ionic}$ (kcal/mol)	% Non-ionic contribution
CDs	1.29	7.17	84%
FDs	0.77	6.80	89%
SDs	0.93	6.59	87%

Figure 62. Salt-dependent AT-CDs equilibrium binding titrations

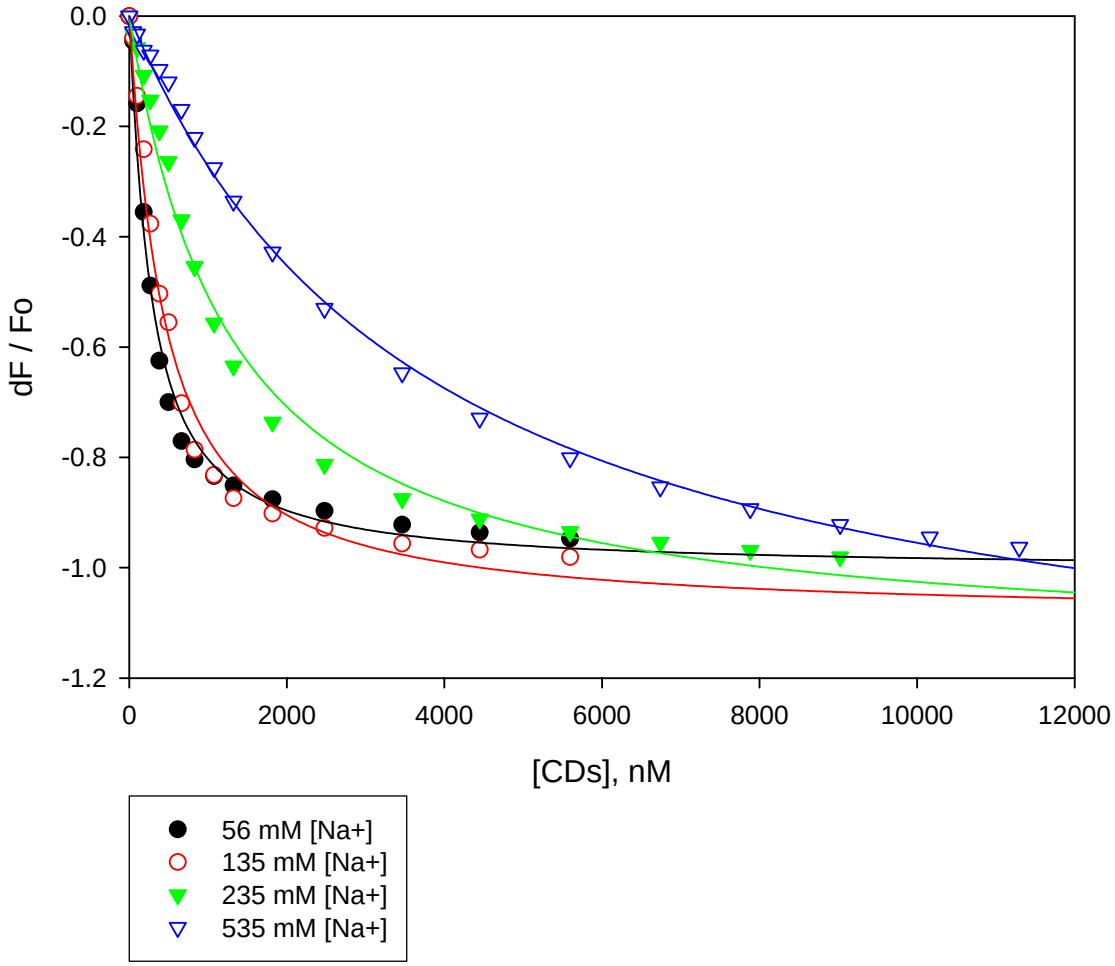

Figure 63. Salt-dependent AT-FDs equilibrium binding titrations

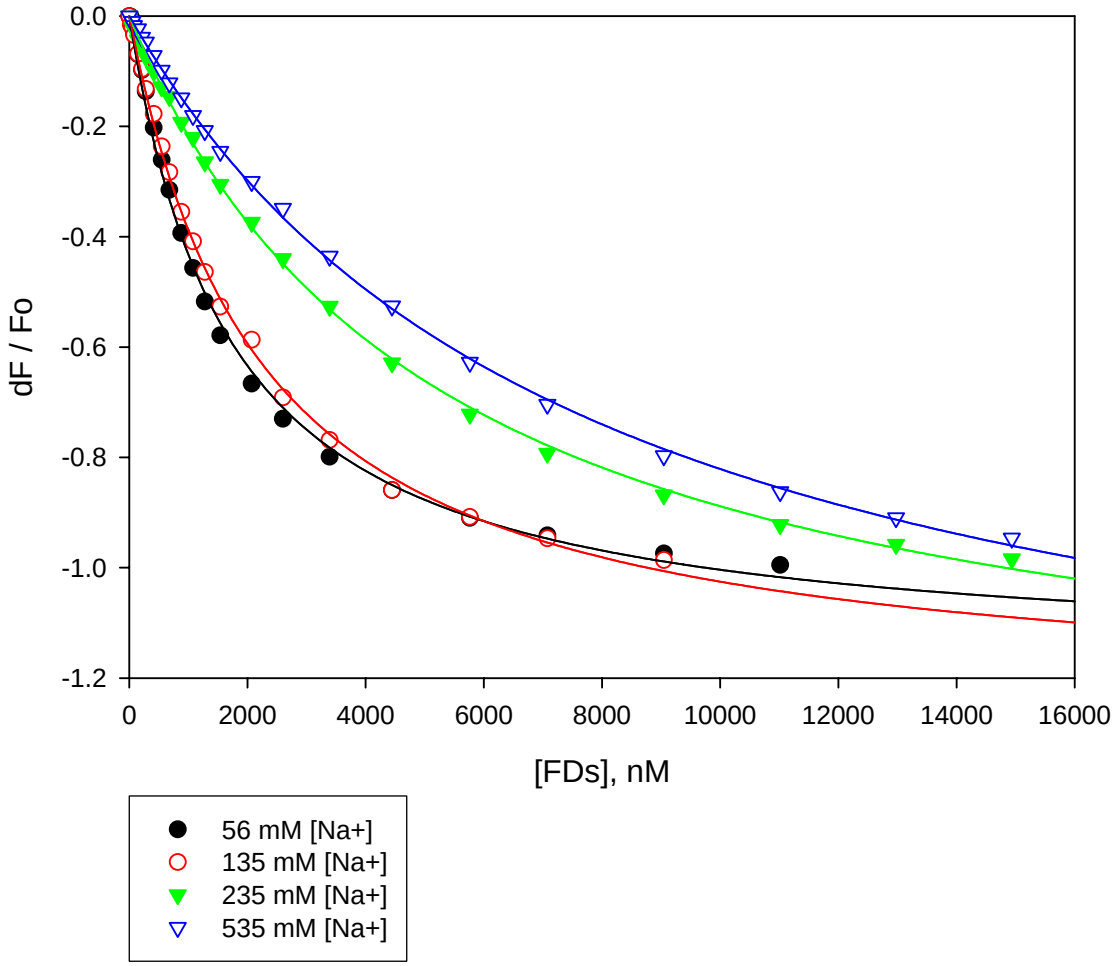

Figure 64. Salt-dependent AT-SDs equilibrium binding titrations

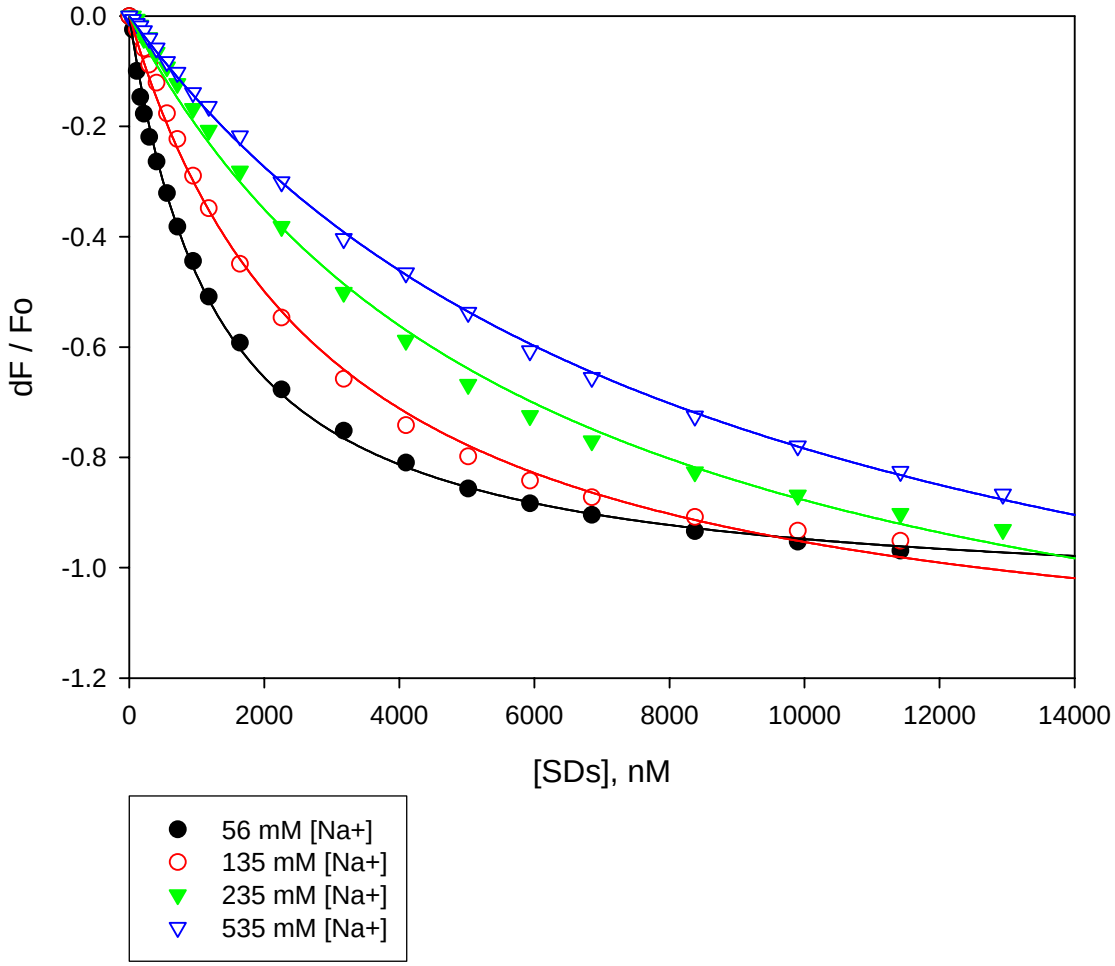

Figure 65. The dependence of AT:CDs on salt concentration (Standard error is shown)

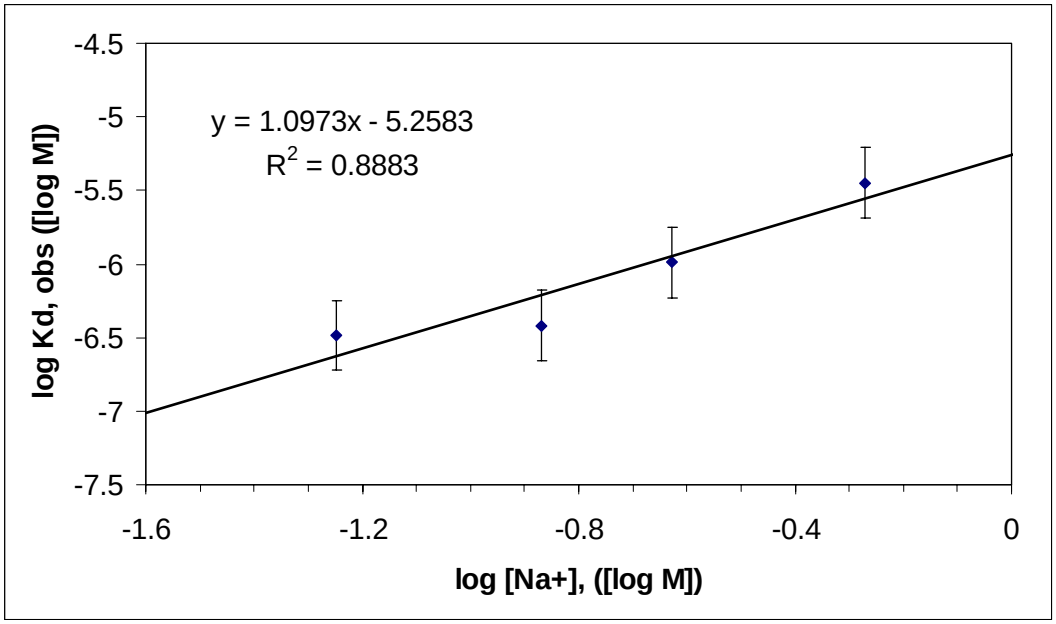

Figure 66. The dependence of AT:FDs on salt concentration (Standard error is shown)

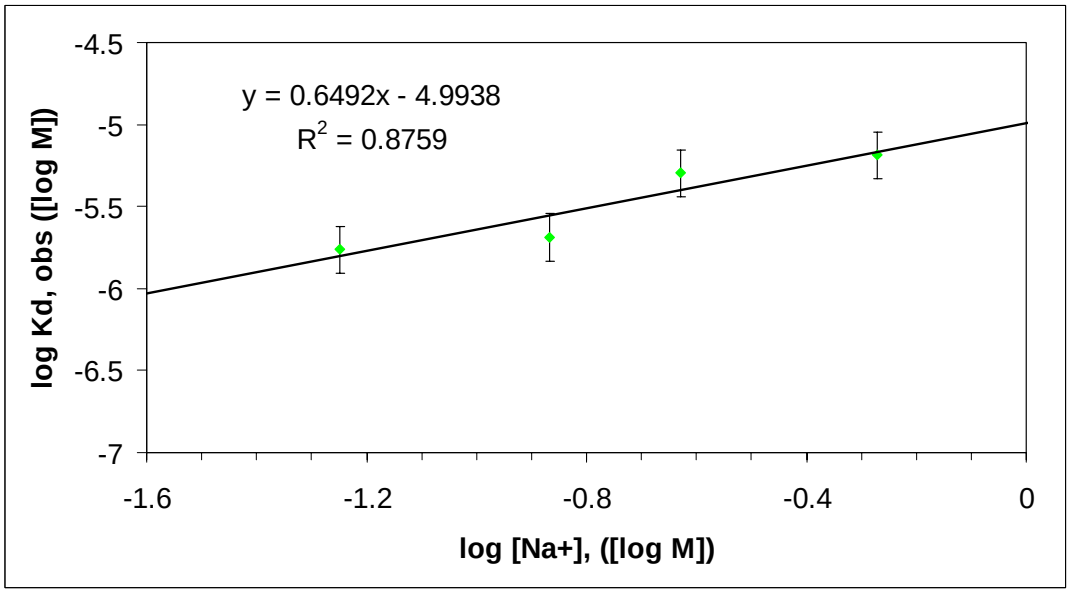

Figure 67. The dependence of AT:SDs on salt concentration (Standard error is shown)

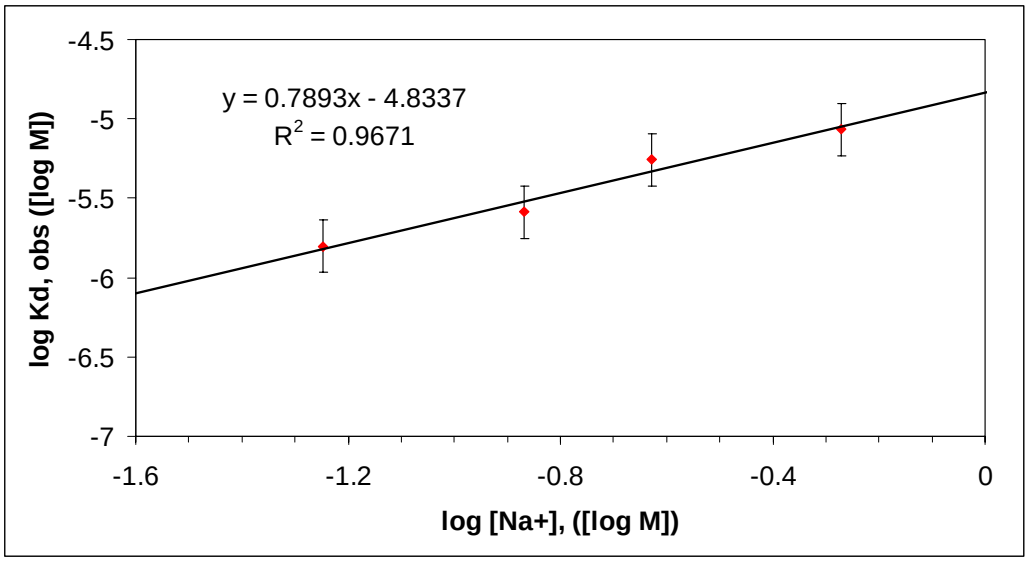

6.5.3 Discussion

The nature of the interaction between the sulfated DHPs and AT was predominantly non-ionic. {Discuss the value of KD,obs as a function of salt concentration.} The relative contribution of non-ionic interactions to total binding was 84-89%. This is a n important result that differentiates sulfated DHPs from all known antithrombin binding ligands. Heparins bind to AT in a manner that is primarily ionic [209]. However, our sulfated DHPs, which bind in a manner similar to heparin, bind in predominantly non-ionic fashion. This data dispels the notion that antithrombin ligands must be highly charged to effectively recognize the PBS and that non-ionic interactions are not important for antithrombin binding. DHPs represent a new strategy of designing AT binding molecules that are less negatively charged and more hydrophobic, which could be useful in the design of orally active anticoagulants.

Literature Cited

Literature Cited

1. Brummel KE, Paradis SG, Butenas S, Mann KG. Thrombin functions during tissue factor-induced blood coagulation. Blood. 2002; 100: 148-52.

2. Golino P. The inhibitors of the tissue factor:factor VII pathway. Thromb Res. 2002; 106:V257-65.

3. Khrenov AV, Ananyeva NM, Griffin JH, Saenko EL. Coagulation pathways in atherothrombosis. Trends Cardiovasc Med. 2002; 12:317-24.

4. Carmeliet P, Collen D. Tissue factor. Int J Biochem Cell Biol. 1998; 30:661-7.

5. Mann KG. Biochemistry and physiology of blood coagulation. Thromb Haemost. 1999; 82:165-74.

6. Giesen PL, Rauch U, Bohrmann B, Kling D, Roqué M, Fallon JT, Badimon JJ, Himber J, Riederer MA, Nemerson Y. Blood-borne tissue factor: another view of thrombosis. Proc Natl Acad Sci U S A. 1999; 96:2311-5.

7. Mann KG, Butenas S, Brummel K. The dynamics of thrombin formation. Arterioscler Thromb Vasc Biol. 2003; 23:17-25.

8. Brufatto N, Nesheim ME. Analysis of the kinetics of prothrombin activation and evidence that two equilibrating forms of prothrombinase are involved in the process. J Biol Chem. 2003; 278:6755-64.

9. Majerus PW, Miletich JP. Relationships between platelets and coagulation factors in hemostasis. Annu Rev Med. 1978; 29:41-9.

10. Fulcher CA, Roberts JR, Zimmerman TS. Thrombin proteolysis of purified factor VIII procoagulant protein: correlation of activation with generation of a specific polypeptide. Blood. 1983; 61:807-11.

11. Suzuki K, Dahlbäck B, Stenflo J. Thrombin-catalyzed activation of human coagulation factor V. J Biol Chem. 1982; 257:6556-64.

12. Naito K, Fujikawa K. Activation of human blood coagulation factor XI independent of factor XII. Factor XI is activated by thrombin and factor XIa in the presence of negatively charged surfaces. J Biol Chem. 1991; 266:7353-8.

13. Gerotziafas GT, Samama MM. Heterogeneity of synthetic factor Xa inhibitors. Curr Pharm Des. 2005; 11:3855-76.

14. Mosesson MW. Fibrinogen and fibrin structure and functions. J Thromb Haemost. 2005; 3:1894-904.

15. Mosesson MW, Siebenlist KR, Meh DA. The structure and biological features of fibrinogen and fibrin. Ann N Y Acad Sci. 2001; 936:11-30.

16. Eisenberg PR, Siegel JE, Abendschein DR, Miletich JP. Importance of factor Xa in determining the procoagulant activity of whole-blood clots. J Clin Invest. 1993; 91:1877-83.

17. Iino M, Takeya H, Takemitsu T, Nakagaki T, Gabazza EC, Suzuki K. Characterization of the binding of factor Xa to fibrinogen/fibrin derivatives and localization of the factor Xa binding site on fibrinogen. Eur J Biochem. 1995; 232:90-7.

18. Hogg PJ, Jackson CM. Fibrin monomer protects thrombin from inactivation by heparin-antithrombin III: implications for heparin efficacy. Proc Natl Acad Sci U S A. 1989; 86:3619-23.

19. Weitz JI, Hudoba M, Massel D, Maraganore J, Hirsh J. Clot-bound thrombin is protected from inhibition by heparin-antithrombin III but is susceptible to inactivation by antithrombin III-independent inhibitors. J Clin Invest. 1990; 86:385-91.

20. Hack CE. Tissue factor pathway of coagulation in sepsis. Crit Care Med. 2000; 28 (Suppl):S25-30.

21. Weitz JI, Hirsh J, Samama MM. New anticoagulant drugs: the Seventh ACCP Conference on Antithrombotic and Thrombolytic Therapy. Chest. 2004; 126 (Suppl):265S-286S.

22. Matyal R, Mahmood F, Park KW. Tifacogin, recombinant tissue factor pathway inhibitor. Int Anesthesiol Clin. 2005; 43:135-44.

23. Bajzar L, Manuel R, Nesheim ME. Purification and characterization of TAFI, a thrombin-activable fibrinolysis inhibitor. J Biol Chem. 1995; 270:14477-84.

24. Bajzar L, Morser J, Nesheim M. TAFI, or plasma procarboxypeptidase B, couples the coagulation and fibrinolytic cascades through the thrombin-thrombomodulin complex. J Biol Chem. 1996; 271:16603-8.

25. Nutescu EA, Wittkowsky AK. Direct thrombin inhibitors for anticoagulation. Ann Pharmacother. 2004; 38:99-109.

26. Sadler JE. Medicine: K is for koagulation. Nature. 2004; 427:493-4.

27. Sasisekharan R, Venkataraman G. Heparin and heparan sulfate: biosynthesis, structure and function. Curr Opin Chem Biol. 2000; 4:626-31.

28. Wu KK, Matijevic-Aleksic N. Molecular aspects of thrombosis and antithrombotic drugs. Crit Rev Clin Lab Sci. 2005; 42:249-77.

29. Capila I, Linhardt RJ. Heparin-protein interactions. Angew Chem Int Ed Engl. 2002; 41:391-412.

30. Frydman A. Low-molecular-weight heparins: an overview of their pharmacodynamics, pharmacokinetics and metabolism in humans. Haemostasis. 1996; 26 Suppl 2:24-38.

31. Boneu B, Necciari J, Cariou R, Sié P, Gabaig AM, Kieffer G, Dickinson J, Lamond G, Moelker H, Mant T, et al. Pharmacokinetics and tolerance of the natural pentasaccharide (SR90107/Org31540) with high affinity to antithrombin III in man. Thromb Haemost. 1995; 74:1468-73.

32. Wallis RB. Hirudins: from leeches to man. Semin Thromb Hemost. 1996; 22:185-96.

33. Salzet M. Leech thrombin inhibitors. Curr Pharm Des. 2002; 8:493-503.

34. DiMaio J, Gibbs B, Munn D, Lefebvre J, Ni F, Konishi Y. Bifunctional thrombin inhibitors based on the sequence of hirudin45-65. J Biol Chem. 1990; 265:21698-703.

35. Römisch J, Diehl KH, Hoffmann D, Krahl-Mateblowski U, Reers M, Stüber W, Pâques EP. Comparison of in vitro and in vivo properties of rhirudin (HBW 023) and a synthetic analogous peptide. Haemostasis. 1993; 23: 249-58.

36. Braun PJ, Dennis S, Hofsteenge J, Stone SR. Use of site-directed mutagenesis to investigate the basis for the specificity of hirudin. Biochemistry. 1988; 27:6517-22.

37. Nutescu EA, Shapiro NL, Chevalier A. New anticoagulant agents: direct thrombin inhibitors. Clin Geriatr Med. 2006; 22:33-56.

38. Warkentin TE. Bivalent direct thrombin inhibitors: hirudin and bivalirudin. Best Pract Res Clin Haematol. 2004; 17:105-25.

39. Rydel TJ, Ravichandran KG, Tulinsky A, Bode W, Huber R, Roitsch C, Fenton JW. The structure of a complex of recombinant hirudin and human alpha-thrombin. Science. 1990; 249:277-80.

40. Maraganore JM, Bourdon P, Jablonski J, Ramachandran KL, Fenton JW. Design and characterization of hirulogs: a novel class of bivalent peptide inhibitors of thrombin. Biochemistry. 1990; 29:7095-101.

41. Skrzypczak-Jankun E, Carperos VE, Ravichandran KG, Tulinsky A, Westbrook M, Maraganore JM. Structure of the hirugen and hirulog 1 complexes of alpha-thrombin. J Mol Biol. 1991; 221:1379-93.

42. Witting JI, Bourdon P, Maraganore JM, Fenton JW. Hirulog-1 and -B2 thrombin specificity. Biochem J. 1992; 287:663-4.

43. Parry MA, Maraganore JM, Stone SR. Kinetic mechanism for the interaction of Hirulog with thrombin. Biochemistry. 1994; 33:14807-14.

44. Fox I, Dawson A, Loynds P, Eisner J, Findlen K, Levin E, Hanson D, Mant T, Wagner J, Maraganore J. Anticoagulant activity of Hirulog, a direct thrombin inhibitor, in humans. Thromb Haemost. 1993; 69:157-63.

45. Hursting MJ, Alford KL, Becker JC, Brooks RL, Joffrion JL, Knappenberger GD, Kogan PW, Kogan TP, McKinney AA, Schwarz RP. Novastan (brand of argatroban): a small-molecule, direct thrombin inhibitor. Semin Thromb Hemost. 1997; 23:503-16.

46. Walenga JM, Ahmad S, Hoppensteadt D, Iqbal O, Hursting MJ, Lewis BE. Argatroban therapy does not generate antibodies that alter its anticoagulant activity in patients with heparin-induced thrombocytopenia. Thromb Res. 2002; 105:401-5.

47. Walenga JM. An overview of the direct thrombin inhibitor argatroban. Pathophysiol Haemost Thromb. 2002; 32 Suppl 3:9-14.

48. Gustafsson D, Nyström J, Carlsson S, Bredberg U, Eriksson U, Gyzander E, Elg M, Antonsson T, Hoffmann K, Ungell A, Sörensen H, Någård S, Abrahamsson A, Bylund R. The direct thrombin inhibitor melagatran and its oral prodrug H 376/95: intestinal absorption properties, biochemical and pharmacodynamic effects. Thromb Res. 2001; 101:171-81.

49. Gustafsson D, Antonsson T, Bylund R, Eriksson U, Gyzander E, Nilsson I, Elg M, Mattsson C, Deinum J, Pehrsson S, Karlsson O, Nilsson A, Sörensen H. Effects of melagatran, a new low-molecular-weight thrombin inhibitor, on thrombin and fibrinolytic enzymes. Thromb Haemost. 1998; 79:110-8.

50. Gustafsson D, Elg M. The pharmacodynamics and pharmacokinetics of the oral direct thrombin inhibitor ximelagatran and its active metabolite melagatran: a mini-review. Thromb Res. 2003; 109 Suppl 1:S9-15.

51. Eriksson UG, Bredberg U, Hoffmann KJ, Thuresson A, Gabrielsson M, Ericsson H, Ahnoff M, Gislén K, Fager G, Gustafsson D. Absorption, distribution, metabolism, and

excretion of ximelagatran, an oral direct thrombin inhibitor, in rats, dogs, and humans. Drug Metab Dispos. 2003 Mar;31(3):294-305.

52. Rewinkel JB, Adang AE. Strategies and progress towards the ideal orally active thrombin inhibitor. Curr Pharm Des. 1999; 5:1043-75.

53. McCullough PA, Dorrell KA, Sandberg KR, Yerkey MW. Ximelagatran: a novel oral direct thrombin inhibitor for long-term anticoagulation. Rev Cardiovasc Med. 2004; 5:99-103.

54. Bredberg E, Andersson TB, Frison L, Thuresson A, Johansson S, Eriksson-Lepkowska M, Larsson M, Eriksson UG. Ximelagatran, an oral direct thrombin inhibitor, has a low potential for cytochrome P450-mediated drug-drug interactions. Clin Pharmacokinet. 2003; 42:765-77.

55. Saiah E, Soares C. Small molecule coagulation cascade inhibitors in the clinic. Curr Top Med Chem. 2005; 5:1677-95.

56. Hirsh, J, Anand, SS, Halperin, JL, Fuster, V. Guide to anticoagulant therapy: Heparin. Circulation 2001; 103: 2994-3018.

57. Bode W, Mayr I, Baumann U, Huber R, Stone SR, Hofsteenge J. The refined 1.9 A crystal structure of human alpha-thrombin: interaction with D-Phe-Pro-Arg chloromethylketone and significance of the Tyr-Pro-Pro-Trp insertion segment. EMBO J. 1989; 8:3467-75.

58. Kraut J. Serine proteases: structure and mechanism of catalysis. Annu Rev Biochem. 1977; 46:331-58.

59. Kranjc A, Kikelj D, Peterlin-Masic L. Recent advances in the discovery of tissue factor/factor VIIa inhibitors and dual inhibitors of factor VIIa/factor Xa. Curr Pharm Des. 2005; 11:4207-27.

60. Girard TJ, Nicholson NS. The role of tissue factor/factor VIIa in the pathophysiology of acute thrombotic formation. Curr Opin Pharmacol. 2001; 1:159-63.

61. Kranjc A, Kikelj D. Dual inhibitors of the blood coagulation enzymes. Curr Med Chem. 2004 Oct; 11:2535-47.

62. Jakobsen P, Pedersen BR, Persson E. Inhibitors of the tissue factor/factor VIIa-induced coagulation: synthesis and in vitro evaluation of novel specific 2-aryl substituted 4H-3,1-benzoxazin-4-ones. Bioorg Med Chem. 2000; 8:2095-103.

63. South MS, Case BL, Wood RS, Jones DE, Hayes MJ, Girard TJ, Lachance RM, Nicholson NS, Clare M, Stevens AM, Stegeman RA, Stallings WC, Kurumbail RG, Parlow JJ. Structure-based drug design of pyrazinone antithrombotics as selective inhibitors of the tissue factor VIIa complex. Bioorg Med Chem Lett. 2003; 13:2319-25.

64. Parlow JJ, Case BL, Dice TA, Fenton RL, Hayes MJ, Jones DE, Neumann WL, Wood RS, Lachance RM, Girard TJ, Nicholson NS, Clare M, Stegeman RA, Stevens AM, Stallings WC, Kurumbail RG, South MS. Design, parallel synthesis, and crystal structures of pyrazinone antithrombotics as selective inhibitors of the tissue factor VIIa complex. J Med Chem. 2003; 46:4050-62.

65. Suleymanov OD, Szalony JA, Salyers AK, LaChance RM, Parlow JJ, South MS, Wood RS, Nicholson NS. Pharmacological interruption of acute thrombus formation with minimal hemorrhagic complications by a small molecule tissue factor/factor VIIa inhibitor:

comparison to factor Xa and thrombin inhibition in a nonhuman primate thrombosis model. J Pharmacol Exp Ther. 2003; 306:1115-21.

66. Parlow JJ, Kurumbail RG, Stegeman RA, Stevens AM, Stallings WC, South MS. Design, synthesis, and crystal structure of selective 2-pyridone tissue factor VIIa inhibitors. J Med Chem. 2003; 46:4696-701.

67. Young WB, Kolesnikov A, Rai R, Sprengeler PA, Leahy EM, Shrader WD, Sangalang J, Burgess-Henry J, Spencer J, Elrod K, Cregar L. Optimization of a screening lead for factor VIIa/TF. Bioorg Med Chem Lett. 2001; 11:2253-6.

68. Klingler O, Matter H, Schudok M, Bajaj SP, Czech J, Lorenz M, Nestler HP, Schreuder H, Wildgoose P. Design, synthesis, and structure-activity relationship of a new class of amidinophenylurea-based factor VIIa inhibitors. Bioorg Med Chem Lett. 2003; 13:1463-7.

69. Linkins LA, Weitz JI. New anticoagulant therapy. Annu Rev Med. 2005; 56:63-77.

70. Lee AY, Vlasuk GP. Recombinant nematode anticoagulant protein c2 and other inhibitors targeting blood coagulation factor VIIa/tissue factor. J Intern Med. 2003; 254:313-21.

71. Bergum PW, Cruikshank A, Maki SL, Kelly CR, Ruf W, Vlasuk GP. Role of zymogen and activated factor X as scaffolds for the inhibition of the blood coagulation factor VIIa-tissue factor complex by recombinant nematode anticoagulant protein c2. J Biol Chem. 2001; 276:10063-71.

72. Buddai SK, Toulokhonova L, Bergum PW, Vlasuk GP, Krishnaswamy S. Nematode anticoagulant protein c2 reveals a site on factor Xa that is important for macromolecular substrate binding to human prothrombinase. J Biol Chem. 2002; 277:26689-98.

73. Stassens P, Bergum PW, Gansemans Y, Jespers L, Laroche Y, Huang S, Maki S, Messens J, Lauwereys M, Cappello M, Hotez PJ, Lasters I, Vlasuk GP. Anticoagulant repertoire of the hookworm Ancylostoma caninum. Proc Natl Acad Sci U S A. 1996; 93:2149-54.

74. Vlasuk GP, Bradbury A, Lopez-Kinninger L, Colón S, Bergum PW, Maki S, Rote WE. Pharmacokinetics and anticoagulant properties of the factor VIIa-tissue factor inhibitor recombinant Nematode Anticoagulant Protein c2 following subcutaneous administration in man. Dependence on the stoichiometric binding to circulating factor X. Thromb Haemost. 2003; 90:803-12.

75. Friederich PW, Levi M, Bauer KA, Vlasuk GP, Rote WE, Breederveld D, Keller T, Spataro M, Barzegar S, Büller HR. Ability of recombinant factor VIIa to generate thrombin during inhibition of tissue factor in human subjects. Circulation. 2001; 103:2555-9.

76. Dennis MS, Eigenbrot C, Skelton NJ, Ultsch MH, Santell L, Dwyer MA, O'Connell MP, Lazarus RA. Peptide exosite inhibitors of factor VIIa as anticoagulants. Nature. 2000; 404:465-70.

77. Dennis MS, Roberge M, Quan C, Lazarus RA. Selection and characterization of a new class of peptide exosite inhibitors of coagulation factor VIIa. Biochemistry. 2001; 40:9513-21.

78. Roberge M, Santell L, Dennis MS, Eigenbrot C, Dwyer MA, Lazarus RA. A novel exosite on coagulation factor VIIa and its molecular interactions with a new class of peptide inhibitors. Biochemistry. 2001; 40:9522-31.

79. Maignan S, Guilloteau JP, Pouzieux S, Choi-Sledeski YM, Becker MR, Klein SI, Ewing WR, Pauls HW, Spada AP, Mikol V. Crystal structures of human factor Xa complexed with potent inhibitors. J Med Chem. 2000; 43:3226-32.

80. Stürzebecher J, Markwardt F, Walsmann P. Synthetic inhibitors of serine proteinases XIV. Inhibition of Factor Xa by derivatives of benzamidine. Thromb Res. 1976; 9:637-46.

81. Hara K, Honma T, Matsuzawa A, Matsuzawa A, Uchida M, Koizumi T, Akahane S, Kojima M. Characteristics of the hemostatic action of KFA-1411, an inhibitor of coagulation factor Xa (FXa), in humans and various animals. J Toxicol Sci. 2003; 28:25-34.

82. Pauls HW, Ewing WR. The design of competitive, small-molecule inhibitors of coagulation factor Xa. Curr Top Med Chem. 2001; 1:83-100.

83. Czekaj M, Klein SI, Guertin KR, Gardner CJ, Zulli AL, Pauls HW, Spada AP, Cheney DL, Brown KD, Colussi DJ, Chu V, Leadley RJ, Dunwiddie CT. Optimization of the beta-aminoester class of factor Xa inhibitors. Part 1: P(4) and side-chain modifications for improved in vitro potency. Bioorg Med Chem Lett. 2002; 12:1667-70.

84. Lin Z, Johnson ME. Proposed cation-pi mediated binding by factor Xa: a novel enzymatic mechanism for molecular recognition. FEBS Lett. 1995; 370:1-5.

85. Guertin KR, Gardner CJ, Klein SI, Zulli AL, Czekaj M, Gong Y, Spada AP, Cheney DL, Maignan S, Guilloteau JP, Brown KD, Colussi DJ, Chu V, Heran CL, Morgan SR, Bentley RG, Dunwiddie CT, Leadley RJ, Pauls HW. Optimization of the beta-aminoester class of factor Xa inhibitors. Part 2: Identification of FXV673 as a potent and selective inhibitor with excellent In vivo anticoagulant activity. Bioorg Med Chem Lett. 2002; 12:1671-4.

86. Light DR, Guilford WJ. Discovery of the factor Xa inhibitor, ZK 807834 (CI-1031). Curr Top Med Chem. 2001; 1:121-36.

87. Adler M, Davey DD, Phillips GB, Kim SH, Jancarik J, Rumennik G, Light DR, Whitlow M. Preparation, characterization, and the crystal structure of the inhibitor ZK-807834 (CI-1031) complexed with factor Xa. Biochemistry. 2000; 39:12534-42.

88. Gong Y, Pauls HW, Spada AP, Czekaj M, Liang G, Chu V, Colussi DJ, Brown KD, Gao J. Amido-(propyl and allyl)-hydroxybenzamidines: development of achiral inhibitors of factor Xa. Bioorg Med Chem Lett. 2000; 10:217-21.

89. Rezaie AR. DX-9065a inhibition of factor Xa and the prothrombinase complex: mechanism of inhibition and comparison with therapeutic heparins. Thromb Haemost. 2003; 89:112-21.

90. Katakura S, Nagahara T, Hara T, Iwamoto M. A novel factor Xa inhibitor: structure-activity relationships and selectivity between factor Xa and thrombin. Biochem Biophys Res Commun. 1993; 197:965-72.

91. Becker RC, Alexander J, Dyke CK, Harrington RA. Development of DX-9065a, a novel direct factor Xa antagonist, in cardiovascular disease. Thromb Haemost. 2004; 92:1182-93.

92. Hirayama F, Koshio H, Katayama N, Kurihara H, Taniuchi Y, Sato K, Hisamichi N, Sakai-Moritani Y, Kawasaki T, Matsumoto Y, Yanagisawa I. The discovery of YM-60828: a potent, selective and orally-bioavailable factor Xa inhibitor. Bioorg Med Chem. 2002; 10:1509-23.

93. Jones SD, Liebeschuetz JW, Morgan PJ, Murray CW, Rimmer AD, Roscoe JM, Waszkowycz B, Welsh PM, Wylie WA, Young SC, Martin H, Mahler J, Brady L, Wilkinson K. The design of phenylglycine containing benzamidine carboxamides as potent and selective inhibitors of factor Xa. Bioorg Med Chem Lett. 2001; 11:733-6.

94. Pinto DJ, Orwat MJ, Wang S, Fevig JM, Quan ML, Amparo E, Cacciola J, Rossi KA, Alexander RS, Smallwood AM, Luettgen JM, Liang L, Aungst BJ, Wright MR, Knabb RM, Wong PC, Wexler RR, Lam PY. Discovery of 1-[3-(aminomethyl)phenyl]-N-3-fluoro-2'-(methylsulfonyl)-[1,1'-biphenyl]-4-yl]-3-(trifluoromethyl)-1H-pyrazole-5-carboxamide (DPC423), a highly potent, selective, and orally bioavailable inhibitor of blood coagulation factor Xa. J Med Chem. 2001; 44:566-78.

95. Quan ML, Liauw AY, Ellis CD, Pruitt JR, Carini DJ, Bostrom LL, Huang PP, Harrison K, Knabb RM, Thoolen MJ, Wong PC, Wexler RR. Design and synthesis of isoxazoline derivatives as factor Xa inhibitors. 1. J Med Chem. 1999; 42:2752-9.

96. Pruitt JR, Pinto DJ, Galemmo RA, Alexander RS, Rossi KA, Wells BL, Drummond S, Bostrom LL, Burdick D, Bruckner R, Chen H, Smallwood A, Wong PC, Wright MR, Bai

S, Luettgen JM, Knabb RM, Lam PY, Wexler RR. Discovery of 1-(2-aminomethylphenyl)-3-trifluoromethyl-N- [3-fluoro-2'-(aminosulfonyl)[1,1'-biphenyl)]-4-yl]-1H-pyrazole-5-carboxyamide (DPC602), a potent, selective, and orally bioavailable factor Xa inhibitor(1). J Med Chem. 2003; 46:5298-315.

97. Pruitt JR, Pinto DJ, Galemmo RA, Alexander RS, Rossi KA, Wells BL, Drummond S, Bostrom LL, Burdick D, Bruckner R, Chen H, Smallwood A, Wong PC, Wright MR, Bai S, Luettgen JM, Knabb RM, Lam PY, Wexler RR. Discovery of 1-(2-aminomethylphenyl)-3-trifluoromethyl-N- [3-fluoro-2'-(aminosulfonyl)[1,1'-biphenyl)]-4-yl]-1H-pyrazole-5-carboxyamide (DPC602), a potent, selective, and orally bioavailable factor Xa inhibitor(1). J Med Chem. 2003; 46:5298-315.

98. Ewing WR, Becker MR, Manetta VE, Davis RS, Pauls HW, Mason H, Choi-Sledeski YM, Green D, Cha D, Spada AP, Cheney DL, Mason JS, Maignan S, Guilloteau JP, Brown K, Colussi D, Bentley R, Bostwick J, Kasiewski CJ, Morgan SR, Leadley RJ, Dunwiddie CT, Perrone MH, Chu V. Design and structure-activity relationships of potent and selective inhibitors of blood coagulation factor Xa. J Med Chem. 1999; 42:3557-71.

99. Choi-Sledeski YM, McGarry DG, Green DM, Mason HJ, Becker MR, Davis RS, Ewing WR, Dankulich WP, Manetta VE, Morris RL, Spada AP, Cheney DL, Brown KD, Colussi DJ, Chu V, Heran CL, Morgan SR, Bentley RG, Leadley RJ, Maignan S, Guilloteau JP, Dunwiddie CT, Pauls HW. Sulfonamidopyrrolidinone factor Xa inhibitors: potency and selectivity enhancements via P-1 and P-4 optimization. J Med Chem. 1999; 42:3572-87.

100. Gong Y, Becker M, Choi-Sledeski YM, Davis RS, Salvino JM, Chu V, Brown KD, Pauls HW. Solid-phase parallel synthesis of azarene pyrrolidinones as factor Xa inhibitors. Bioorg Med Chem Lett. 2000;10:1033-6.

101. Maignan S, Guilloteau JP, Choi-Sledeski YM, Becker MR, Ewing WR, Pauls HW, Spada AP, Mikol V. Molecular structures of human factor Xa complexed with ketopiperazine inhibitors: preference for a neutral group in the S1 pocket. J Med Chem. 2003; 46:685-90.

102. Claeson G. Synthetic peptides and peptidomimetics as substrates and inhibitors of thrombin and other proteases in the blood coagulation system. Blood Coagul Fibrinolysis. 1994; 5:411-36.

103. Zhu BY, Huang W, Su T, Marlowe C, Sinha U, Hollenbach S, Scarborough RM. Discovery of transition state factor Xa inhibitors as potential anticoagulant agents. Curr Top Med Chem. 2001; 1:101-19.

104. Neeper MP, Waxman L, Smith DE, Schulman CA, Sardana M, Ellis RW, Schaffer LW, Siegl PK, Vlasuk GP. Characterization of recombinant tick anticoagulant peptide. A highly selective inhibitor of blood coagulation factor Xa. J Biol Chem. 1990; 265:17746-52.

105. Lehman ED, Schaefer TF, Przysiecki CT, Joyce JG, Bailey FJ, Schulman CA, Burke CJ, Ramjit HG, Miller WJ. Large-scale purification and characterization of recombinant tick anticoagulant peptide. J Chromatogr. 1992; 574:225-35.

106. Waxman L, Smith DE, Arcuri KE, Vlasuk GP. Tick anticoagulant peptide (TAP) is a novel inhibitor of blood coagulation factor Xa. Science. 1990; 248:593-6.

107. Jordan SP, Waxman L, Smith DE, Vlasuk GP. Tick anticoagulant peptide: kinetic analysis of the recombinant inhibitor with blood coagulation factor Xa. Biochemistry. 1990; 29:11095-100.

108. Dunwiddie CT, Neeper MP, Nutt EM, Waxman L, Smith DE, Hofmann KJ, Lumma PK, Garsky VM, Vlasuk GP. Site-directed analysis of the functional domains in the factor Xa inhibitor tick anticoagulant peptide: identification of two distinct regions that constitute the enzyme recognition sites. Biochemistry. 1992; 31:12126-31.

109. Vlasuk GP. Structural and functional characterization of tick anticoagulant peptide (TAP): a potent and selective inhibitor of blood coagulation factor Xa. Thromb Haemost. 1993; 70:212-6.

110. Dunwiddie CT, Smith DE, Nutt EM, Vlasuk GP. Anticoagulant effects of the selective factor XA inhibitors tick anticoagulant peptide and antistasin in the APTT assay are determined by the relative rate of prothrombinase inhibition. Thromb Res. 1991; 64:787-94.

111. Seymour JL, Lindquist RN, Dennis MS, Moffat B, Yansura D, Reilly D, Wessinger ME, Lazarus RA. Ecotin is a potent anticoagulant and reversible tight-binding inhibitor of factor Xa. Biochemistry. 1994; 33:3949-58.

112. Tuszynski GP, Gasic TB, Gasic GJ. Isolation and characterization of antistasin. An inhibitor of metastasis and coagulation. J Biol Chem. 1987; 262:9718-23.

113. Nutt E, Gasic T, Rodkey J, Gasic GJ, Jacobs JW, Friedman PA, Simpson E. The amino acid sequence of antistasin. A potent inhibitor of factor Xa reveals a repeated internal structure. J Biol Chem. 1988; 263:10162-7.

114. Han JH, Law SW, Keller PM, Kniskern PJ, Silberklang M, Tung JS, Gasic TB, Gasic GJ, Friedman PA, Ellis RW. Cloning and expression of cDNA encoding antistasin, a leech-derived protein having anti-coagulant and anti-metastatic properties. Gene. 1989; 75:47-57.

115. Dunwiddie C, Thornberry NA, Bull HG, Sardana M, Friedman PA, Jacobs JW, Simpson E. Antistasin, a leech-derived inhibitor of factor Xa. Kinetic analysis of enzyme inhibition and identification of the reactive site. J Biol Chem. 1989; 264:16694-9.

116. Ohta N, Brush M, Jacobs JW. Interaction of antistasin-related peptides with factor Xa: identification of a core inhibitory sequence. Thromb Haemost. 1994; 72:825-30.

117. Chopin V, Salzet M, Baert J, Vandenbulcke F, Sautiére PE, Kerckaert JP, Malecha J. Therostasin, a novel clotting factor Xa inhibitor from the rhynchobdellid leech, Theromyzon tessulatum. J Biol Chem. 2000; 275:32701-7.

118. Arocha-Piñango CL, Marchi R, Carvajal Z, Guerrero B. Invertebrate compounds acting on the hemostatic mechanism. Blood Coagul Fibrinolysis. 1999; 10:43-68.

119. Condra C, Nutt E, Petroski CJ, Simpson E, Friedman PA, Jacobs JW. Isolation and structural characterization of a potent inhibitor of coagulation factor Xa from the leech Haementeria ghilianii. Thromb Haemost. 1989; 61:437-41.

120. Brankamp RG, Manley GG, Blankenship DT, Bowlin TL, Cardin AD. Studies on the anticoagulant, antimetastatic and heparin-binding properties of ghilanten-related inhibitors. Blood Coagul Fibrinolysis. 1991; 2:161-6.

121. Cappello M, Clyne LP, McPhedran P, Hotez PJ. J Infect Dis. Ancylostoma factor Xa inhibitor: partial purification and its identification as a major hookworm-derived anticoagulant in vitro. 1993; 167:1474-7.

122. Cappello M, Vlasuk GP, Bergum PW, Huang S, Hotez PJ. Ancylostoma caninum anticoagulant peptide: a hookworm-derived inhibitor of human coagulation factor Xa. Proc Natl Acad Sci U S A. 1995; 92:6152-6.

123. Donnelly KM, Bromberg ME, Milstone A, Madison McNiff JM, Terwilliger G, Konigsberg WH, Cappello M. Ancylostoma caninum anticoagulant peptide blocks metastasis in vivo and inhibits factor Xa binding to melanoma cells in vitro. Thromb Haemost. 1998; 79:1041-7.

124. Faria F, Kelen EM, Sampaio CA, Bon C, Duval N, Chudzinski-Tavassi AM. A new factor Xa inhibitor (lefaxin) from the Haementeria depressa leech. Thromb Haemost. 1999; 82:1469-73.

125. Hopfner KP, Lang A, Karcher A, Sichler K, Kopetzki E, Brandstetter H, Huber R, Bode W, Engh RA. Coagulation factor IXa: the relaxed conformation of Tyr99 blocks substrate binding. Structure. 1999; 7:989-96.

126. Lottenberg R, Christensen U, Jackson CM, Coleman PL. Assay of coagulation proteases using peptide chromogenic and fluorogenic substrates. Methods Enzymol. 1981; 80:341-61.

127. Brandstetter H, Bauer M, Huber R, Lollar P, Bode W. X-ray structure of clotting factor IXa: active site and module structure related to Xase activity and hemophilia B. Proc Natl Acad Sci U S A. 1995; 92:9796-800.

128. Greer J. Comparative modeling methods: application to the family of the mammalian serine proteases. Proteins. 1990; 7:317-34.

129. Bode W, Brandstetter H, Mather T, Stubbs MT. Comparative analysis of haemostatic proteinases: structural aspects of thrombin, factor Xa, factor IXa and protein C. Thromb Haemost. 1997; 78:501-11.

130. Weitz JI, Bates SM. New anticoagulants. J Thromb Haemost. 2005; 3:1843-53.

131. Bajaj SP, Joist JH. New insights into how blood clots: implications for the use of APTT and PT as coagulation screening tests and in monitoring of anticoagulant therapy. Semin Thromb Hemost. 1999; 25:407-18.

132. Vijaykumar D, Sprengeler PA, Shaghafi M, Spencer JR, Katz BA, Yu C, Rai R, Young WB, Schultz B, Janc J. Discovery of novel hydroxy pyrazole based factor IXa inhibitor. Bioorg Med Chem Lett. 2006; 16:2796-9.

133. Katz BA, Elrod K, Verner E, Mackman RL, Luong C, Shrader WD, Sendzik M, Spencer JR, Sprengeler PA, Kolesnikov A, Tai VW, Hui HC, Breitenbucher JG, Allen D, Janc JW. Elaborate manifold of short hydrogen bond arrays mediating binding of active site-directed serine protease inhibitors. J Mol Biol. 2003; 329:93-120.

134. Sun J, Yamaguchi M, Yuda M, Miura K, Takeya H, Hirai M, Matsuoka H, Ando K, Watanabe T, Suzuki K, Chinzei Y. Purification, characterization and cDNA cloning of a novel anticoagulant of the intrinsic pathway, (prolixin-S) from salivary glands of the blood sucking bug, Rhodnius prolixus. Thromb Haemost. 1996; 75:573-7.

135. Schwienhorst A. Direct thrombin inhibitors - a survey of recent developments. Cell Mol Life Sci. 2006; 63:2773-91.

136. Bates SM, Weitz JI. The status of new anticoagulants. Br J Haematol. 2006; 134:3-19.

137. Nierodzik ML, Karpatkin S. Thrombin induces tumor growth, metastasis, and angiogenesis: Evidence for a thrombin-regulated dormant tumor phenotype. Cancer Cell. 2006; 10:355-62.

138. Davie EW, Kulman JD. An overview of the structure and function of thrombin. Semin Thromb Hemost. 2006; 32 Suppl 1:3-15.

139. Higaki JN, Evnin LB, Craik CS. Introduction of a cysteine protease active site into trypsin. Biochemistry. 1989; 28:9256-63.

140. Huntington JA. Molecular recognition mechanisms of thrombin. J Thromb Haemost. 2005; 3:1861-72.

141. Tsiang M, Jain AK, Dunn KE, Rojas ME, Leung LL, Gibbs CS. Functional mapping of the surface residues of human thrombin. J Biol Chem. 1995; 270:16854-63.

142. Mathews II, Padmanabhan KP, Ganesh V, Tulinsky A, Ishii M, Chen J, Turck CW, Coughlin SR, Fenton JW. Crystallographic structures of thrombin complexed with thrombin receptor peptides: existence of expected and novel binding modes. Biochemistry. 1994; 33:3266-79.

143. Esmon CT, Lollar P. Involvement of thrombin anion-binding exosites 1 and 2 in the activation of factor V and factor VIII. J Biol Chem. 1996; 271:13882-7.

144. Ye J, Liu LW, Esmon CT, Johnson AE. The fifth and sixth growth factor-like domains of thrombomodulin bind to the anion-binding exosite of thrombin and alter its specificity. J Biol Chem. 1992; 267:11023-8.

145. De Cristofaro R, De Candia E, Landolfi R, Rutella S, Hall SW. Structural and functional mapping of the thrombin domain involved in the binding to the platelet glycoprotein Ib. Biochemistry. 2001; 40:13268-73.

146. Sheehan JP, Wu Q, Tollefsen DM, Sadler JE. Mutagenesis of thrombin selectively modulates inhibition by serpins heparin cofactor II and antithrombin III. Interaction with the anion-binding exosite determines heparin cofactor II specificity. J Biol Chem. 1993; 268:3639-45.

147. Stone SR, Braun PJ, Hofsteenge J. Identification of regions of alpha-thrombin involved in its interaction with hirudin. Biochemistry. 1987; 26:4617-24.

148. Sheehan JP, Sadler JE. Molecular mapping of the heparin-binding exosite of thrombin. Proc Natl Acad Sci U S A. 1994; 91:5518-22.

149. Dumas JJ, Kumar R, Seehra J, Somers WS, Mosyak L. Crystal structure of the GpIbalpha-thrombin complex essential for platelet aggregation. Science. 2003; 301:222-6.

150. Richardson JL, Kröger B, Hoeffken W, Sadler JE, Pereira P, Huber R, Bode W, Fuentes-Prior P. Crystal structure of the human alpha-thrombin-haemadin complex: an exosite II-binding inhibitor. EMBO J. 2000; 19:5650-60.

151. Di Cera E, Guinto ER, Vindigni A, Dang QD, Ayala YM, Wuyi M, Tulinsky A. The Na+ binding site of thrombin. J Biol Chem. 1995; 270:22089-92.

152. Kettner C, Shaw E. D-Phe-Pro-ArgCH2C1-A selective affinity label for thrombin. Thromb Res. 1979; 14:969-73.

153. Kettner C, Mersinger L, Knabb R. The selective inhibition of thrombin by peptides of boroarginine. J Biol Chem. 1990; 265:18289-97.

154. A.Maryanoff BE, Qiu X, Padmanabhan KP, Tulinsky A, Almond HR, Andrade-Gordon P, Greco MN, Kauffman JA, Nicolaou KC, Liu A, et al. Molecular basis for the inhibition of human alpha-thrombin by the macrocyclic peptide cyclotheonamide . Proc Natl Acad Sci U S A. 1993; 90:8048-52.

155. Mungall D. BIBR-1048 Boehringer Ingelheim. Curr Opin Investig Drugs. 2002; 3:905-7.

156. Hauel NH, Nar H, Priepke H, Ries U, Stassen JM, Wienen W. Structure-based design of novel potent nonpeptide thrombin inhibitors. J Med Chem. 2002; 45:1757-66.

157. Tomczuk B, Lu T, Soll RM, Fedde C, Wang A, Murphy L, Crysler C, Dasgupta M, Eisennagel S, Spurlino J, Bone R. Oxyguanidines: application to non-peptidic phenyl-based thrombin inhibitors. Bioorg Med Chem Lett. 2003; 13:1495-8.

158. Katz BA, Luong C. Recruiting Zn2+ to mediate potent, specific inhibition of serine proteases. J Mol Biol. 1999; 292:669-84.

159. Katz BA, Clark JM, Finer-Moore JS, Jenkins TE, Johnson CR, Ross MJ, Luong C, Moore WR, Stroud RM. Design of potent selective zinc-mediated serine protease inhibitors. Nature. 1998; 391:608-12.

160. Altenburger JM, Lassalle GY, Matrougui M, Galtier D, Jetha JC, Bocskei Z, Berry CN, Lunven C, Lorrain J, Herault JP, Schaeffer P, O'Connor SE, Herbert JM. SSR182289A, a selective and potent orally active thrombin inhibitor. Bioorg Med Chem. 2004; 12:1713-30.

161. Deadman JJ, Elgendy S, Goodwin CA, Green D, Baban JA, Patel G, Skordalakes E, Chino N, Claeson G, Kakkar VV, et al. Characterization of a class of peptide boronates

with neutral P1 side chains as highly selective inhibitors of thrombin. J Med Chem. 1995; 38:1511-22.

162. Lee K, Jung WH, Hwang SY, Lee SH. Fluorobenzamidrazone thrombin inhibitors: influence of fluorine on enhancing oral absorption. Bioorg Med Chem Lett. 1999; 9:2483-6.

163. Lee K, Park CW, Jung WH, Park HD, Lee SH, Chung KH, Park SK, Kwon OH, Kang M, Park DH, Lee SK, Kim EE, Yoon SK, Kim A. Efficacious and orally bioavailable thrombin inhibitors based on a 2,5-thienylamidine at the P1 position: discovery of N-carboxymethyl-d-diphenylalanyl-l-prolyl[(5-amidino-2-thienyl)methyl]amide. J Med Chem. 2003; 46:3612-22.

164. Burgey CS, Robinson KA, Lyle TA, Nantermet PG, Selnick HG, Isaacs RC, Lewis SD, Lucas BJ, Krueger JA, Singh R, Miller-Stein C, White RB, Wong B, Lyle EA, Stranieri MT, Cook JJ, McMasters DR, Pellicore JM, Pal S, Wallace AA, Clayton FC, Bohn D, Welsh DC, Lynch JJ, Yan Y, Chen Z, Kuo L, Gardell SJ, Shafer JA, Vacca JP. Pharmacokinetic optimization of 3-amino-6-chloropyrazinone acetamide thrombin inhibitors. Implementation of P3 pyridine N-oxides to deliver an orally bioavailable series containing P1 N-benzylamides. Bioorg Med Chem Lett. 2003; 13:1353-7.

165. Nantermet PG, Burgey CS, Robinson KA, Pellicore JM, Newton CL, Deng JZ, Selnick HG, Lewis SD, Lucas BJ, Krueger JA, Miller-Stein C, White RB, Wong B, McMasters DR, Wallace AA, Lynch JJ, Yan Y, Chen Z, Kuo L, Gardell SJ, Shafer JA, Vacca JP, Lyle TA. P2 pyridine N-oxide thrombin inhibitors: a novel peptidomimetic scaffold. Bioorg Med Chem Lett. 2005; 15:2771-5.

166. Salzet M, Chopin V, Baert J, Matias I, Malecha J. Theromin, a novel leech thrombin inhibitor. J Biol Chem. 2000; 275:30774-80.

167. Strube KH, Kröger B, Bialojan S, Otte M, Dodt J. Isolation, sequence analysis, and cloning of haemadin. An anticoagulant peptide from the Indian leech. J Biol Chem. 1993; 268:8590-5.

168. Electricwala A, Sawyer RT, Jones CP, Atkinson T. Isolation of thrombin inhibitor from the leech Hirudinaria manillensis. Blood Coagul Fibrinolysis. 1991; 2:83-9.

169. Noeske-Jungblut C, Haendler B, Donner P, Alagon A, Possani L, Schleuning WD. Triabin, a highly potent exosite inhibitor of thrombin. J Biol Chem. 1995; 270:28629-34.

170. Glusa E, Bretschneider E, Daum J, Noeske-Jungblut C. Inhibition of thrombin-mediated cellular effects by triabin, a highly potent anion-binding exosite thrombin inhibitor. Thromb Haemost. 1997; 77:1196-200.

171. Fuentes-Prior P, Noeske-Jungblut C, Donner P, Schleuning WD, Huber R, Bode W. Structure of the thrombin complex with triabin, a lipocalin-like exosite-binding inhibitor derived from a triatomine bug. Proc Natl Acad Sci U S A. 1997; 94:11845-50.

172. Zingali RB, Jandrot-Perrus M, Guillin MC, Bon C. Bothrojaracin, a new thrombin inhibitor isolated from Bothrops jararaca venom: characterization and mechanism of thrombin inhibition. Biochemistry. 1993; 32:10794-802.

173. Arocas V, Zingali RB, Guillin MC, Bon C, Jandrot-Perrus M. Bothrojaracin: a potent two-site-directed thrombin inhibitor. Biochemistry. 1996; 35:9083-9.

174. Friedrich T, Kröger B, Bialojan S, Lemaire HG, Höffken HW, Reuschenbach P, Otte M, Dodt J. A Kazal-type inhibitor with thrombin specificity from Rhodnius prolixus. J Biol Chem. 1993;268:16216-22.

175. van de Locht A, Lamba D, Bauer M, Huber R, Friedrich T, Kröger B, Höffken W, Bode W. Two heads are better than one: crystal structure of the insect derived double domain Kazal inhibitor rhodniin in complex with thrombin. EMBO J. 1995; 14:5149-57.

176. Bralet J, Schwartz JC. Vasopeptidase inhibitors: an emerging class of cardiovascular drugs. Trends Pharmacol Sci. 2001; 22:106-9.

177. Brandstetter H, Kühne A, Bode W, Huber R, von der Saal W, Wirthensohn K, Engh RA. X-ray structure of active site-inhibited clotting factor Xa. Implications for drug design and substrate recognition. J Biol Chem. 1996; 271:29988-92.

178. Nar H, Bauer M, Schmid A, Stassen JM, Wienen W, Priepke HW, Kauffmann IK, Ries UJ, Hauel NH. Structural basis for inhibition promiscuity of dual specific thrombin and factor Xa blood coagulation inhibitors. Structure. 2001; 9:29-37.

179. Deng JZ, McMasters DR, Rabbat PM, Williams PD, Coburn CA, Yan Y, Kuo LC, Lewis SD, Lucas BJ, Krueger JA, Strulovici B, Vacca JP, Lyle TA, Burgey CS. Development of an oxazolopyridine series of dual thrombin/factor Xa inhibitors via structure-guided lead optimization. Bioorg Med Chem Lett. 2005; 15:4411-6.

180. Hanessian S, Therrien E, Granberg K, Nilsson I. Targeting thrombin and factor VIIa: design, synthesis, and inhibitory activity of functionally relevant indolizidinones. Bioorg Med Chem Lett. 2002; 12:2907-11.

181. Carroll AR, Pierens GK, Fechner G, De Almeida Leone P, Ngo A, Simpson M, Hyde E, Hooper JN, Boström SL, Musil D, Quinn RJ. Dysinosin A: a novel inhibitor of Factor VIIa and thrombin from a new genus and species of Australian sponge of the family Dysideidae. J Am Chem Soc. 2002; 124:13340-1.

182. Qiao JX, Cheng X, Modi DP, Rossi KA, Luettgen JM, Knabb RM, Jadhav PK, Wexler RR. 5-Amidinobenzo[b]thiophenes as dual inhibitors of factors IXa and Xa. Bioorg Med Chem Lett. 2005; 15:29-35.

183. First oral anticoagulant in new class of direct thrombin inhibitors, Exanta™. (21 June 2004). Medical News Today. Retrieved 16 November 2005, from http://www.medicalnewstoday.com/medicalnews.php?newsid=9724

184. Murray CJ, Lopez AD. Mortality by cause for eight regions of the world: Global Burden of Disease Study. Lancet 1997; 349:1269-1276.

185. Cushman M, Tsai AW, White RH, Heckbert SR, Rosamond WD, Enright P, Folsom AR. Deep vein thrombosis and pulmonary embolism in two cohorts: the longitudinal investigation of thromboembolism etiology. Am. J. Med. 2004; 117:19-25.

186. Lopez JA, Kearon C, Lee AY. Deep venous thrombosis. Hematology Am Soc Hematol Educ Program. 2004; 439-456.

187. Desai UR. New antithrombin-based anticoagulants. Med. Res. Rev. 2004; 24:151-181.

188. Petitou M, van Boeckel CAA. A synthetic antithrombin III binding pentasaccharide is now a drug! What comes next? Angew. Chem. Int. Ed. Engl. 2004, 43, 3118-3133.

189. de Kort M, Buijsman RC, van Boeckel CA. Synthetic heparin derivatives as new anticoagulant drugs. Drug Discovery Today. 2005; 10:769-79.

190. Gunnarsson GT, Desai UR. Designing small, non-sugar activators of antithrombin using hydropathic interaction analyses. J. Med. Chem. 2002; 45:1233-1243.

191. Gunnarsson GT, Desai UR. Interaction of sulfated flavanoids with antithrombin: Lessons on the design of organic activators. J. Med. Chem. 2002; 45:4460-4470.

192. Gunnarsson GT, Desai UR. Exploring new non-sugar sulfated molecules as activators of antithrombin. Bioorg. Med. Chem. Lett. 2003; 13:579-583.

193. Monien BH, Desai UR. Antithrombin activation by nonsulfated, non-polysaccharide organic polymer. J Med Chem. 2005; 48:1269-73.

194. Monien BH, Cheang KI, Desai UR. Mechanism of poly(acrylic acid) acceleration of antithrombin inhibition of thrombin: implications for the design of novel heparin mimics. J Med Chem. 2005; 48:5360-8.

195. Freudenberg K, Neish AC. Constitution and biosynthesis of lignin (molecular biology, biochemistry and biophysics). New York, Springer Verlag, 1968; 132-182.

196. Adler E. Lignin chemistry – past, present and future. Wood. Sci. Technol. 1977; 11:169-218.

197. Kobayashi S, Uyama H, Kimura S. Enzymatic polymerization. Chem. Rev. 2001; 101:3793-3818.

198. Ralph J, Hatfield RD, Piquemal J, Yahiaoui N, Pean M, Lapierre C, Boudet AM. NMR characterization of altered lignins extracted from tobacco plants down-regulated for

lignification enzymes cinnamylalcohol dehydrogenase and cinnamoyl-CoA reductase. Proc. Natl. Acad. Sci. U S A. 1998; 95:12803-12808.

199. Syriänen K, Brunow G. Regioselectivity I lignin biosynthesis. The influence of dimerization and cross-coupling. J. Chem. Soc., Perkin Trans. 2000; 1:183-187.

200. Ferreira D, Slade D. Oligomeric proanthocyanidins: naturally occurring O-heterocycles. Nat Prod Rep. 2002; 19:517-41.

201. Ferreira D, Li XC. Oligomeric proanthocyanidins: naturally occurring O-heterocycles. Nat Prod Rep. 2000; 17:193-212.

202. Glasser WG. In Pulp and Paper – Chemistry and Chemical Technology; Casey, J. P. Ed. Wiley and Sons, New York, 1980, pp. 39.

203. Sarkanen KV. In Lignins: Occurrence, Formation, Structure, and Reactions; Sarkanen, K. V.; Ludwig, C. H. Eds.; Wiley-Interscience, New York, 1971, pp. 95.

204. Ward G, Hadar Y, Bilkis I, Konstantinovsky L, Dosoretz CG. Initial steps of ferulic acid polymerization by lignin peroxidase. J Biol Chem. 2001; 276:18734-41.

205. Boerjan W, Ralph J, Baucher M. Lignin biosynthesis. Annu Rev Plant Biol. 2003; 54:519-46.

206. Touzel JP, Chabbert B, Monties B, Debeire P, Cathala B. Synthesis and characterization of dehydrogenation polymers in Gluconacetobacter xylinus cellulose and cellulose/pectin composite. J Agric Food Chem. 2003; 51:981-6.

207. Xia Z, Akim LG, Argyropoulos DS. Quantitative (13)C NMR analysis of lignins with internal standards. J Agric Food Chem. 2001; 49:3573-8.

208. Banoub JH, Delmas M. Structural elucidation of the wheat straw lignin polymer by atmospheric pressure chemical ionization tandem mass spectrometry and matrix-assisted laser desorption/ionization time-of-flight mass spectrometry. J Mass Spectrom. 2003; 38:900-3.

209. Desai, U. R. In Chemistry and Biology of Heparin and Heparan Sulfate; Garg, H. G.; Linhardt, R. J.; Hales, C. A. Eds.; Elsevier, New York, 2005, pp. 483.

210. Gettins PG. Serpin structure, mechanism, and function. Chem Rev. 2002; 102:4751-804.

211. Björk, I.; Olson, S. T. In Chemistry and Biology of Serpins; Church, F. C.; Cunnigham, D. D.; Ginsburg, D.; Hoffman, M.; Stone, S. R.; Tollefsen, D. M. Eds.; Plenum Press, New York, 1997, pp. 17.

212. Monien BH, Henry BL, Raghuraman A, Hindle M, Desai UR. Novel chemo-enzymatic oligomers of cinnamic acids as direct and indirect inhibitors of coagulation proteinases. Bioorg Med Chem 2006; 14: 7988-98.

213. Olson ST, Swanson R, Raub-Segall E, Bedsted T, Sadri M, Petitou M, Herault JP, Herbert JM, Bjork I. Accelerating ability of synthetic oligosaccharides on antithrombin inhibition of proteinases of the clotting and fibrinolytic systems. Comparison with heparin and low-molecular-weight heparin. Thromb Haemost 2004; 92: 929-39.

214. Menajovsky LB. Heparin-induced thrombocytopenia: clinical manifestations and management strategies. Am J Med 2005; 118 Suppl 8A: 21S-30S.

215. Bauersachs RM. Fondaparinux: an update on new study results. Eur J Clin Invest 2005; 35 Suppl 1: 27-32.

216. Turpie AG. The safety of fondaparinux for the prevention and treatment of venous thromboembolism. Expert Opin Drug Saf 2005; 4: 707-21.

217. Ramjee MK. The use of fluorogenic substrates to monitor thrombin generation for the analysis of plasma and whole blood coagulation. Anal Biochem 2000; 277: 11-8.

218. Prasa D, Svendsen L, Sturzebecher J. The ability of thrombin inhibitors to reduce the thrombin activity generated in plasma on extrinsic and intrinsic activation. Thromb Haemost 1997; 77: 498-503.

219. Boström SL, Hansson GF, Sarich TC, Wolzt M. The inhibitory effect of melagatran, the active form of the oral direct thrombin inhibitor ximelagatran, compared with enoxaparin and r-hirudin on ex vivo thrombin generation in human plasma. Thromb Res 2004; 113: 85-91.

220. Petros S, Siegemund T, Siegemund A, Engelmann L. The effect of different anticoagulants on thrombin generation. Blood Coagul Fibrinolysis 2006; 17: 131-7.

221. Salooja N, Perry DJ. Thromboelastography. Blood Coagul Fibrinol 2001; 12: 327-37.

222. Carr ME Jr, Martin EJ, Kuhn JG, Ambrose H, Fern S, Bryant PC. Monitoring of hemostatic status in four patients being treated with recombinant factor VIIa. Clin Lab 2004; 50: 529-538.

223. Klein SM, Slaughter TF, Vail PT, Ginsberg B, El-Moalem HE, Alexander R, D'Ercole F, Greengrass RA, Perumal TT, Welsby I, Gan TJ. Thromboelastography as a perioperative measure of anticoagulation resulting from low molecular weight heparin: a comparison with anti-Xa concentrations. Anesth Analg 2000; 91: 1091-5.

224. Chandler WL. The thromboelastography and the thromboelastograph technique. Semin Thromb Hemostasis 1995; 21 Suppl 4: 1-6.

225. Carr ME, Martin EJ, Kuhn JG, Spiess BD. Onset of force development as a marker of thrombin generation in whole blood: the thrombin generation time (TGT). J Thromb Haemost 2003; 1: 1977-83.

226. Carr ME. Development of platelet contractile force as a research and clinical measure of platelet function. Cell Biochem Biophys 2003; 38: 55-78.

227. Carr ME, Carr SL, Greilich PE. Heparin ablates force development during platelet mediated clot retraction. Thromb Haemost 1996; 75: 674-8.

228. Carr ME, Carr SL, Tildon T, Fischer LM, Martin EJ. Batroxobin-induced clots exhibit delayed and reduced platelet contractile force in some patients with clotting factor deficiencies. J Thromb Haemost 2003; 1: 243-9.

229. Carr ME, Carr SL, Hantgan RR, Braaten J. Glycoprotein IIb/IIIa blockade inhibits platelet-mediated force development and reduces gel elastic modulus Thromb Haemost 1995; 73: 499-505.

230. Vongchan P, Warda M, Toyoda H, Marks M, Linhardt RJ. Structural characterization of human liver heparan sulfate. Biochim Biophys Acta 2005; 1721: 1-8.

231. Bedsted T, Swanson R, Chuang YJ, Bock PE, Björk I, Olson ST. Heparin and calcium ions dramatically enhance antithrombin reactivity with factor IXa by generating new interaction exosites. Biochemistry. 2003; 42:8143-52.

232. Neuenschwander PF, Branam DE, Morrissey JH. Importance of substrate composition, pH and other variables on tissue factor enhancement of factor VIIa activity. Thromb Haemost. 1993; 70:970-7.

233. Chase T, Shaw E. Comparison of the esterase activities of trypsin, plasmin, and thrombin on guanidinobenzoate esters. Titration of the enzymes. Biochemistry. 1969; 8:2212-24.

234. Sonder SA, Fenton JW. Thrombin specificity with tripeptide chromogenic substrates: comparison of human and bovine thrombins with and without fibrinogen clotting activities. Clin Chem. 1986; 32:934-7.

235. Berliner LJ, Shen YY. Physical evidence for an apolar binding site near the catalytic center of human alpha-thrombin. Biochemistry. 1977; 16:4622-6.

236. Linhardt RJ, Loganathan D, al-Hakim A, Wang HM, Walenga JM, Hoppensteadt D, Fareed J. Oligosaccharide mapping of low molecular weight heparins: structure and activity differences. J Med Chem. 1990; 33:1639-45.

237. Olson ST, Halvorson HR, Björk I. Quantitative characterization of the thrombin-heparin interaction. Discrimination between specific and nonspecific binding models. J Biol Chem. 1991; 266:6342-52.

238. Bock PE, Olson ST, Björk I. Inactivation of thrombin by antithrombin is accompanied by inactivation of regulatory exosite I. J Biol Chem. 1997; 272:19837-45.

239. Davin LB, Lewis NG. Lignin primary structures and dirigent sites. Curr Opin Biotechnol. 2005; 16:407-15.

240. Rezaie AR. Identification of basic residues in the heparin-binding exosite of factor Xa critical for heparin and factor Va binding. J Biol Chem. 2000; 275:3320-7.

241. Bianchini EP, Pike RN, Le Bonniec BF. The elusive role of the potential factor X cation-binding exosite-1 in substrate and inhibitor interactions. J Biol Chem. 2004; 279:3671-9.

242. Carter WJ, Cama E, Huntington JA. Crystal structure of thrombin bound to heparin. J Biol Chem. 2005; 280:2745-9.

243. Streusand VJ, Björk I, Gettins PG, Petitou M, Olson ST. Mechanism of acceleration of antithrombin-proteinase reactions by low affinity heparin. Role of the antithrombin binding pentasaccharide in heparin rate enhancement. J. Biol. Chem. 1995; 270:9043-9051.

244. Liu LW, Vu TK, Esmon CT, Coughlin SR. The region of the thrombin receptor resembling hirudin binds to thrombin and alters enzyme specificity. J. Biol. Chem. 1991; 266:16977-16980.

245. Desai UR, Petitou M, Björk I, Olson ST. Mechanism of heparin activation of antithrombin. Role of individual residues of the pentasaccharide activating sequence in the recognition of native and activated states of antithrombin. J. Biol. Chem. 1998; 273:7478-7487.

APPENDIX A

Abbreviations used: AT, antithrombin; APTT, activated partial thromboplastin time; CA, caffeic acid; CD, dehydropolymer of caffeic acid; CD_{AC}, acetylated dehydropolymer of caffeic acid; CD_S, sulfated dehydropolymer of caffeic acid; CDSO3, sulfated dehydropolymer of caffeic acid; (+)-CS, (+)-catechin sulfate; DHP, dehydrogenation polymer; DTI, direct thrombin inhibitor; FA, ferulic acid; FD, dehydropolymer of ferulic acid; FD_{AC}, acetylated dehydropolymer of ferulic acid; FD_S, sulfated dehydropolymer of ferulic acid; FDSO3, sulfated dehydropolymer of ferulic acid; [5F]-Hir[54-65](SO_3^-), Tyr63-sulfated hirudin-(54-65) labeled with fluorescein; GAG, glycosaminoglycan; H8, heparin octasaccharide; HRP, horseradish peroxidase; IC_{50}, concentration of inhibitor that results in 50% inhibition; LMWH, low-molecular-weight heparin; MES, 2-(*N*-morpholino)ethanesulfonic acid sodium; M_N, number average molecular weights;M_W, weight average molecular weights; NPGB, *p*-nitrophenyl-*p'*-guanidinobenzoate; PABA, *p*-aminobenzamidine; PEG, polyethylene glycol; PT, prothrombin time; SA, sapinic acid; SD, dehydropolymer of sapinic acid; SD_{AC}, acetylated dehydropolymer of sapinic acid; SD_S, sulfated dehydropolymer of sapinic acid; SDSO3, sulfated dehydropolymer of sinapic acid; SEC, size-exclusion chromatography; THF, tetrahydrofuran

VITA

Brian Henry was born on May 15, 1980 in Stanford, CA. Brian graduated from Middletown High School in 1998. He matriculated to James Madison University in the fall of 1998 and received his B.S. in biology (Magna Cum Laude) in December 2001. While at James Madison University, Brian was the recipient of the Excellence in Biology Award, a George W. Chappelear Jr. scholar and was inducted into the Phi Kappa Phi National Honor Society. After college, Brian entered the MD/PhD program at the Medical College of Virginia in fall 2002. After completing the first two years of medical school, Brian transitioned to the Department of Medicinal Chemistry to pursue the PhD portion of his training. While in the Department of Medicinal Chemistry, Brian was selected by the VCU School of Pharmacy as its representative to present his research at the Virginia Council of Graduate School's Graduate Student Research Forum. He was also the winner for best poster at the 2006 VCU School of Pharmacy Research day and at the 2007 VCU Graduate Student Research Symposium.